

**Precast Concrete Inlay Panels:  
Rehabilitation Strategy for  
High-Volume Highways in Ontario**

by

Daniel John Pickel

A thesis  
presented to the University of Waterloo  
in fulfilment of the  
thesis requirement for the degree of  
Doctor of Philosophy  
in  
Civil Engineering

Waterloo, Ontario, Canada, 2018

© Daniel John Pickel 2018

## EXAMINING COMMITTEE MEMBERSHIP

The following served on the Examining Committee for this thesis. The decision of the Examining Committee is by majority vote.

External Examiner	<b>Dr. Shiraz Tayabji</b> President, Advanced Concrete Pavement Consultancy
Supervisor(s)	<b>Dr. Susan Tighe</b> Deputy Provost and Associate Vice-President Int. Planning & Budgeting Norman W. McLeod Professor in Sustainable Pavement Engineering University of Waterloo, Department of Civil & Environmental Engineering
Internal Member	<b>Dr. Jeffrey West</b> Adjunct Professor University of Waterloo, Department of Civil & Environmental Engineering
Internal-external Member	<b>Dr. Duane Cronin</b> Adjunct Professor University of Waterloo, Department of Mechanical & Mechatronic Engineering
Other Member(s)	<b>Dr. Hassan Baaj</b> Professor University of Waterloo, Department of Civil & Environmental Engineering

## **AUTHOR'S DECLARATION**

This thesis consists of material all of which I authored or co-authored: see Statement of Contributions included throughout the thesis. This is a true copy of the thesis, including any required final revisions, as accepted by my examiners.

I understand that my thesis may be made electronically available to the public.

## STATEMENT OF CONTRIBUTIONS

Chapter 4 of this thesis contains parts of a paper co-authored by myself, my supervisor (Dr. Tighe), Rico Fung, Stephen Lee, Peter Smith, Tom Kazmierowski, and Mark Snyder. I wrote the paper based on the PCIP design that was developed by the full group of co-authors, including myself. The co-authors also provided some editing and reviews during the paper's production.

Chapter 5.5 of this thesis has been incorporated within a paper submitted for publication. The paper is co-authored by myself, Dahlia Malek, an MASc student, and my supervisor (Dr. Tighe). I developed the methodology and research design of the paper, with input from Dr. Tighe, while Ms. Malek assisted in the writing of the paper and collecting background information relating the Analytical Hierarchy Process. Ms. Malek and I collectively analyzed and summarized the experimental data.

Chapter 6.2 of this thesis contains parts of a paper co-authored by myself, my supervisor (Dr. Tighe), Warren Lee, and Rico Fung. I developed the methodology for the analysis, with input from Dr. Tighe, and wrote the paper based on the findings. The co-authors provided technical input regarding the analysis of data. The co-authors also provided editing and review during the paper's production.

Chapter 6.3 of this thesis contains parts of a paper that was submitted for publication and co-authored by myself and my supervisor (Dr. Tighe). I developed the methodology for the analysis, analyzed the data, developed the new joint analysis model, and wrote the paper based on the findings, all with input from Dr. Tighe.

## ABSTRACT

The Ministry of Transportation of Ontario (MTO) has responsibility for many high-volume highways throughout the province of Ontario, including the 400-series highways. Several of these highways have exhibited a premature rutting failure three to seven years after the placement of new hot-mix asphalt (HMA) in the pavement surface layers. This failure indicates the presence of deep-seated pavement issues that are likely located in the base layers or subgrade beneath the HMA pavement layers. To address these deep-seated issues directly, a full-depth pavement rehabilitation is required wherein the pavement structure is fully removed to the depth of the problematic layer. This type of rehabilitation is time-consuming, particularly when these issues extend for substantial lengths of the given highway.

The time-consuming nature of full-depth pavement rehabilitation precludes it from use on the 400-series highways due to the MTO's practice of limiting construction windows to the time between 10 pm and 6 am. Outside of this time, traffic must be reinstated to full capacity in all lanes. For this reason, the deep-seated rutting issues have been consistently addressed with mill and overlay procedures, wherein the upper 40 mm or 80 mm of HMA is milled from the pavement and replaced with an equivalent thickness, which then exhibits the same failure after another three to seven years.

In order to address this issue for a longer term, the MTO was interested in the development of a new rehabilitation technique using precast concrete panels inlaid into the HMA pavement structure. The design of a trial section to evaluate the precast concrete inlay panels (PCIP) was developed in conjunction with the MTO, the Fort Miller Company, the Cement Association of Canada, and Golder Associates. The PCIP design was based off typical precast concrete pavements but was modified to address the unique conditions of inlay within HMA pavement. The trial was 100 m in length and was comprised of 22 panels.

The support conditions beneath precast concrete pavements have been found to be a significant factor in determining their performance. For this reason, three support conditions were designed, each with different costs and benefits in terms of overall constructability; the support conditions were Asphalt-supported (AS), Grade-supported (GraS), and Grout-supported (GroS).

The construction of the trial section took place between September 19<sup>th</sup> and September 23<sup>rd</sup>, 2016, with the installation of each support condition taking place on a separate night. Dufferin Construction was the head contractor who undertook the construction. The timing of the individual construction activities and any issues that arose were monitored throughout the course of the construction.

Following construction, an analytical hierarchy process was used to analyze the three support conditions in terms of their relative constructability. The analysis was performed with input from both Dufferin Construction and the MTO. It was found that the GroS panels were the most ideal choice in terms of construction, based on the criteria that were used in the analysis.

Data from instrumentation that was installed beneath the PCIP trial during construction indicate that moisture penetrated beneath the panels shortly after the completion of construction, indicating that the joints should be improved and that a drainage detail is required. The instrumentation also indicated a higher load concentration beneath the joints of a loaded panel in relation to the mid-panel location.

Various surface analyses were undertaken during highway closures, including visual analyses, surface texture scanning, and roughness and friction measurement. The three support conditions were found to behave similarly for all tests except surface roughness, in which the GroS section was found to be significantly less rough than the other two support conditions. This was due to the high degree of control over panel elevation differences in this design.

A life cycle cost analysis was undertaken to compare the PCIP strategy to the mill and overlay strategy that had been used in the past. It was found that the PCIP strategy generally has a higher life cycle cost because of its high initial costs, and the present worth cost difference between the two strategies was sensitive to factors that affected the initial cost, such as the panel unit cost and the installation rate. The analysis was based on several cost and maintenance assumptions that will be further clarified as the service life of the PCIP rehabilitation is better defined.

Finally, several design improvements suggestions were made based on the performance and construction of the PCIP trial. These include increased strength specifications, advanced milling control, improved HMA edge protection, joint material design, drainage details, and diamond grinding following the complete installation of the PCIP rehabilitation.

## **ACKNOWLEDGEMENTS**

I would like to acknowledge and express my deep gratitude to the many people who have supported me during the completion of this research. Firstly, to Dr. Susan Tighe, whose support and guidance have been irreplaceable. Secondly, I would like to thank Jazmine for her tireless support and patience. Thirdly, thanks to my family, Lee, Bill, Jessica, Burton (and family), and Charlotte, for every type of support they provide me.

I would also like to acknowledge the other members of the design team whose expertise has been invaluable: Rico Fung formerly of the Cement Association of Canada, Stephen Lee, Warren Lee, and Susanne Chan of the Ministry of Transportation of Ontario, Peter Smith of the Fort Miller Company, Tom Kazmierowski of Golder Associates Ltd., and Mark Snyder.

Thanks to Aaron Toth, John Snow, Chris Esbah, and the full construction team of Dufferin Construction for their help and involvement even following the completion of construction.

Further thanks to all the members of the Centre for Pavement and Transportation Technology group (both current and former) who have never failed to help when asked. Special thanks to Andy (Zhong) Jian, Ata Nahidi, Dahlia Malek, Donghui Lu, Eskedil Melese, Frank (Yang) Liu, Frank Mi-Way Ni, Qingfan Liu, Raha Wafa, Sergey Averyanov, Taha Younes, Yashar Alamdary, and Zaid Alyami for their help during the trial construction and data collection trips.

A special thank you also to Terry Ridgway, Anne Allen, Mark Sobon, Richard Morrison, Doug Hirst, Laura Bland, Jessica Rossi, and Bev Seibel for their generous help and patience with me.

I would like to acknowledge the following sponsoring partners of this research project:

- The Centre for Pavement and Transportation Technology (CPATT), Norman W. McLeod Chair, University of Waterloo;
- The Ministry of Transportation Ontario (MTO);
- The Cement Association of Canada (CAC)
- The Natural Sciences and Engineering Research Council of Canada (NSERC) Collaborative Research and Development Program.

## DEDICATION

*This thesis is dedicated to my partner and family,  
whose support, patience, and love have made this a possibility.*

# TABLE OF CONTENTS

Examining Committee Membership .....	ii
Author's Declaration.....	iii
Statement of Contributions .....	iv
Abstract .....	v
Acknowledgements.....	vii
Dedication.....	viii
Table of Contents.....	ix
List of Figures .....	xiv
List of Tables .....	xix
List of Abbreviations .....	xx
CHAPTER 1 : Introduction .....	1
1.1 Statement of the Problem .....	1
1.2 Research Hypothesis .....	2
1.3 Objectives of the Research.....	3
1.4 Methodology of Study.....	4
1.4.1 Construction Monitoring/ Discussions with Contractor .....	4
1.4.2 Instrumentation .....	4
1.4.3 Falling Weight Deflectometer Testing.....	5
1.4.4 Pavement Surface Testing.....	6
1.4.5 Visual Inspection .....	7
1.4.6 Life Cycle Cost .....	7
1.5 Thesis Organization.....	7
CHAPTER 2 : Literature Review .....	9
2.1 Current Practices .....	9
2.2 Precast Concrete Panels .....	12
2.3 Life Cycle Cost Analyses.....	19
2.4 User Costs .....	20
2.5 Least Significant Difference Test.....	22
2.6 Chapter Summary.....	24
CHAPTER 3 : Research Methodology .....	26
CHAPTER 4 : Precast Concrete Inlay Panel Trial Design .....	29

4.1	General Rehabilitation Strategy .....	29
4.2	Panel Support Conditions.....	33
4.2.1	Grade-supported (GraS).....	33
4.2.2	Asphalt-supported (AS) .....	36
4.2.3	Grout-supported (GroS) .....	37
4.2.4	Summary of Support Options .....	38
4.3	Precast Panel Design .....	38
4.3.1	PCIP Materials .....	38
4.3.2	PCIP Thickness Design.....	40
4.3.3	PCIP Details.....	47
4.4	PCIP Trial Design .....	54
4.5	Chapter Summary.....	55
CHAPTER 5 : Trial Section Construction.....		56
5.1	Project Site .....	56
5.2	Preliminary Plans .....	60
5.2.1	Order of Installation.....	60
5.2.2	Nightly Number of Panels Installed.....	60
5.2.3	Precast Panel Delivery .....	61
5.2.4	Lifting Inserts/Levelling Inserts.....	61
5.2.5	CPATT Installation Plans .....	62
5.2.6	Lane Closures.....	62
5.3	Construction Activities.....	63
5.3.1	Panel Production (Late August – Early September).....	63
5.3.2	Site Layout (September 15 <sup>th</sup> , 2016).....	66
5.3.3	Saw-cutting (September 19 <sup>th</sup> , 2016) .....	67
5.3.4	Asphalt-Supported Trial Section (September 20 <sup>th</sup> , 2016).....	68
5.3.5	Grade-Supported Trial Section (September 21 <sup>st</sup> , 2016).....	75
5.3.6	Grout-Supported Trial Section (September 22 <sup>nd</sup> , 2016) .....	86
5.4	Construction Summary.....	91
5.4.1	General Findings.....	93
5.4.2	Asphalt-Supported Trial.....	94
5.4.3	Grade-Supported Trial .....	95
5.4.4	Grout-Supported Trial.....	95
5.5	Constructability Analytical Hierarchy Process .....	96

5.5.1	Construction Activities .....	96
5.5.2	AHP Methodology .....	98
5.5.3	Confidence in the AHP Ranking Results & Significance.....	106
5.6	Construction Conclusions .....	110
5.6.1	Saw-Cutting Requirements .....	110
5.6.2	Milling.....	111
5.6.3	Cost .....	113
5.6.4	Grout .....	114
5.6.5	Surface Finish .....	115
5.6.6	Ideal Support Condition based on Construction .....	115
5.7	Chapter Summary.....	116
CHAPTER 6	: In-service panel performance .....	117
6.1	Visual Assessment.....	117
6.1.1	Longitudinal Asphalt/PCIP Joint .....	118
6.1.2	Transverse Asphalt/PCIP Joint .....	122
6.1.3	Typical Transverse Joints .....	123
6.1.4	Grout Injection .....	124
6.1.5	Panel Cracking.....	127
6.2	PCIP Instrumentation .....	129
6.2.1	Instrumentation .....	130
6.2.2	Methodology.....	135
6.2.3	Results.....	139
6.2.4	Conclusions and Recommendations .....	156
6.3	Joint Performance.....	158
6.3.1	Joint Evaluation Methodology.....	161
6.3.2	Incorporating RD <sub>75</sub> into Joint Evaluation .....	171
6.3.3	Conclusions.....	174
6.4	Panel Surface Analysis.....	176
6.4.1	Surface Texture Measurement .....	179
6.4.2	PCIP Surface Roughness Properties .....	190
6.4.3	PCIP Frictional Properties .....	200
6.4.4	Conclusions.....	213
CHAPTER 7	: Life Cycle Cost Analysis .....	216
7.1	Rehabilitation Techniques.....	218

7.1.1	Scope of Comparison .....	218
7.1.2	Social Discount Rate.....	218
7.1.3	Required Activities .....	219
7.1.4	Unit Costs.....	222
7.1.5	User Costs .....	225
7.2	Life Cycle Cost.....	228
7.2.1	Sensitivity Analysis .....	230
7.3	Tipping Point Analysis.....	235
7.4	Initial Cost Reduction Estimate.....	237
7.5	Life Cycle Cost Analysis Conclusions.....	238
CHAPTER 8: Conclusions and Recommendations .....		240
8.1	Thickness Design .....	240
8.2	Construction Conclusions .....	241
8.3	Visual Assessment.....	242
8.4	Instrumentation.....	243
8.5	Joint Performance.....	244
8.6	Panel Surface Evaluation .....	245
8.7	Life Cycle Cost Analysis.....	247
8.8	Overall Feasibility .....	248
CHAPTER 9: Improvements and Selection Procedure for PCIP Projects .....		249
9.1	Proposed Changes to the Initial PCIP Design .....	249
9.1.1	Concrete Strength Specification .....	249
9.1.2	Advanced Milling Control .....	250
9.1.3	Edge Protection.....	251
9.1.4	Full Depth Mastic .....	253
9.1.5	Drainage Details.....	260
9.1.6	PCIP Surface Diamond Grinding.....	263
9.2	Selection Procedure for PCIP.....	266
CHAPTER 10: Specifications for Future Applications .....		268
References.....		287
Appendix A: Least Significant Difference Calculation .....		296
Appendix B: Trial Specifications and Design Drawings.....		299
Appendix C: Visual Assessment Results .....		316



## LIST OF FIGURES

FIGURE 1.1:	TYPICAL SENSOR CONFIGURATION FOR FWD LOAD TRANSFER TEST (APPROACH AND LEAVE PANEL) (CHAN & LANE, 2005).....	5
FIGURE 2.1:	BONDED AND UNBONDED CONCRETE OVERLAY STRESS DISTRIBUTIONS .....	11
FIGURE 2.2:	PLACEMENT OF ASPHALT SEPARATION LAYER FOR UNBONDED OVERLAY OF COMPOSITE PAVEMENT .	12
FIGURE 2.3:	ROCKAWAY BLVD. INTERSECTION AT JFK AIRPORT .....	14
FIGURE 2.4:	PRECAST CONCRETE PANEL REPAIR TYPES (ADAPTED FROM (TAYABJI, YE, & BUCH, 2012)).....	15
FIGURE 3.1:	RESEARCH METHODOLOGY FOR STUDYING PRECAST CONCRETE INLAY PANELS.....	27
FIGURE 4.1:	STEPS REQUIRED FOR PCIP REHABILITATION.....	30
FIGURE 4.2:	LARGE SCREED LEVELLING BASE MATERIAL .....	34
FIGURE 4.3:	CROSS-SECTION OF GRAS PANEL (THE FORT MILLER COMPANY INC., 2015).....	35
FIGURE 4.4:	TYPICAL SUB-PANEL DETAILS .....	36
FIGURE 4.5:	GRACIE LEVELING LIFT™ .....	37
FIGURE 4.6:	28-DAY CONCRETE COMPRESSIVE STRENGTH RESULTS FOR PCIP .....	45
FIGURE 4.7:	DEEP TINING (LEFT) AND SHALLOW TINING (RIGHT).....	48
FIGURE 4.8:	BROOM FINISH (LEFT) AND BURLAP DRAG (RIGHT) .....	48
FIGURE 4.9:	TYPICAL PRECAST PANEL LAYOUT (THE FORT MILLER Co., INC. 2015) .....	50
FIGURE 4.10:	TEMPORARY END PANEL DETAIL (THE FORT MILLER Co., INC. 2015) .....	52
FIGURE 4.11:	TEMPORARY AND PERMANENT LONGITUDINAL EDGE DETAILS (THE FORT MILLER Co., INC. 2015)...	53
FIGURE 4.12:	TERMINAL TRANSVERSE EDGE DETAIL (THE FORT MILLER Co., INC. 2015) .....	54
FIGURE 4.13:	GENERAL TRIAL SECTION LAYOUT AND PANEL NUMBERING .....	55
FIGURE 5.1:	APPROXIMATE LOCATION OF TRIAL SECTION (GOOGLE, CNES 2016).....	57
FIGURE 5.2:	TRIAL SECTION LOCATION (GOOGLE MAPS, 2015).....	58
FIGURE 5.3:	TRAFFIC PLANS FOR LANE CLOSURE (MINISTRY OF TRANSPORTATION OF ONTARIO, 2014).....	63
FIGURE 5.4:	CONCRETE BATCHING PLANT AT ARMTEC, MITCHELL .....	65
FIGURE 5.5:	LAYING OUT PANEL FORMWORK .....	65
FIGURE 5.6:	PANEL FORM READY FOR CONCRETE PLACEMENT .....	66
FIGURE 5.7:	LONGITUDINAL TINING APPARATUS .....	66
FIGURE 5.8:	GENERAL SITE LAYOUT (NOT TO SCALE) .....	67
FIGURE 5.9:	SAW-CUTTING FIRST PASS .....	68
FIGURE 5.10:	SECOND PASS OF MILLING MACHINE .....	69
FIGURE 5.11:	ROUNDED HMA PORTION LEFT BY CYLINDRICAL MILLING HEAD .....	70
FIGURE 5.12:	END AFTER LONGITUDINAL AND TRANSVERSE PASSES .....	71
FIGURE 5.13:	FORT MILLER'S GRADE CHECKING APPARATUS .....	71
FIGURE 5.14:	PANEL-CARRYING TRUCK UNLOADED ADJACENT TO TRAFFIC .....	73
FIGURE 5.15:	CHECKING THE RE-MILLED SURFACE WITH A STRINGLINE.....	73

FIGURE 5.16:	PLACING PANEL #2; FIRST GAP (INSET).....	74
FIGURE 5.17:	TEMPORARY END PANEL .....	75
FIGURE 5.18:	HMA MILLING BEGUN ADJACENT TO TEMPORARY PANEL.....	76
FIGURE 5.19:	CORE HOLE ENCOUNTERED IN GRADE-SUPPORTED SECTION.....	77
FIGURE 5.20:	SPRAY FOAM SEPARATING JOINTS (L), LONGITUDINAL REINFORCING AT EDGES (R).....	77
FIGURE 5.21:	DOWEL GROUT BEING PUMPED INTO DOWEL SLOTS.....	78
FIGURE 5.22:	EDGE GROUT BEING PLACED USING SMALL HOPPER; INSIDE VIEW OF HOPPER (INSET) .....	79
FIGURE 5.23:	EVIDENCE OF SEGREGATION IN EDGE GROUT .....	80
FIGURE 5.24:	MEMBERS OF FORT MILLER, DUFFERIN, AND CPATT LAYING OUT RAILS.....	80
FIGURE 5.25:	CONSOLIDATED BALLS OF CTBM.....	81
FIGURE 5.26:	COMPACTING CTBM WITH PLATE TAMPER WHILE CPATT INSTALLS INSTRUMENTATION .....	82
FIGURE 5.27:	BOND BREAKER AGENT BEING APPLIED TO PANEL EDGE .....	83
FIGURE 5.28:	GROUT MIXER STEAMING .....	84
FIGURE 5.29:	LOCATION WHERE MILLED PORTION WAS WIDENED .....	85
FIGURE 5.30:	EDGE GROUT SAW-CUT AT TRANSVERSE JOINT; SAW-CUTTING (INSET) .....	87
FIGURE 5.31:	CRANE POSITIONED AHEAD OF PANEL BEING PLACED .....	89
FIGURE 5.32:	THREE MIXERS PRODUCING EDGE GROUT .....	89
FIGURE 5.33:	FINAL PANEL BEING PLACED .....	90
FIGURE 5.34:	PNEUMATIC IMPACT WRENCH (LEFT); EXTENDED PIPE WRENCH (RIGHT).....	90
FIGURE 5.35:	PANELS WITH LEVELLING BOLTS INSERTED.....	91
FIGURE 5.36:	CONSTRUCTION ACTIVITY TIMING FOR EACH SUPPORT CONDITION .....	97
FIGURE 5.37:	AHP HIERARCHY FOR THE PCIP EVALUATION.....	100
FIGURE 5.38:	FLOW CHART OF AHP STEPS FOR RANKING SUPPORT CONDITIONS.....	101
FIGURE 5.39:	ALTERNATIVE SCORE SENSITIVITY ANALYSIS RESULTS.....	108
FIGURE 5.40:	VERTICAL MILLED SURFACE .....	111
FIGURE 6.1:	FREQUENCY OF OBSERVED DISTRESSES AND ISSUES ON PCIP TRIAL SECTION (SEPT. 6, 2017).....	118
FIGURE 6.2:	LONGITUDINAL JOINT GROUT RAVELLING (MEDIUM SEVERITY).....	120
FIGURE 6.3:	EDGE GROUT/ASPHALT INTERFACE GAP .....	120
FIGURE 6.4:	PCIP/HMA GAP AND SEVERE RAVELLING .....	121
FIGURE 6.5:	FINAL TRANSVERSE JOINT BETWEEN PCIP AND HMA (RIGHT WHEEL PATH).....	123
FIGURE 6.6:	INCOMPRESSIBLE MATERIALS LODGED IN TRANSVERSE JOINT.....	125
FIGURE 6.7:	GROUT OVERFLOW AT INJECTION PORT.....	126
FIGURE 6.8:	GROUT OVERFLOW AT TRANSVERSE JOINT.....	126
FIGURE 6.9:	CRACKING OBSERVED IN PANEL #1 (CRACKS HIGHLIGHTED FOR CLARITY) .....	128
FIGURE 6.10:	CRACKING OBSERVED IN PANEL #2 (CRACK HIGHLIGHTED FOR CLARITY) .....	129
FIGURE 6.11:	TYPICAL TOTAL EARTH PRESSURE CELL.....	131
FIGURE 6.12:	SOIL WATER CONTENT REFLECTOMETER (CAMPBELL SCIENTIFIC, 2017).....	132

FIGURE 6.13:	DATA LOGGING EQUIPMENT SETUP (LEFT), INSTALLATION ON SITE (RIGHT) .....	133
FIGURE 6.14:	PROJECT INSTRUMENTATION SCHEMATIC.....	134
FIGURE 6.15:	INSTRUMENTATION CLUSTER INSTALLATION .....	135
FIGURE 6.16:	LOADED TRUCK AXLE CONFIGURATIONS FOR STATIC TESTING.....	137
FIGURE 6.17:	VOLUMETRIC WATER CONTENT OCTOBER 3 – NOVEMBER 7, 2016 .....	139
FIGURE 6.18:	VOLUMETRIC WATER CONTENT APRIL 25 TO JUNE 13, 2017 .....	141
FIGURE 6.19:	VOLUMETRIC WATER CONTENT JUNE 13, 2017 TO NOVEMBER 30, 2017 .....	142
FIGURE 6.20:	AVERAGE VOLUMETRIC MOISTURE CONTENT AND DAILY PRECIPITATION FOR 2016 .....	144
FIGURE 6.21:	AVERAGE VOLUMETRIC MOISTURE CONTENT AND DAILY PRECIPITATION FOR 2017 .....	144
FIGURE 6.22:	AVERAGE VOLUMETRIC MOISTURE CONTENT AND DAILY PRECIPITATION FOR 2018 .....	145
FIGURE 6.23:	STATIC LOAD TEST RESULTS FOR PANEL INSTRUMENTED WITH EPC 9/10 .....	146
FIGURE 6.24:	DISPLACEMENT SHAPE UNDER STATIC LOAD POSITIONS (NOT TO SCALE).....	147
FIGURE 6.25:	INSTRUMENT CLUSTER PRESSURE DIFFERENCES AND TEMPERATURE DIFFERENTIAL (OCT 2016).....	149
FIGURE 6.26:	INSTRUMENT CLUSTER PRESSURE DIFFERENCES AND TEMPERATURE DIFFERENTIAL (JUNE 2017).....	150
FIGURE 6.27:	INSTRUMENT CLUSTER PRESSURE DIFFERENCES AND TEMPERATURE DIFFERENTIAL (FEBRUARY 2018) .....	151
FIGURE 6.28:	EDGE STRESS DISTRIBUTION 07/10/2016 TO 07/10/2017 (HALF HOUR INTERVALS).....	152
FIGURE 6.29:	EDGE STRESS DISTRIBUTION 24/04/2017 TO 24/04/2018 (HALF HOUR INTERVALS).....	152
FIGURE 6.30:	CALCULATED EDGE STRESS DURING HOT WEATHER PERIOD (20/09/2017 – 27/09/2017) .....	154
FIGURE 6.31:	CALCULATED EDGE STRESS DURING WARM WEATHER PERIOD (10/08/2017 – 17/08/2017).....	154
FIGURE 6.32:	CALCULATED EDGE STRESS DURING COLD WEATHER PERIOD (04/02/2018 – 11/02/2018) .....	155
FIGURE 6.33:	DAILY MAXIMUM AND MINIMUM TEMPERATURE DIFFERENTIALS, OCTOBER 3, 2016 – OCTOBER 3, 2017 .....	156
FIGURE 6.34:	ILLUSTRATION OF JOINT WITH NO LOAD TRANSFER (A), AND A JOINT WITH EXCELLENT LOAD TRANSFER (B).....	160
FIGURE 6.35:	LTE <sub>8</sub> RESULTS FOR OCT. 6, 2016 (INITIAL CONSTRUCTION) AND SEPT. 19, 2017 (ONE YEAR OF SERVICE).....	164
FIGURE 6.36:	SUB-JOINT VOID ANALYSIS RESULTS .....	167
FIGURE 6.37:	RD <sub>75</sub> RESULTS FOR OCT. 6, 2016 (INITIAL CONSTRUCTION) AND SEPT. 19, 2017 (ONE YEAR OF SERVICE).....	170
FIGURE 6.38:	CORRELATION BETWEEN LTE <sub>8</sub> AND RD <sub>75</sub> .....	172
FIGURE 6.39:	CORRELATION BETWEEN D <sub>0</sub> AND RD <sub>75</sub> .....	173
FIGURE 6.40:	CORRELATION BETWEEN D <sub>0</sub> AND LTE <sub>8</sub> .....	173
FIGURE 6.41:	SIMPLIFIED PAVEMENT SURFACE AS COMBINATION OF DIFFERENT SINE WAVES.....	177
FIGURE 6.42:	MATERIAL BEARING AREA CURVE FOR PAVEMENT TEXTURE (LIU, 2015) .....	181
FIGURE 6.43:	EFFECT OF MICRO-TEXTURE AND MACRO-TEXTURE ON PAVEMENT-TIRE FRICTION AT DIFFERENT SLIDING SPEEDS (FLINTSCH, AL-QADI, DAVIS, & MCGHEE, 2002).....	182

FIGURE 6.44:	RECOVERED 3-D SURFACE TEXTURE HEIGHT MAP OF RIGHT WHEEL PATH ON PANEL #1 .....	184
FIGURE 6.45:	RECOVERED 3-D SURFACE TEXTURE HEIGHT MAP OF CENTRE OF PANEL #1 .....	185
FIGURE 6.46:	SIMULATED MEAN TEXTURE DEPTH RESULTS FOR ALL PANELS (RIGHT WHEEL PATH AND CENTRE) ..	187
FIGURE 6.47:	KURTOSIS OF MEASURED SURFACE TEXTURE FOR ALL PANELS (RIGHT WHEEL PATH AND CENTRE) ..	187
FIGURE 6.48:	SKEWNESS OF MEASURED SURFACE TEXTURE FOR ALL PANELS (RIGHT WHEEL PATH AND CENTRE) .	188
FIGURE 6.49:	CORE VOID VOLUME OF MEASURED SURFACE TEXTURE FOR ALL PANELS (RIGHT WHEEL PATH AND CENTRE) .....	189
FIGURE 6.50:	NORMALIZED POWER SPECTRA ENERGY FOR ALL PANELS (RIGHT WHEEL PATH AND CENTRE) .....	189
FIGURE 6.51:	THE IRI ROUGHNESS SCALE (FROM SAYERS <i>ET AL.</i> 1986).....	192
FIGURE 6.52:	SURPRO 4000 MEASURING SURFACE PROFILES ON PCIP TRIAL SITE.....	193
FIGURE 6.53:	A PARTIAL DISPLAY OF PROFILE DATA AS COLLECTED BY SURPRO 4000.....	194
FIGURE 6.54:	IRI VALUES ON 1 M INTERVALS FOR ONE DATA COLLECTION PASS (SURPRO).....	195
FIGURE 6.55:	AVERAGE IRI VALUES FOR EACH SECTION OF THE TRIAL SECTION.....	196
FIGURE 6.56:	IRI VALUES ON 10 M INTERVALS FOR ONE DATA COLLECTION PASS (ARAN) .....	199
FIGURE 6.57:	ADHESION AND HYSTERESIS, THE TWO PRINCIPLE COMPONENTS OF PAVEMENT-TIRE FRICTION (GLENNON & HILL, 2004).....	201
FIGURE 6.58:	PAVEMENT FRICTION VERSUS TIRE SLIP (HALL, SMITH, & TITUS-GLOVER, 2006) .....	202
FIGURE 6.59:	BRITISH PENDULUM SKID RESISTANCE TESTER (GONZALEZ, 2014) .....	204
FIGURE 6.60:	BRITISH PENDULUM RESULTS FOR TESTING AT ARMTEC FACILITY (SEPT. 7, 2016) .....	205
FIGURE 6.61:	BRITISH PENDULUM RESULTS FOR IN-SITU TESTING (SEPT. 6, 2017) .....	206
FIGURE 6.62:	T2GO TESTING ON AN URBAN CONCRETE STREET (Wafa, 2018) .....	207
FIGURE 6.63:	COEFFICIENT OF FRICTION (DRY) FOR PCIP TRIAL (SEPT. 6, 2017) .....	208
FIGURE 6.64:	AVERAGE COEFFICIENT OF FRICTION (DRY) PER PANEL FOR PCIP TRIAL (SEPT. 6, 2017) .....	210
FIGURE 6.65:	PREDICTED FRICTION NUMBERS FROM SURFACE TEXTURE MEASUREMENT .....	212
FIGURE 7.1:	TYPICAL AND OBSERVED CONSTRUCTION AND MAINTENANCE SCHEDULE FOR DEEP STRENGTH ASPHALT CEMENT PAVEMENT .....	220
FIGURE 7.2:	ASSUMED CONSTRUCTION AND MAINTENANCE SCHEDULE FOR PCIP REHABILITATION MODELLED ON JPCP .....	222
FIGURE 7.3:	TEMPORARY CLOSURE LAYOUT FOR M/O AND PCIP REHABILITATIONS (MINISTRY OF TRANSPORTATION OF ONTARIO, 2014) .....	227
FIGURE 7.4:	QUEUE DEVELOPMENT FOR PCIP CONSTRUCTION OPERATIONS .....	228
FIGURE 7.5:	PRESENT WORTH COSTS FOR PCIP AND M/O REHABILITATION TECHNIQUES .....	230
FIGURE 7.6:	SENSITIVITY ANALYSES FOR DISCOUNT RATE (UPPER LEFT), AVERAGE DAILY USER COST (UPPER RIGHT), COST PER PANEL (CENTRE LEFT), FREQUENCY OF M/O OPERATION (CENTRE RIGHT), AND PANEL PLACEMENT RATE (LOWER LEFT) .....	233
FIGURE 7.7:	SENSITIVITY ANALYSIS FACTORIAL COMBINATION RESULTS.....	235
FIGURE 7.8:	LIFE CYCLE COSTS OF PCIP AND M/O STRATEGIES AT “TIPPING POINT” .....	237

FIGURE 9.1:	CROSS-SECTION OF HMA CORNER PROTECTION DETAIL .....	252
FIGURE 9.2:	PLAN VIEW OF HMA CORNER PROTECTION DETAIL .....	252
FIGURE 9.3:	SIMPLIFIED LONGITUDINAL HMA STRESSES UNDER TIRE LOAD.....	255
FIGURE 9.4:	ASTM D5329 COHESION/ADHESION SAMPLE (VARAMINI, 2018).....	257
FIGURE 9.5:	PCIP TRIAL TRANSVERSE EDGE DESIGN DETAIL .....	258
FIGURE 9.6:	PROPOSED PCIP TRANSVERSE EDGE DETAIL .....	259
FIGURE 9.7:	PROPOSED PCIP LONGITUDINAL JOINT DETAIL .....	260
FIGURE 9.8:	PROPOSED DRAINAGE DETAIL FOR PCIP REHABILITATIONS .....	261
FIGURE 9.9:	PVC DRAINAGE DETAIL END DURING PANEL PLACEMENT (LEFT), FOLLOWING BLOCK REMOVAL (RIGHT) .....	262
FIGURE 9.10:	DIAMOND GRINDING HEAD FOR NEXT GENERATION CONCRETE SURFACE (ADAPTED FROM (SCOFIELD, 2017)) .....	263
FIGURE 9.11:	NEXT GENERATION CONCRETE SURFACE TEXTURE (ADAPTED FROM (SCOFIELD, 2017)) .....	264
FIGURE 9.12:	NGCS AND CONVENTIONAL DIAMOND GRINDING SURFACE PROFILES .....	265
FIGURE 9.13:	SELECTION TREE FOR PRECAST CONCRETE INLAY PANEL USE.....	267

## LIST OF TABLES

TABLE 2.1:	LOAD TRANSFER EFFICIENCY OF SELECTED PCP PROJECTS .....	18
TABLE 4.1:	COST/BENEFIT COMPARISON OF SUPPORT CONDITIONS .....	39
TABLE 4.2:	FATIGUE LIFE ANALYSIS.....	44
TABLE 4.3:	TRUCK TYPES, FACTORS, AND COMPOSITION FOR HIGHWAY 400 (ADAPTED FROM (APPLIED RESEARCH ASSOCIATES, 2012)) .....	46
TABLE 4.4:	TRAFFIC CALCULATION ASSUMPTIONS.....	46
TABLE 5.1:	CORING RESULTS.....	59
TABLE 5.2:	MEASURED CROSS SLOPES AT LEADING PANEL EDGE (%) .....	59
TABLE 5.3:	SUMMARY OF CONSTRUCTION ACTIVITIES .....	92
TABLE 5.4:	PAIRWISE COMPARISON MATRIX EXAMPLE.....	103
TABLE 5.5:	QUANTITATIVE VALUES OF EVALUATION CRITERIA.....	105
TABLE 5.6:	OVERALL SCORING OF SUPPORT CONDITIONS .....	105
TABLE 5.7:	CRITERIA WEIGHTING SENSITIVITY ANALYSIS .....	107
TABLE 6.1:	SENSOR SUMMARY .....	132
TABLE 6.2:	SUMMARY OF SUPPORT CONDITIONS STUDIED .....	159
TABLE 6.3:	SUMMARY OF LTE <sub>δ</sub> RESULTS FOR OCT. 6, 2016 (INITIAL CONSTRUCTION) AND .....	163
TABLE 6.4:	SUMMARY OF D <sub>0</sub> RESULTS FOR OCT. 6, 2016 (INITIAL CONSTRUCTION) AND SEPT. 19, 2017 (ONE YEAR OF SERVICE).....	166
TABLE 6.5:	ILLUSTRATION OF POTENTIAL ISSUES WITH LTE <sub>δ</sub> .....	167
TABLE 6.6:	SUMMARY OF RD75 RESULTS FOR OCT. 6, 2016 (INITIAL CONSTRUCTION) AND SEPT. 19, 2017 (ONE YEAR OF SERVICE).....	169
TABLE 6.7:	3-DIMENSIONAL PAVEMENT TEXTURE INDICES (LIU, 2015).....	180
TABLE 6.8:	AVERAGE RESULTS FOR PRE-INSTALLATION MEASUREMENTS.....	186
TABLE 6.9:	LEAST SIGNIFICANT DIFFERENCE ANALYSIS FOR IRI VALUES.....	197
TABLE 6.10:	PANEL ADJUSTMENT PRACTICES AND IRI VALUES.....	198
TABLE 6.11:	LEAST SIGNIFICANT DIFFERENCE ANALYSIS FOR COEFFICIENT OF FRICTION VALUES (T2Go) .....	209
TABLE 6.12:	FRICTION TEST RESULTS FOR RIGHT WHEEL PATH AND PANEL CENTRE.....	213
TABLE 7.1:	PANEL UNIT COST ESTIMATES FOR FULL-SCALE PCIP PROJECTS .....	223
TABLE 7.2:	UNIT COSTS USED FOR CALCULATION OF CONSTRUCTION COSTS .....	224
TABLE 7.3:	UNIT COSTS AND ESTIMATED SERVICE LIVES FOR MAINTENANCE/REHABILITATION ACTIVITIES....	225
TABLE 7.4:	INITIAL COST REDUCTION EFFECTS .....	238

## **LIST OF ABBREVIATIONS**

- PCIP** – Precast concrete inlay panel
- HMA** – Hot mix asphalt
- AS** – Asphalt-supported panels
- GraS** – Grade-supported panels
- GroS** – Grout-supported panels
- LSD** – Least significant difference, post hoc data analysis test
- PCC** – Portland cement concrete
- PCP** – Precast concrete pavement
- IRI** – International roughness index
- MTO** – Ministry of Transportation of Ontario
- PWC** – Present worth cost
- FWD** – Falling weight deflectometer
- LCCA** – Life Cycle Cost Analysis
- PWC** – Present Worth Cost

# CHAPTER 1: INTRODUCTION

## 1.1 Statement of the Problem

The Ministry of Transportation of Ontario (MTO) has responsibility for the maintenance of several high-volume roadways within the province. The most highly travelled of these roadways are generally located in and around the Greater Toronto Area (GTA), which is a metropolitan area with a population of more than six million people (Statistics Canada, 2015). For instance, portions of the King's Highway 401 in the GTA have average annual daily truck traffic levels higher than 26 000 trucks per day (Ministry of Transportation of Ontario, 2016).

Highways with traffic levels this high are affected in two major ways by the traffic. Firstly, the high traffic loading increases the rate of pavement degradation in the most heavily travelled lanes. Secondly, the user costs associated with delays on the highway increase greatly. These two effects have a considerable impact on the maintenance and rehabilitation strategies that can be effectively employed on these highways.

The MTO has identified that several of their high volume HMA highways are experiencing deep rutting failure due to the high levels of traffic. This failure has been seen most commonly in the rightmost lanes, which typically see the highest percentage of the overall truck traffic. In the past, the MTO has addressed this issue with shallow (1- or 2-lift) HMA cold-planing and replacement strategies, however these repairs were found to last only 3-4 years, in some cases, before requiring further rehabilitation.

Work zone road user costs are significant considerations for all construction activities on roadways. These user costs are defined as the additional costs incurred by motorists and the larger community as a result of construction activities. The costs can be used as a measure of the impacts that a given roadway construction activity has on people. These costs can be considered to be a combination of several components, not all of which are easily considered as a monetary value. Some of the components that can be monetized include costs associated with travel delay, vehicle operation, crashes, and emissions. Other components of the user cost, including noise, business impacts, and inconvenience to local residents, are more difficult to monetize but are just as

important when assessing the effects of a given construction activity (US Department of Transportation Federal Highway Administration, 2015).

In the case of construction activities on Ontario's high volume highways, night construction is often used in order to reduce the number of users that are directly affected by the activity. The user costs are minimized by performing construction activities when the traffic levels are at their lowest point of the day. The construction time window that is often prescribed by the MTO is between the hours of 10 pm and 6 am the following morning.

At the end of this construction window, the MTO typically specifies that all construction equipment and materials need to be removed from the roadway and shoulders to allow for the full reinstatement of unimpeded traffic the following morning.

Even given this method, construction activities can have a significant impact on traffic and not all user costs and worker safety issues can be avoided; minimizing the number of required construction activities for a given roadway is a high priority concern for the MTO.

The MTO is interested in studying a new method for rehabilitating the high volume highways in Ontario. They are interested in finding a method that has a longer service life than the current method of rehabilitation but that can still be installed during overnight construction windows without significantly affecting daytime traffic.

## **1.2 Research Hypothesis**

The main hypotheses for this research are as follows:

- The use of precast concrete inlay panels as a rehabilitation strategy can prolong the usable life of the repairs to high volume highways in the province of Ontario.
- The prolonged usable life of the rehabilitation strategy will reduce the frequency and magnitude of future construction operations on the highway, thereby reducing the associated user costs.
- The increase in life cycle length will reduce the life cycle cost of the new rehabilitation strategy that will make it a viable option for future lane repairs.
- The performance of precast concrete inlay panels in asphalt will depend on the panel support conditions, which may be adversely affected by the presence of moisture.

- The precast concrete inlay panel performance will also depend on the performance of joints which affect structural performance and moisture infiltration.

### **1.3 Objectives of the Research**

This research is focused on the production and evaluation of an innovative rehabilitation strategy for high volume highways. The strategy will apply to asphalt highways that are experiencing premature deep seated rutting failure due to high traffic loading. This has been identified by the MTO as a significant issue and the results of this research could affect the rehabilitation strategy for many high volume highways, including the 400 series highways.

The rehabilitation strategy will include precast concrete inlay panels (PCIP) within the asphalt pavement section to provide significant increases in stiffness and to distribute traffic loads across greater surface areas of the remaining asphalt and subgrade material.

The design of the strategy that is the focus of this research was developed in collaboration with several individuals and organizations. These include Rico Fung of the Cement Association of Canada, Stephen Lee of the Ontario Ministry of Transportation, Peter Smith of the Fort Miller Company, Tom Kazmierowski of Golder Associates Ltd., and Mark Snyder, Independent Consultant. The evaluation of the strategy will be focused on determining the feasibility of this rehabilitation strategy for a department of transportation. Feasibility is a broad term, but in the context of this problem it will involve durability, cost, and constructability, and the levels of each that MTO requires.

The main objectives of this research are:

- To develop a detailed construction plan for a trial application of this rehabilitation strategy, including detailed design drawings and construction specifications.
- To evaluate the rehabilitation strategy in terms of its cost, durability, and constructability, using a combination of field testing, inspection, and stakeholder surveys.
- To develop a set of specifications for use by departments of transportation in any future applications of this strategy.
- To analyze the life cycle cost of the rehabilitation strategy, including a comparison to the current industry-standard methods of repair and rehabilitation .

## **1.4 Methodology of Study**

The evaluation of this rehabilitation method has many components to gain a comprehensive understanding of its feasibility for regular use by the MTO. The evaluation plan includes six broad components, which are evaluated with regard to each support condition being investigated as well as the overall rehabilitation method, as described below.

### **1.4.1 Construction Monitoring/ Discussions with Contractor**

During the construction of the test sections, members of the Centre for Pavement and Transportation Technology (CPATT) conducted on-site monitoring and recording of each night's activities. This included timing individual construction processes and noting any issues that arose throughout the course of the process.

This is a new strategy and there is an expected learning curve, so consideration was given to the types of difficulties associated with any new construction practice. Night-to-night improvements in repeated construction practices were considered to assess each practice's constructability.

On-going discussions were held with the installation contractor, Dufferin Construction, to help determine which activities posed the most difficulties or concerns. A wrap-up meeting was scheduled following the completion of the project to give the contractor an opportunity to summarize any concerns and suggestions for future implementation that were identified and documented.

### **1.4.2 Instrumentation**

During the installation of the precast panels, several pieces of sensing technology were installed. This technology included both earth pressure cells and moisture probes.

The earth pressure cells were installed at the interface between the panels and the HMA to allow for the collection of information relating to the pressure being imparted by the precast panels into the underlying HMA. This information provides insight into the effectiveness of this rehabilitation strategy in extending the pavement life. Each earth pressure cell has a built-in temperature sensor; in combination with surface temperatures, this measurement provided information regarding the temperature gradients being experienced by the precast panels under both day and night conditions.

Moisture probes were also placed at the panel/HMA interface. Any moisture that permeates this interface could have an adverse effect on the durability of the repair method when it is exposed to freeze-thaw cycles throughout the course of a Canadian winter. The moisture probes were used to monitor for the presence of moisture.

### 1.4.3 Falling Weight Deflectometer Testing

The Falling Weight Deflectometer (FWD) is a pavement testing tool that imparts a deflection in the pavement using a mass falling from a prescribed height and then measures the deflections at set distances from the point of impact using sensors. When considering rigid pavements, FWDs can be used to assess the load transfer across joints and cracks and also to detect voids beneath the pavement.

FWD testing was performed on the test section after the completion of construction and after one year of service. In both cases, the testing was performed using the testing configuration shown in Figure 1.1, which was taken from the Falling Weight Deflectometer Testing Guideline produced by the MTO (Chan & Lane, 2005).

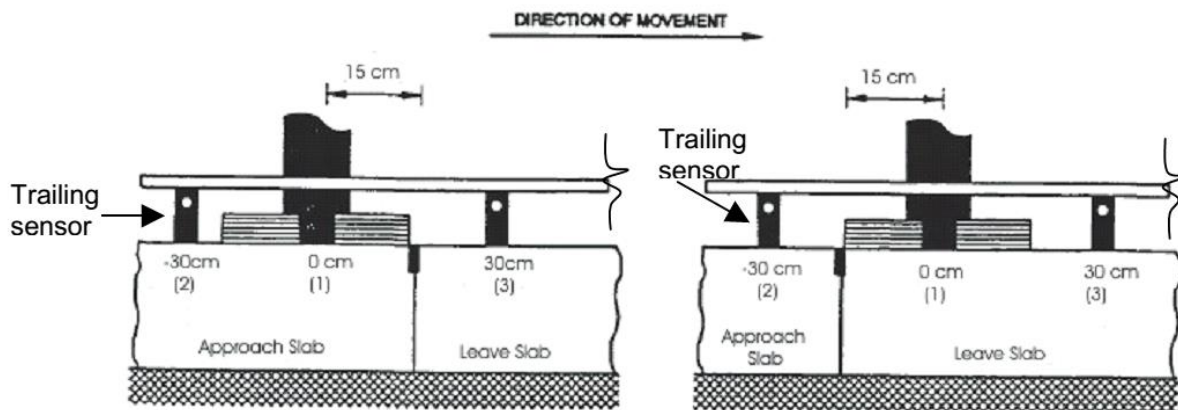


**Figure 1.1: Typical Sensor Configuration for FWD Load Transfer Test (Approach and Leave Panel) (Chan & Lane, 2005)**

As shown in Figure 1.1, two sensors are located at an equal distance ahead of and behind the excitation source. A test is performed spanning the joint with each sensor, and the signal loss across the joint is compared to the signal loss measured at the sensor on the same panel as the excitation for each test. These values are then used to calculate the efficiency of load transfer across the joint.

Load transfer efficiency (LTE) above 70% is considered adequate by the MTO, depending on the severity of the joint condition. Below this threshold value, a full depth repair is generally recommended. LTE considers the ratio of the two deflections, but does not consider the deflection differential between the panels. This can result in low LTE values at small total joint deflections in joints that are performing well. Conversely, the LTE value of a poorly supported joint can be acceptable even with significant total deflection (Snyder, 2011). The LTE provides a component for assessing joint performance, but the deflection differential will also be considered. This should provide a better indication of overall joint performance.

Testing was performed at all joints within the extents of the project, according to the testing procedure specified by the MTO. All dowelled joints between adjacent panels as well as the transverse joints between asphalt and the precast panels at the two ends of the test section were tested. The results of the initial FWD test provide a baseline for future load transfer testing undertaken throughout the test section's life cycle. Remedial action will be considered on any joints found to not meet the 70% threshold for load transfer efficiency

If degradation of the panel support is suspected due to freeze thaw cycling, FWD testing will be used to determine if any loss of support can be detected. This testing will also be performed in accordance with the MTO's Falling Weight Deflectometer Testing Guideline (Chan & Lane, 2005).

#### **1.4.4 Pavement Surface Testing**

The interaction between a pavement's surface and the vehicles that use the pavement are an important consideration in the performance of said pavement. The components of this interaction most commonly considered include friction, roughness, and noise. Each of these components can be partially dependent on the surface texture of the pavement.

The surface of the panels was evaluated for these characteristics in order to evaluate how the PCIP trial was performing. Due to the limited access to the site, this testing was performed on one occasion following one year of service.

### **1.4.5 Visual Inspection**

Visual inspections were carried out initially and after one year of service. Specific attention was paid to joint condition and panel cracking as these are the most common surface defects associated with precast pavements. Furthermore, the condition of the HMA-to-precast and precast-to-HMA joints at each end of the test section was monitored to assess the performance of this joint type.

Visual inspections were performed on a panel-by-panel basis, which was feasible due to the relatively small scale of the project. This provides insight into the effects of the different panel support conditions.

### **1.4.6 Life Cycle Cost**

The cost of a given rehabilitation is a very significant consideration in its feasibility. This cost should include life cycle considerations in addition to the costs associated with initial construction.

A Life Cycle Cost Analysis was undertaken to provide insight into the feasibility of PCIPs. This was performed using the MTO guidelines outlined in their MERO-018 document as a guideline (Lane & Kazmierowski, 2005). The analysis considered the costs associated with the trial section, for which there are no probabilistic information due to the strategy's novelty. Therefore a deterministic analysis was undertaken that incorporated sensitivity analyses to gauge the effects of changes in the inputs. Since the construction window restraints drove the design of the PCIP, the effects of user costs were also considered as part of the analysis.

## **1.5 Thesis Organization**

The thesis is divided into ten chapters. Chapter One provides an introduction to the research study. Chapter Two outlines the literature review undertaken to frame the research in the current state of the practice. Chapter Three outlines the methodology that was followed for the research. Chapter Four discusses the design of the Precast Concrete Inlay Panels (PCIP) and the trial section used to analyze them. Chapter Five describes the construction of the trial section and the analysis that was subsequently undertaken to compare the different support methods included within the trial. Chapter Six outlines the performance of the trial section with respect to data gathered from visual inspections, instrumentation, joint analyses, and surface analyses. Chapter Seven includes an analysis of the PCIP rehabilitation technique in terms of life cycle cost in comparison to existing rehabilitation techniques. Chapter Eight summarizes the conclusions drawn throughout the study

and recommendations for future applications of the PCIP technology. Chapter Nine outlines specific improvements that are recommended for implementation of future PCIP installations. Chapter Ten presents a set of general specifications for the use of PCIP technology that incorporate the findings of this research study.

## **CHAPTER 2: LITERATURE REVIEW**

This chapter summarizes the current state-of-the-practice relevant to the use of precast concrete panel inlays and the proposed methodology of this study.

### **2.1 Current Practices**

The impetus behind this study was the observed premature rutting failure of high volume asphalt highways in Ontario. These failures have generally been observed in the outside traffic lanes (Lane #3) and are assumed to be caused by high levels of truck traffic. The observed rutting failure has been classified as a deep-seated failure, which implies that rutting is observed throughout the depth of the pavement's asphalt and granular layers due to an issue located deep within the pavement structure.

Typically, this type of pavement failure is addressed with a pavement rehabilitation as opposed to pavement repairs or maintenance. A rehabilitation strategy includes significant changes or material replacements within the pavement to return the level of serviceability to a like new condition (Transportation Association of Canada (TAC), 2013). Generally, a rehabilitation strategy is employed when repair and maintenance of a given pavement is no longer cost effective.

High volume highways have several characteristics that make the choice of rehabilitation strategy more complex. Generally, long closures of the highway are not acceptable to the owner. In the case of the MTO, they have specified that most construction operations on the 400 series highways must occur during overnight periods in order to minimize the disruption to traffic. This overnight period is generally between the hours of 10 pm and 5 am or 6 am. The stipulation with this specification is that traffic must be fully reinstated each morning. This specification limits the number of conventional rehabilitation strategies that are feasible for rehabilitating a high volume highway.

The use of Portland cement concrete (PCC) overlays is a pavement rehabilitation technique that includes the placement of cast-in-place concrete over a deteriorated pavement. Generally, this improves the structural capacity of the highway and requires very few repairs prior to the PCC

placement (Harrington & Fick, 2014). Concrete overlays are typically categorized as either bonded or unbonded.

As the name suggests, bonded overlays involve PCC bonded to the underlying asphalt causing both pavements to act as one integral section. This integral action generally distributes stresses from traffic loading as shown in Figure 2.1, such that the concrete generally only is subjected to compression forces. This results in a thinner required depth of concrete (typically about 50-150mm). Bonded overlays can only be used on pavements that are in fair to good condition, and cracks within the existing asphalt pavement must be aligned with joints in the concrete to ensure acceptable composite action.

Unbonded PCC overlays are a rehabilitation option that restore structural capacity to pavements that are in significantly deteriorated to fair condition. This rehabilitation option does not depend on the structural capacity of the underlying layer, so much as it is designed by treating the existing pavement as a stable base material. Due to the non-integral action, the stress distribution within the pavement section is as shown in Figure 2.1, with compression and tension components in both layers.

While concrete overlays may address the premature rutting issue observed on the 400 series highways, both overlay types would require a construction period longer than 7 hours in order to re-open to full traffic. This is because cast-in-place PCC requires significant curing time for the material to gain sufficient strength to support traffic loads. This curing time is generally greater than 24 hours. Fast-track PCC is a material that gains strength much more quickly than conventional PCC. It is generally achieved by using mixture designs with high cement contents and low water-to-cement ratios. This can increase material shrinkage during curing and makes the timing of pavement saw-cutting critical to control shrinkage stresses. The material has been found to require careful control and early-age monitoring. Improper mixture proportioning, placement, curing, or saw-cutting can result in uncontrolled cracking that can affect the pavement's durability. Anecdotally, the MTO has had durability issues with the use of fast track PCC.

Furthermore, if rutting is only observed in Lane #3 of the highway, this rehabilitation technique would be required on all lanes to avoid elevation differential between lanes.

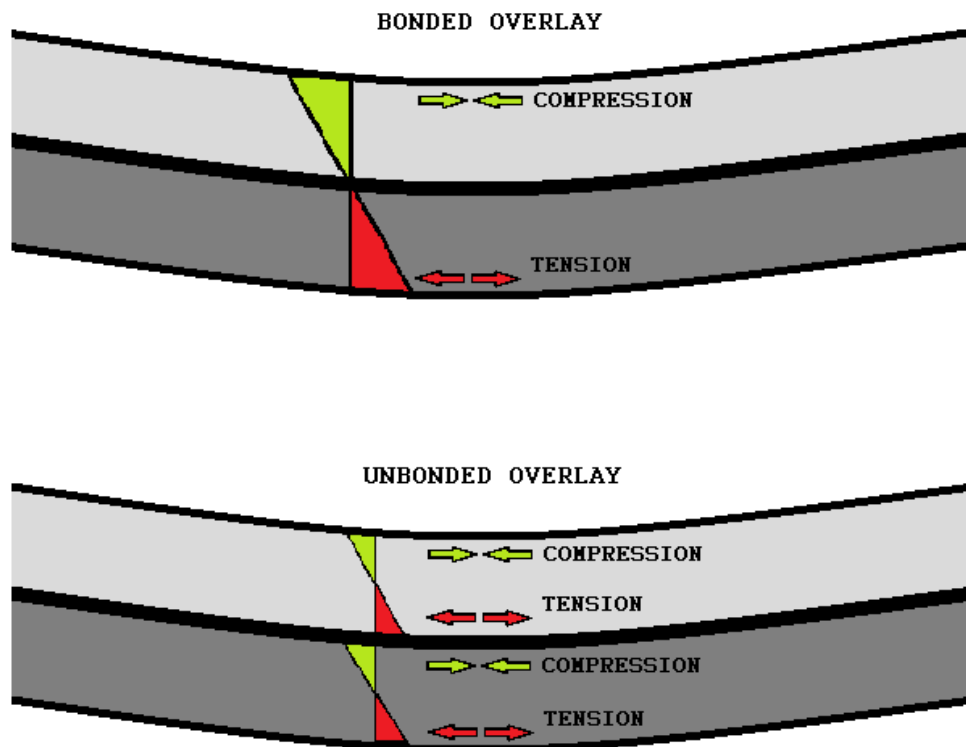


**Figure 2.1: Bonded and unbonded concrete overlay stress distributions**

Figure 2.2 shows the placement of an asphalt separation layer on an unbonded overlay project in the Region of Waterloo. The figure shows the relative elevation difference between the lanes with and without the concrete overlay.

Another rehabilitation strategy that could potentially be employed is milling and structural resurfacing of the rutted lanes. In this strategy, asphalt milling machines are used to remove the rutted pavement to a specified depth, and this is then replaced with new asphalt, typically placed in two lifts (Transportation Association of Canada (TAC), 2013).

Generally this strategy is designed to remove the full depth of the failed pavement in order to replace it with new material. This ensures that there are no issues with the underlying material that would compromise the performance of the surface material.



**Figure 2.2: Placement of asphalt separation layer for unbonded overlay of composite pavement**

In this case, the deep-seated failure that has been observed may extend into the subgrade of the pavement. The asphalt layers of the pavement are at least 300 mm thick in most locations of the highway. Considering the restrictive construction windows and the thick pavement structure, the requirement to expose and improve the subgrade material prior to placing several lifts of hot mix asphalt make this strategy complex.

Previously, this method has been employed to address the rutting failure observed. The depth of the asphalt milling was less than full depth, usually 40 mm or 80 mm of a 300+ mm thick pavement. This indicates that the observed rutting is a function of subgrade or base/subbase layer rutting or potentially asphalt material issues, as rutting is observed 3-7 years after placement.

As discussed previously, the asphalt that is placed is designed specifically for high volume roadways. This is done through grade bumps in the performance graded asphalt cement that produce stiffer asphalt concretes. The increased stiffness theoretically improves the rutting resistance of the concrete. This may indicate that the rutting is related to issues in the subgrade or base/subbase.

## **2.2 Precast Concrete Panels**

Since the failure of the pavement appears to be due to issues with the subgrade or base/subbase material, the MTO is interested in the study of a concrete pavement, which through beam action, would distribute traffic loads over a greater area, and thereby reduce the stresses on the subgrade

materials. However, the previously mentioned construction issues make this difficult. The use of fast-track concrete mixes that gain strength quickly is considered to be problematic by the MTO. Temperamental mixes combined with long term durability concerns make this material less desirable as a pavement option (Lane & Kazmierowski, 2011).

The MTO has experience with the use of precast concrete panels. In 2004 they began a study on the performance of precast concrete panels used as a repair strategy for concrete pavement structures. In this study, panels produced using the Michigan, Fort Miller Intermittent, and Fort Miller Continuous Methods were installed and monitored. All panels were found to perform well with the only issues being related to workmanship. When the panels were being installed using the Michigan method that requires that dowel slots be cut in the adjacent pavement, the contractor often over cut these slots. This eventually led to joint deterioration in the panels installed using this method. The ride quality of the precast panels was noted to be comparable to that of fast track concrete sections that had been constructed in other portions of the same highway (Lane & Kazmierowski, 2011).

Currently, precast concrete pavement (PCP) panels are generally used as a repair technique for conventional concrete pavements. The Pavement Asset Design and Management Guide developed by the Transportation Association of Canada, notes the use of precast concrete by the MTO and the Ministère des Transport du Québec for this purpose, and also the potential for PCP to be used as a continuous concrete pavement. Furthermore, the use of PCP as a means to upgrade asphalt intersections that have experienced rutting (Transportation Association of Canada (TAC), 2013). One such instance of this technique was the upgrade of Rockaway Boulevard that runs alongside the John F. Kennedy Airport in New York City. The approaches to several intersections were upgraded with PCP during nighttime closures, due to rutting and shoving caused by transport trucks entering the airport. The traffic was maintained during the daytime periods as any disruption would have had a significant impact on the shipping activities at the airport (Smith, 2014).

Figure 2.3 shows the interface between the PCP and the asphalt within the intersection on the east side of JFK Airport.



**Figure 2.3: Rockaway Blvd. intersection at JFK Airport**

The main reason for the use of PCPs is that they provide the ability to repair high volume roadways with minimal disruption to daytime traffic, as seen in the Rockaway Blvd case. Other benefits of PCP include stricter controls over material quality and curing practices as both are controlled at the precasting plant, fewer weather restrictions on placement as curing temperatures are not an issue, and elimination of construction related failures such as late or shallow concrete joint cuts (Tayabji, Ye, & Buch, 2012).

PCPs are also being investigated as a means of repairing airfield pavements. In this case, the driving force behind their use is also short construction windows, which can often be as short as 4-6 hours. This type of pavement undergoes significant loading, but has been found to perform comparably to typical cast-in-place concrete pavements in controlled test sections (Priddy, Bly, Jackson, & Flintsch, 2014).

There are several different general types of PCP repairs, as shown in Figure 2.4. They include intermittent repairs, which are used when individual panels deteriorate, joint repairs, which replace a failed joint, short length continuous, in which several panels are placed adjacent to one another

to repair deterioration that extended beyond the length of one panel, and continuous repair, in which an entire section of concrete pavement is replaced with PCP. In each PCP type, the width of the panels is the width of one traffic lane, and the length is either determined by the length of deterioration being repaired or by the maximum length that can be transported to site. In order to rehabilitate a rutted lane, a continuous placement of precast concrete panels will be necessary.

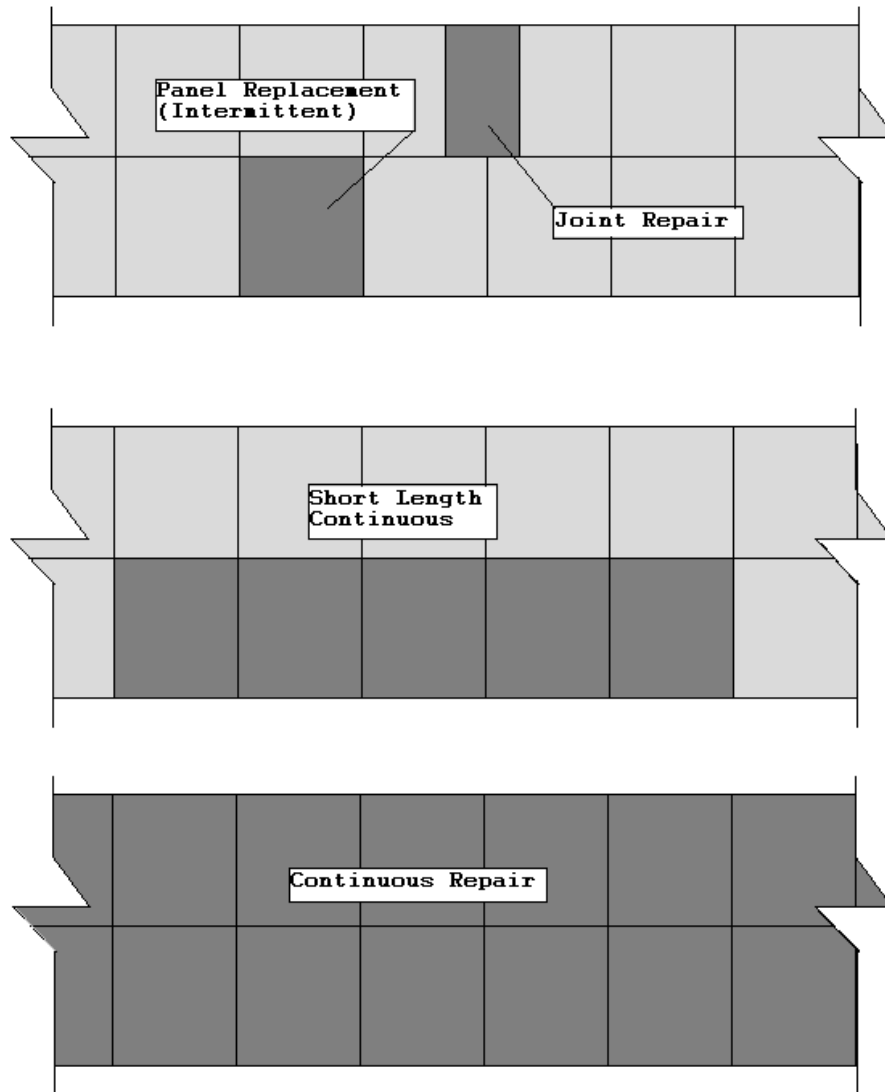


**Figure 2.4: Precast concrete panel repair types (adapted from (Tayabji, Ye, & Buch, 2012))**

While precast concrete has been used as a pavement material for over 40 years in different capacities, very little effort was made to document the performance of these early applications. Recently, the Strategic Highway Research Program 2 (SHRP2) carried out a concerted effort to monitor and collect relevant data from various PCP projects throughout the United States.

This effort included, but was not limited to the collection of the following data types:

1. Condition Data
2. Ride (smoothness)
3. Joint Elevation Difference
4. Joint Width Measurement
5. FWD Deflection testing for load transfer efficiency and the presence of voids

Several lessons were learned as part of the SHRP2 study regarding the construction of projects, but the importance of assessing the existing base and preparing the panel support were two of the most important (Tayabji, Ye, & Buch, 2012). The improper placement and compaction of base material has contributed to issues noted within the SHRP2 study. Intermittent repairs were performed in 2007 and 2008 on the I-295 highway in New Jersey using Fort Miller's Super Slabs. When damaged concrete was removed, it was noted that the sandy granular base beneath was disturbed. Panel settlement was observed to occur and this was attributed to the improper re-compaction of the base material. Panel cracking, assumed to be due to insufficient base compaction, was also noted at a Virginia I-66 onramp, California I-15, and a project in Reno (Tayabji, Ye, & Buch, 2012).

Another issue that has been found to reduce the durability of PCP repairs is over saw-cutting the existing concrete. This is a construction error that results in deterioration of the concrete surrounding the PCP at the time of installation. The results of this error is generally accelerated joint deterioration and the progression of cracks into the existing concrete that had not been present previously. This issue was noted on the Highway 427 repairs in Ontario (Lane & Kazmierowski, 2011) as well as during the field testing of airport pavements (Priddy, Bly, Jackson, & Flintsch, 2014).

Load transfer efficiency (LTE) is a measure of PCP performance and provides an indicator of the performance of the joints between adjacent panels. Joint deterioration is considered to be a concern of PCPs secondary only to support conditions.

LTE is measured through falling weight deflectometer (FWD) testing. FWD testing involves dropping a weight of known mass from a known height in order to impart an impact load of known force onto the surface of a pavement. Using sensors placed at set intervals from the location of the impact, the deflections of the pavements are measured.

LTE testing places the sensors on either side of a joint or crack at equal distances from the impact load. The deflections at these points indicate how well the impact load is being transferred across the joint or crack. Equation 1 is generally used to calculate LTE (Ashtiani, Jackson, Saeed, & Hammons, 2010).

$$LTE(\%) = \frac{\delta_U}{\delta_L} \times 100\% \quad (1)$$

Where  $\delta_U$  represents the deflection measured on the unloaded panel and  $\delta_L$  represents the deflection measured on the loaded panel.

The MTO generally uses 70% LTE as a minimum allowable load transfer value for concrete pavements (Chan & Lane, 2005). Beyond this value, repair of the joint or crack is generally recommended.

As part of the SHRP2 study, the LTE of several PCP projects were tested. The results of these tests as well as an accelerated airfield pavement test are summarized in Table 2.1. The average of all results was above the 70% LTE threshold. The average taken is typically across ten or more panels within the project and some individual LTE values would be below the 70% level. Furthermore, >70% LTE was observed in several joints that were physically deteriorated, specifically in the accelerated airfield pavement test. In this case, sufficient LTE did not necessarily reflect an acceptable joint.

According to the mechanistic MEPDG published by the National Cooperative Highway Research Program, the LTE of a given interface can be broken down into 3 components: 1) aggregate interlock and joint stiffness, 2) load transfer through dowels, and 3) load transfer through the supporting materials. It is estimated that the supporting materials can provide between 20% and 40% of the total load transfer, depending on the behaviour of the material. Asphalt treated bases are assumed to provide about 30% of the load transfer (Applied Research Associates: ERES Division, 2003). Support by approximately 100mm of asphalt pavement structure could presumably provide greater support, as in the case of the proposed research.

**Table 2.1: Load Transfer Efficiency of Selected PCP Projects**

<b>Project</b>	<b>Type</b>	<b>Installed</b>	<b>Tested</b>	<b>Average LTE</b>
I-295, New Jersey	Intermittent Super Slab	2007-2008	2010	80%
I-280, New Jersey	Continuous Super Slab	2008-2009	2010	82%
Route 27, New York State	Intermittent Roman Stone	2009	2010	70%
I-675 Michigan	Intermittent, Michigan Method	2003	2010	80%
Tappan Zee Toll Plaza, New York	Continuous Super Slab	2001-2002	2010	90%
TH62, Minnesota	Continuous Super Slab	2005	2010	90%
I-66 Ramp, Virginia	Continuous Super Slab	2009	2009	90%
I-15, California*	Continuous Super Slab	2010	2010	90%
NJ-130, New Jersey**	Continuous Super Slab	2010	2010	83%
Aircraft Pavement Field Study	Intermittent Michigan Method	Accelerated Testing (10,000 C-17 passes)		>70%

\*included both support grouted and non-support grouted

\*\*included both steel and FRP dowel bars

PCPs are typically installed in situations where installation time is restricted. As such, there is generally little time devoted to excavation and removal of subgrade material for the installation of pressure cells, followed by replacement and compaction. Furthermore, this would result in a disturbed base, which has been cited as a potential cause of premature PCP failure in field trials.

Earth pressure cells have been used to instrument PCP installations in the past, but generally only in experimental, non-service applications. Typically, these instruments are installed in the subgrade material beneath the panels to measure the vertical stress imparted by traffic or testing loads onto the subgrade (Priddy, Bly, Jackson, & Flintsch, 2014; Khanal, Tighe, & Bowers, 2013).

Efforts have been made to install sensors at the interface between precast panels and the supporting material, with some success. This operation requires careful installation practices to avoid damage to the sensors during the panel placement. The layout of these sensors determine the conclusions that can be drawn. In an evaluation of a new PCP joint design, placement of the pressure cells beneath adjacent panels provided insight into the load transfer across joints as well as the mechanism by which the adjacent panels deflected (Gaspard, 2008).

### **2.3 Life Cycle Cost Analyses**

Life cycle costing is defined by the International Organization for Standardization as being “economic assessment considering all agreed projected significant and relevant cost flows over a period of analysis expressed in monetary value. The projected costs are those needed to achieve defined levels of performance, including reliability, safety and availability.” (International Organization for Standardization, 2008). The importance of this assessment tool for use in public procurement is being more widely realized as the push for sustainability in practice gains acceptance (Perera, Morton, & Perfrement, 2009).

In many cases, the initial costs of sustainable assets are higher than their less-sustainable counterparts, however these costs can be largely offset by efficiency gains and cost savings throughout the course of the asset’s lifespan. Considering this lifespan through life cycle costing helps public entities to justify procurement of sustainable assets despite the higher initial costs (Perera, Morton, & Perfrement, 2009).

Life cycle costing will be considered as part of this research as a means by which to determine whether the proposed rehabilitation technique is feasible. The justification of the use of precast concrete is its lifespan that is assumed to far exceed that of mill and replace HMA rehabilitations. In this way, it can be considered as a more sustainable rehabilitation option. While a potential decrease in user costs is a major consideration, the overall feasibility of the rehabilitation strategy will largely depend on whether it costs the owner and therefore the public less money over its lifespan.

In 2005, the MTO developed guidelines for the use of life cycle cost analysis (LCCA) on freeway projects (Lane & Kazmierowski, 2005). Generally, the guidelines are used to establish net present worth values for different design alternatives based on discount rates, analysis periods, service life

and activity timing (repairs and rehabilitations), construction, repair, and rehabilitation costs, and salvage value. Net present worth is calculated using Equation 2 (Tighe, 2001).

$$Net\ Present\ Worth = \sum \frac{Costs}{(1 + i)^n} \quad (2)$$

where

*Costs* = initial construction, maintenance, rehabilitation costs or salvage value

*i* = the discount rate

*n* = year in which cost occurs

These guidelines are often used as a means to facilitate alternative bidding for freeway contracts. Contractors are invited to submit bids for asphalt or concrete pavement construction and their bid is adjusted using an adjustment factor that has been calculated based on an LCCA of each pavement type.

The MTO requires that all LCCAs for high volume roads (ESAL > 1 million per year) and 400 series highways be performed according to their guidelines (Lane & Kazmierowski, 2005).

Generally, a probabilistic LCCA is required for high volume roads. This LCCA type incorporates the means and standard deviations for all observed data in order to provide insight into the uncertainty and associated variability in construction practices, and therefore their present worth value. Probabilistic LCCA can also be used to gauge the sensitivity of a present worth value to changes in a given variable.

MERO-018 provides recommended values for Probabilistic LCCA, however these values are outdated. Furthermore, the costs associated with precast panels are not included for reference. Finally, the guide recommends normal distribution of variables, but some research has found lognormal distributions to be better representations of construction variables (Tighe, 2001).

## **2.4 User Costs**

Work zone road user costs are a significant consideration for all construction activities on roadways. These user costs are defined as the additional costs incurred by motorists and the larger community as a result of construction activities. The costs can be used as a metric to measure the

impacts that a given construction activity on a roadway has on people. These costs can be considered a combination of several components, not all of which are easily considered as a monetary value. Some of the components that can be monetized include costs associated with travel delay, vehicle operation, crashes, and emissions. Other components of the user cost, including noise, business impacts, and inconvenience to local residents, are more difficult to monetize but are just as important when assessing the effects of a given construction activity (US Department of Transportation Federal Highway Administration, 2015).

In the case of construction activities on Ontario's high volume highways, night construction is often used in order to reduce the number of users that are directly affected by the activity. By performing construction activities when the traffic levels are at their lowest point of the day, the user costs are minimized. Reducing the amount of nearby traffic by scheduling work at night has the added benefit of improving worker safety. The construction time window that is often prescribed by the MTO is between the hours of 11 pm and 6 am the following morning.

MicroBENCOST is an evaluation software that was developed in the 1990's in order to quantify the effects of construction on traffic. While there are many inputs required to make calculations of this type, the governing input is the number of vehicles that are attempting to use the roadway at a given time. MicroBENCOST uses tables that separate the average annual daily traffic into hourly amounts distributed throughout the day. These tables are dependent on site-specific factors, however there is a default table for an urban interstate type highway that can be used in the absence of site-specific data as a reasonable estimate. According to this default table, 7.3% of the average annual daily traffic will be seen during the period between 11pm and 6am, or an average of approximately 1% AADT/hour. For reference, the lowest hourly value outside of this period is 2.3% AADT between 10pm and 11pm while the highest hourly value is 8.5% AADT between 5pm and 6pm (Walls III & Smith, 1998).

At the end of the 11pm-6am construction window, the MTO typically specifies that all construction equipment and materials need to be removed from the roadway and shoulders to allow for the full reinstatement of unimpeded traffic the following morning. This is an effort to incur no user delay costs during the busiest traffic hours.

Even given this method, construction activities can have an impact on traffic and all user costs and worker safety issues cannot be avoided; minimizing the amount of required construction activities for a given roadway is a high priority concern for the MTO.

User delay costs have been used in LCCAs, however they are not included as part of the LCCA Guidelines specified by the MTO (Lane & Kazmierowski, 2005).

## **2.5 Least Significant Difference Test**

Throughout this research, groups of data are often compared to one another to determine whether they can be confidently considered distinct. This is due to the nature of the research wherein three different Precast Concrete Inlay Panel (PCIP) designs are considered. When data are collected across these three distinct groups for comparison purposes, it is important to determine if any of the three groups is performing significantly differently than the others.

The Least Significant Difference (LSD) test is a method by which to compare three sets of data in this way. The original LSD test was developed by Fisher in 1935 (Williams & Abdi, 2010). It is a post hoc analysis that is undertaken following an analysis of variance (ANOVA) test. Typically the LSD is a protected method meaning that the ANOVA test should indicate that there is a significant difference between means, prior to undertaking the LSD analysis. A Dunn/Sidák modification is used in this research to account for family-wise errors that can occur with multiple comparison analyses. These errors are Type I, indicating the null hypothesis is false, when it is actually true.

In order to undertake an LSD test, an ANOVA test is first undertaken on the multiple data sets (typically three data sets in this research). The results of this test indicate whether there is a significant difference within the group of data sets. When the F-value is larger than the F-critical value, the null hypothesis that all of the means are statistically similar can be rejected at the chosen confidence level. An ANOVA analysis indicates that there is a difference between the means, but not the pairs between which the difference is significant. The LSD provides insight into that question.

The first step of an LSD is an analysis of variance. For this research, the ANOVA test was performed using Excel software. The ANOVA is performed at a 95% confidence level ( $\alpha=0.05$ )

and provides insight into whether or not there is a significantly distinct group in those being tested. If so, the LSD can be undertaken.

The LSD is the product of the standard error and  $t_{\text{critical}}$  values associated with the data. The standard error is calculated according to Equation 3.

$$SE = \sqrt{\frac{2MS}{n^*}} \quad (3)$$

where: SE = Standard error  
 MS = Mean square (sum of squares divided by degrees of freedom)  
 n\* = Average number of samples per group

The  $t_{\text{critical}}$  value is based on tabulated data for two-tail t-statistics, which depends on the alpha value and degrees of freedom in the comparison. The degrees of freedom depend on the number of data points and groups in the comparison. The alpha value is found using the Dunn/Sidák modification, as shown in Equation 4.

$$\alpha_{\text{mod}} = 1 - (1 - \alpha_{\text{overall}})^{\frac{1}{k}} \quad (4)$$

where:  $\alpha_{\text{mod}}$  = Modified alpha value  
 $\alpha_{\text{overall}}$  = Original alpha value (typically 0.05)  
 k = Number of groups being compared (typically 3)

The LSD is then calculated using these values according to Equation 5.

$$LSD = t_{\alpha_{\text{mod}}} \times SE \quad (5)$$

where: LSD = Least significant difference  
 $t_{\alpha}$  = t-value based on  $\alpha_{\text{mod}}$   
 $\alpha_{\text{mod}}$  = Modified alpha value  
 SE = Standard error

The LSD is then compared to the differences between the means of the groups being compared. If the difference is larger than LSD, then the two groups can be considered statistically distinct at 95% confidence.

Appendix A shows a sample calculation for the determination of LSD.

## **2.6 Chapter Summary**

The main points discussed in this chapter include:

- Practices of rehabilitating hot mix asphalt (HMA) pavements using Portland cement concrete (PCC), which generally includes concrete overlays using cast-in-place PCC. This practice requires significant time as cast-in-place PCC requires curing time after placement to achieve enough strength to support traffic loads. Fast track PCC, which reduces the required curing time has durability concerns associated with its use.
- Current rehabilitation practices for MTO 400-series highways exhibiting premature rutting involve milling and structural resurfacing. This generally is done to a depth of 40 mm or 80 mm and does not address the deep-seated cause of the rutting. Accessing and repairing the deep-seated issue requires more time than the current MTO closure windows allow.
- Precast concrete pavement (PCP) is produced using relatively small panels that can be transported to and placed on site. The PCP panels are produced in controlled factory conditions and placed on site following the early age curing. PCP is most commonly used to repair existing PCC pavements intermittently or in short or long continuous repairs. A large-scale evaluation of PCP technology was completed by SHRP2 in the United States and this indicated that the support conditions provided beneath the PCP have been found to have the most impact of all factors on their performance.
- Load transfer efficiency (LTE) is a method of evaluating concrete pavement joints based on relative deflections of opposite sides of a joint under loading. A 70% LTE criterion is generally used by the MTO to indicate an acceptable joint. PCP sections studied in the SHRP2 report have been found to maintain acceptable LTE.
- The life cycle cost (LCC) of a pavement is a way of analyzing its cost over the course of its service life, by including costs of maintenance activities and user costs over the course of its service life, in addition to the initial construction costs. The MTO has an LCC

methodology for analyzing pavements (MERO-018) that will be used for this study, as the study was performed to support the MTO decision-making process.

- The Least Significant Difference (LSD) test is the method of statistical analysis used throughout this study. The method is well-suited to analyzing the statistical significance of differences between the means of three groups. Since three support conditions are to be considered as part of this study, the method is well suited.

The primary gaps in the existing knowledge of PCP rehabilitations relate to their use on HMA sections. Specifically, the questions that need to be answered include:

- What alterations to typical PCP designs are required for installation within a milled HMA section?
- Can the precast concrete inlay panel (PCIP) sections be constructed in short over night construction windows?
- Which method of providing panel support is most consistently constructible?
- Which method of panel support is most appealing to a specifying agency, considering a range of criteria relevant to said agency?
- How well can a trial installation of PCIP perform under service conditions, in terms of visual distresses, sub-panel moisture and load distributions, joint performance, and panel surface performance? Which support condition performs best considering each of these considerations?
- Can a PCIP rehabilitation be considered feasible in terms of life cycle cost, when compared to current rehabilitation practices?

The research that is outlined in this thesis addresses these gaps in order to evaluate to overall feasibility of PCIP as a rehabilitation technique for high-volume HMA highways.

## **CHAPTER 3: RESEARCH METHODOLOGY**

To address the gaps in the existing knowledge laid out in Chapter 2.6 an overall research methodology was developed. This methodology, which is laid out in Figure 3.1, is composed of five broad phases: Initial Planning, Detailed Design, Construction, Monitoring, and Synthesis.

Initial planning consisted of identifying the problem and proposing the general solution to the problem. This stage was completed in close conversation with members of the MTO who had firsthand knowledge of the problem and comprehensive experience with precast concrete pavements (PCP) as a repair strategy. Additionally, this stage included the literature review of typical practices using PCP.

The second phase was detailed design. Since this research study was based primarily on a precast concrete inlay panel (PCIP) trial section, this phase considers the design of this section. Based on the literature review, the key concerns for the design were identified, which included PCIP durability, support conditions, and constructability. Each of these concerns were co-related but represented a focus during design. This phase was completed with the design team described in Chapter 1.3. Many of the features were developed based on the experience-based knowledge of the design team. Following the general design, a thickness design check was also performed. This phase is generally included in Chapter 4 of this thesis.

Following the design phase, the trial section was constructed, and this process represents the third phase of the methodology. Dufferin Construction was the contractor hired by the MTO to complete the construction of the trial section. Prior to construction, several meetings were held with the contractor and sub-contractors to develop a construction plan, which was completed in September 2016. Instrumentation was installed beneath select panels during the construction phase. Cost tracking was performed during construction; however, this proprietary information was not made available to the researchers. Unit costs were supplied, and the cost estimates were evaluated by the contractor following construction. This phase is generally included within Chapter 5 of this thesis.

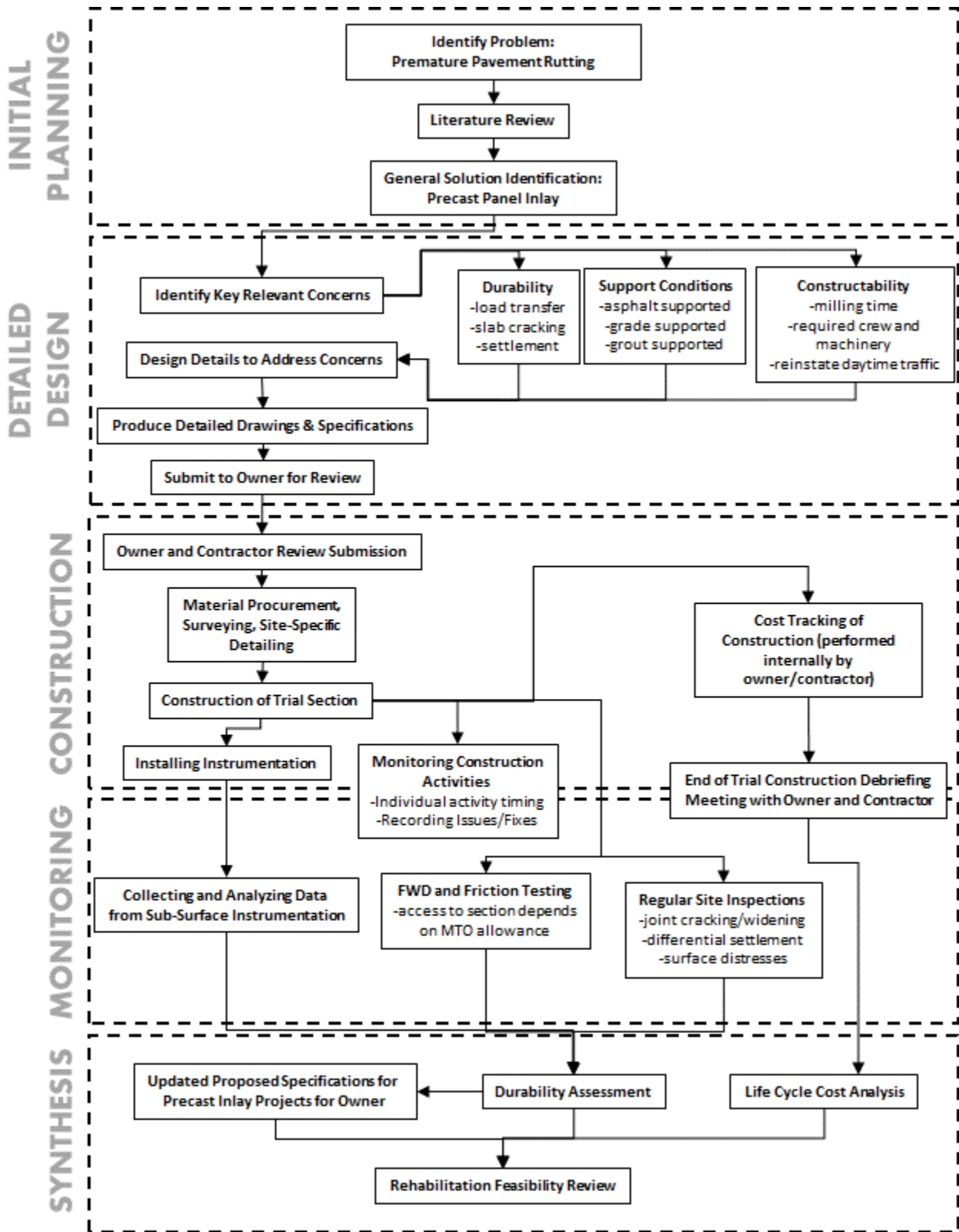


Figure 3.1: Research methodology for studying Precast Concrete Inlay Panels

The monitoring phase included the collection of relevant data from various sources. These sources include on-site monitoring during the construction process, surveys of contractors and MTO personnel, moisture probes and pressure cells beneath the PCIP, climatic data from local weather stations, traffic information from published MTO sources, Falling Weight Deflectometer joint testing, in-service friction and roughness testing, and on-site testing during closures (friction, texture, roughness, visual survey). Further information was collected from MTO personnel relating to costing and maintenance data relating to life cycle cost analysis.

Each of the aspects of the monitoring phase fed directly into analysis that made up the final phase of the methodology, synthesis. This phase involved taking the information gathered from the PCIP trial section and using it to meet the objectives listed in Chapter 1.3 and to answer the questions outlined previously in Chapter 2.6.

The monitoring and synthesis phases generally correspond to Chapters 6 and 7 of this thesis.

## **CHAPTER 4:**

### **PRECAST CONCRETE INLAY PANEL TRIAL DESIGN<sup>1</sup>**

This chapter outlines the design developed for the MTO trial section in order to investigate whether using precast panels to rehabilitate existing HMA pavement is a feasible option for the MTO. This includes descriptions of the panel designs, support conditions designs, construction plan, and testing plan.

#### **4.1 General Rehabilitation Strategy**

A mill-and-replace strategy with precast concrete pavement (PCP) was decided upon to rehabilitate HMA sections. The goal of the strategy was to provide a rehabilitation method for high-volume highways, with a particular focus on the 400-series highways in Ontario. The typical pavement structure of these highways includes a thick HMA component up to and including the riding surface. These HMA layers are often 300 mm thick, or more.

The conventional method of using PCP for repair or rehabilitation includes fully removing the existing pavement surface material, usually Portland cement concrete (PCC), and replacing it with a PCP of approximately equal thickness. Fully replacing the HMA pavement layer thickness in a 400-series highway with PCP would have several drawbacks, such as:

- It would require substantial milling, including multiple passes, to remove material that is mostly sound beneath the surface rutting.
- Equivalent thickness of PCP would be considerably larger than necessary based on typical concrete design theory.
- The edges of the extents of HMA removal would provide a path of ingress for water beneath the HMA pavements.

---

<sup>1</sup> The contents of this chapter have been incorporated within a paper that has been published as part of a conference proceedings. D. Pickel, S. Tighe, R. Fung, S. Lee, P. Smith, T. Kazmierowski, and M. Snyder “*Using Precast Concrete Inlay Panels for Rut Repair on High Volume Flexible Pavements*” Published for the 11<sup>th</sup> International Conference on Concrete Pavements. Date August 28 – September 1, 2016

- Following the removal of HMA, the underlying granular pavement layers would require repair and recompaction that could be substantial, especially where deep-seated rutting issues are observed.
- The HMA beneath the surface course in sound condition could provide a stable base for the PCP, which is a primary design consideration for PCC pavements.

Considering these factors, the general concept for the PCP repair was developed to include milling the HMA in the lane to a partial depth, then placing PCPs within the milled-out recess. Milling the HMA only to a depth that would accommodate the required thickness of PCP would address all of the issues listed above. Based on the plan to place the PCP within the HMA, the overall rehabilitation strategy is referred to as Precast Concrete Inlay Panels (PCIP). The PCIPs are designed to be supported by the remaining HMA and the surfaces of the PCIP will provide the riding surface of the roadway.

Following the definition of the general rehabilitation plan, the broad steps required to undertake the rehabilitation were formulated. These steps are illustrated in Figure 4.1.

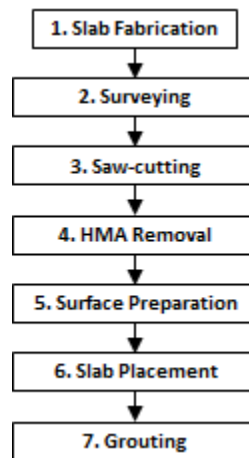


**Figure 4.1: Steps required for PCIP rehabilitation**

Each step had unique requirements that were considered in the development of the detailed rehabilitation strategy. The plan to implement the PCIP rehabilitation method consists of the following general steps:

## 1. **Panel Fabrication**

- a. Fabrication of the precast panels must take place at least two weeks prior to the beginning of construction, in order to provide sufficient time for concrete curing and construction time tolerances.
- b. Fabrication depends on the delivery of the concrete mixture design and approved fabrication drawings to the precast producers from the contractor.
- c. The production capacity of the fabricator must be considered during the timing of the construction operation. Based on current capacity, the fabricator could cast approximately 2 PCIPs per day.

## 2. **Surveying**

- a. The lane to be rehabilitated must be surveyed completely prior to the beginning of construction, to provide the elevation details necessary to ensure that asphalt removal is performed to the correct depth and that the proper pavement cross-slope is maintained.
- b. In addition to measuring existing pavement elevations, the survey must lay out the location of each panel end and each required saw-cut. These locations must be marked using durable methods that do not interfere with traffic, such as nails driven flush with the pavement surface.

## 3. **Saw-cutting**

- a. The night before the precast panels are installed, precise saw-cuts will be made in the asphalt delineating the area of asphalt that is to be removed via milling on the following night.
- b. The saw-cuts will be based on the survey data and must be precise in order that no large gaps remain after asphalt is removed and precast panels are placed. The depth of the saw-cut will correspond to the specified HMA removal depth. For instance, the total overall depth of the asphalt pavement may be 300 mm  $\pm$ , but the depth of removal and therefore the saw-cut will be approximately 215 mm  $\pm$ .
- c. To avoid saw-cut meandering that can be associated with deep cuts, the saw-cuts should be done progressively.

#### **4. HMA Removal**

- a. The HMA within the sawcut-delineated area will be removed via milling to the specified depth.
- b. This portion of the construction process is expected to require a significant proportion of the available time during each night of construction.
- c. Milled HMA will be trucked off-site as it is removed.
- d. At each end of the nightly milling extents, a radiused portion will be left by the cylindrical milling head. This portion must be removed in order to provide a vertical face against which the precast panels can be placed.

#### **5. Surface Preparation**

- a. Following HMA removal, the surface of the remaining asphalt will be prepared for precast panel placement. The first step in this preparation will be the removal of detritus left by the asphalt milling equipment, using power brooms.
- b. Once the asphalt surface is free of debris, the support material for the precast panels can be placed. The support conditions will vary throughout the project but cement-treated bedding material will be used where graded support material is required.

#### **6. Panel Placement**

- a. Following fabrication and curing, the PCIPs are transported to site via flat-bed truck and are brought to site as needed due to the limited space available on a highway construction job.
- b. The PCIPs are picked from the truck and lowered into place using the four lifting inserts installed in each and a crane or other suitable lifting device. Care must be taken to ensure that all dowels and dowel slots align during placement and that the maximum spacing limits between panels are observed.

#### **7. Grouting**

- a. Grout will be placed in order to fill any voids around or beneath the precast panels. Four distinct types of grout are required, based on different requirements:
  - i. Bedding Grout: thin, non-structural grout, pumped beneath panels that are supported by surfaces within a  $\pm 3$  mm tolerance, via cast-in grout ports. Used to fill small voids and provide uniform support.

- ii. Rapid-Setting Bedding Grout: thin, non-structural bedding grout as described above that reaches a compressive strength of 5 MPa in one hour or less. This grout is used to support panels that incorporate levelling bolts and have larger gaps between the panel and the underlying asphalt.
  - iii. Dowel Grout: a non-shrink, non-expansive structural grout that is pumped into dowel slots to engage dowels in load transfer between panels. The dowel grout will have a minimum design compressive strength of 30 MPa and must attain a strength of 20 MPa before it is deemed acceptable to carry traffic loads.
  - iv. Edge Grout: dowel grout that is extended 60% by weight with 9.5 mm pea gravel. This grout is used to fill gaps between the precast panels and the vertical cut faces of the adjacent asphalt pavement.
- b. Dowel and edge grout must be installed prior to bedding grout. This ensures that these more structural grouts fill their intended locations and are not displaced by the weaker bedding grout.

## **4.2 Panel Support Conditions**

The support provided to a precast concrete panel is one of the most important factors in determining how well that panel will perform (Smith & Snyder, 2017; Tayabji, Ye, & Buch, 2012). Non-uniform support can lead to premature cracking, loss of load transfer, and ultimately premature panel failure. The process of preparing the proper panel support has also been identified as a construction activity where potential time savings can be made.

For these reasons, the precast panel support conditions are a primary focus of this research study. Three different panel support conditions are designed and investigated with seven or eight panels of each support conditions type constructed as part of the trial. This study is designed to assess the feasibility of PCIP rehabilitation of HMA highways so each support condition will be evaluated based on its constructability and performance. The three support conditions to be evaluated are outlined in the following sections.

### **4.2.1 Grade-supported (GraS)**

The grade-supported (GraS) condition involves the placement of graded and compacted cement-treated bedding material (CTBM) between the PCIP and the milled HMA surface. The CTBM is

placed on the supporting HMA surface and levelled using a screed, such as the one pictured in Figure 4.2. The screed is positioned based on the elevation and cross slope information determined as part of the pre-construction surveying. After levelling, the material is compacted using plate tampers to a desired density, and this process is repeated until the required surface elevation of the compacted CTBM is met. The final surface of the CTBM must be within a  $\pm 3$  mm tolerance prior to placing the panels and thoroughly dampened with sprayed water.



**Figure 4.2: Large screed levelling base material**

Once panels are placed on the CTBM, they can support traffic loads and can be opened to traffic, however dowel, edge, and bedding grout must be installed (in that order) during the next construction shift (typically the following night). Dowel and bedding grout are pumped through the panel through ports in the panel's surface. Adjacent port holes are observed during pumping until grout is observed to come out, which indicates that the dowel chambers or the voids beneath the panel are filled with grout. Figure 4.3 shows a cross-section of a grade-supported panel as installed. Pavement cross-slopes shown in the figure were assumed based on typical values of MTO highways, but will be adjusted to meet the requirements of the existing cross slopes

encountered on site. As shown, a space of approximately 75 mm is left on either side of the panels in order to facilitate placement within the asphalt.

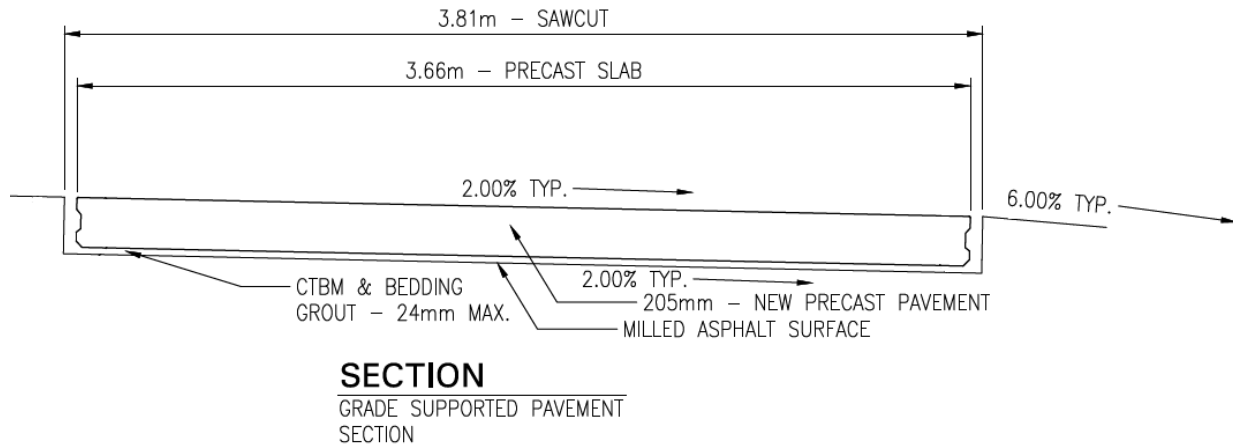


**Figure 4.3: Cross-section of GraS panel (The Fort Miller Company Inc., 2015)**

Flowable bedding grout is pumped from the surface of the panel into any voids between the panel and the bedding material. This provides the uniform support that is required for precast panels. Dowel grout is a non-shrink, non-expansive structural grout that is pumped into slots around dowels in order to provide load transfer between adjacent panels.

Dowel and bedding grout are pumped through different ports from the panel surface. Separate port holes that are connected to the same sub-surface void are observed until grout is observed issuing from them, which indicates that the voids beneath the panel are filled with grout. In the case of bedding grout, panel-bottom channels run between grout ports to facilitate the flow of the grout between ports and to all areas beneath the panel. An example of this detail is shown in Figure 4.4.

Edge grout is produced by extending dowel grout 60% by weight using 9.5 mm pea gravel. It is placed between the vertical edge of the panel and the existing asphalt to fill the gap and provide a uniform driving surface.

Foam gaskets are placed beneath the panel and form barriers between the dowel slots, edges, and the sub-panel voids. These gaskets prevent the grout types from blending that could reduce the effectiveness of the structural grouts. An example of this detail is shown in Figure 4.4.

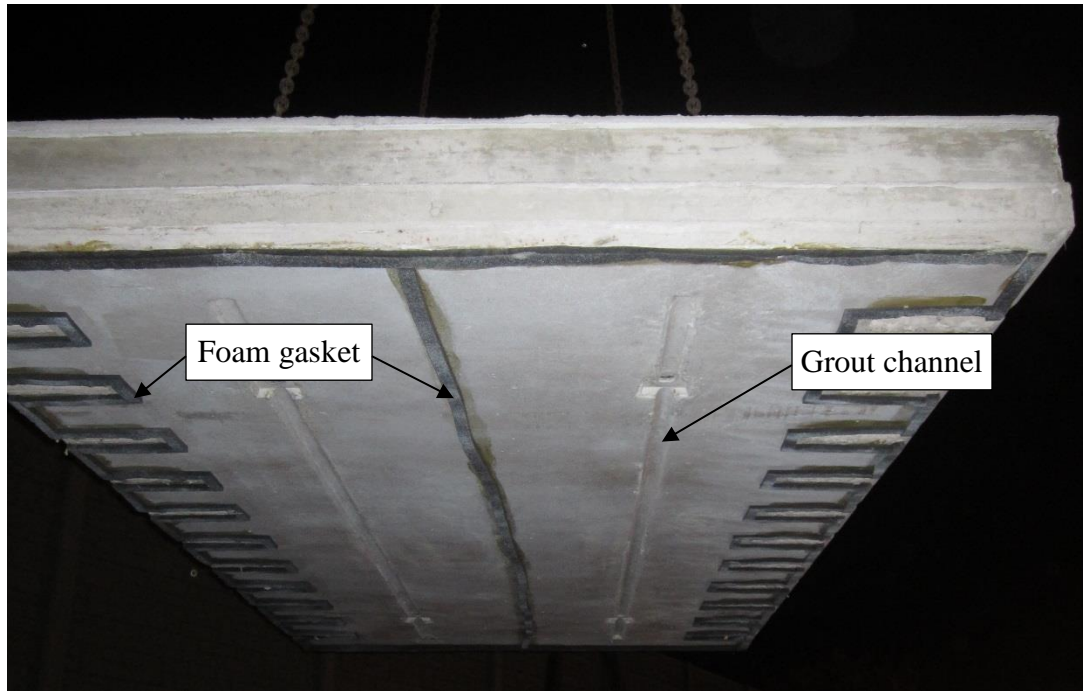


**Figure 4.4: Typical sub-panel details**

This support condition most closely resembles the typical method used with Fort Miller Super Slabs on MTO highway projects. The method has shown good results in full depth panel repair projects in the past.

#### **4.2.2 Asphalt-supported (AS)**

The second support condition to be evaluated is asphalt-supported (AS). This condition involves placement of PCC panels directly onto the milled asphalt surface that has been micro milled to within the same  $\pm 3$  mm surface tolerance specified for the GraS condition. If this tolerance can be achieved, then panels can support traffic as soon as they are placed and grouting can take place on the following night, similar to grade-supported panels. The feasibility of achieving the required surface tolerances with micro milling will be considered as part of this project.

Micro milling is similar to conventional pavement milling, but uses more bits spaced more closely together on the milling drum. This drum layout results in smaller amplitudes between the ridges and valleys of the milled asphalt surface, on the order of 3-4 mm (Pavement Interactive, 2011). This value would fall into the  $\pm 3$  mm surface tolerance that is required of a precast panel support surface. In order to achieve this tolerance, slower progress and shallower milling depths may be required. Both of these factors are relevant for the project's restrictive construction windows.

It is presumed that this method will provide benefits in terms of time in relation to the other two methods because a CTBM layer is not required and the panel can support traffic immediately after placement. However, the extra time required for asphalt micro milling to precise tolerances will be monitored to determine the overall time benefit.

### 4.2.3 Grout-supported (GroS)

The third support condition is grout-supported (GroS). Grout-supported panels are fabricated with integrally cast levelling lifts and are placed directly on the asphalt surface following the milling and cleaning operations. The levelling lifts are then deployed until the surface of the panel has the correct elevation and cross-slope characteristics.

Figure 4.5 illustrates a levelling lift as it is deployed under a precast panel. The detachable base plate is pushed out of the bottom of the panel with the threaded bar until the surface of the panel is in the desired location. Rapid setting bedding grout is then pumped beneath the panel to provide full support. Once the grout attains sufficient strength, the threaded bars are removed and the grout bears the weight of the panel.

Typically a grout strength of 3.4 MPa is required prior to allowing vehicles to travel on the surface of the panel (Tayabji, Ye, & Buch, 2012).

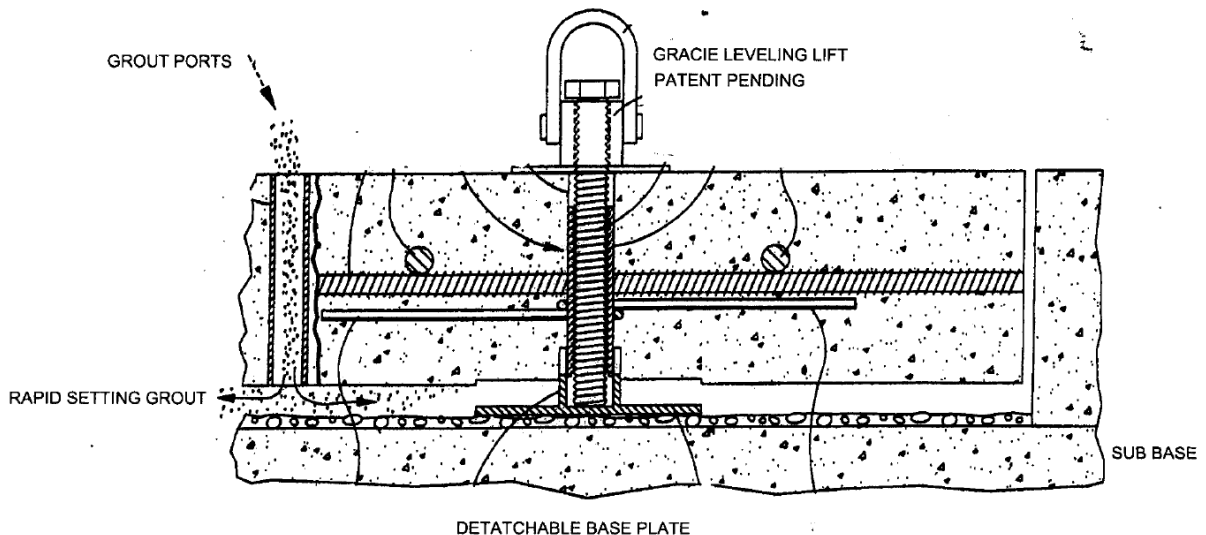


Figure 4.5: Gracie Leveling Lift™

Unlike the previously discussed support conditions, GroS panels cannot support traffic prior to the placement of grout. The non-uniform support of the milled asphalt or the deployed levelling bolts would result in stress concentrations under vehicle loading that would cause premature cracking. Therefore dowel, edge, and rapid setting bedding grout must be installed the same night as the panel is placed. While this has implications for the nightly construction schedule and additional costs associated with bedding grout, it is also presumed that time will be saved relative to grade-supported panels by not requiring the placement and compaction of bedding material.

There is no base material required for this support condition so the depth of asphalt milling can be slightly reduced in relation to the grade-supported panels.

#### **4.2.4 Summary of Support Options**

Each option provides potential relative costs and benefits. The magnitude of the effects of each were monitored throughout the project's construction to determine the best option for this new pavement rehabilitation strategy and are discussed in Section 5.5.

Based on the development of the proposed support conditions, Table 4.1 summarizes the costs and benefits of each support condition that are expected.

### **4.3 Precast Panel Design**

The design of the panels to be used in the project was multifaceted. The broad design details were developed by the Fort Miller Company, whose patented Super Slab was selected for the trial. Specific details of the design were selected to suit MTO pavement requirements or the requirements of the PCIP design problem. The various aspects of the panel design are presented here.

#### **4.3.1 PCIP Materials**

The concrete used to produce the precast panels was specified to meet a minimum compressive strength of 30 MPa at an age of 28 days and have a minimum of 3% entrained air with a maximum spacing factor of 0.230mm. These specifications were selected to suit the Ontario Provincial Standard Specifications (OPSS) for Construction of Concrete Pavement (Ontario Provincial Standards (OPS), 1998). The concrete material and aggregate were specified to adhere to

OPSS.PROV 1350 and OPSS.PROV 1002 (Ontario Provincial Standards (OPS), 2016; Ontario Provincial Standards (OPS), 2013).

**Table 4.1: Cost/Benefit Comparison of Support Conditions**

<b>Support Condition</b>	<b>Benefits</b>	<b>Costs</b>
<b>Grade-supported</b>	<ul style="list-style-type: none"> <li>· Contractor familiarity with method</li> <li>· Pavement can open as soon as panel is placed</li> <li>· High smoothness of asphalt surface not a requirement</li> </ul>	<ul style="list-style-type: none"> <li>· Time/Effort required to place CTBM</li> <li>· Requires extra material (CTBM, water) and machines (laser level, compaction equipment) be brought on site</li> </ul>
<b>Asphalt-supported</b>	<ul style="list-style-type: none"> <li>· No extra support material required (CTBM, rapid setting grout)</li> <li>· Pavement can open as soon as panel is placed</li> </ul>	<ul style="list-style-type: none"> <li>· Unknown time requirement for precision milling</li> <li>· Two milling machines may be necessary</li> <li>· Requires pre-construction proof of concept</li> <li>· Asphalt surface must be entirely clear of any debris &gt;3mm in nominal diameter</li> </ul>
<b>Grout-supported</b>	<ul style="list-style-type: none"> <li>· Panels can be easily adjusted to suit grade/cross-slope requirements</li> <li>· Intensive surface preparation is not required prior to panel placement</li> <li>· High smoothness of asphalt surface not a requirement</li> </ul>	<ul style="list-style-type: none"> <li>· Time is required for rapid setting grout to achieve sufficient strength to support vehicles</li> <li>· Cost of levelling lift is approximately 3-4 times higher than standard lifting insert</li> <li>· Cost of rapid setting grout is expected to be high</li> </ul>

These specifications provide a general baseline for materials, however the requirements of precast concrete fabrication generally govern the selection and design of materials. In order to facilitate timely production, the fabricator generally plans to strip the panels from their forms within one day after pouring. The typical target compressive strength of the concrete prior to stripping is 15 MPa to 21 MPa, so that the panels are not damaged during stripping and subsequent lifting off of the casting bed (Tayabji, Ye, & Buch, 2012). To achieve these early strengths, the fabricator was expected to use a high-early strength cement, which will have compressive strength beyond the specified value.

### **4.3.2 PCIP Thickness Design**

The typical panel design includes a 205 mm thickness, reinforced with two mats of reinforcement steel spaced at 300 mm centres. This thickness was used for the development of the PCIP design in the absence of site-related traffic information. When the design was submitted to the MTO, a site was chosen and the appropriateness of this design was checked using Pavement ME and other softwares.

The current ME software available does not consider this type of pavement. Pavement ME, considering a pavement with no reinforcement, and unbonded condition, estimated a 7-year service life, which would be unacceptable to the MTO. Based on the reinforcement, base conditions, and overall pavement structure, this intuitively seems like a very conservative estimate, which indicates that the software is underestimating the design.

Warehouse floor design software with two layers of reinforcement was used to justify the design (35-year service life). The reinforcement in these floors is often welded-wire mesh that is used to avoid shrinkage cracking, and still may not fully consider the reinforcement benefits of the reinforcing steel in the panels.

Designs considered that the panels were unbonded to the asphalt, but the true nature of the bond is currently unknown. Panels are constructed in forms with form oil applied to ease stripping. Residual oil is expected on the panels, though the amount is not known. Presumably, some amount of residual oil after form stripping will disperse during storage in the precasters' yard. Fort Miller has assessed reusable panels in a Brooklyn project, and when the panels are pulled up the grout under the panel is difficult to remove. This anecdotally indicates that the form oil is not present on the bottom of the panel or does not largely inhibit the bond between the grout and the panel.

The appropriateness of the 205 mm design thickness was checked using fatigue design principles. "Fatigue is the degradation of a material's strength caused by a cyclically applied tensile load that is usually below the yield strength of the material. Fatigue is a concern because a material designed to withstand an allowable safe load one time may fail when the same load is applied cyclically one time too many. The cyclically applied load causes a crack to initiate and propagate from the area of highest stress concentrations. The material finally fails when the crack grows to a sufficient

length so that applied load causes a stress that exceeds the material's ultimate strength" (Titus-Glover, Mallela, Darter, Voigt, & Waalkes, 2005).

While the substantial reinforcement of a precast panel should arrest the propagation of fatigue cracks, the fatigue behaviour of the material under loads is still an important consideration in the behaviour of the pavement.

Fatigue design for concrete pavements is based on the stress ratio (SR), which is the ratio between the stress imparted by loading and the flexural strength of the concrete. The ration is shown in Equation 6.

$$SR = \frac{\sigma}{MOR} \quad (6)$$

where:      SR      = Stress ratio (unitless)  
                  $\sigma$       = Stress induced in pavement by loading (MPa)  
                 MOR    = Flexural strength, or Modulus of Rupture of concrete (MPa)

The SR is defined by both material properties (MOR) and traffic/environmental properties ( $\sigma$ ), which are both project specific. The closer that SR is to unity, the fewer repetitions are required to reach the fatigue life. When the induced stress equals or exceeds the flexural strength, the pavement will fail under a single load. For the purposes of the preliminary fatigue calculation, the approximation of each value was made based on a set of assumptions defined later. When the design SR is determined, the number of repetitions of that condition that can occur before fatigue failure, can be determined. A fatigue model was developed for the American Concrete Pavement Association design software, StreetPave. The model, shown in Equation 7, was developed based on accumulated data from various sources, and finds the expected number of repetitions to failure based on the SR and design probability.

$$\log N_f = \left[ \frac{-SR^{-10.24} \log(1 - P)}{0.0112} \right]^{0.217} \quad (7)$$

where:  $N_f$  = Number of repetitions to failure  
 $SR$  = Stress ratio (unitless)  
 $P$  = Probability of premature failure  
 $(1 - P)$  = Probability of survival

To determine the  $SR$ , the design stress under loading must be calculated for the panel in service. Delatte (2014) suggests that unless pavement corners are heavily loaded or unsupported, the stress associated with edge loading should be considered in design. For the case of the PCIP design, the corner support should be consistent and dependable as it is provided by milled HMA. Edge loading is the case wherein panel is loaded on its edge, which results in tensile stress in the middle of the bottom of the panel. The conditions can result in mid-panel cracking. The stress related to edge loading can be calculated according to Equation 8, developed by Ioannides et al. (1985). The equation is based on the assumption that a given load is applied at the edge of a panel and the footprint of the load is circular in shape.

$$\sigma_e = \frac{-6P(1 + 0.5\nu)}{h^2} \left[ 0.489 \log \left( \frac{a}{l} \right) - 0.012 - 0.063 \left( \frac{a}{l} \right) \right] \quad (8)$$

where:  $\sigma_e$  = Stress at edge (kPa)  
 $P$  = Applied load (kN)  
 $\nu$  = Poisson's ratio for concrete (0.15 assumed)  
 $h$  = Panel thickness (m)  
 $a$  = Radius of circular tire-pavement interface (m)  
 $l$  = Radius of relative stiffness (m)

The radius of relative stiffness is a measure of the stiffness of a concrete panel in relation to the foundation it rests on. It is calculated using Equation 9.

$$l = \sqrt[4]{\frac{Eh^3}{12(1-\nu^2)k}} \quad (9)$$

where:  $l$  = Radius of relative stiffness (m)  
 $E$  = Modulus of elasticity of the concrete (MPa)  
 $h$  = Panel thickness (m)  
 $\nu$  = Poisson's ratio for concrete (0.15 assumed)  
 $k$  = Modulus of subgrade reaction (MPa/m)

The modulus of elasticity of the concrete can be reasonably estimated using Equation 10 (American Concrete Institute, 2005).

$$E = 4.73(f'_c)^{0.5} \quad (10)$$

where:  $E$  = Modulus of elasticity of the concrete (GPa)  
 $f'_c$  = Concrete compressive strength (MPa)

The relationship between compressive strength and flexural strength of concrete was analyzed by Ahmed et al. (2014), who found that the 2/3 power model shown in Equation 11 to be a good estimate.

$$MOR = 0.45(f'_c)^{\frac{2}{3}} \quad (11)$$

where:  $MOR$  = Modulus of rupture of the concrete (MPa)  
 $f'_c$  = Concrete compressive strength (MPa)

Delatte (2014) suggests that a k-value of 145 MPa/m can be assumed for concrete overlays of asphalt to account for the high stiffness of the support material. Using these values and relationships, and the assumptions summarized in Table 4.2, the fatigue life of the panels was estimated.

**Table 4.2: Fatigue Life Analysis**

v	0.15						
a	0.15 m						
k	145 MPa/m						
P	40 kN						
h	205 mm						

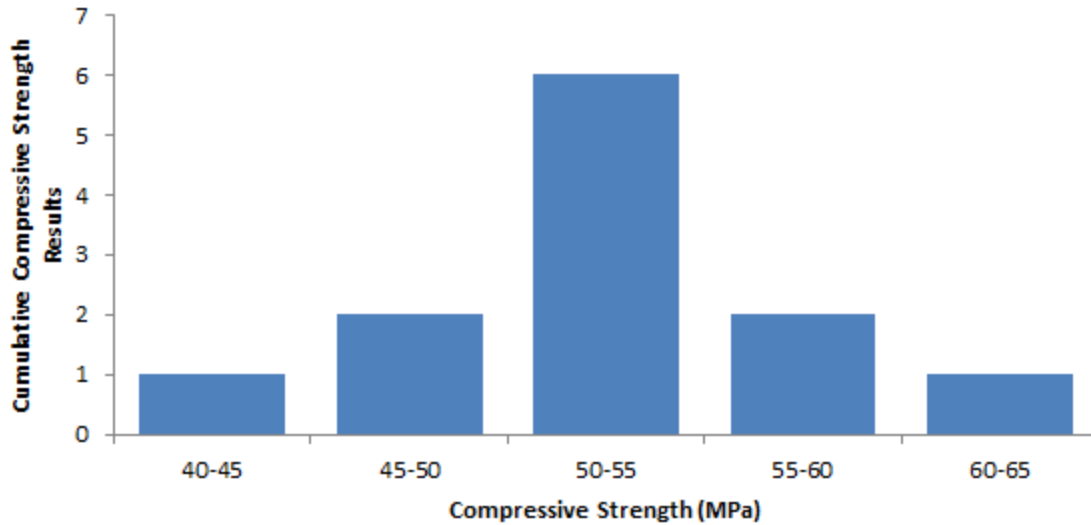
  

Probability of Failure	f'c (MPa)	E (GPa)	MOR (MPa)	l (m)	$\sigma_e$ (MPa)	SR	$N_f$
0.01	30	25.9	4.34	0.602	1.98	0.456	4.62E+04
0.01	40	29.9	5.26	0.624	2.03	0.385	6.41E+06
0.01	45	31.7	5.69	0.633	2.04	0.359	8.88E+07
0.01	50	33.4	6.11	0.642	2.06	0.337	1.35E+09
0.01	60.9	36.9	6.97	0.658	2.09	0.300	6.98E+11

The table assumes a loading condition of one 40 kN load applied directly on the edge of the concrete panel. This corresponds to the standard single axle considered in the development of Equivalent Standard Axle Loads (ESAL) in pavement design, which is an 80 kN single axle (40kN per tire).

According to the analysis, if the strength of the pavement were actually constructed to have a 30 MPa 28 day strength, the panel would be expected to crack due to fatigue after approximately 46,200 edge loads of a 40 kN tire. As the strength of the concrete increases however, the expected fatigue life increases.

The actual concrete strength results were found 28 days after casting, and these results are summarized in Figure 4.6. The strength results represent average values based on all tests done on a single concrete batch. A concrete batch would typically produce enough concrete for two panels.



**Figure 4.6: 28-day concrete compressive strength results for PCIP**

The average 28 day strength of the PCIP concrete was found to be 52.0 MPa, with a range from 41.7 MPa to 60.9 MPa. When this compressive strength range is considered, the fatigue life is found to be between  $1.55 \times 10^7$  and  $6.98 \times 10^{11}$  40 kN edge loads.

The section eventually chosen for the PCIP trial was located on the northbound Lane #3 of Highway 400, as outlined in Chapter 5.1. While this section was not known at the time of design, it provides good context for the analysis of the pavement. The total truck loading for the section can be estimated based on traffic volume and composition surveys that have been performed for the highway. The design of the HMA pavement in the location of the trial section, was performed by Applied Research Associates in 2012. In it, the composition of the truck traffic on the highway was determined based on a recent MTO survey. The truck composition was broken into the nine truck classes that were observed on the highway. The composition, as well as the typical Truck Factor (TF) are shown in Table 4.3. The TF represents the typical number of ESALs associated with each truck type.

**Table 4.3: Truck types, factors, and composition for Highway 400 (adapted from (Applied Research Associates, 2012))**

<b>FHWA Class</b>	<b>Description</b>	<b>TF</b>	<b>Commercial Vehicle Distribution (CV)</b>	<b>TFxCV</b>
5	2-axle, single unit trucks	0.3	17.4%	0.052
6	3-axle, single unit truck	0.9	9.7%	0.087
7	4+ axle, single unit truck	4	1.5%	0.060
8	4 or fewer axle, single trailer trucks	1.1	3.0%	0.033
9	5-axle, single trailer trucks	1.6	40.2%	0.643
10	6+ axle single trailer trucks	4	22.8%	0.912
11	5 or fewer axle, multi-trailer trucks	1	0.0%	0.000
12	6-axle, multi-trailer truck	4.3	0.2%	0.009
13	7+ axle, multi-trailer truck	5.6	5.2%	0.291
		<b>Total</b>	<b>100.0%</b>	<b>2.09</b>

Based on the distribution, it was calculated that the average number of ESALs per truck could be approximated by 2.09. Considering this value, and the design assumptions outlined in Table 4.4, the total expected number of ESALs can be calculated.

**Table 4.4: Traffic Calculation Assumptions**

Annual Traffic Growth Rate (%)	2.4
Initial Traffic Level (AADT)	92, 800
Percentage of Trucks in Design Lane (%)	70
Percentage of Total Traffic made up of Trucks (%)	12
Design Life (years)	25

The growth rate, percentage of trucks in the design lane, and percentage of total trucks were taken from the previously discussed design report (Applied Research Associates, 2012). The initial traffic level was found using the MTO database of network traffic volumes (Ministry of Transportation of Ontario, 2016). The 25 year design life is only an estimate of a typical pavement. Considering these values, the section can be expected to encounter  $1 \times 10^8$  ESALs during the course of its service life.

This value should be considered only as reference for the purposes of fatigue life estimation. While the applied load, N, was chosen to correspond to one tire of a standard axle load, the total number

of ESALs does not indicate the number of 40 kN loads applied to the panel. One ESAL is defined based on a loss of serviceability associated with the standard load, while the fatigue calculation is based on the number of load repetitions at a given magnitude.

Each of the truck classes in Table 4.3, the truck factor for each is consistently less than the number of axles for the given truck type. This implies that each axle for a given truck would have an average TF component less than one ESAL. This combined with the definitions of ESALs and fatigue indicate that each axle of a given truck generally has a smaller tire load than the assumed 40 kN.

The nature of the stress equation (Equation 8) is such that a small reduction in the applied load results in an exponential increase in the number of load repetitions sustained until failure. For instance, a 10% decrease in applied load (from 40 kN to 36 kN) causes the number of repetitions until fatigue failure for a 40 MPa strength concrete to increase from  $6.41 \times 10^6$  to  $4.01 \times 10^8$ , an approximately 6300% increase.

This consideration, combined with the actual measured compressive strengths and the distribution of traffic within the width of the lane (not solely on the outside edge), indicate that the panels are likely sufficient for a 25-year service life in fatigue, given the support conditions are maintained. It should be noted that this post-hoc analysis was completed based on site-specific information and can not be applied to all high-volume highways without site-specific thickness design.

As mentioned previously, fatigue cracks once begun will be kept closed by the reinforcement included in the panels.

### **4.3.3 PCIP Details**

The PCIP trial design was developed for the MTO. The submission to the MTO consisted of a set of detailed construction drawings, drafted by the Fort Miller Company at the direction of the design team, and a Non-Standard Special Provision Specification. This section of the chapter describes the design, but Appendix B should be referenced for these documents.

#### **4.3.3.1 Surface Finish**

The surfaces of the precast panels were finished with a combination of broom finish in the direction of vehicle travel, followed by 3-5 mm wide longitudinal grooving spaced at 19 mm. This surface

texture was determined following a demonstration by Armtec, the fabricator of the panels. The longitudinal tines could be applied at a high pressure and a low pressure setting, resulting in deep tines or shallow tines, respectively. Both were constructed for demonstration, and the difference between the two is shown in Figure 4.7. The MTO representative chose the deep longitudinal tines.



**Figure 4.7: Deep tining (left) and shallow tining (right)**



**Figure 4.8: Broom finish (left) and burlap drag (right)**

A similar demonstration was performed using a burlap drag and broom finish prior to tining. The difference between the two is shown in Figure 4.8. The MTO representative chose the broom finish in order to provide the most surface texture.

#### **4.3.3.2 Panel Size and Details**

For the purposes of the trial, a precast panel of typical plan dimensions 3.66 m by 4.57m was chosen. These dimensions were decided upon based on the design lane width and extensive precast panel experience. The dowels to provide load transfer are 38 mm in diameter, 355 mm long, located at the mid height of the panel, and spaced at 300 mm on centre. The panel reinforcement includes two mats of 10M bars spaced at 300 mm on centre in both directions. The panels are to be Fort Miller Super Slabs<sup>®</sup>. Figure 4.9 presents a plan view of the typical panel design, with the traffic direction from left to right.

Several design details can be seen in Figure 4.9. Super Slabs have patented dovetail dowel slots on the bottoms of the panels, as shown on the left edge of the panel pictured in Figure 4.9. The slots are cast such that they align with the embedded dowels shown on the right side of the figure. These slots differ from several other precast panel types that have dowel bar slots that are exposed to the surface of the pavement. The key benefits associated with the bottom-slot design are that it allows for traffic to pass safely over the un-grouted slots prior to placing dowel bar grout and it protects the dowel grout from de-icing chemicals that are applied to the pavement surface.

The dowels and dowel slots are cast integrally into the panels and therefore greater precision of alignment can be met under the controlled casting conditions as compared to typical concrete pavements cast on site. The only drawback to these details is that they require a greater level of precision during the placement of the precast panels on site to ensure that slots are lowered directly over the dowels. This has typically not been observed to be a problem for experienced construction crews.

The dowel slots are open to the bottom of the panel; therefore, panel-bottom gaskets are required to provide separation between the dowel grout and the much weaker and more flowable bedding grout, which is pumped beneath the panel. The bedding grout is also not designed for freeze-thaw durability and could result in rapid deterioration of joints, if it is placed therein. In order to ensure that the bedding grout is not installed around the dowels, the dowel grout is pumped into the slots

first. The thinner bedding grout is unlikely to displace the dowel grout when it is installed subsequently.

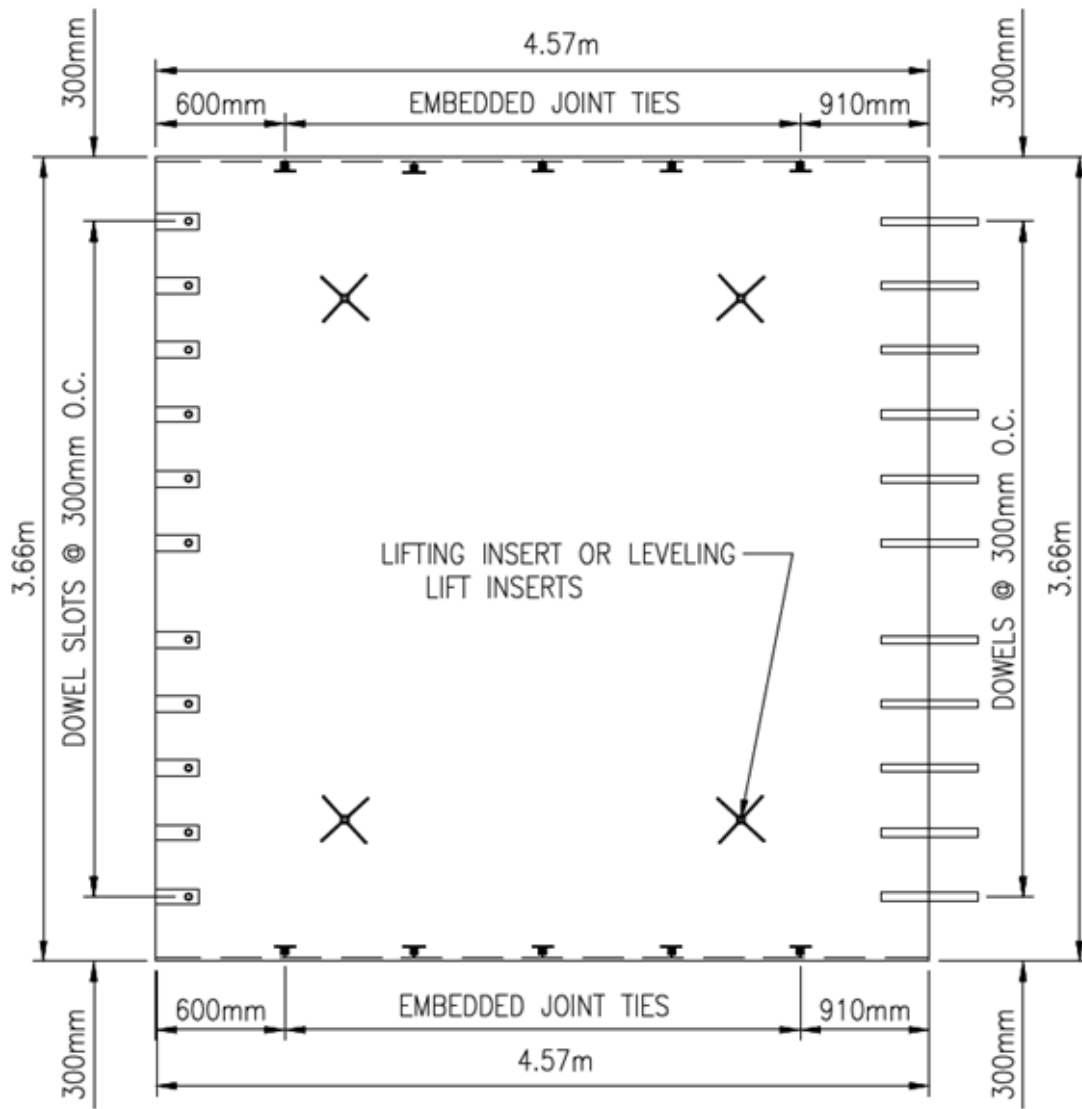


**Figure 4.9: Typical precast panel layout (The Fort Miller Co., Inc. 2015)**

The second panel support option described previously is grout-supported. In order to place this support condition, the precast panels require integrally cast levelling bolts. The bolts provide the mechanism by which the panel is raised to the desired position (elevation and cross-slope) before the bedding grout is pumped beneath it to provide support. As shown in Figure 4.9, this support system requires that levelling-lifting inserts be cast integrally within the PCIPs, instead of the typical lifting inserts.

#### ***4.3.3.3 Temporary End Detail***

At the end of each night of construction, the dowels protruding from the last panel placed are exposed. These dowels will be covered by the dowel slots of the first panel placed during the next construction shift, but they cannot be left exposed while maintaining daytime traffic. In order to provide a safe driving surface, a 1 m long temporary end panel with one set of Super Slab inverted dovetail slots (see Figure 4.10) was designed. This temporary panel is the same width as the typical precast panels to fit into the same milled recess in the HMA pavement. One transverse edge of the temporary end panel fits over the exposed dowels, while the other abuts against the vertical cut face of the HMA at the nightly terminus of construction. At the beginning of the next night's construction activities, the temporary panel is removed, and typical construction can recommence.

The use of the temporary panel requires that the removal of asphalt be performed with high precision. The length of the removed asphalt requires enough precision that the temporary panel can be installed without leaving a gap larger than 12 mm between the remaining HMA and the end of the temporary panel. The temporary panel locations must be considered during the surveying and saw-cutting operations discussed previously in order to lay out the extents of the nightly milling.

#### ***4.3.3.4 Temporary Longitudinal Edge Detail***

In order to place precast panels between the vertical asphalt faces left by saw-cutting and removing asphalt, the vertical faces must be spaced far enough apart to allow for placement without risk of damaging the adjacent asphalt. To provide this space, a 75 mm gap was designed along both longitudinal edges of each precast panel.

While this plan allows for safe panel placement, it leaves two edge gaps that cannot be present when traffic resumes. These gaps are grouted when the dowel and bedding grout is placed, typically on the night following the panel placement. Delayed grouting is a benefit of the PCIP strategy that helps with the restrictive time constraints associated with construction on a 400-series highway.

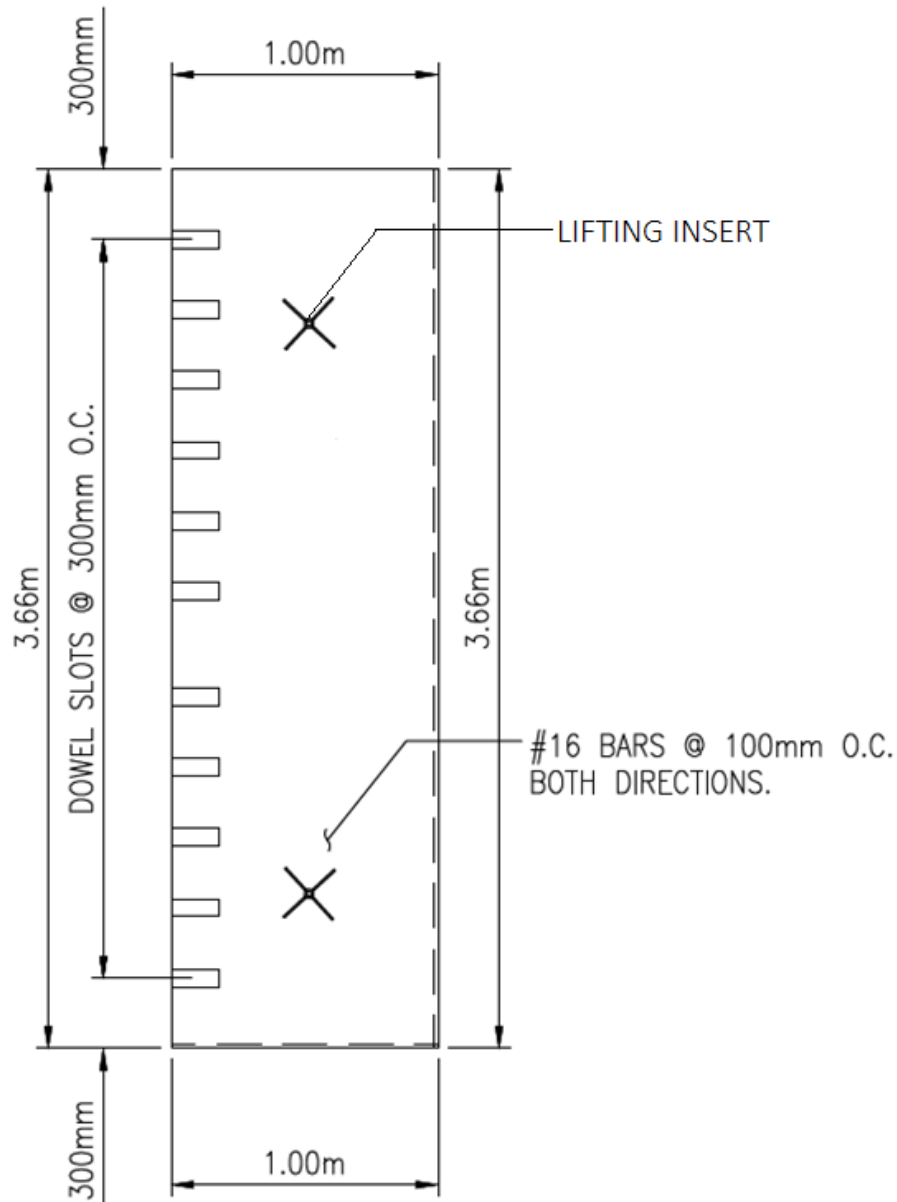


**Figure 4.10: Temporary end panel detail (The Fort Miller Co., Inc. 2015)**

A temporary longitudinal joint insert, shown in Figure 4.11, was designed to fill a portion of this gap and support traffic until grouting occurred. The detail consists of a temporary re-usable hollow steel section bolted to the longitudinal edge of the precast panel and secured in place with bolts screwed into threaded inserts embedded in the edges of the PCIP, as shown in Figure 4.11.

During the next construction shift, the temporary insert is removed, headed studs are attached to the threaded inserts, and a #5 reinforcing bar is placed in the longitudinal gap in order to secure

the grout within the edge gap as is also shown in Figure 4.11. The gap is then filled with the edge grout, discussed previously.

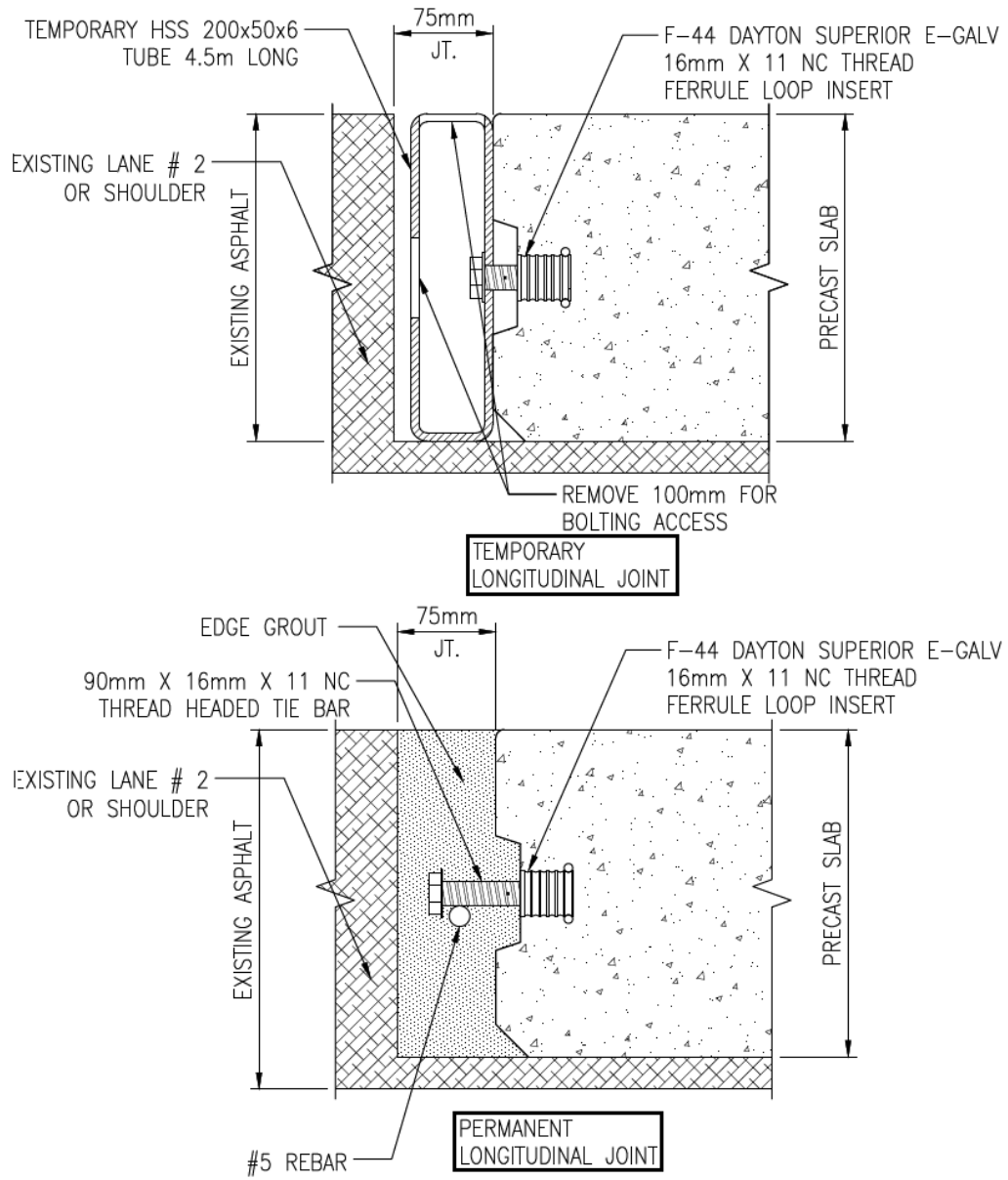


**Figure 4.11: Temporary and permanent longitudinal edge details (The Fort Miller Co., Inc. 2015)**

#### 4.3.3.5 First and Last Transverse Joint Detail

Figure 4.12 illustrates the terminal transverse edge detail where the inlay panels abut the existing HMA pavement. This joint is designed with a keyway cast integrally in the precast panel and is specified to be placed approximately 12 mm from the vertically cut face of the existing pavement. This 12 mm gap was designed to be filled with the same grout used for the typical transverse joints. This joint represents an area of concern that will be closely monitored throughout the life of the trial section. Unlike the longitudinal joints, this joint will be exposed to high traffic loading. Additionally, the interface being between materials of different moduli could result in differential deformation over time, which in turn could lead to increased stresses and surface water ingress.

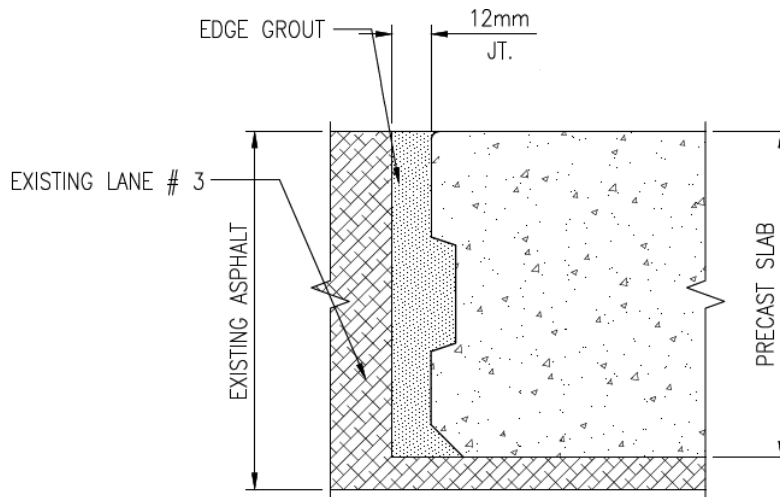


Figure 4.12: Terminal transverse edge detail (The Fort Miller Co., Inc. 2015)

#### 4.4 PCIP Trial Design

The final design of the trial section itself was dependant on the location and contractor input, however some details were determined for the design submission to the MTO. In general, the design included 22 PCIPs to be installed in Lane #3 (the right-hand lane) of a three-lane highway. The grade of the section was suggested to be approximately level (0%) in order to diminish the complexity of the first PCIP installation.

The three support conditions, AS, GraS, and GroS would be installed consecutively, with 8, 7, and 7 panels of each type installed, respectively.

For the purposes of differentiation, the PCIPs were numbers sequentially in the direction of travel. Therefore, Panels #1 to #8 were AS, Panels #9 to #15 were GraS, and Panels #16 to #22 were GroS. Figure 4.13 shows a general schematic of the site layout, including the numbering associated with the different panels and support conditions.

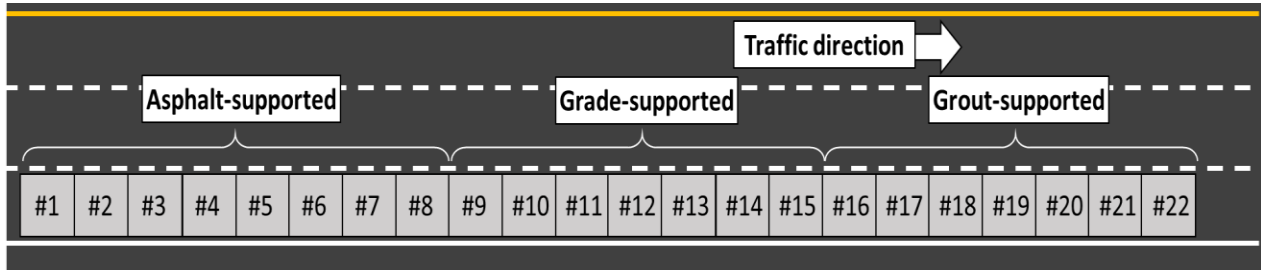


**Figure 4.13: General trial section layout and panel numbering**

## 4.5 Chapter Summary

In this chapter, the design of the PCIP trial rehabilitation was outlined. This included a description of the broad steps required for inlay panels, which are panel fabrication, surveying, saw-cutting, HMA removal, surface preparation, panel placement, and grouting.

The support conditions beneath the PCIP are a main focus of the study, and each of the three support condition types designed for the trial PCIP section are described in detail. These support conditions are Grade-supported (GraS), Asphalt-supported (AS), and Grout-supported (GroS). Each support condition was developed in consideration of assumed costs and benefits related to construction. The relative magnitude of these costs and benefits would determine the best option of the three. These costs and benefits were described and summarized.

The thickness of the PCIP panels used on the trial was evaluated using fatigue design principles. Based on the stresses associated with edge loading, the concrete strength, and traffic estimates, the design of the panels was found to be generally acceptable. It was noted that the panels are substantially reinforced, and therefore fatigue cracking is not expected to propagate following initiation.

The surface finish and design details that were developed specifically for this trial were also outlined and discussed.

## **CHAPTER 5: TRIAL SECTION CONSTRUCTION**

The detailed design described in the previous chapter was accepted by the MTO and it was decided that an existing highway resurfacing contract would provide the best opportunity for the construction of a trial section. For this reason, the trial section was implemented as a change order to an existing contract underway between Dufferin Construction (Dufferin) and the MTO. WSP Canada was serving as contract administrator for the contract.

This choice was based on several factors, including but not limited to contractor familiarity with precast panel installation, and suitable HMA pavement thickness, elevation, and cross slopes for trial.

The original contract scope involved “shaving and paving” sections of Highway 400 south of Barrie. Shave and pave consists of milling surface HMA and replacing it with an equivalent thickness of new HMA to repair the highway’s surface, which is the typical repair strategy for this and similar highways.

Several subcontractors were contracted by Dufferin as part of the trial project. These included:

- Armtec, the precast panel fabricator/supplier
- RotoMill, for milling HMA in area of the rehabilitation
- Basic Cutting and Coring, for saw-cutting the extents of HMA removal
- Amherst Crane Rentals, for lifting panels into place

This chapter outlines the construction of the trial section, including the descriptions of the different support conditions, issues encountered, and the post-construction analysis used to analyze the different methods of constructing the PCIPs.

### **5.1 Project Site**

The final location determined for the project site was chosen by Dufferin and WSP through discussions with the MTO and the design team. It was located on the northbound section of Highway 400 between the intersections with highways 88 (to the south) and 89 (to the north). The geographic Cartesian coordinates of the site are 44°06'44.0"N 79°38'01.9"W.

The average annual daily traffic (AADT) in both directions for the section was estimated to be 87300 vehicles in 2013. This was a 13% increase as compared to 2008 and a 27 % increase over the 2003 levels. It is estimated that this traffic consists of approximately 12% trucks, for an estimated average annual daily truck traffic of 5250 trucks in one direction (Ministry of Transportation of Ontario: Highway Standards Branch, 2013; Ministry of Transportation Ontario, 2016). This corresponds to approximately 13500 ESALs per day (Hajek, Smith, Rao, & Darter, 2008). It is estimated that by 2026 there will be approximately 9.6 M ESALs per year per direction on this section of highway. A 2016 traffic volume estimate for the section indicated that the AADT for the section was 92800 vehicles per day (Ministry of Transportation Ontario, 2016).

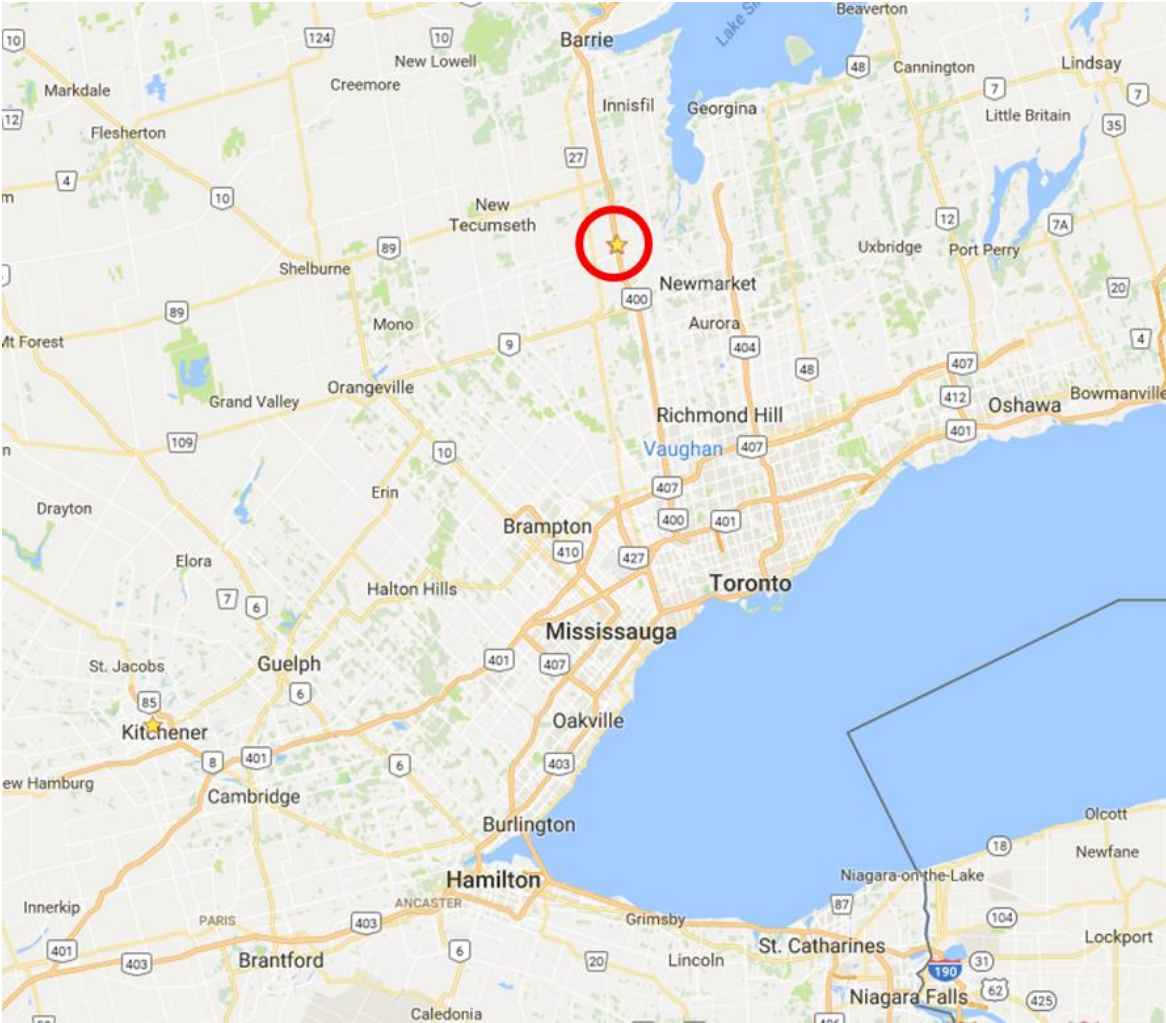


**Figure 5.1: Approximate location of trial section (Google, CNES 2016)**

This section has three lanes in each direction that are separated by an approximately 2 m wide divider with guiderails. The trial was planned for a 100 m section of Lane #3, adjacent to the outside shoulder. A 2.5 m HMA shoulder was located adjacent to Lane 3. The section of roadway was in a cut section, with a sloped berm in the clear zone beyond a shallow ditch adjacent to the shoulder. Figure 5.2 illustrates the site from its southernmost extents facing north.

The site conformed to the initial requirement that it be flat and straight.

The HMA pavement on the project site had been replaced in 2015 as part of the existing contract between Dufferin and the MTO, and thus it was known that this section of highway had sufficient HMA depth to support this rehabilitation strategy. In addition, cores were taken prior to the beginning of construction to ensure the pavement depths were sufficient. Cores were also taken in the middle of the shoulder for insight into the pavement structure in these areas. Table 5.1 summarizes the results of this coring.



**Figure 5.2: Trial section location (Google Maps, 2015)**

**Table 5.1: Coring Results**

Station	NBLN3	NB RT Shoulder
17+570	375mm	210mm
17+600	355mm	195mm
17+630	370mm	200mm

The minimum pavement thickness requirement for a PCIP installation was 300 mm, and sufficient pavement thickness was found in each of the cores taken from Lane #3. Each shoulder core was found to be slightly larger than half of the Lane #3 thickness.

The cross slope of the highway was designed to be 2% down towards the shoulder and towards the centre median, with the crown located between Lanes #2 and #3. As HMA highways are continuously repaired over time, the design cross slope can often be lost. Cross slope was measured at the proposed location of each panel edge as part of the site layout activities to gain insight into existing conditions and in order to produce a design cross slope. These values are summarized in Table 5.2. The final value in the Grout-Supported column represents the cross slope measured at the trailing edge of the last panel.

**Table 5.2: Measured Cross slopes at Leading Panel Edge (%)**

Slab Number for Support Condition	Asphalt Supported	Grade-Supported	Grout-Supported
1	2.4	2.37	2.64
2	2.08	2.53	2.49
3	2.23	2.49	2.63
4	2.35	2.51	2.49
5	2.51	2.67	2.84
6	2.37	2.73	2.94
7	2.57	2.7	2.94
8	2.27		3.04*
<b>Average</b>	<b>2.3</b>	<b>2.6</b>	<b>2.7</b>

\* denotes trailing edge of final slab

As shown, there was considerable variability in the cross slopes within each section. Within a section, the largest variation in cross slope was 0.55%. Across a 3.66 m lane width, this corresponds to an elevation difference of approximately 20 mm between two points that should be at approximately the same level. This variation was noted prior to milling the HMA.

## **5.2 Preliminary Plans**

No substantial changes were made to the detailed design package that was submitted to the MTO, shown in Appendix B, however some changes were proposed by Dufferin to address concerns they identified.

### **5.2.1 Order of Installation**

While no order of installation was explicitly stated, it was originally recommended that the order of installation would be, Grade-Supported, Asphalt-Supported, then Grout-Supported panels. This recommendation was made with the intention to simplify the beginning of construction. Since the Grade-Supported procedure was most similar to previous installations, and because the CTBM could correct some issues associated with milling, it appeared to provide the least problematic installation procedure of the three support conditions.

After seeing the efficacy of the milling machine, Dufferin elected to install the Asphalt-Supported panels first. After confirming that the milling machine could provide a surface within the specified tolerance, this support condition was viewed to have fewer uncertainties than the others. After the Asphalt-Supported condition, the installation of Grade-Supported and Grout-Supported panels were chosen to follow.

### **5.2.2 Nightly Number of Panels Installed**

During the initial design phase, it was presumed that approximately half of each support condition (3 or 4 panels) would be installed in any given night. This assumption was based on precast panel experience, wherein a new job has typically required a steep learning curve to achieve the final production rates. Since each support condition would essentially be a new construction method, it was assumed that a conservative initial production rate would be chosen.

Dufferin did not identify that any of the learning curve considerations would slow their rate of production and instead decided to install all panels of a given support condition type in one night.

It was conceded that if the first night exposed issues with this plan, then subsequent installation nights could be scaled back as deemed necessary; transverse saw-cuts were planned for locations that demarcate the full installation of the Grout- and Grade-Supported panels as well at locations corresponding to four of the potential seven panels each night.

### **5.2.3 Precast Panel Delivery**

The delivery of panels to site was a staging consideration between Armtec and Dufferin. Two main plans that were discussed included storing the panels in one of Dufferin's nearby yards or delivering panels required for each night's construction just-in-time (JIT) to the site.

It was decided that the extra considerations associated with storage on site, such as unloading and reloading and space concerns, made JIT delivery more feasible. Armtec indicated that due to the wide load considerations associated with moving the panels, they must be on site no later than one half hour after sunset (Heavy Haul Trucking, 2016). At the time of construction, this meant that trucks could arrive on site no later than 7:50 pm. It was decided that these trucks could be parked on the highway shoulder with a crash truck subcontracted by Dufferin to wait until lane closures began.

Due to the special circumstances of this construction project, lane closures were allowed by the MTO to begin at 8 pm each night, which meant that the trucks loaded with panels would not have to wait for very long periods of time before they move into the lane closure. Furthermore, because the site was located immediately north of a highway exit, the lane closure extended to the merge lane onto the northbound portion of the highway. This allowed the trucks to park at a parking lot located near the exit, and enter the site directly from the merge lane without entering into the highway traffic.

### **5.2.4 Lifting Inserts/Levelling Inserts**

The original design included levelling inserts to be installed as the lifting insert in the panels used for the Grout-Supported condition. These inserts allow the panels to be manually elevated to the required elevation once placed.

Dufferin and Armtec agreed to include these lifting inserts in all panel types as a measure of redundancy. The cost associated with the more-expensive lifts was deemed to be worthwhile in

case the HMA milling left a pavement surface that was too low and needed to be remedied before the pavement was opened to traffic.

### **5.2.5 CPATT Installation Plans**

The installation of instrumentation and data-logging units required input and help from Dufferin throughout the construction process. The instrumentation, in total, included 12 vibrating wire pressure cells and 6 moisture probes, installed at 6 different locations.

In order, this included:

- Ordering a data-logger cabinet.
- Laying out and constructing a concrete base for cabinet on site.
- Saw-cutting trenches through the HMA shoulder for the running of cable.
- Digging a trench adjacent to the shoulder through which to run cabling (nightly).
- Saw-cutting/removing HMA in milled section for installation of sensors (nightly).
- Placing conduit for cables.
- Affixing the cabinet to the concrete base.
- Miscellaneous help during installation (providing sand and other materials, saw-cutting conduit, etc.).

### **5.2.6 Lane Closures**

The typical traffic plan for closures during construction had two stages. Each stage was laid out in accordance with the Ontario Traffic Manual Book 7 (Ministry of Transportation of Ontario, 2014).

The first stage each night began at 8 pm and followed a TL-29 layout for one lane closure on a multi-lane freeway. At 11 pm, a TL-38 lane closure for two lanes closed was instituted. Figure 5.3 illustrates each of these lane closures as specified in the Ontario Traffic Manual.

The staggered lane closures allowed the construction crews to access the site earlier than typical, two lane closures beginning at 11 pm. During the 8-11 pm periods each night, any work that was confined to the shoulder or the outermost portions of lane #3 would be conducted. This work would not interfere with traffic but would extend the total time allowed on site.

At 11 pm, the remainder of the work that was immediately adjacent to or on Lane #2 could begin. This included finishing the milling and transporting panels and other materials beside the milled section.

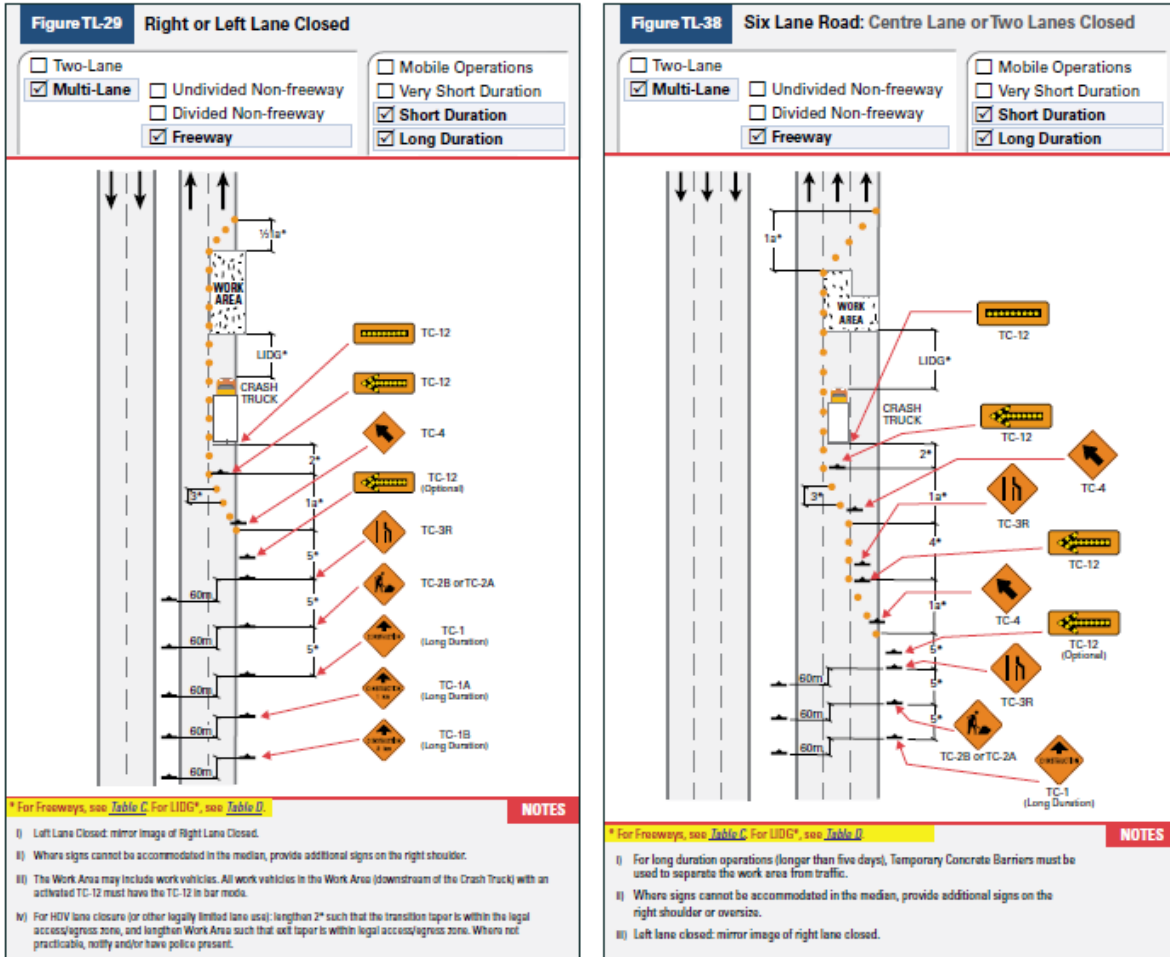


Figure 5.3: Traffic plans for lane closure (Ministry of Transportation of Ontario, 2014)

### 5.3 Construction Activities

The construction of the trial section consisted of several individual activities.

#### 5.3.1 Panel Production (Late August – Early September)

Panel production took place at the Armtec production facility located in Mitchell, Ontario. The plant produces precast concrete products as well as wood-chip sound barriers under the name Durisol.

The factory produces its own concrete mixtures for the production of precast products in its batching plant, pictured in Figure 5.4. The mixer distributes concrete into a portable hopper (pictured) that is then used to transport the concrete to the precast forms.

The forms for the panels were constructed on large steel casting beds, shown in Figure 5.5.

After the side rail forms were positioned, slot formers (including grout port formers) and penetrating dowel bars were attached to them. Bedding grout channels and associated grout port formers were then attached to the beds. Finally, epoxied steel reinforcement and lifting/levelling inserts were placed as indicated on the approved shop drawings. Figure 5.6 illustrates a panel form with all of these features installed awaiting concrete placement. The inset to Figure 5.6 shows a bedding grout port former attached to a bedding grout channel former and a lifting/levelling insert.

Concrete was poured into the forms in layers and vibrated to ensure full consolidation. The surface of the concrete was then finished with a roller screed, before longitudinal broom and tine finishes were placed on the final surface. Figure 5.7 shows the rolling apparatus that was used to place the tined finish at a consistent pressure and direction.

After the concrete in the panels had attained the 20 MPa minimum stripping strength, the panels were stripped from the formwork, placed in stacks using dunnage, and moist cured using burlap. The moist curing period was specified to last a minimum of 96 hours. Following the curing period, the panels were stored in the outside yard of the plant on the flatbed trailers that would later be used for transporting the panels.



**Figure 5.4: Concrete batching plant at Armtec, Mitchell**

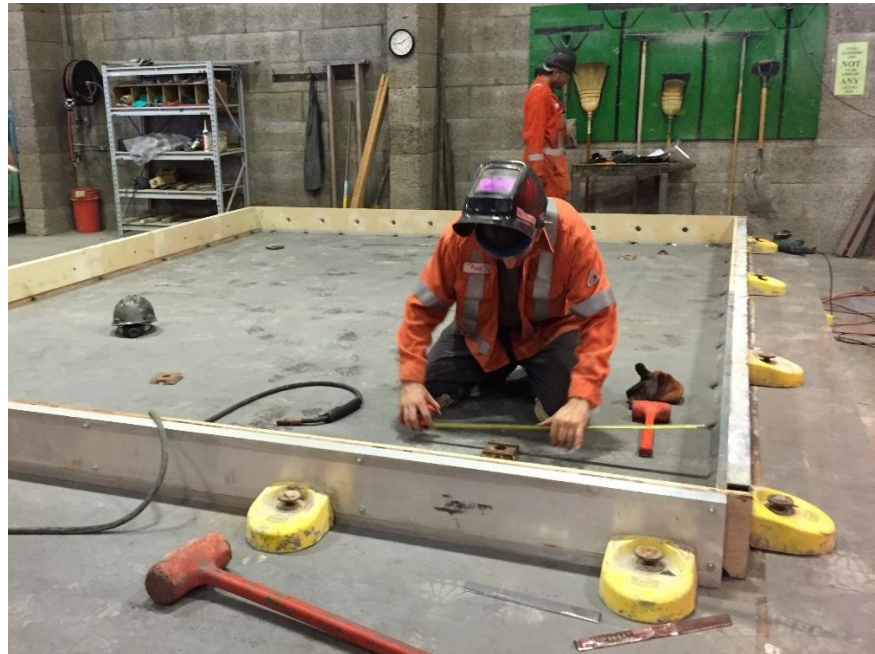


**Figure 5.5: Laying out panel formwork**



**Figure 5.6: Panel form ready for concrete placement**



**Figure 5.7: Longitudinal tining apparatus**

### **5.3.2 Site Layout (September 15<sup>th</sup>, 2016)**

On the evening of September 15<sup>th</sup>, Dufferin had a surveying crew visit and lay out the site. Two lanes of Highway 400 were closed at the site location beginning at 11 pm. Using a total station, the survey crew laid out longitudinal and transverse saw-cuts, laid out the leading edge of each panel at both the shoulder and inside edge of the lane, and recorded existing pavement elevations at the proposed location of the transverse corners of each new panel so cross slopes of the pavement

at each new transverse saw-cut could be determined. The general layout for the site is illustrated in Figure 5.8.

During this lane closure, the trenches that would be used to run cabling from the lane through the shoulder to the ditch were laid out. The ditch was located beyond the right-hand shoulder.

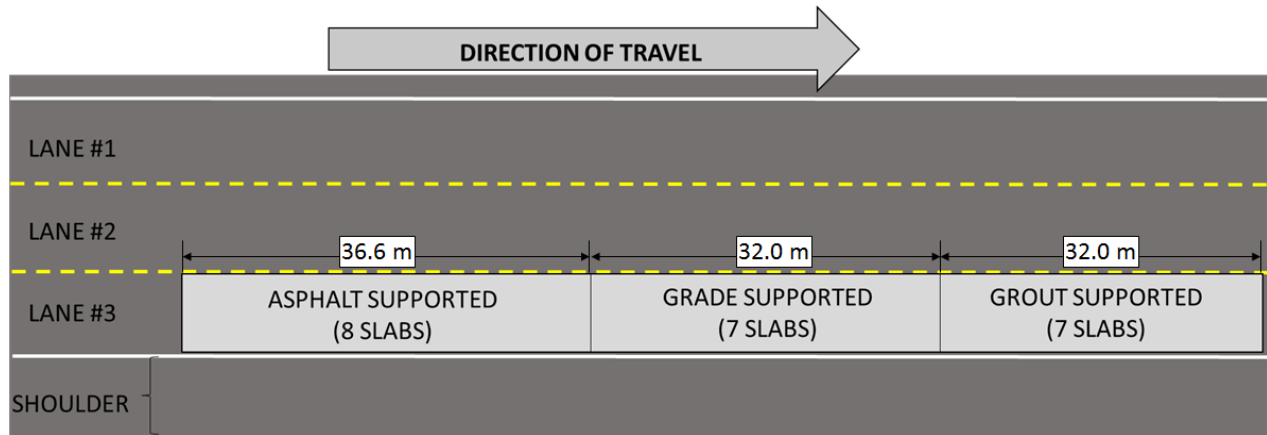


**Figure 5.8: General site layout (Not to Scale)**

### 5.3.3 Saw-cutting (September 19<sup>th</sup>, 2016)

The saw-cutting specified in the NSSP began on the evening of September 19<sup>th</sup>. The weather was clear, with an average temperature of approximately 20°C. Both longitudinal edges, and several transverse sections were cut throughout the extents of the project.

The typical staged lane closure began at 8 pm and allowed for the shoulder edge of Lane #3 to be saw-cut. Each saw-cut was done in two passes. The first pass was to a depth of approximately 50 mm, while the second cut was to the full depth of the section, 206 mm. A shallow cut using the sawing machine can be easily controlled and therefore any wandering of the blade could be quickly and easily corrected, therefore the first cut was done to accurately cut along the prescribed lines. This cut would then serve as a guide for the subsequent cut, allowing for accurate, full-depth cuts. Figure 5.9 shows a first pass of the saw-cutting machine.



**Figure 5.9: Saw-cutting first pass**

After the longitudinal edge along the shoulder had been cut, the trenches for instrumentation cabling were cut. These cuts were the same depth as the other saw-cuts to align the bottom of the trench with the bottom of the milled section.

When the second lane was closed at 11 pm, the longitudinal edge between Lane #2 and Lane #3 was cut.

The cutting operation was completed by approximately 3 am on the morning of September 20<sup>th</sup>, including lane closures, the operation took approximately 5 hours to complete by one labourer.

#### **5.3.4 Asphalt-Supported Trial Section (September 20<sup>th</sup>, 2016)**

The first night of panel installation began on the evening of September 20<sup>th</sup>. The weather was clear, with an average temperature throughout the evening of approximately 10°C. Traffic control was begun at 8 pm, and the milling machine was unloaded and beginning to mill the section by 8:30 pm. The milling machine itself was a Wirtgen Model W120 CFI, with a 1.2 m-wide milling head.

The initial target cross slope for the milled surface was 2.4% (towards the shoulder). This was chosen as a median value based on the measured cross slopes presented previously. This cross slope was manually checked behind the milling machine using a 1200mm long level. After setting

the cross slope and depth, the milling machine progressed at a speed of approximately 8-10 m/minute.

The milling was performed in the direction of traffic and the milled HMA was directed into a dump truck that was moving in the same direction (pictured in Figure 5.10). When the truck was full it would exit out of the lane closure to dump the material and would then return to continue hauling.

The milled surface was cleaned using a power broom attached to a skid-steer loader, which is pictured in the inset in Figure 5.10.



**Figure 5.10: Second pass of milling machine**

The first two passes of the milling machine were completed by 10:15 pm, and the second lane closure began at 10:50 pm. By 10:56 pm, the third pass of the milling machine had begun.

After the second pass of the milling machine, the spot removals to facilitate instrumentation placement began. The two areas were laid out, saw-cut using a quick-cut saw, and then chipped out using a pneumatic hammer. The work was paused when the milling operation encroached on the areas being removed.

Due to the cylindrical shape of the milling head, an intact portion of HMA remained at each end of the milled section that could not be removed as part of the longitudinal passes of the milling machine, shown in Figure 5.11.



**Figure 5.11: Rounded HMA portion left by cylindrical milling head**

Initially, it was assumed that removing this material would be done with chipping hammers, however the milling crew was able to turn the milling machine 90° to do a transverse pass at each end. This left only two small rounded portions in each corner that were removed with chipping hammers (Figure 5.12).

By 11:30 pm, the first round of bulk milling had been finished, including the transverse passes. The milling machine was loaded onto a flat-bed trailer and transported off the site. At this point, the Fort Miller representatives began to place their grade checker (Figure 5.13), which was made up of several pins connected to a levelling screed. The height of the movable pins indicated the level of the milled surface relative to the required depth.



**Figure 5.12: End after longitudinal and transverse passes**



**Figure 5.13: Fort Miller's grade checking apparatus**

The grade checker found that the height of the milled surface was too high in several places throughout the milled extents, however an attempt was made to place the panels on the milled surface, regardless.

The first panel was placed at approximately 12:45 am and it was obvious that the elevation difference between the panel and the adjacent HMA was too large to proceed, so Dufferin recalled the milling crew and equipment.

The second milling crew arrived on site at approximately 1:50 am and began to re-mill the surface. The instrumentation that had been placed during the placement of the first panel, was removed during the re-milling operation. The goal of the second re-mill was to remove approximately 12 mm of asphalt, based on the readings from Fort Miller's grade checker.

Following the milling operation, a stringline was used with a measuring tape to measure the depth of the milled recess. This operation is shown in Figure 5.15. The recessed area for instrumentation (filled with milled asphalt) can also be seen in this figure.

The re-milling operation was finished by 3:10 am, and the first panel was re-lowered into place by 3:20 am.

The crane used to place the panels was a National truck crane rated at 45 tons. Due to the restrictions on site, the 45 ton crane could only place one panel from any one position, and had to be re-positioned for each subsequent panel. On this night, the crane was generally located on the previously-set panel in order to place the next.

The work zone on this site was limited to the two right-hand lanes (Lanes #2 and #3) and the adjacent shoulder since it was necessary for highway traffic to use all of the left lane (Lane #1). This limited working width, typical of lane replacement projects on a three lane highway, prevented the outriggers on the left side of the crane from being extended fully, thereby reducing the allowable lifting capacity of the crane. Figure 5.14 illustrates uneven outrigger extension on the crane and how close the operation of unloading panels was to the maintained traffic lane. Furthermore, because of the requirement to place rails to use Fort Miller's grade checking apparatus, the panel-carrying truck was unable to drive past the crane to allow a 90° or less swing while placing the panels. For this reason, the crane was required to lift the panels and then rotate ~270° around the back of the crane to place them. This required that panels be lifted over the ditch, which was the location of some construction activities and the main route for personnel to cross the site. Great care was taken with no incidents, however this situation should be avoided in the future.



**Figure 5.14: Panel-carrying truck unloaded adjacent to traffic**



**Figure 5.15: Checking the re-milled surface with a stringline**

At the first transverse joint between the HMA and the precast panels, the panel was found to be approximately 9 mm high. There were also no surveyed marks to show where the panel should be placed, and when the second panel was placed, a gap of approximately 15 mm was observed. The placement of the second panel and the gap between the first two panels are shown in Figure 5.16. The vertical difference between adjacent panels was found to be within the 3 mm tolerance for the remainder of the panels.

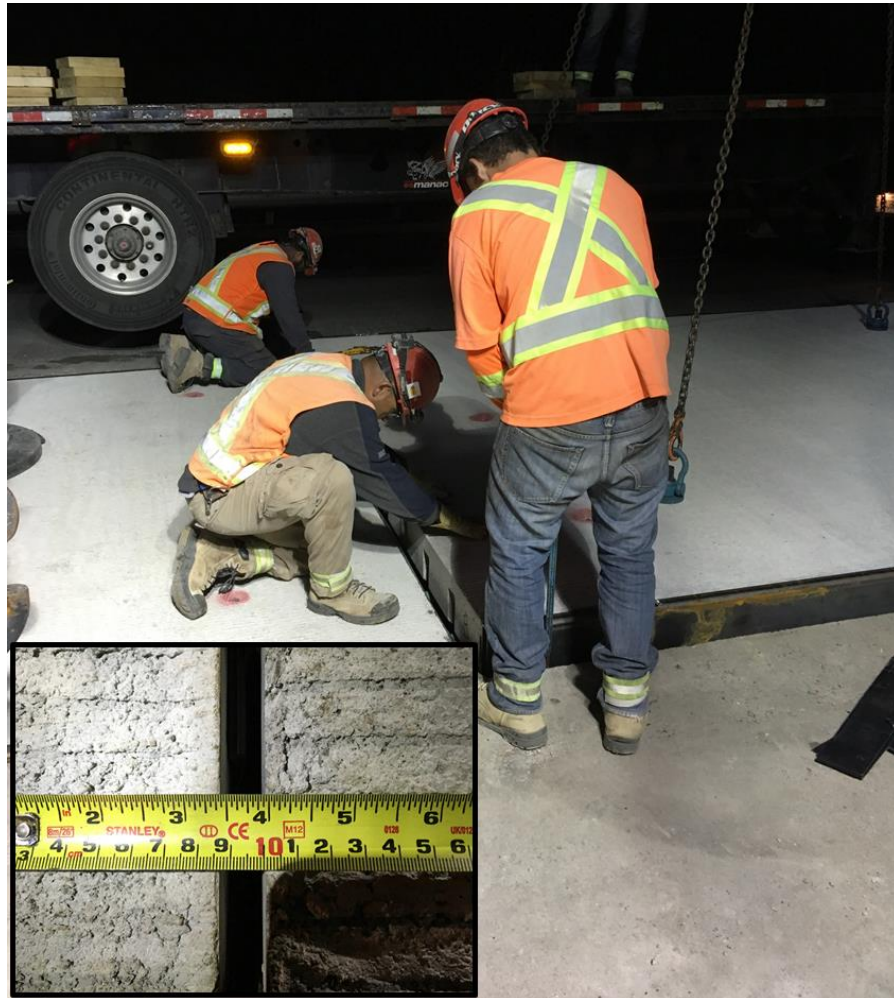


**Figure 5.16: Placing panel #2; first gap (inset)**

Each panel had the doweled edge sprayed with bond-breaking agent up to the point 25 mm below the top edge. This was done to ensure that grout would only bond with the dowel-slot edge of the joint.

The final asphalt-supported permanent panel was placed at approximately 4:30 am, while the temporary end panel (shown in Figure 5.17) was placed by 4:45 am. Excluding the temporary panel, 8 panels were placed in approximately 1 hr 10 minutes, for an average of approximately 8.75 minutes/panel.



**Figure 5.17: Temporary end panel**

After the placement of the final panel, site clean-up took place ensuring that all debris was removed from the site prior to opening for traffic.

### **5.3.5 Grade-Supported Trial Section (September 21<sup>st</sup>, 2016)**

The Grade-Supported panels were placed during the construction period beginning on the evening of Wednesday, September 21<sup>st</sup>. The weather was slightly hazy, with an average temperature throughout the evening of approximately 12°C.

Traffic control was completed similarly to the previous night, however access to the site was not granted until approximately 8:45 pm. Visual inspections of the panels placed the previous night found no instances of cracking had occurred during the day. The labourers from Dufferin began removing the temporary longitudinal steel tubing when they arrived on site.

Once the lane was closed, the milling crew entered Lane #3 and began milling on the right-hand side of the lane. The specified depth of the milling for this section was 218 mm while the cross slope was specified to be 2.6%, based on the pre-existing cross slope of the section.

Due to staging difficulties, the crane was not present on site at the beginning of the night, and therefore the temporary panel remained in place at the beginning of milling (Figure 5.18). This plan resulted in the continuing need to make special considerations for removing the HMA left at the beginning of HMA milling.



**Figure 5.18: HMA milling begun adjacent to temporary panel**

During milling, a core hole was discovered from a previous investigation. This provided insight into the base layer of HMA on which the panels were being placed. From the bottom of the HMA to the milled surface measured approximately 160 mm, as shown in Figure 5.19.

The second lane closure was begun early (approximately 10:15 pm) and the final pass of milling was completed at approximately 11:15 pm.

Some small corrections in panel height were discussed. The levelling lifts that were cast into each panel would have allowed for some “fine-tuning”, however the proper-sized sockets were not available on-site, and as such, the original elevations were used.

After the temporary steel tubing was removed, the joints (longitudinal and transverse) were prepared for grouting. This included placing a single steel reinforcing bar in the longitudinal joints at either edge of the lane, and applying barriers made of spray foam at the ends of the transverse joint to separate the dowel grout and the extended grout (Figure 5.20).



**Figure 5.19: Core hole encountered in Grade-Supported section**

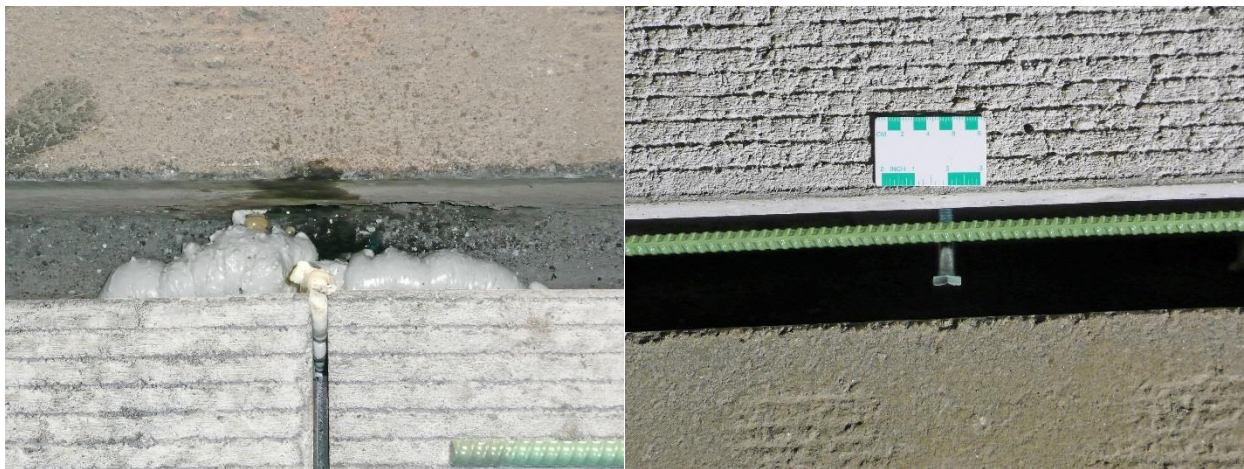


**Figure 5.20: Spray foam separating joints (L), Longitudinal reinforcing at edges (R)**

While the milling was still taking place, set-up for the grouting operation began. The panels that had been placed the previous night were to be grouted by half of the labourers on site. Initially the mixer was placed on the panels with a plastic sheet used to protect the surface of the panels from spillage. As the night progressed, the mixer was moved onto the shoulder to simplify this procedure.

The transverse joints were the first to be grouted, using dowel grout. The dowel grout, as outlined in the NSSP, was specified to have a 17 MPa compressive strength in two hours and 30 MPa strength at 28 days. The dowel grout used on this project was ProSpec's "Slab Dowel Grout". This grout was injected into the dowel slots through the grout ports that were cast into the panels, using the pressurized hose running from the mixer, pictured in Figure 5.21.

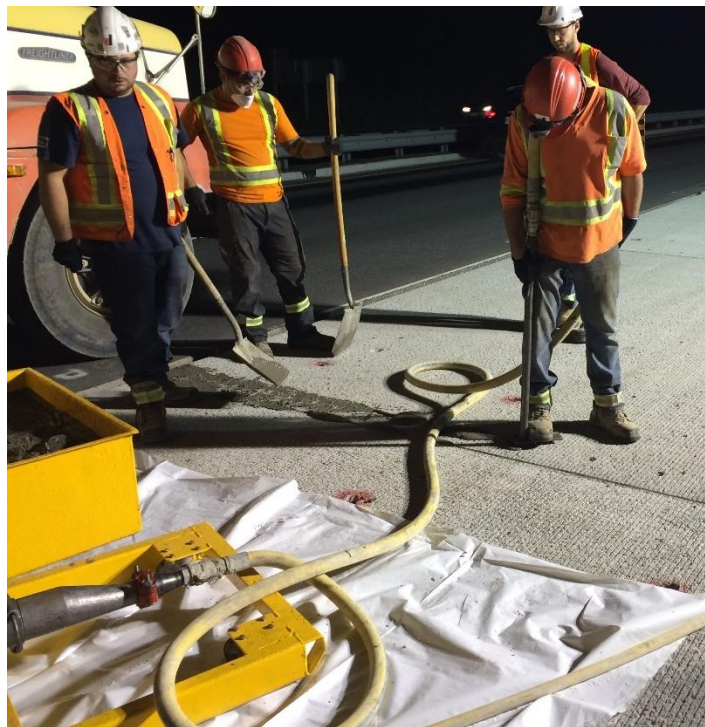


**Figure 5.21: Dowel grout being pumped into dowel slots**

Following the dowel grouting procedure, the longitudinal joints were grouted using the same grout used for the dowels, extended with 60% pea-gravel by weight. The extended grout was made by adding four parts pea-gravel for every one part grout. This material was mixed on-site in a concrete drum mixer and then placed in the joints using a hopper constructed out of plywood, pictured in Figure 5.22.

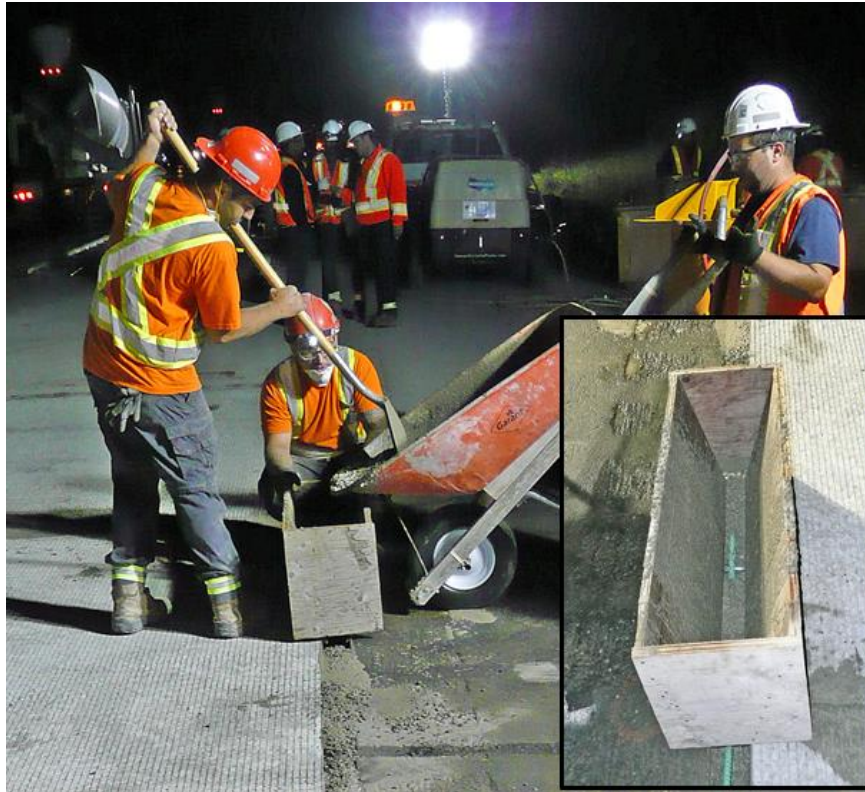


**Figure 5.22: Edge grout being placed using small hopper; Inside view of hopper (inset)**

The water contained in the pea-gravel made on-site proportioning difficult. The material appeared to have a water content that was too high, resulting in some material segregation that could be observed in some places. An instance of this segregation is shown in Figure 5.23.

As the grouting procedure took place, the rails on which the levelling screed ran were being laid out adjacent the grade-supported panel area that was about to be graded. For this operation, the shoulder side edge of the lane was used as a benchmark and the pre-determined cross slope (2.6%) was achieved by adjusting the rail height on the edge of Lane #3 that abutted Lane #2. Figure 5.24 shows the shoulder edge being set before the lane edge is adjusted to meet the proper cross slope.

After the rails were placed, the screed was moved into position. At this point, two issues were encountered. Firstly, it was found that the milling operation had not left the specified 13 mm between the surface of the milled surface and the presumed bottom of the panel. When the screed was pulled across the surface, it scraped almost all the bedding material from the milled surface.



**Figure 5.23: Evidence of segregation in edge grout**



**Figure 5.24: Members of Fort Miller, Dufferin, and CPATT laying out rails**

The screed was adjusted up by 5 mm to enable the placement of a layer of CTBM beneath the panels. The second issue was that the CTBM, intended to be a fine, “dry”, easy to grade and compact material, instead consisted of balls between approximately 10 to 25 mm in diameter (Figure 5.25). This presented further difficulties to the screeding operation as the balls would be pushed by the screed instead of graded. The plate tamper for compacting the material, seen in Figure 5.26, would break up the CTBM because it had not yet been fully hydrated, but the screed could not distribute and level the material evenly beforehand. Approximately the first 8 m of the milled area was prepared using the first (balled) batch of CTBM, however at this point it was determined that the material was not satisfactory, and the load was rejected for a new load, at approximately 2:20 am. Using the area leveled using the first batch of CTBM, the first two panels were placed at approximately 2:30 am.



**Figure 5.25: Consolidated balls of CTBM**

The clumping (balling) issue was likely due to high water content in the sand that was used to create the material. The intent was to have the CTBM be placed dry, and wetted in place. The moisture in the sand would have caused the material to begin to hydrate and adhere to itself before it was discharged from the truck. The trucks also arrived on site early, and remained in place with periodic mixing, causing the CTBM in the truck to ball further.



**Figure 5.26: Compacting CTBM with plate tamper while CPATT installs instrumentation**

The truck with the new CTBM arrived at 3:15 am, and the material was placed immediately. Clumps were still present, but it was not made up entirely of balls like the previous load. The material was screeded using the levelling screed and compacted using the plate tamper. The typical Fort Miller procedure is to place and grade the CTBM approximately 3mm high. That operation is followed by a second screeding operation during which the screed is placed to the correct elevation. After the second grading pass is complete, the material is wetted to begin hydration and the panels are placed directly upon the newly screeded bedding layer. Due to the initial issues with milling on this project, however, the material was placed, screeded, and compacted in one pass. The grading operation was finished at approximately 4:10 am.

As the panels were placed, the same procedure as described previously was followed. Figure 5.27 shows the bond breaker agent being applied to the dowelled face of a panel in position. The tape along the upper edge of the panel's face was to prevent bond-breaking agent from being applied to the upper 25 mm.

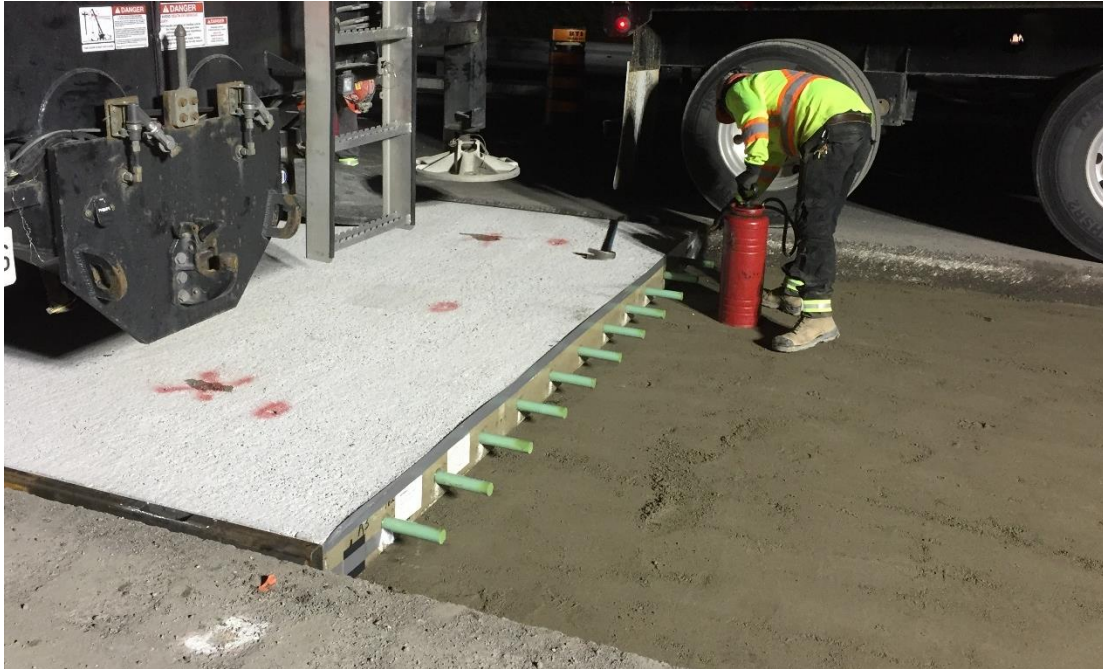


**Figure 5.27: Bond breaker agent being applied to panel edge**

At approximately 3:30 am, the fast-setting bedding grout was being proportioned and readied for installation under the asphalt-supported panels. The water content for the mixture was being proportioned by testing the mixture for its flow-rate characteristics. Originally, 27.3 L (7.2 gallons) were used to mix 4 bags (one batch), but this had a very slow flow rate as measured by a standard ASTM C939 flow cone. Several iterations were tried until a mixture with 30.3 L (8 gallons) of water exhibited an acceptable flow rate of 17.5 seconds. The first panel took approximately 3 batches, or 12 bags of grout mixture.

During the fifth batch, steam was observed coming out of the mixer. This is typically a sign that the material is hardening in the mixer. The mixer was promptly emptied and cleaned and no hardened grout was left in the mixer, however this indicated that mixer cleaning should take place every four batches to prevent the machine from seizing up. Figure 5.28 shows the steam as observed coming from the mixer.



**Figure 5.28: Grout mixer steaming**

As the CTBM was being placed and compacted, the panels were being placed on the compacted material. The final panel was placed at approximately 4:40 am. During the placement of panels, it became apparent that the milling operation had milled wider than was specified, leaving a large gap on both longitudinal edges of the panels. This was found to be a milling mistake rather than a layout or saw-cut mistake at the point shown in Figure 5.29. The saw-cut edge was over-milled by approximately 30 - 40 mm.

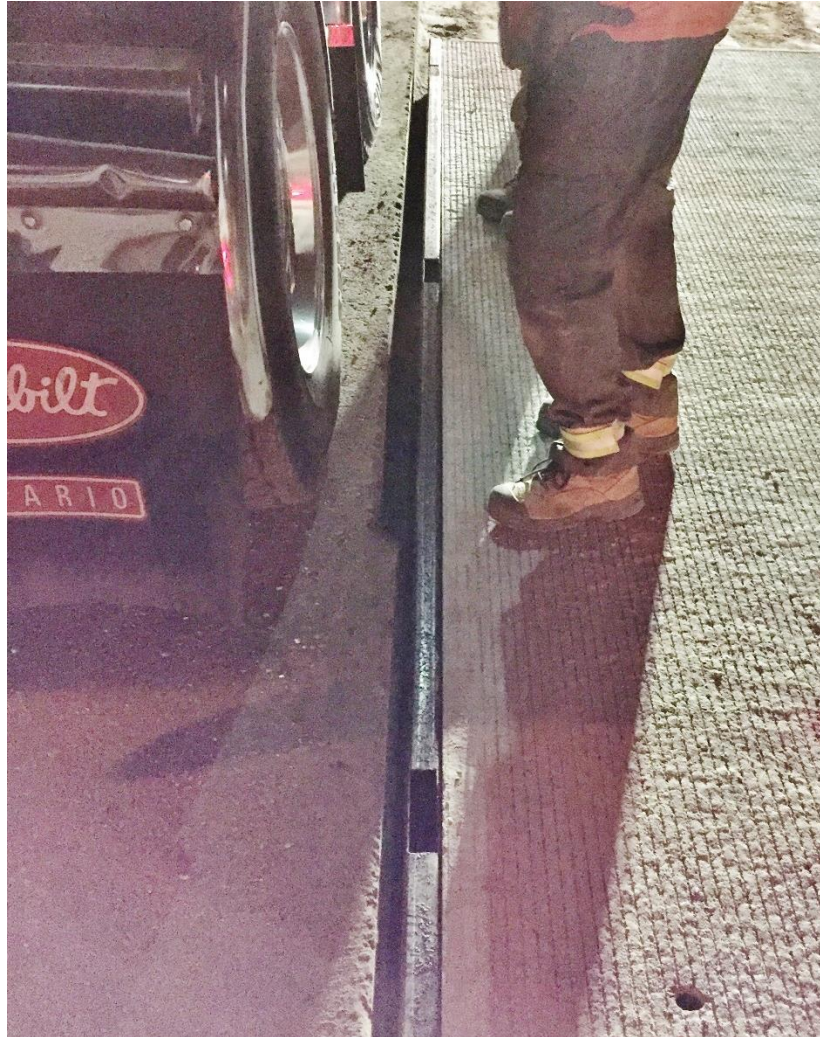


**Figure 5.29: Location where milled portion was widened**

This substantial gap presented a safety issue for opening the lane to traffic, even with the hollow steel tubes in the longitudinal joint. Dufferin made the judgement call to remove the steel tubes and place edge grout on one edge to fill this gap. The grouting crew was pulled off of the bedding grout on the Asphalt-Supported panels, and asked to begin placing the edge grout on one edge of the Grade-Supported panels.

This represented a significant change in the staging plan for the construction, and Dufferin began to make arrangements for extending the lane closure beyond the original 6 am opening time.

The final edge grout was placed by approximately 5:30 am, and Dufferin reported to have exited the roadway by 6:30 am.

### **5.3.6 Grout-Supported Trial Section (September 22<sup>nd</sup>, 2016)**

The Grout-Supported panels were placed during the construction period beginning on the evening of Thursday, September 22<sup>nd</sup>. The weather had intermittent light showers, with an average temperature throughout the evening of approximately 19°C.

The traffic control began at approximately 8:15 pm and access was granted to the site by approximately 8:30 pm. At this time the milling and grouting crews came on to the site and began preparing for their work. While the grouting operation did not begin immediately the previous night, this night they did. In part, this was because the Grout-Supported panels typically require same-night grouting. This meant that the previous night's as well as the current night's panels would require grouting.

The milling began at approximately 8:45 pm and the first pass was finished by 9:00 pm, the 32 m of required milling was performed in 12 minutes.

The grouting operation began at approximately 9:00 pm by completing the placement of bedding grout that had not been completed the previous night. The flow rate of the bedding grout was initially too low, and required additional water be added to the mix to achieve the proper flow.

The bedding grout had been completed for the Asphalt-Supported panels by approximately 10:00 pm. Following this, the grouting team switched to dowel grouting all the panels from the first two nights that had not yet been grouted. This was finished by approximately 11:00pm, at which point the crew switched to begin the bedding grout for the Grade-Supported panels.

The second lane was closed at approximately 10 pm, allowing for the final milling passes to begin early.

While grouting was taking place, saw-cuts were being made in the edge grout aligning with the transverse joints. The purpose of this was to induce cracking at these points, which would be preferable because this is where joint sealant would be applied and where there was no reinforcement in the longitudinal joint. Figure 5.30 illustrates the saw-cut crack control joint as well as the saw-cutting operation in the inset photo.

The main passes of HMA milling were completed by 10:30 pm, and the transverse pass of the milling machine at the first edge was completed by 10:45 pm.

The location of the first set of instrumentation was beneath the first Grout-Supported panel due to an alignment/cabbling issue. Therefore, the recessed section in which the instrumentation was placed could not be removed until after the transverse pass of the milling machine had occurred. Therefore, placement of panels could not begin until marking, saw-cutting, and chipping of this recessed area was completed. Generally, this was the first time that the instrumentation installation caused a delay in the construction operation.

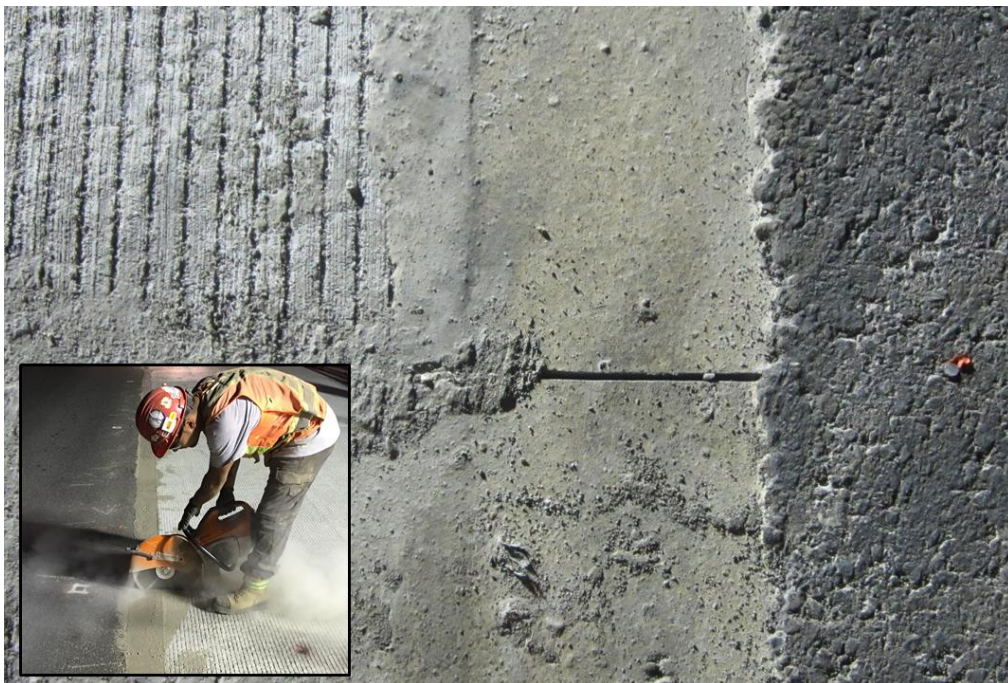


**Figure 5.30: Edge grout saw-cut at transverse joint; Saw-cutting (Inset)**

Instrumentation clusters were placed under the first and fourth Grout-Supported panels, panels number 16 and 19 overall.

After the instrumentation was placed, the first panel was lowered into place at approximately 11:45 pm, however it was immediately observed that the panel was not sitting flush on the roadway. This was attributed to several factors, including CTBM from beneath the temporary panel and imperfect milling at the ends of the lane. The CTBM was removed with crow-bars by the labourers, and

eventually high spots were removed using chipping hammers. The first panel was placed at approximately 12:15 am.

On this evening, the crane was placed ahead of the panel being placed, as opposed to behind like on previous evenings, to avoid cracking panels that may not have been completely supported – as may be the case when HMA is not milled to the same tolerance as that required for Asphalt-supported panels. Figure 5.31 shows the typical crane/panel orientation used to place the Grout-Supported panels.

The bedding grout for Asphalt-supported and Grade-supported panels was finished by 12:10 pm.

The placement of the edge grout for the remaining ungrouted edge of the Grade-Supported began at approximately 12:45 am. The excess moisture in the pea gravel again resulted in a mixture that segregated during placement, leaving a “honeycombed” surface texture. Three mixers (Figure 5.32) were used to produce the edge grout, resulting in efficient placement of the edge grout.

The final panel was placed at approximately 1:10 am (Figure 5.33), leaving a gap between the trailing panel edge and the milled HMA edge of approximately 25 mm.

After placement, the grout-supported panels were raised to the proper elevations using the integrally cast levelling lifts. This procedure began at 1:30 am. The pneumatic impact wrench that was brought to site to turn the levelling bolts was found to have insufficient torque to raise the panels. For this reason, a pipe wrench with an extended handle for higher torque was used to deploy the levelling lifts. Both of these methods for deploying the levelling lifts are shown in Figure 5.34.

By 2:00 am, all panels had been raised to the appropriate height and grouting could begin. Most of the levelling bolts were used on the Lane #2 side of the panels, as shown in Figure 5.35.

Grouting began with the transverse dowelled joints and the longitudinal edge joints at 2:15 am. The dowel grouting included all seven of the Grout-Supported panels, plus one Grade-Supported panel that had not been grouted earlier in the evening. The edge grouting began along the left-hand edge. The dowel grouting and the left-hand longitudinal edge grouting finished by 3:20 am and at this point the placement of bedding grout and the right-hand longitudinal edge grout began.

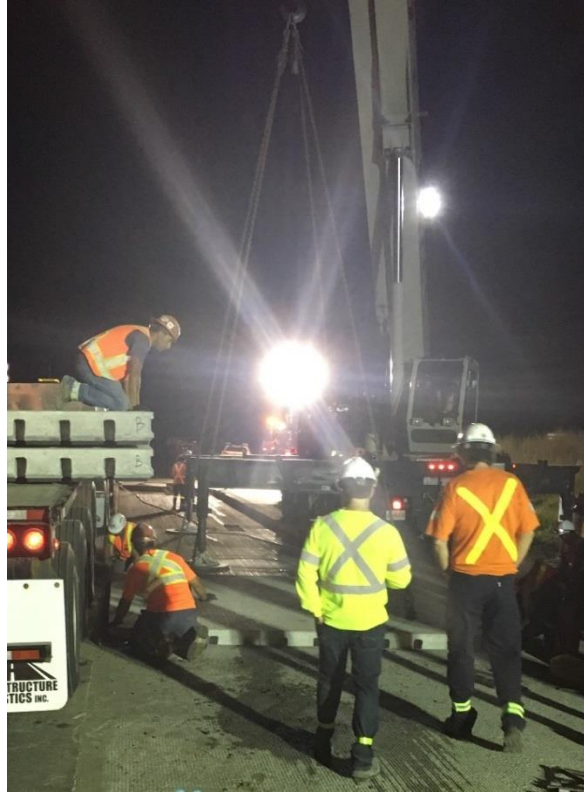


**Figure 5.31: Crane positioned ahead of panel being placed**



**Figure 5.32: Three mixers producing edge grout**



**Figure 5.33: Final panel being placed**

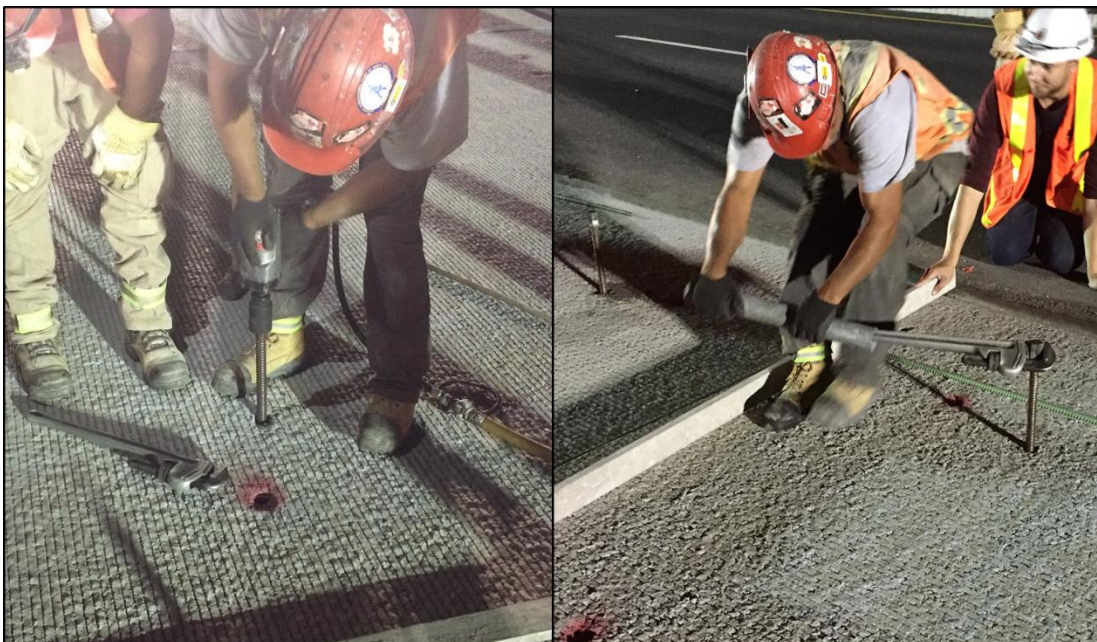


**Figure 5.34: Pneumatic Impact Wrench (Left); Extended Pipe Wrench (Right)**



**Figure 5.35: Panels with levelling bolts inserted**

During installation of bedding grout, the clean-out frequency of the mixer was extended to allow for the grout beneath two panels to be placed between cleanings. Each panel required approximately 14 bags of bedding grout, meaning approximately 27-28 bags of grout were mixed between each cleaning of the mixer.

The longitudinal edge grout was completed at approximately 4:00 am, and the final bedding grout was placed at 4:30 am. After cleaning and loading up, the site was vacated by 5:30 am.

#### **5.4 Construction Summary**

Table 5.3 summarizes some of the statistics regarding each support condition type. The time estimates are approximate based on notes taken on site as well as time-stamped photos and videos. It should be noted that eight panels were placed for the Asphalt-Supported condition, so the milling and panel placement times are referring to a slightly larger section. Furthermore, the milling time for Asphalt-Supported panels includes the time for both the original milling, and the second round of milling when the crew was called back to the site.

**Table 5.3: Summary of Construction Activities**

	<b>Asphalt-Supported Installed Sept 20/16</b>	<b>Grade-Supported Installed Sept 21/16</b>	<b>Grout-Supported Installed Sept 22/16</b>
<b>Number of Slabs</b>	8	7	7
<b>Milling Time (min)</b>	215	120	75
<b>Milling Time (min/m)*</b>	5.9	3.8	2.3
<b>Slab Placement Time (min)</b>	70	90	85
<b>Time per Slab (min)</b>	8.8	12.9	12.1
<b>Bedding Grout Bags per slab</b>	12	4	14
<b>Overall Time On Site (hr:min)</b>	9:00	10:00	9:15
<b>Time of 2nd Lane Closure</b>	10:50 PM	10:15 PM	10:00 PM

\*average time per meter length of 3.66m lane. Milling machine was considerably faster at 1.2 m width

As shown in Table 5.3, the required amount of bedding grout varied between the different support conditions. The Grout-supported panels required the most bedding grout and this was an expected result as the levelling bolts were used to produce a void beneath the panels to be filled by grout. The Grade-supported panels required the least bedding grout, indicating that the graded material and the bottom surface of the panels aligned well, with few voids between the two surfaces. The relatively high bedding grout requirement of the Asphalt-supported panels indicates that the  $\pm 3\text{mm}$  surface tolerance of the milled surface was not achieved, and substantial voids beneath the panels required filling with bedding grout.

Each night, two 6-person crews of Dufferin workers were on site. Generally, they divided up as panel placement and grouting crews, however these divisions were fluid as each night required different activities, including helping to install instrumentation.

Grouting was not performed in a linear order, and often included parallel tasks occurring at once. Therefore, estimating the times of each grouting operation was not undertaken. Generally, it was found that there was sufficient time in each case to grout the panels that were placed the previous night. On September 21<sup>st</sup> and 22<sup>nd</sup> portions of two sections were grouted in one night, though for different reasons.

The following section summarizes some of the findings and notable points from each night of construction. The findings applicable to all support conditions are outlined first, followed by those specific to each separate support condition.

#### **5.4.1 General Findings**

- 1) Some flexibility was observed in lane closure times (specifically Lane #2). The effects of stricter closure times are difficult to gauge based on this trial procedure.
- 2) Milling equipment can do a transverse milling pass, which greatly reduces the amount of handwork required at nightly milling extents although this process did inflict damage on the adjacent HMA pavement. Some chipping of remaining HMA is still required, but only at the corners, as opposed to the full lane width.
- 3) The milling method used on this project could not accommodate depth and cross slope inputs as originally hoped for. By referencing the milling off of a ski riding along the edge of the existing shoulder, the depth and cross slope can only be made relative to that reference plane. After all passes were finished, the depth and cross slope needed to be checked before the milling team can leave the work zone . This was done using stringlines, levels, and measuring tapes on site, with some success. Ideally, the miller should start on the high side of the lane (ie. adjacent to Lane 2 for Lane 3 milling) to ensure the cross slope is maintained across the lane width.
- 4) Care should be taken to adhere to the limits of the milled area. Accidentally extending the milled width resulted in a need to install edge grout on the same night that the panels were placed. This could have greater impact in future applications in which the edge gap is significantly smaller to avoid hollow structural steel.
- 5) As a follow up to Point 4), the edge grout detail on this project provided a level of redundancy in the case of milling errors such as the one experienced. The edge-grouting crew was able to fill the void in order to reinstate traffic with little delay.
- 6) Overall, milling time was significantly reduced as familiarity with the strategy was gained.
- 7) It was found that the remaining HMA thickness after milling was approximately 140 mm.
- 8) The first panel in each support condition presented difficulties with base preparation. It was found to be very difficult to achieve a smooth surface using chipping hammers. This

would be remedied in part by removing the temporary end panel prior to milling, which is a consideration for future applications.

- 9) Unloading procedure should be reviewed for safety. The panel truck parked in lane adjacent to traffic made potential interactions between the two possible. Cranes with long cable lengths appear to make the possibility of a panel swinging out into traffic likely although that risk can be managed by mandating the use of tie ropes during placement. Positioning the panels on the shoulder or in the same lane may provide a larger buffer between the panels and traffic, however this alignment is often not practical or possible on three lane highways.
- 10) Bedding grout initially required mixer clean-outs every 4 batches (16 bags), but this was eventually reduced to clean-outs every 7 batches (28 bags). This is partially due to increased efficiency of mixer discharge as soon as grout is prepared. This improved throughout the course of construction. Grout crew members need to be careful to observe for signs of grout setting-up (steam), as this can bring grouting to a stop for the night.
- 11) Water content of constituent materials needs to be accounted for. In the case of edge grout, the high moisture in the pea-gravel caused the material to segregate upon placement, leaving a honeycombed surface that is expected to ravel relatively quickly. The water proportioning of the grout should be done incrementally if the moisture contents of the materials are unknown. In the case of the CTBM, the water content in the sand caused the material to clump and begin hydrating on site while being mixed in the concrete truck. A trial batch of CTBM should be made before it is sent to the job site to make sure it is dry enough to be graded and compacted efficiently, to avoid the clumping observed on this project. Alternately, the cement could be added and mixed with the sand on site just prior to placement.

#### **5.4.2 Asphalt-Supported Trial**

- 1) This strategy was not flexible in responding to milling mistakes. The precise HMA profile that is required means that milling must be done to tight tolerances. Depth and slope tolerances of the milled surface were found to be the most difficult to achieve.
- 2) Once milling tolerances were achieved, the placement of panels progressed quickly.

### **5.4.3 Grade-Supported Trial**

- 1) Depth of milled surface presented problems. Changes in milling depth from the previous night may have contributed to this. This strategy allowed for flexibility to accommodate changes in milled depth.
- 2) Placement of screeding rails requires a minimum of three persons. Proper planning is required for their placement.
- 3) Extra machinery (screed, rails, and tamper) produces greater potential for break-down on site, (ie. the handle on the screed was broken on site). Also, the rails that the screed ran on have the potential for tripping workers entering and leaving the milled area. The rails also interfered with the location of the trucks bringing the panels to be unloaded.
- 4) Hardened CTBM beneath temporary panel required extra effort for removal the following night. This issue would not be critical if temporary panels were removed prior to milling, or if there wasn't a transition between support conditions between nights.

### **5.4.4 Grout-Supported Trial**

- 1) Positioning the crane ahead of the panels being placed worked reasonably well. This orientation meant that the cab of the truck was not an obstacle as panels were rotated away from the cab.
- 2) High-torque impact wrench is required in order to effectively lift panels prior to grouting. Extended pipe wrench was found to work well as a redundancy but required significantly more effort and time.
- 3) When raising the panels, enough levelling bolts should be present on-site to engage all levelling lifts. Issues were avoided in this instance, but if all levelling lifts were required, there were not enough bolts.

## 5.5 Constructability Analytical Hierarchy Process<sup>2</sup>

As part of the trial, three methods for providing sub-panel support (AS, GraS, and GroS) were designed and constructed, each with inherent advantages and disadvantages relating to PCIP's constructability. Following construction, the support methods were analyzed with respect to construction-related criteria, using the Analytic Hierarchy Process (AHP). The relative weighting of these criteria was determined based on input from MTO staff while the relative performance with respect to the criteria, was provided by members of the trial section's construction contractor. This analysis identifies the support method that provides an overall advantage in the construction of a PCIP rehabilitation.

The in-situ performance of each of the different PCIP support conditions will ultimately provide insight into its viability as a rehabilitation technique, but feasible overnight construction of the support condition is essential to successfully implementing PCIP.

### 5.5.1 Construction Activities

While each support condition's construction is unique, as outlined previously, general aspects of the construction are shared. Figure 5.36 shows each support condition's construction according to these general aspects.

The extents of the HMA removal were demarcated during the first night of construction using full-depth saw-cuts. These saw-cuts were intended to provide a clean vertical surface following HMA milling. Saw-cutting is the first night of construction for each support condition in Figure 5.36.

It should be noted that the AS condition included the placement of eight panels while the GraS and GroS conditions included seven.

---

<sup>2</sup> The contents of this section of the chapter have been incorporated within a paper that has been submitted for publication. D. Pickel, D. Malek, and S. Tighe, "Using Analytic Hierarchy Process for Assessment of Precast Concrete Inlay Panel Construction: A Canadian Case Study" Submitted to Precast/Prestressed Concrete Institute Journal. Submission date: January 25, 2018.

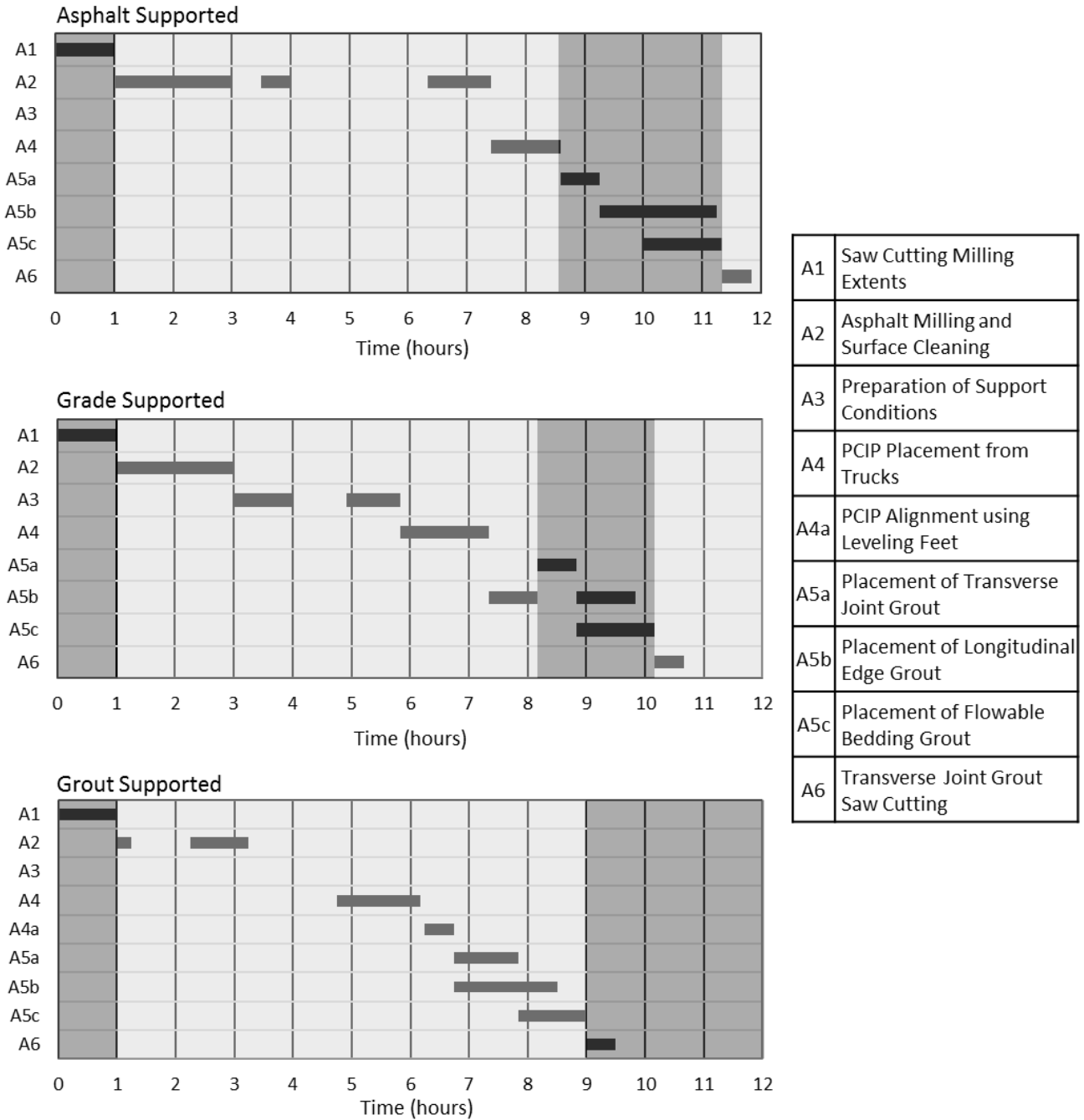


**Figure 5.36: Construction activity timing for each support condition**

The times in Figure 5.36 are as-observed during the construction periods, beginning with saw-cutting on the first night. Notable gaps in a construction activity, such as those in AS: A2 (asphalt milling) indicate a pause in that activity. In this case, the first small pause indicates the period between the first pass of the milling machine and the second. As a result of the use of progressive closures, only the right side of Lane #3 was initially milled to avoid encroaching on traffic in Lane

#2. When Lane #2 was closed, the rest of the milling was done. The second pause represents the period during which the milled surface was checked for compliance to the specifications after the first milling crew had left the site. More milling was required, so a second milling crew was brought onto site, at which point the final milling took place.

A similar pause can be seen in GraS: A3 due to the material issues encountered with the CTBM, discussed previously. In addition, the GraS: A4 (panel placement) and A5b (longitudinal edge grouting) took place the same night, despite the original plan to grout the following night. This was due to the over-milling, which resulted in wider-than-intended milled recesses.

A pause can be seen between GroS: A2 (milling) and A4 (panel placement). This represents a period when manual chipping of the HMA surface was performed due to improper milling. Following chipping and cleaning, panel placement began.

In typical construction projects wherein repetitive steps are undertaken, the efficiency of the completion of these steps tends to improve over time as the construction team progresses along a learning curve. Since the nightly trial construction represented the first time that each support method was constructed, improvements in construction efficiency were not realized on this trial project. In future applications, addressing the concerns that resulted in construction process pauses would result in higher installation rates. Furthermore, if the PCIP design was implemented on a larger scale, different aspects of the construction could be undertaken concurrently by several crews. The relatively small scale of the trial resulted in the work being undertaken by two construction crews; one focused on grouting the previous night's panels while the other focused on placing the panels. This organization resulted in the sequential order of construction operations that can be seen throughout Figure 5.36.

### **5.5.2 AHP Methodology**

The feasibility of the PCIP rehabilitation technique is highly dependant on its constructability, which varies for each of the three support conditions. The constructability of the support conditions was compared through use of the Analytic Hierarchy Process (AHP).

The AHP is a multi-criteria decision-making tool widely used in the engineering field (Vaidya & Sushil, 2006). The AHP provides a method of reaching sound, justifiable decisions based on both

quantitative and qualitative criteria. For qualitative criteria, input is required from users to determine the importance, preference, or value of one criterion over another based on the individual's personal experience and rationale. Based on these inputs and quantitative data, weightings of the criteria and rankings of the alternatives are established (Saaty T. L., 2013).

The AHP can be easily constructed, does not require those providing input to have technical expertise of decision-making tools, and can incorporate input from many individuals enabling groups to reach a consensus on shared values (Saaty T. L., 2013). The statistical significance of AHP results has been questioned in the past, and the traditional AHP method does not quantify uncertainty due to variations in assigned values (Banuelas & Antony, 2004; Scott, 2002). Therefore, for the assessment of the support conditions, sensitivity analyses, using limits set within a reasonable context of a given decision, were performed to provide some insight into the significance of the results.

An AHP is conducted through four main steps. Firstly, the goal of the analysis is determined, which in this case is determining the PCIP support condition that is most ideal for construction. Secondly, alternatives are identified, and a set of criteria are established that can be used to compare and differentiate the alternatives. Thirdly, the performance of each alternative is compared with regards to the criteria. These comparisons are made pair-wise such that each alternative is compared to each other alternative. A similar comparison is performed between each of the criteria to determine the relative importance or weight of each criteria. Finally, the alternative priorities for each criterion are synthesized into an overall or global priority, which indicates the ideal alternative given the relative performances of each alternative for each criteria.

An AHP was implemented to rank the three support condition alternatives (AS, GraS, and GroS) based on four constructability criteria: relative cost, installation rate, repeatability, and resiliency. The AHP organizes the problem into a hierarchy that includes the goal, criteria, and alternatives, illustrated by Figure 5.37.

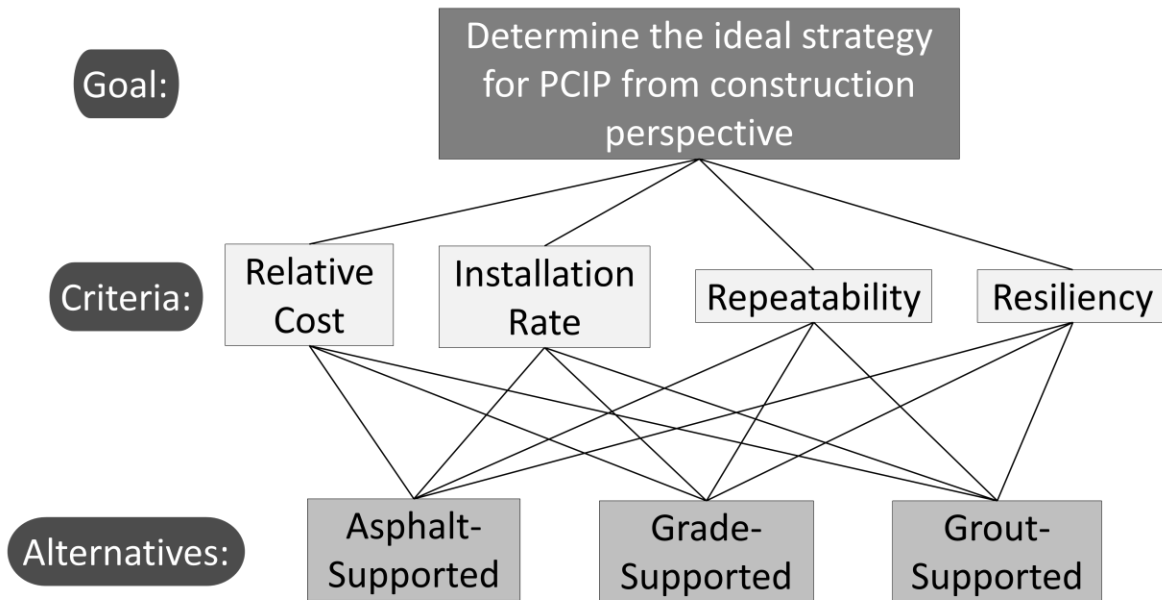


**Figure 5.37: AHP hierarchy for the PCIP evaluation**

An overview of the AHP procedure for ranking the alternatives based on constructability is illustrated in Figure 5.38. As shown, the input from MTO staff was used to determine the relative importance of the criteria used for the analysis. Input from the contractor’s construction team was then used to compare the three alternatives according to the four criteria. These inputs were then synthesized into a final priority that took the shape of an overall ranking.

Each of the steps of this analysis are described in the following sections to outline the process of obtaining the overall ranking of the support conditions.

### **5.5.2.1 Constructability Criteria**

The comparison criteria form the bases for comparing the alternatives. These criteria were developed based on input from the various stakeholders in the trial project. Each criterion was developed to represent a different factor an agency would consider when comparing various rehabilitation options.

**Relative Costs** This criterion reflects the cost of each support condition relative to the others. The cost of a given rehabilitation technique is typically important for a transportation agency, as they must justify all costs to taxpayers. The PCIP strategy is a specialized rehabilitation technique developed to address the high user-costs associated with the short service life and frequent repairs

using the mill-and-replace strategy. For this reason, a higher unit cost might be acceptable, under the assumption that PCIP would provide longer service life without needing substantial road reconstruction necessitating long-term road closures. Costs only reflect the initial construction costs, as the life-cycle costs will depend on the strategy's service life, which is currently unknown.

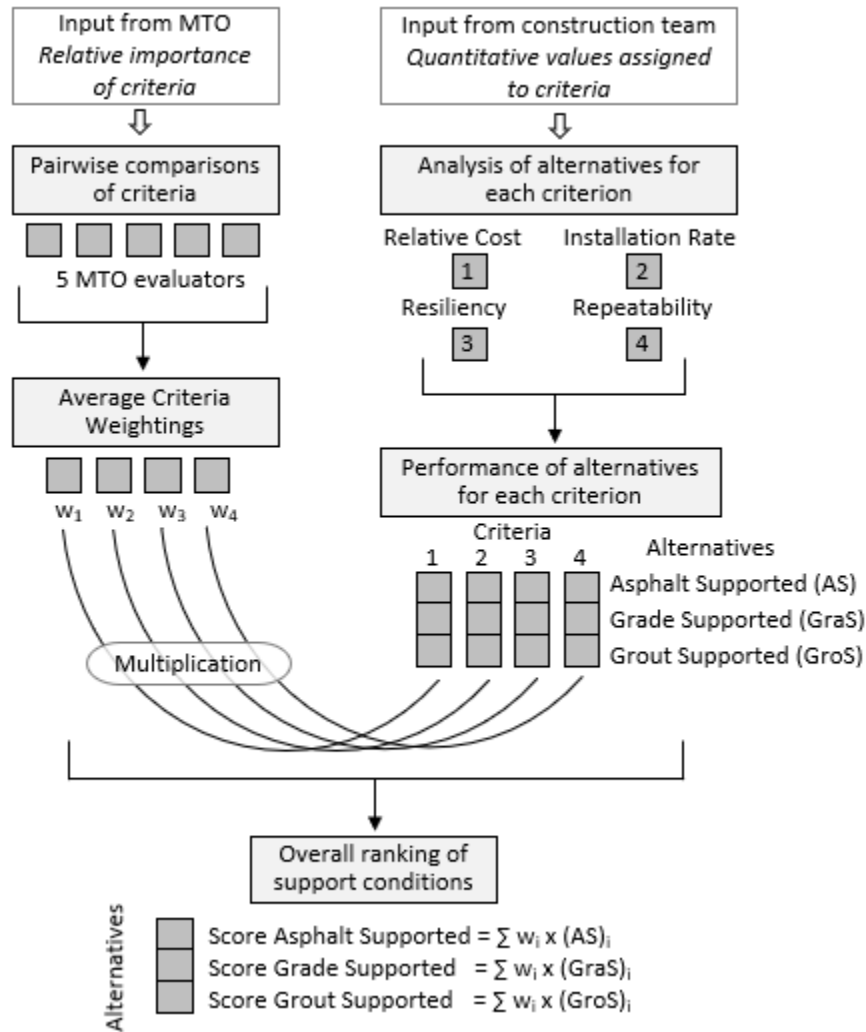


**Figure 5.38: Flow chart of AHP steps for ranking support conditions**

**Installation Rate** The second criterion relates to the rate at which the panels could be installed under typical conditions. Agencies have an interest in reducing the construction times on their high-volume roads to minimize the impacts on users. The time required to repair a given length of road is a function of the installation rate. While actual construction times were measured, these measurements do not account for any benefits of learning curves that are typically realized in

construction applications and are not expected to be representative of a full-scale PCIP project. Therefore, the nightly installation rates used in the AHP are estimates based on the contractor's experience with the trial section and road construction.

**Repeatability** Repeatability is a subjective criterion that indicates the ease of installation. This criterion reflects the benefits for construction of having fewer, simpler installation steps. While construction on a high-volume highway project is likely to be performed by a trained and effective construction crew, a highly repeatable operation would have fewer sources for error during construction, resulting in fewer opportunities for cost and time overruns. The repeatability criterion is related to installation rate but provides insight into the potential for errors that can have repercussions beyond installation rate.

**Resiliency** The resiliency criterion is also subjective and reflects the ability of the given support condition to be adjusted during construction to accommodate unforeseen on-site conditions. Unforeseen on-site conditions are difficult to predict, but might include insufficient HMA depth following milling, over-milling (both depth and width), unexpected weather events, and deteriorated HMA base layers.

#### ***5.5.2.2 Pairwise Comparisons of Criteria***

A pairwise comparison consists of comparing two components at a time and assigning a value representing the ratio of importance of component A to component B ( $w_A/w_B$ ). The evaluator selects a value from the “fundamental scale” that contains integer values ranging from 1 to 9 and their reciprocals (1/9 to 1/1), where a value of 1 indicates that the components are of equal importance, a value of 9 indicates that component A is extremely dominant over component B, and the reciprocals are assigned to indicate the dominance of component B over component A. This fundamental scale was derived mathematically to ensure that a small change in the selected scale value will not have an unduly large influence on the resulting priorities determined by the AHP. The scale is also designed to be intuitive to use and assign values to comparisons (Saaty T. L., 2013).

Past and present MTO engineers performed the pairwise comparisons, and this input was used to calculate weightings of the constructability criteria. Table 5.4 illustrates an example of a pairwise matrix used to develop rankings of relative importance of the criteria. This matrix contains the

input from one evaluator, and each evaluator completed a similar matrix. In the example shown, Relative Cost was deemed to be five times more important than Resiliency to PCIP construction while Resiliency is shown to be 1/9 as important as Installation Rate.

**Table 5.4: Pairwise Comparison Matrix Example**

Criterion A \ Criterion B	Ratio of Importance of Criterion A to Criterion B ( $w_A/w_B$ )				Relative Criteria Weighting
	Cost	Installation Rate	Repeatability	Resiliency	
Relative Costs	1	1/3	3	5	0.250
Installation Rate	3	1	5	9	0.566
Repeatability	1/3	1/5	1	5	0.138
Resiliency	1/5	1/9	1/5	1	0.046

The normalised eigenvector of the pairwise comparison matrix values then represent the relative weightings for each criteria, shown in the last column of Table 5.4. These weightings were compared to a consistency ratio of 10% to ensure that the pairwise comparisons were made to an acceptable level of consistency, throughout. The consistency ratio is a function of the maximum eigenvalue compared to that of a random matrix. The consistency measure ensures that if component A is found to be more important than component B, and B is found to be more important than component C, then component A should be more important than component C. (Saaty T. L., 2005)

The individual weightings were averaged to produce the average relative criteria weightings shown in Table 5.5.

Installation rate and cost, weighted at 0.497 and 0.272, respectively, were determined to be the most important criteria. Repeatability and resiliency were relatively less important with weightings of 0.154 and 0.077, respectively. MTO feedback indicated that the contractor should meet a minimum level of competency and that the repeatability should not be a deciding factor. Similarly, it was stated that comprehensive site investigation prior to construction could reduce the risk of unexpected site conditions, thereby reducing the importance of resilience. These statements indicate that these relative weightings would be subject to change under other construction and contracting conditions.

### ***5.5.2.3 Evaluation of Support Conditions***

Contractor personnel closely involved in the trial construction provided feedback regarding the constructability of each support condition, informed by their experience with the trial construction. The personnel included crew foremen and project managers. Each evaluator assigned values for the three support conditions indicating installation rate, repeatability, and resiliency. The installation rate is an estimated number of panels that could be installed per night, and repeatability and resiliency are scores on a scale of 1 to 10.

The cost of each support condition was considered to be private information, however typical unit costs for the various construction operations were provided to develop a cost estimate. This estimate was based on the cost of installing 10 panels and was afterwards deemed by the contractor to be a reasonable approximation of the costs.

The assigned values correspond to observations and comments made by the contractors regarding the construction process. For example, the asphalt-supported condition was deemed to have the lowest repeatability, as seen from the average values in Table 5.5. This can be partly attributed to the inconsistent control of the milling depth that was found to be a limiting factor for the AS panels.

The grout-supported option was identified as being the most “stress-free” alternative, due to less stringent milling requirements and a forgiving levelling procedure. Levelling lifts were installed in all panels as a precaution, though they were only deployed in the GroS alternative. The levelling feet are an integral design feature to the GroS, and a resiliency-increasing contingency in the other alternatives, which indicates a higher level of inherent resiliency in the GroS method. The contractor comments indicated that this feature should be a contingency system built into all future applications of PCIP.

The grade-supported panels were noted to require extra steps in comparison to the other support conditions due to the preparation of the CTBM. This resulted in a slower installation rate for the GraS than other alternatives. The feedback received was that the additional steps for this alternative seem counter-productive since the overall goal of PCIP is to minimize the construction periods.

The evaluations from all the surveyed members of the construction company were amalgamated to produce average values for these criteria for each of the support conditions, summarized in Table 5.5.

**Table 5.5: Quantitative Values of Evaluation Criteria**

Criterion	Average Relative Criteria Weighting	Average Values				Performance Weighting of Alternatives in each criterion		
		Unit	AS	GraS	GroS	AS	GraS	GroS
Cost	0.272	\$	106,855	108,621	107,072	0.335	0.330	0.335
Installation Rate	0.497	panels /night	40	30	43	0.354	0.265	0.381
Repeatability	0.154	/10	5.4	8	8	0.252	0.374	0.374
Resiliency	0.077	/10	6.4	5.8	6.2	0.348	0.315	0.337

The average values were then subjected to an eigenvector analysis, similar to that outlined for the criteria weighting, which produced a performance weighting for each support condition alternative within each evaluation criterion. The product of these performance values and the average relative weightings of the criteria produced overall scores.

#### 5.5.2.4 Overall Scores of Support Conditions

Table 5.6 summarizes the overall scores of each support condition, based on the products of the relative criteria weightings and performance weightings. The overall score is the summation of these products across all criteria for a given support condition.

**Table 5.6: Overall Scoring of Support Conditions**

Support Condition	Contribution of Alternative's Performance in each Criterion				Overall Score
	Cost	Installation Rate	Repeatability	Resiliency	
AS	0.085	0.176	0.039	0.027	<b>0.326</b>
GraS	0.084	0.132	0.058	0.024	<b>0.297</b>
GroS	0.104	0.189	0.058	0.026	<b>0.376</b>
$\Sigma$	0.272	0.497	0.154	0.077	1

Based on the construction-related criteria, the Grout-Supported condition was the highest scoring method for PCIP installation. The Asphalt-Supported technique was the second highest ranked option.

All three options were ranked closely to one another, with only an approximately 20% difference between the highest and lowest ranked techniques. This finding is supported by the results of the trial section construction. Each technique had challenges, but all methods produced functioning panels without any substantial issues.

This result does not preclude any of the three support techniques, and it is possible that project-specific circumstances could relatively improve any of the three studied conditions. However, based on the circumstances of this construction, the GroS condition is the support technique recommended for future PCIP applications.

### **5.5.3 Confidence in the AHP Ranking Results & Significance**

The AHP is well-suited to consolidating various subjective and objective criteria into one result for the purposes of decision making. However, the AHP does not include a method of measuring the statistical significance of its results (Banuelas & Antony, 2004; Scott, 2002). One method for analyzing the significance of a given result is to use sensitivity analyses to determine the effects of changes in the input values on the analysis results.

Two separate sensitivity analyses to determine the reliability of the results. The first investigated the effects of changes in the criteria weighting (provided by MTO personnel), and the second investigated the effects of changes in the average quantitative values (assigned to the criteria by contractor personnel).

#### **5.5.3.1 Criteria Weighting Sensitivity Analysis**

The individual criteria weightings were generally consistent across all submissions, but some variability was observed. To investigate the sensitivity of the result to this variability, a sensitivity analysis was undertaken. Using the normalised eigenvectors of each pairwise matrix submitted by MTO staff, the maximum and minimum weighting for each criterion was noted. Then, to undertake the sensitivity analysis, one criterion's maximum weighting was considered while the remaining criteria were factored down such that the sum of all weightings remained 1, which is a requirement

of an AHP. The weighting of each remaining criteria was not factored below the minimum value observed for that criterion. In this way, the maximum and minimum submitted responses provided the bounds of the sensitivity analysis. The AHP was then re-conducted based on the adjusted weightings, producing overall scores for the three support conditions. This process was repeated, maximizing each constructability criterion based on its maximum observed weighting. Table 5.7 summarizes the results of this analysis.

**Table 5.7: Criteria Weighting Sensitivity Analysis**

Support Condition	Overall Scores adjusted for the Maximized Criterion Weighting				Unadjusted Overall Score
	Cost	Installation Rate	Repeatability	Resiliency	
AS	0.331	0.337	0.327	0.334	0.333
GraS	0.317	0.295	0.308	0.305	0.304
GroS	<b>0.352</b>	<b>0.367</b>	<b>0.364</b>	<b>0.361</b>	<b>0.364</b>

It was found that the results of the AHP were not sensitive to changes in the criterion weights within the limits set for the analysis. Only slight changes to the overall scores for each alternative were observed, and the relative ranking of the alternatives did not change in any case. This provides a degree of confidence in the results, considering the variability that was observed in the criteria weightings.

### **5.5.3.2 Contractor Scoring Sensitivity Analysis**

The relative performance of each alternative for each criterion used in the AHP was based on average values collected from several members of the contracting team. As such, a range of responses was collected, and the maximum and minimum value in each case were chosen to provide the bounds of a second sensitivity analysis.

In this analysis, the effects of changes to these values for one criterion were analyzed while keeping the other criteria at their average values. For each criterion, the optimum value observed for one alternative was selected while the least-optimum values were selected for the other two alternatives. The overall score of the different alternatives was then determined based on an AHP using these adjusted values.

For instance, while considering the effects of skewing the input values of installation rate, the input values for cost, repeatability and resiliency were kept at their average. The installation rate was skewed in the favour of one alternative by selecting the maximum installation rate (optimum) observed for that alternative while selecting the minimum installation rate (least optimum) observed for the other two alternatives. The AHP analysis was performed using these adjusted values. Then the process was repeated to skew the criterion in favour of a different alternative. After repeating this process for each of the three alternatives for one criterion, this process was repeated for a new criterion. This required 12 iterations in total.

The results of this analysis are illustrated in Figure 5.39. The results, in terms of overall scores of the three alternatives, are segregated by the criterion being manipulated. The original scores of each alternative are included as horizontal lines to provide context.

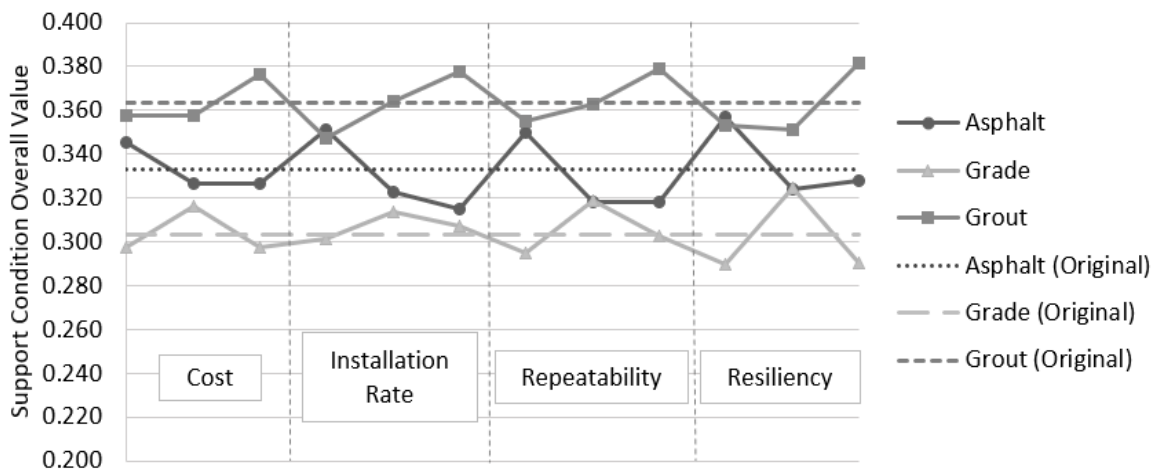


**Figure 5.39: Alternative score sensitivity analysis results**

The cost values were developed based on unit costs and did not have a maximum and minimum response to define the range of the sensitivity analysis. In this case, a 10% decrease in the calculated cost was defined as the optimum value while a 10% increase in cost was considered the least-optimum value.

This sensitivity analysis reflects the possible results when considering the entire range of performance values that were provided by members of the contracting team. The results of this analysis indicate that even considering potential fluctuations in the values assigned for each criterion and each alternative, the grout-supported alternative was still consistently ranked as the

most favourable choice. Under two conditions, the asphalt-supported condition was slightly favoured above the grout-supported alternative by 0.4%, or approximately equal.

Based on this analysis, the overall score of the alternatives was largely found to not be sensitive to the effects of changing the quantitative values within the defined bounds. This bolsters the conclusion, that based on this trial installation of PCIP technology, the grout-supported alternative was found to be the most favourable from a construction viewpoint.

It should be noted that the conclusions drawn from the AHP analysis are based only on the relative constructability of the different support conditions, and the long-term durability and life cycle costs were not a part of the analysis.

### ***5.5.3.3 AHP Conclusions***

An Analytic Hierarchy Process (AHP) was undertaken to compare the different construction types based on their relative performances in four evaluation criteria: cost, installation rate, repeatability, and resiliency. The importance of each criterion to a transportation agency was established by pairwise comparisons of the criteria, performed by members of the MTO. The average results of these comparisons indicated that the order of the criteria, from most to least important, was installation rate, cost, repeatability, then resiliency.

The contracting company that installed the trial PCIP project assigned quantitative values to installation rate, repeatability, and resiliency for each of the construction types. Actual cost information was not made available, so the cost of each construction type was based on unit costs. The averages of these quantitative values were used for the AHP. General comments about the construction types were also collected. Generally, it was felt that the GroS design was straightforward and repeatable. The AS design was reliant on milling performance, which was found to be variable during the trial. The extra material involved in the GraS condition were expected to reduce the installation rate.

The AHP analysis indicated that the GroS construction type was the most favourable from a construction standpoint, with AS and GraS ranking second and third, respectively. While the reliability of results obtained using the AHP cannot be quantified, the results indicate a reasonable basis upon which an agency could specify a PCIP construction type. Two separate sensitivity

analyses were conducted considering the effects of changes in both the criteria weighting and the contractor's assigned values. The limits of these analyses were set to the maximum and minimum responses obtained from both the MTO and contractor. Based on these analyses, it was found that the ranking of the construction types was largely insensitive to reasonable changes. Under some conditions the AS and GroS construction types were found to be approximately equally favourable, but most of tested circumstances still indicated that the GroS was most favourable.

Constructability of the support condition is a critical factor for the success of PCIP as a repair strategy, since rapid construction is an essential requirement. The constructability evaluation demonstrates the feasibility of an adequate PCIP support condition and should inform any future applications of this strategy. Furthermore, the concepts of constructability and decision criteria described in this section may be applied to other applications of precast concrete pavement.

## **5.6 Construction Conclusions**

### **5.6.1 Saw-Cutting Requirements**

During and after the construction, consideration was given to the necessity of saw-cuts prior to milling the HMA lane. From a construction staging stand-point, it required that an additional night of work be scheduled prior to the placement of panels because saw-cutting and panel placement cannot occur on the same night. The straightness and accuracy of the milled surfaces on site were generally found to be of good quality.

The vertical face of the milled surface was observed to be rougher than the vertical saw-cut faces. There is no standard for smoothness of a vertical face in this type of rehabilitation, so the acceptability of this surface is subjective. Figure 5.40 shows the vertical face.

There are many considerations required to determine the best practice for this rehabilitation strategy. A rougher face may help to form a bond between the grout and HMA allowing it to behave more monolithically. Conversely, the saw-cut could serve as a guide for the milling operation. It was found on the second night of milling that the milling machine over milled the section such that the widths of the gaps on either edge of the precast panels were too large to open traffic. This indicates that the milling on this project was not precise, even with a saw-cut serving as a guide. The precision of the milling operation will serve to inform the necessity of saw-cutting

going forward. If the milling machine is not remotely guided using survey data, then at least a highly visible line denoting the extents of milling may be necessary.



**Figure 5.40: Vertical milled surface**

Transverse saw-cuts were also considered unnecessary by the contractor, although they were detailed in order to better facilitate the hand-removal of HMA that cannot be done by the cylindrical milling head. The contractor expressed that in future applications of this project, a small milling head would be fitted to a skid-steer loader to ease this removal operation. This may somewhat negate the benefits of a transverse saw-cut.

### **5.6.2 Milling**

Surveying and laying-out joints beforehand was generally found to be worthwhile and aided in the proper placement of the panels.

The grade control of the milling operation presents the biggest challenge remaining for the application of this technology. Challenges include inputting the existing and final surface

characteristics into the milling machine as well as checking the milled surface for conformance. Manually checking using a stringline was the contractor's preferred method, which seemed to work well during construction. The four points representing the corners of each panel were thought to be the critical considerations, and elsewhere the only consideration was that the depth could not be less than the prescribed depth. Based on experience, Fort Miller cautions against the stringline method as it relies on only two points (lane side and shoulder side) per measurement. The surfaces of the existing pavement were found to have considerable variations, and therefore these points may not catch the full variability beneath any given panel. A rail system or scan system captures and accounts for this variability better.

One option is to develop some easily-implemented QC methods that could be used to immediately check the depth and cross slope of a milled surface.

A "design cross slope" for each section was developed based on the surveyed cross slopes within the section extents and provided to the milling machine operator, however this was found to be troublesome to the operator and not practical or easily implemented in the milling process. One potential solution that the MTO is currently exploring is the use of total scans (possibly provided by ARAN technology) to be fed into milling machines to provide a more uniform base for the placement of HMA. This is currently being considered in order to address issues with final pavement surfaces that are straying further and further from design drawings on several sections. Similar technology could be implemented here. Future applications of PCIP should explicitly specify the use of milling equipment that can be accurately guided off of a previously developed 3-D surface model or a reliable reference (such as a Global Navigation Satellite System reference or levelled rail) to produce a planar surface at a constant cross slope. The use of milling machine-mounted skis running on the surface of the shoulder or adjacent lane as a reference point cannot produce a consistent cross slope.

In future MTO applications, levelling bolts would be incorporated into all panels to provide a "safety net" for improper milling. The cost of Gracie lifts was not prohibitively expensive, and incorporation into all panels would not drastically alter their cost.

One more consideration was the width of the milling head. Typical HMA milling is performed with a 2.2 m wide milling head (as opposed to the 1.2 m head used on this project). The wider

head would streamline the milling operation, reducing the time required for the milling component of the construction even further.

The milling accuracy on site indicated that the HSS tubes were unnecessary and could likely be removed from the design in future iterations. A narrower gap could be milled to place grout along the longitudinal edges of the panels without reinforcement, and allowing the edges to be opened to traffic prior to grouting. This would also negate the requirement for pea gravel-extended grout, which added a level of complexity on site (on-site mix design, effects of excess moisture in mix design resulting in some segregation, etc.). Removing the HSS tubes simplifies the procedure and remove some cost. The maximum acceptable width of gaps between panels and HMA should be agreed upon and specified by the MTO. Some uncertainty was encountered on site regarding when edge grouting was necessary on the same night due to large gaps. Furthermore, to ensure that panel placement is not impeded, a tight tolerance for milling and sawing will be required. Milling to this tolerance was not observed in this trial, and would need to be closely monitored for if included in the specifications.

The use of a specialized protection measure for the HMA edge beside the milled area should be used if the width of the longitudinal edge gaps are reduced substantially.

In future applications, a skid-steer with a grinder attached to the bucket would be useful for removing HMA at the beginning and ending of each night's run, minimizing the amount that needs to be removed by hand. The temporary panel used at the end of each night's work can easily be removed by a full sized loader – before the milling operation - without encroaching into Lane No. 2. On this project there actually was such a loader on site that could have been used to do that. Removal of the temporary panel would allow the milling machine to remove the HMA entirely at the beginning of each night's run.

### **5.6.3 Cost**

The contractors involved in the construction warn against considering the cost of this trial to be even somewhat representative of a full-scale project. A full week is usually required to get everyone past the learning curve, and three consecutive “first nights” are not typical.

The MTO is aware of this and indicates that this is widely accepted. In the case of precast repairs on the 401 and 427, there was an approximate reduction in cost of 2.5 times between the trial project and the full-scale implementation, and some reduction in cost would be expected for this rehabilitation strategy as well.

Furthermore, the cost is not the only influence in this case, as the strategy would be implemented in situations where less expensive options will not address the issues being remedied.

#### **5.6.4 Grout**

Bedding grout was used at the following estimated rates: Asphalt-supported: 12 bags/panel, Grout-supported: 14 bags/panel, Grade-supported: 4 bags/panel. This presents a significant cost consideration for design, though it was suggested that when the cost of CTBM, and labour to place it is considered, the overall cost savings associated with using less grout in Grade-Supported condition may not be as substantial. More labour may be required for greater amounts of grout that is a further consideration. Dufferin estimates that the grout cost between \$20-\$25/bag. This issue would be more clearly defined on larger scale projects where the average costs could be better defined. It should also be noted that the asphalt-supported panels would be expected to require less grout if more a more-precisely milled surface had been achieved.

Dufferin stated that using the same grout for bedding and joints/edges would greatly enhance production capabilities; there would be fewer stops to wash out the mixer and the order of installation would no longer be critical. This would allow for a single grouting pass to follow behind the placement of panels.

This is a common request from contractors, but the flow characteristics required for bedding grout and the strength/durability required for dowel grout tend to conflict with each other. Research into highly-flowable dowel grout is being done, but no current product can reliably provide acceptable performance in both cases.

One option on large projects is to use two grouting crews, which would minimize the change over required to wash out mixers. This is often the grouting method that is used on large-scale California jobs.

While it was not found to be a factor on this small-scale trial, future large-scale applications must consider that grout-supported panels require at least an hour of grout curing time before they can be opened to traffic loads. This is a staging consideration, though this can correspond with site clean-up activities required at the end of a night's construction.

### **5.6.5 Surface Finish**

Some transverse joints on the section had noticeable elevation differences due to the support conditions and would require diamond grinding once installed to achieve a smooth riding surface. Initial diamond grinding is not a problem, if it is considered early in the design/planning/staging process. In future applications, a "sacrificial layer" could be designed to account for diamond grinding both initially and throughout the pavement's life. This would allow for adequate reinforcement cover to be maintained throughout the pavement's service life. It is reasonable to expect 3±1 rounds of diamond grinding throughout a concrete pavement's life cycle and this would be 4±1 if an initial diamond grind is required to smooth joint transitions.

Some rough surface textures were observed on some panels, however the MTO indicates that a more aggressive surface texture is better, considering that public safety and liability play huge roles in the decision making.

### **5.6.6 Ideal Support Condition based on Construction**

From the ministry's perspective, the current ranking of the three support conditions is 1) Asphalt-Supported, 2) Grout-Supported, and 3) Grade-Supported. Considering the ultimate goal of installing long sections of the panels, asphalt-supported panels showed the most potential of the three, though some significant changes to the milling procedure are required. These changes include more accurate grade control and more accurate grade reference to provide consistent cross slopes on the milled surface.

In addition to the production concerns, there are long-term concerns with placing a permeable (CTBM) layer between two impermeable layers. A hybrid of the asphalt- and grout-supported conditions would be the preference going forward from Dufferin's perspective. The less-stringent milling tolerance combined with the adjustable feet would provide the greatest potential for production rate. However, the lower milling tolerance requires same-night grouting and restricts the crane from sitting on the panels to place subsequent panels. These considerations both have

implications to production rates that were not significant on the small-scale trial, but could be significant on full-scale installations.

These preferences were both reflected in the results of the AHP used to compare the different support conditions. In general, the GroS panel was found to be most constructable, based on the criteria used in the analysis, with AS ranking second. Under some conditions explored as part of the sensitivity analysis, it was found that the AS panels could be considered more ideal than the GroS panels, though this was generally not the case.

## **5.7 Chapter Summary**

This chapter focused on the construction of the PCIP trial section that took place on the right-hand northbound lane (Lane #3) of Highway 400, south of Barrie Ontario. Firstly, the site-specific conditions were outlined. Next the construction plans relating to installation order, placement rate, panel delivery, lifting inserts, instrumentation, and lane closures were summarized.

The construction activities were next outlined, starting with panel fabrication and site layout and saw-cutting. Since each of the different support conditions were largely constructed on separate nights, the construction of each is summarized separately.

An overall summary of construction, including general findings was then provided.

The construction process was then analyzed through the use of an Analytical Hierarchy Process. This process was performed using input from the various stakeholders, including both MTO and Dufferin Construction personnel. Each of the support conditions were graded on four criteria that included relative cost, installation rate, repeatability, and resiliency. These gradings were then analyzed using criteria weightings developed with input from the MTO in order to determine the ideal support condition. This analysis indicated that the Grout-supported condition was the ideal PCIP design, in terms of constructability. A sensitivity analysis was undertaken on this result, which reinforced this finding.

## **CHAPTER 6: IN-SERVICE PANEL PERFORMANCE**

### **6.1 Visual Assessment**

One of the most basic types of assessment for a pavement includes making visual observations and noting what is observed. This can provide insight into some issues that manifest on the pavement surface, such as cracking, spalling, rutting, potholing, etc.

The PCIP trial section is located on a busy portion of Highway 400, and therefore access to the site is limited as it requires lane closures. A visual inspection of the trial section was performed on September 6<sup>th</sup>, 2017, during a lane closure that was scheduled in order to perform Falling Weight Deflectometer testing. During the visual inspection, notes and photographs were taken of any distresses or issues that were found.

The Manual for Condition Rating of Rigid Pavements (Chong & Wrong, 1995), which was developed for use by the MTO, was used as a reference for the visual inspection. The extents of distress occurrence guidelines were not used because the limited scale of the project allowed for observation of all individual panels on site. Only those distresses that were observed are remarked upon in this section.

Appendix C contains a summary of the distresses that were observed on site during the September 6<sup>th</sup>, 2017 site assessment.

Figure 6.1 summarizes the distresses and issues that were observed on site and the frequency at which they were observed. In each case, the frequency represents the number of panels that showed the given concern out of the total 22 panels of the trial. The frequency does not represent the total number of instances of a given distress or issue.

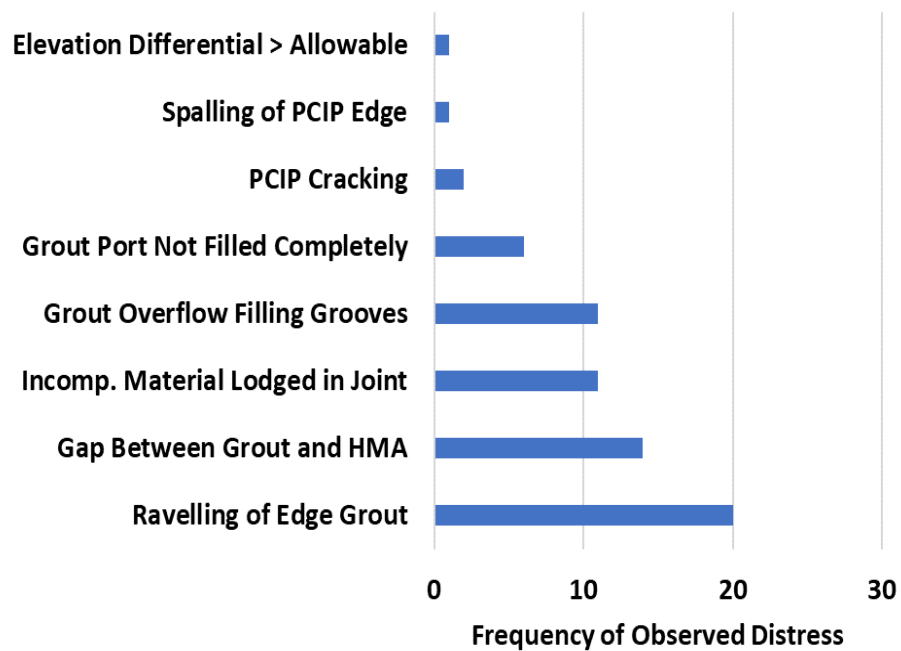


**Figure 6.1: Frequency of observed distresses and issues on PCIP Trial Section (Sept. 6, 2017)**

As shown, the most prevalent issue that was observed was ravelling of the grout that was placed in the longitudinal gap between the PCIPs and the adjacent asphalt in either Lane #2 or the shoulder, while a gap forming between the edge grout and the adjacent asphalt was the second most prevalent issue.

The observed issues, their severity and potential impact, and future considerations are addressed in this chapter. It should be noted that the PCIP trial section was found to be performing very well in general.

The PCIP rehabilitation strategy is a novel one, and therefore identification of likely distress types is an important aspect of developing a state-of-practice for the installation and maintenance of this strategy. Another purpose of highlighting the issues that were observed is to subsequently improve the PCIP rehabilitation strategy in order that future applications can avoid these issues.

### **6.1.1 Longitudinal Asphalt/PCIP Joint**

The most prevalent issue that was observed during the visual inspection was deterioration of the longitudinal joints between the PCIP and the adjacent asphalt in either Lane #2 or the shoulder.

This deterioration largely manifested in two ways: ravelling of the edge grout and a gap forming between the grout and the asphalt.

The PCIP design included 75 mm gaps along each longitudinal edge between the PCIPs and the vertical cut asphalt face. The gaps were included to ensure that the PCIP panels would be placed without damaging the adjacent asphalt. After the panels were placed, these gaps were to be filled with edge grout, which was structural dowel grout that had been extended 60% by weight by 9.5 mm pea gravel. This is outlined in Section 4.3

During construction, some of this extended grout was found to exhibit honeycombing upon placement. This may have been due to incomplete mixing on site, or due to the method of placing the grout by dumping grout from a bucket into a small funnel, resulting in aggregate segregation.

In some areas this existing segregation was made worse under traffic conditions, breaking the exposed aggregate away from the cementitious grout matrix. The severity of the ravelling was considered slight, medium, or severe based on the depth of the material that had become lost from the grout. Slight severity corresponded to only surficial material loss, medium corresponded to material loss less than 25 mm in depth, while severe material loss was greater than 25 mm in depth. Figure 6.2 shows an example of medium severity ravelling.

Throughout the trial section, the longitudinal joints of seven panels showed slight ravelling, eight panels showed medium ravelling, and five panels showed severe ravelling. Each panel joint was classified by its most severe instance of ravelling.

These localized areas present a poor riding surface, and if the deterioration were to become extensive enough could result in a safety issue for road users.

Another longitudinal joint issue noted during the visual inspection involved gaps between the edge grout and the adjacent asphalt material. These gaps are likely a result of differential temperature effects between the Portland cement concrete and the asphalt material. They were generally observed to be small, but represent a route for the ingress of surface water beneath the panels, and further deterioration.



**Figure 6.2:** Longitudinal joint grout ravelling (medium severity)

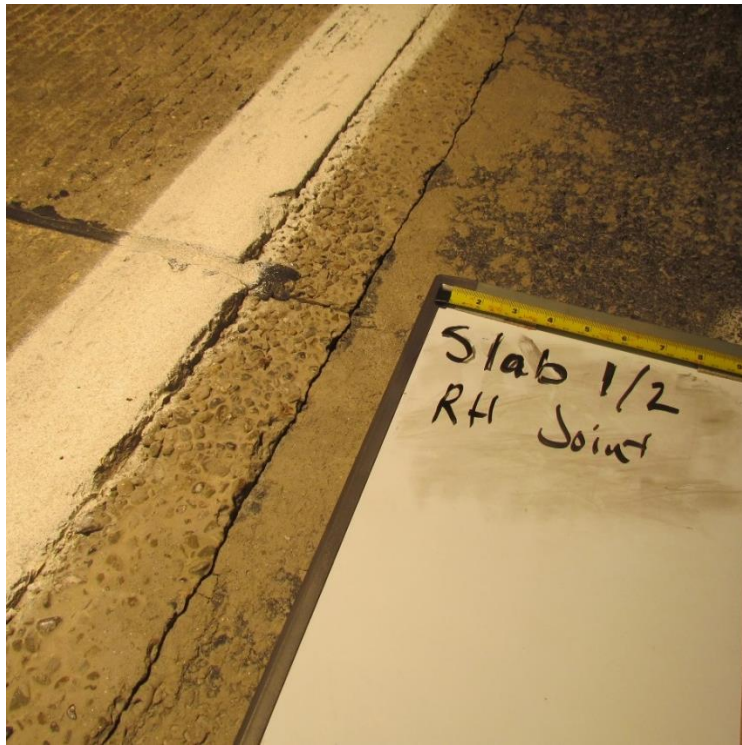


**Figure 6.3:** Edge grout/asphalt interface gap

Gaps between the grout and the adjacent asphalt were observed in 14 of the 22 panels of the project. This was probably due to the considerably different material behaviour characteristics under both temperature and traffic-related loading. Differential thermal strains along the interface could result in stresses larger than the shear capacity of the grout/asphalt interface. In areas where both ravelling and this gap were found, they appeared to compound, resulting in more severe material loss, as shown in Figure 6.4. This was commonly found where the transverse saw-cut, which was made as part of the joint-sealant application, extended through the edge grout.

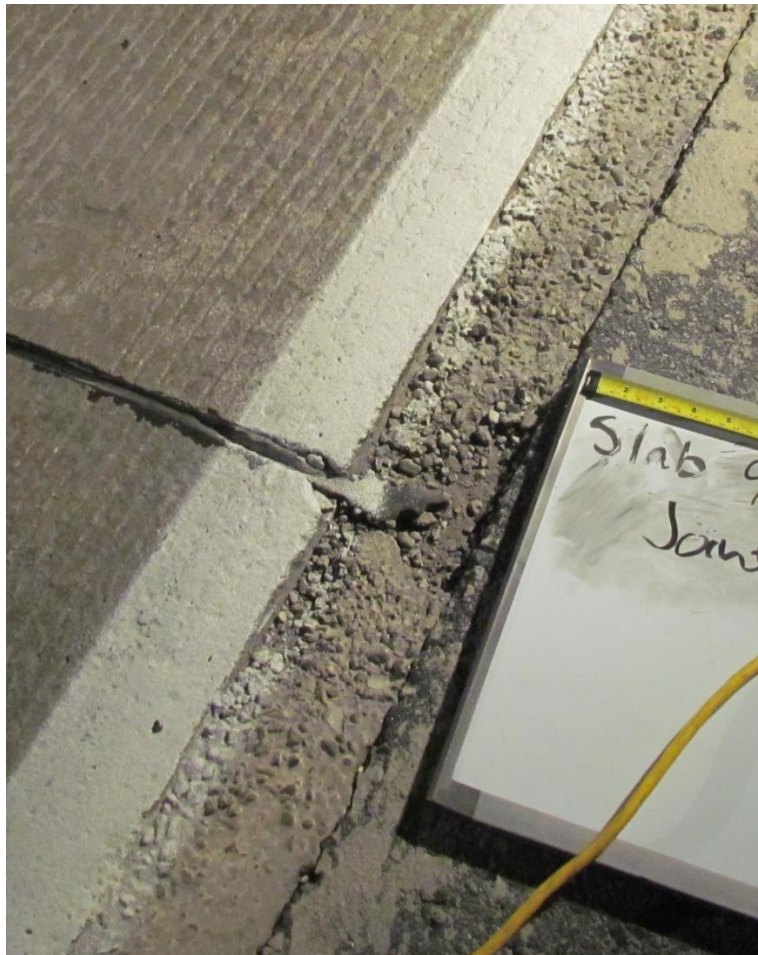


**Figure 6.4: PCIP/HMA gap and severe ravelling**

Based on the findings of the visual survey, the longitudinal joint detail of the PCIP rehabilitation technique requires refinement. One of the principle benefits of precast concrete pavement is the quality of material placement practices that can be maintained in a controlled fabrication

environment. This benefit is negated by the current design's requirement for a significant width of grout material that is exposed to traffic.

It is recommended that future applications of the PCIP minimize the width of the longitudinal edge gap and maintain the integrity of the adjacent asphalt during panel installation using a different method. A proposed method for protecting HMA edges is outlined in Section 9.1.3.

Minimizing the width of the gap will reduce the effects of tires on the edge grout, avoid the need for pea gravel-extended grout, and potentially allow for the use of sealant materials on the panel edges to reduce water ingress beneath the panels.

### **6.1.2 Transverse Asphalt/PCIP Joint**

Similar to the longitudinal edge joint, the transverse joint at the leave end of the trial section displayed signs of deterioration where the PCIP abutted the existing asphalt. The deterioration was located where vehicles travelled from the PCIP surface to the HMA surface. The observed deterioration included a widening gap between the PCIP and the HMA, which appeared to be the result of the HMA being pulled away from the PCIP. The sealant initially placed into the joint had become detached from one edge of the joint or the other within the wheel path areas of the transverse joint.

Incompressible materials and detritus were observed within the gap. The materials generally appeared to be small aggregate that could have potentially come from the ravelled grout in the longitudinal joints. Figure 6.5 shows a portion of the final transverse joint. In this portion of the panel, the sealant has generally become detached from the PCIP, but was still largely attached to the HMA surface.

This deterioration results in the sealant becoming effectively useless and a substantial means of ingress for surface water to reach the bottom of the panels. If the deterioration continues, it will eventually effect the ride quality of the pavement; a wider gap will result in an impact as the vehicle's tires hit the corner of the HMA pavement. The presence of water and increased impact forces from vehicle wheels hitting the HMA corner could lead to accelerated deterioration of the HMA in the area.

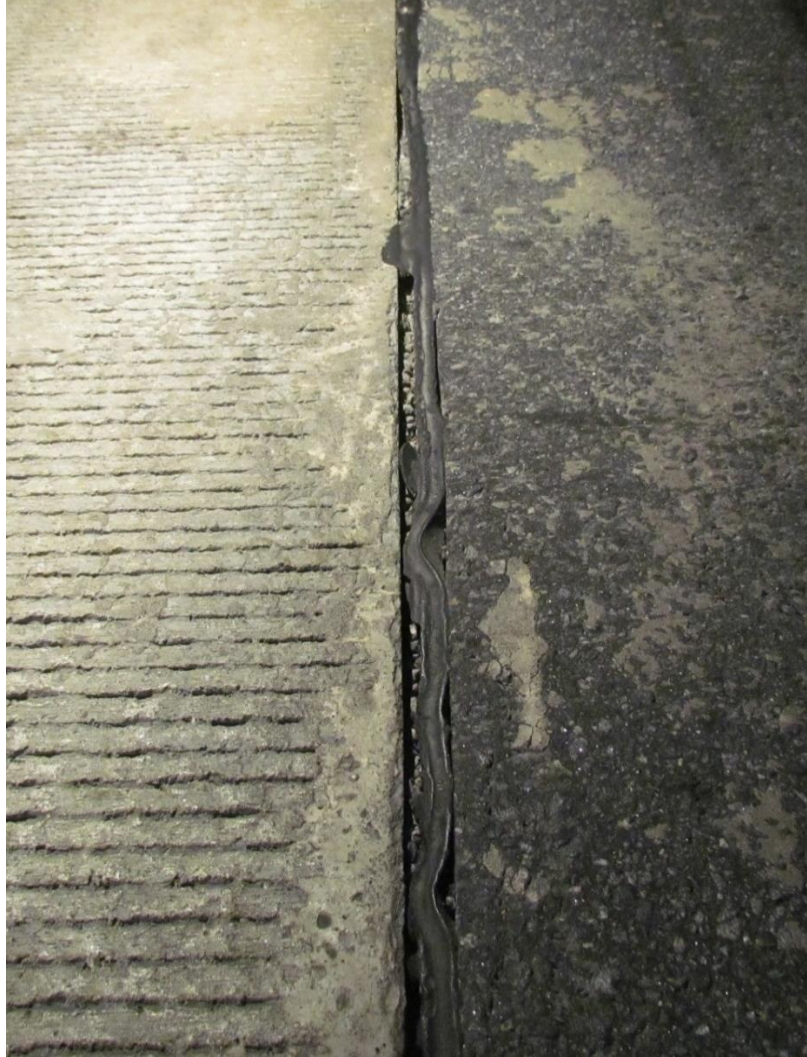


**Figure 6.5: Final transverse joint between PCIP and HMA (right wheel path)**

In order to avoid these potential issues, the design of this transverse joint should be changed. Generally, the use of grouts in the PCIP/HMA interface was found to be ineffective as the bond between the materials did not last. It is recommended that a better bonding and more flexible material, such as a hot-applied mastic, be used in these joints to preserve a bond between the two elements even under differential movements caused by traffic or temperature-related loading.

### **6.1.3 Typical Transverse Joints**

The inter-panel transverse joints were generally found to be in good condition throughout the project. Within the driving surface, no instances of joint sealant pulling from the joint were observed.

The width of the transverse joint between adjacent panels was measured in three locations, left wheel path, right wheel path, and centre. The average of these three readings was used to determine the average joint width. The average joint widths, as measured, ranged from 13.7 mm to 18.3 mm. The typical joint width specified in the design documents was 12 mm, though some variance is expected due to panel construction and installation tolerances.

Eleven of the panels were found to have incompressible materials lodged in the joints. These materials were often pieces of aggregate that appeared to be from the ravelled edge grout discussed previously. The pea-gravel used to extend the edge grout had a nominal maximum aggregate size of 9.5 mm, while the average width of the transverse joints was found to be 15 mm. This allowed the displaced aggregate to lodge easily in the sealed joints. Figure 6.6 shows a typical example of incompressible materials lodged in a transverse joint.

One small (>25 mm diameter) spall was observed in a PCIP panel at the transverse joint. This could have been caused by the combination of thermal panel expansion and incompressible materials in the joint, though this is not certain.

As discussed previously, the presence of incompressible materials is expected to largely be due to the longitudinal edge detail. This detail should be improved such that a significant source of incompressible materials is not so close to the joints.

The maximum allowable vertical differential between adjacent panels was specified to be 3 mm, and this limit was observed to be generally adhered to, based on visual assessments made without measuring. The vertical differentials between adjacent panels were not typically measured on site, however the joint between panels #13 and #14 was found to have a vertical differential of approximately 10 mm. It is unclear whether this displacement occurred during or following construction.

#### **6.1.4 Grout Injection**

Throughout the trial, there was evidence of overflows during sub-surface grout injection. Grout was observed to fill the tined surface texture in the areas surrounding grout ports and at panel edges. Generally the affected areas surrounding grout ports were quite small, with diameters of



**Figure 6.6: Incompressible materials lodged in transverse joint**

less than 30 cm. Figure 6.7 shows a typical grout injection port with overflowed material filling tines.

Ten transverse joints were found to have grout filling the adjacent tines, such as shown in Figure 6.8. In general, this issue was confined to the area approximately 5 cm to either side of the joint.

In these area, the benefits of the longitudinal tines are negated. These benefits include improvements in friction and noise between the pavement surface and the tires of vehicles using the pavement. This issue can have negative effects on these properties, though the magnitude is not large due to the small size of the affected areas.



**Figure 6.7: Grout overflow at injection port**



**Figure 6.8: Grout overflow at transverse joint**

This issue could be addressed by specifying the use of a hand-held power broom following grouting to clean out affected tines. Efforts to contain the grout should also be made during injection, however this is difficult, especially when the grout is pumped beneath the panels until it is observed to issue from other grout ports. Additionally, surface grinding following the installation of panels would negate the effects of this issue by removing the material entirely. Surface grinding

is not appropriate to address only grout overflow, but it is discussed in Section 6.4.2 as a method to improve the roughness characteristics of the PCIP rehabilitation strategy.

### **6.1.5 Panel Cracking**

Cracking was observed in two panels (Panel #1 and #2). Figure 6.9 and Figure 6.10 show the cracking observed in Panel #1 and #2, respectively. In each case, the cracks are highlighted for clarity.

Panel #1 and #2 were the first panels to be installed, and were placed in the first area to be milled. When Panel #1 was initially placed, it was found that the milling depth was insufficient and the milling crew was recalled to site to mill the section to a further depth. This inconsistent milling may have resulted in the cracks that were found. The cracking in Panel #1 are consistent with a relative high point in the support material below where the cracks converge, with relative low points along the longitudinal edges. Similarly, the cracking observed in Panel #2 indicates a low support area beneath the corner. The bedding grout pumped beneath the panels should typically address milling issues such as these, indicating that either the cracks were formed following the first night of construction when the panels were exposed to traffic loads while not grouted, or that the bedding grout was not installed effectively.

In both cases, the cracks were not active and were visible only due to the presence of moisture, indicating that the panel reinforcement is holding the crack together. Falling weight deflectometer (FWD) testing, which is discussed in detail in Section 6.3, confirmed that the cracks maintained high load transfer efficiency. The cracks will be monitored, but are not expected to worsen due to their reinforced condition.

The cracking highlights the importance of milling accuracy, particularly when the panels are in the asphalt-supported condition. This support condition provides very little resiliency to milling issues, and requires significant milling control to be considered feasible. Improvements to milling machine accuracy would greatly improve the relative benefits of the asphalt-supported support condition.

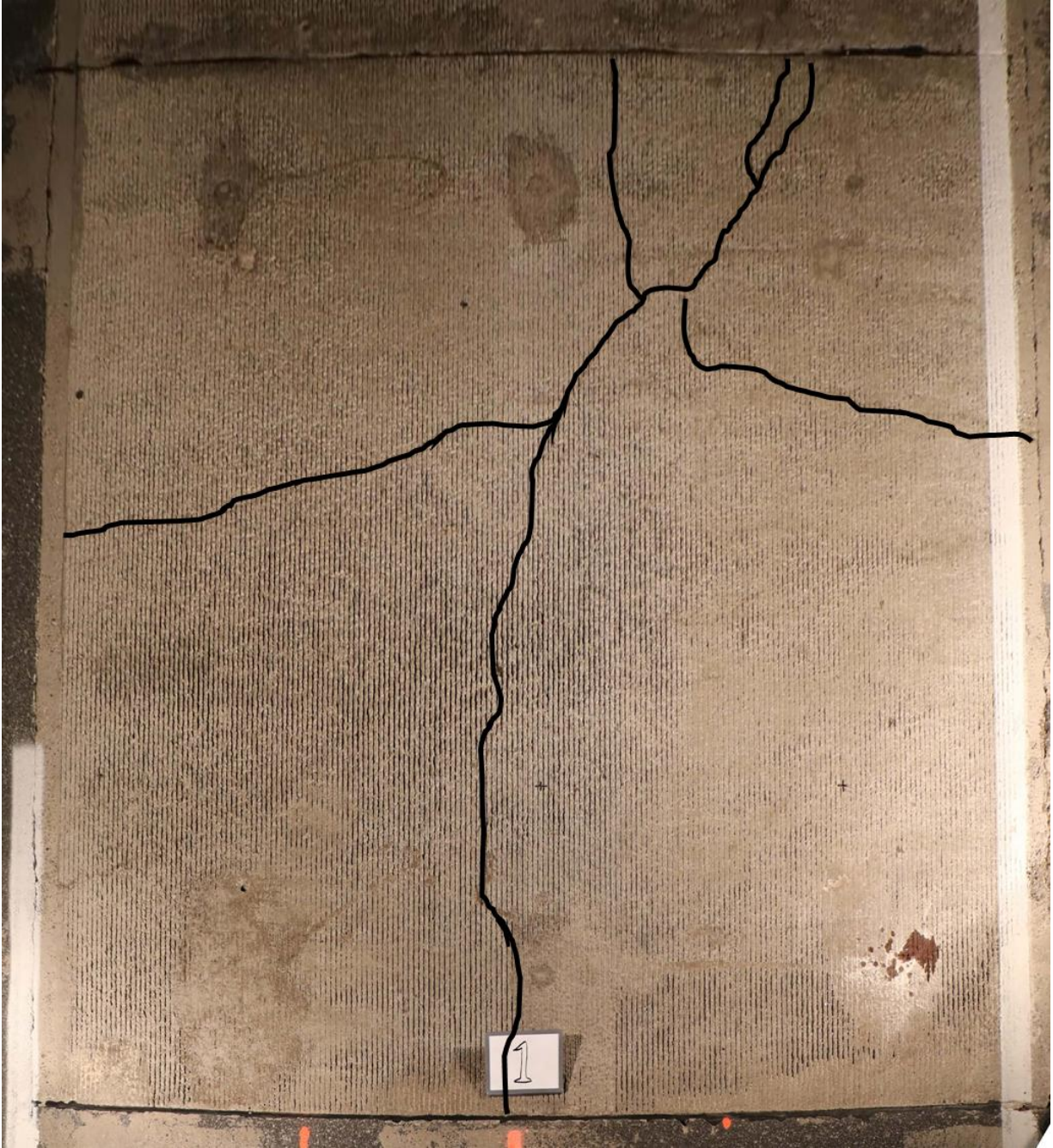


**Figure 6.9:** Cracking observed in Panel #1 (cracks highlighted for clarity)

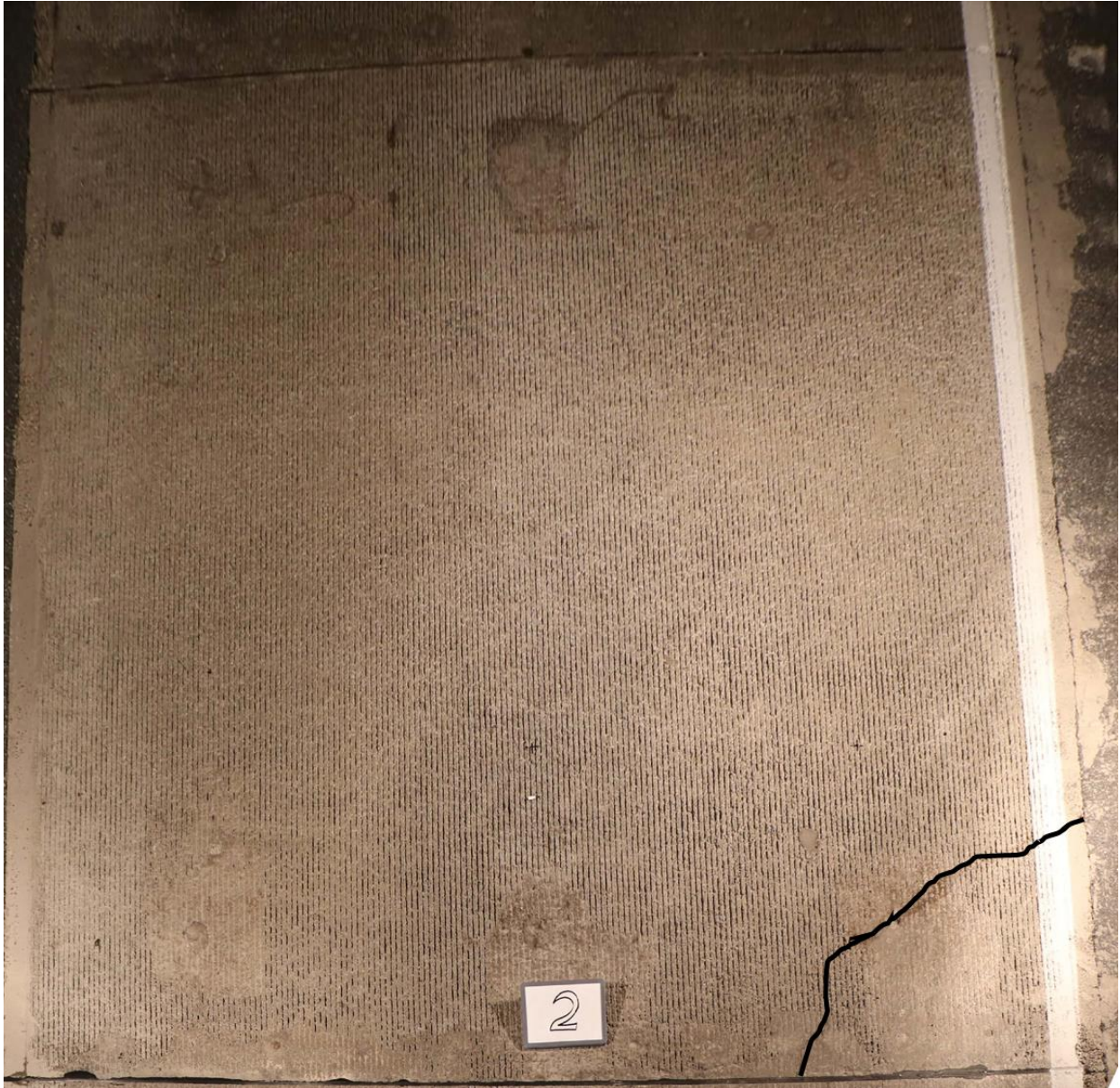


**Figure 6.10: Cracking observed in Panel #2 (crack highlighted for clarity)**

## **6.2 PCIP Instrumentation<sup>3</sup>**

Precast panel pavements have been used successfully in the past; however, precast concrete inlay panels (PCIP) are a new and novel application of the technology. Several methods were proposed to investigate the behaviour of the panels, including the placement of instrumentation at the interface between the PCIP and the milled asphalt. This chapter discusses the information gathered from this instrumentation and its potential impacts to the performance of the PCIP trial. This

information relates to thermal and static loading, sub-surface moisture levels, and temperature gradients throughout the PCIP.

### **6.2.1 Instrumentation**

The novel nature of this application made gathering information on the behaviour of the PCIP trial a priority. This information gathering consisted of two parts: post-construction testing, and sub-surface instrumentation. The post-construction testing is discussed in other chapters of this thesis.

The sub-surface instrumentation involved the collection of data from sensors installed beneath the panels during the construction operation. An instrumentation plan was submitted as part of the design package that was produced for the MTO, and included the sensor types, installation plans, and positions within the project extents.

#### ***6.2.1.1 Instrumentation Types***

Two types of sensors were installed as part of this project: earth-pressure cells (EPCs) and moisture sensors. The sensors were installed at the PCIP-asphalt interface in order to provide information relating to the support conditions beneath the panel.

Internal sensors within the PCIPs were initially considered in order to gauge strains throughout the panel depth, but ultimately these were not used due to concerns with cabling during panel casting, transportation, and placement, combined with uncertainty related to positioning on the site.

The EPCs were LPTPC09-V model total earth pressure cells, manufactured by RST Instruments. The sensors are plate type cells, shown in Figure 6.11, which include two circular stainless steel plates that are welded together around their circumference. Between the two plates is a void that is filled with de-aired glycol. A hollow stem is connected between the plates and a pressure transducer, shown on the left of Figure 6.11, such that all three components (plates, stem, and transducer housing) are filled with a continuous glycol reservoir. As pressure is applied to the plate

---

<sup>3</sup> The contents of this section of the chapter are from an accepted manuscript of an article accepted for publication by NRC Research Press in The Canadian Journal of Civil Engineering on April 30, 2018, available online, DOI: 10.1139/cjce-2018-0044. D. Pickel, S. Tighe, W. Lee, and R. Fung “*Highway 400 Precast Concrete Inlay Panel Project: Instrumentation Plan, Installation, and Preliminary Results*”

surface, the glycol fluid is also pressurized. The pressure transducer then measures the pressure of the fluid, which is recorded by an external data logger. The EPCs installed in this project used a vibrating wire type pressure transducer.

The EPCs had an applicable range of 0 to 2000 kPa applied pressure, with a calibrated accuracy of 0.15% of full range (3 kPa). Each EPC was calibrated prior to installation in the field. Each EPC also had a 3 k $\Omega$  thermistor located in the transducer housing for measurement of temperature in the sensor's glycol.

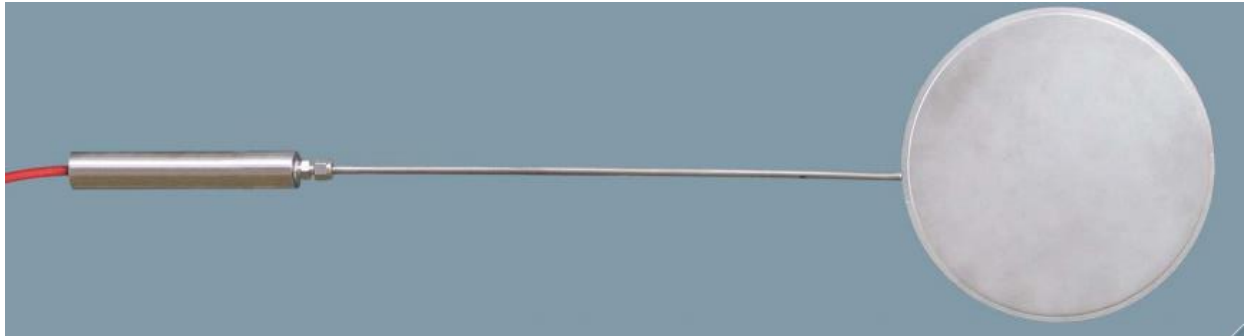


**Figure 6.11: Typical total earth pressure cell**

The vibrating wire sensor measures the frequency at which the wire vibrates after being activated. This frequency, the barometric pressure, the glycol temperature, and the calibration values can be used to calculate the pressure using Equation 12.

$$P = CF \times (L_i - L_c) + 0.1 \times (B_i - B_c) + T_k \times (T_i - T_c) \quad (12)$$

where:

P	= Pressure in EPC (kPa)
CF	= Calibration Factor (kPa/B unit)
L <sub>i,c</sub>	= Initial and current readings (B units)
B <sub>i,c</sub>	= Initial and current barometric pressure (millibars)
T <sub>k</sub>	= Temperature calibration coefficient (kPa/°C)
T <sub>i,c</sub>	= Initial and current temperature (°C)

All calibration factors for each sensor were determined by the manufacturer.

The moisture sensors were CS-655 model soil water content reflectometers, manufactured by Campbell Scientific. The sensor, shown in Figure 6.12, consists of two probes extending parallel from the sensor base. The probes measure the electrical conductivity of the material spanning

between them. This information is used to determine the volumetric water content of the soil surrounding the probes. The temperature is also measured using a 3 k $\Omega$  thermistor located near where a probe connects to the sensor base.

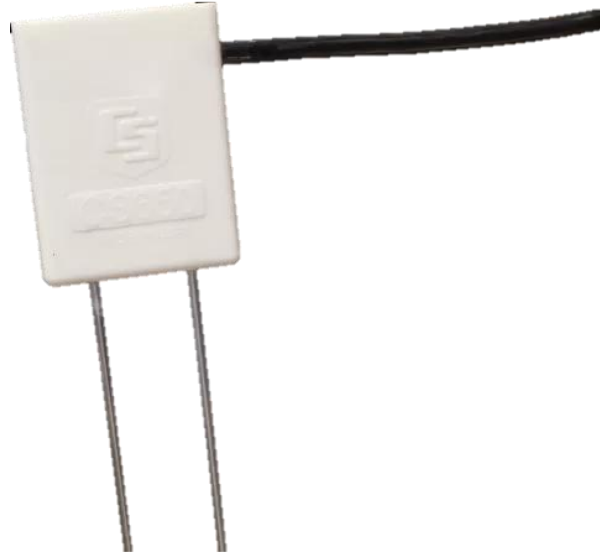


**Figure 6.12: Soil water content reflectometer (Campbell Scientific, 2017)**

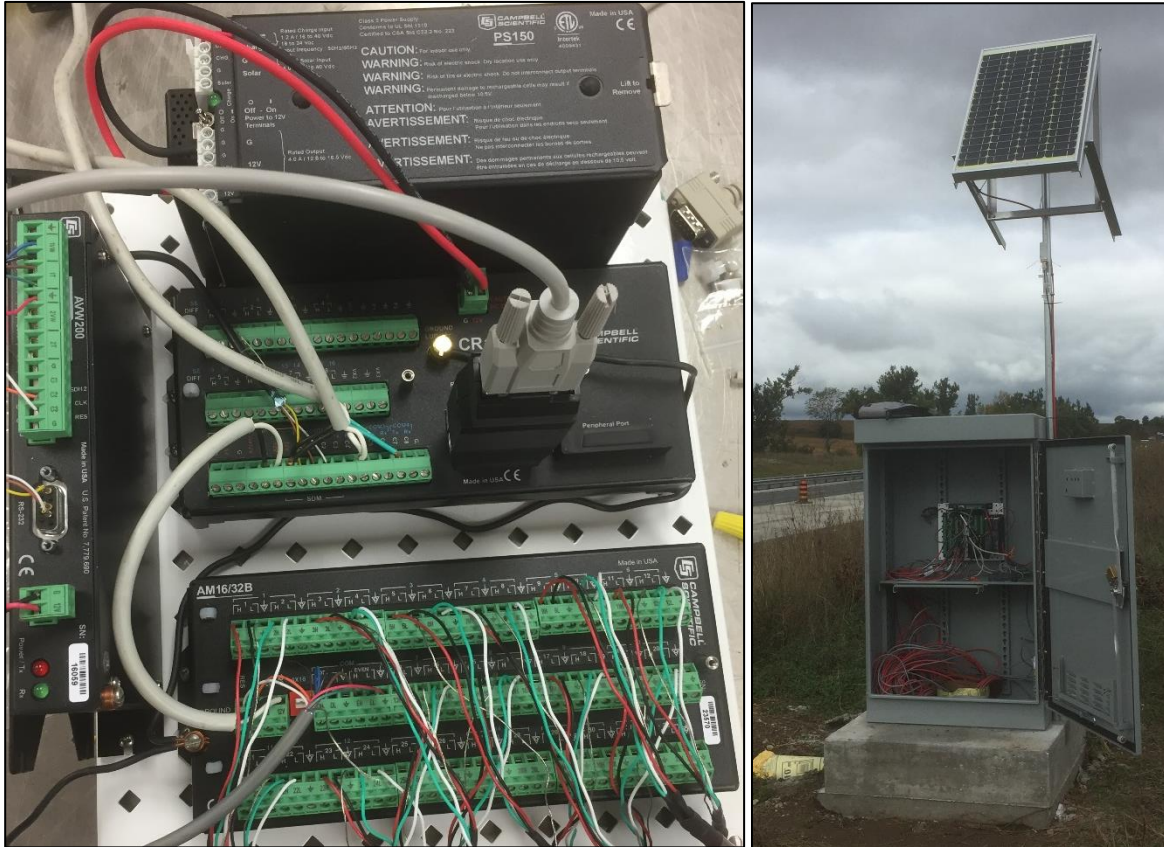
The accuracy of the volumetric water content measurements are  $\pm 3\%$ , with a precision of  $< 0.05\%$ . The accuracy of the temperature measurements are  $\pm 0.5^\circ\text{C}$ , with a precision of  $\pm 0.02^\circ\text{C}$ .

Table 6.1 summarizes the two types of sensors that were employed as part of this project.

**Table 6.1: Sensor Summary**

<b>Sensor Type</b>	<b>Model</b>	<b>Sensors Installed</b>	<b>Measurements Made</b>	<b>Sampling Frequency (readings/hour)</b>
Earth Pressure Cell (EPC)	LPTPC09-V	12	· VW Frequency (Hz) · Therm. Resistance (ohm)	4
Moisture Probe	CS-655	6	· Volumetric Water Content ( $\text{m}^3/\text{m}^3$ ) · Temperature ( $^\circ\text{C}$ )	1

Both sensor types were connected via cabling to a data logging setup consisting of a CR1000 data logger, AVW 200 vibrating wire analyzer, AM16/32B multiplexer, and a PS150 power source, all manufactured by Campbell Scientific. The setup for this equipment is shown in Figure 6.13.



**Figure 6.13: Data logging equipment setup (left), installation on site (right)**

The power source in the data logging equipment is recharged using a pole-mounted solar panel, shown in Figure 6.13 as installed on site. The setup was installed in a locking cabinet that cables were run to through buried pipe.

### **6.2.1.2 Instrumentation Installation**

Two clusters of sensors were installed for each support condition type during construction. Each cluster of sensors was located beneath the right wheel path and included two EPCs (one 300 mm from the leading edge and one beneath the centre of the panel being instrumented) and one moisture sensor. In total, twelve (12) EPCs and six (6) moisture sensors were installed. Figure 6.14

illustrates the layout of the site and the positions of the six instrument clusters within the project extents.

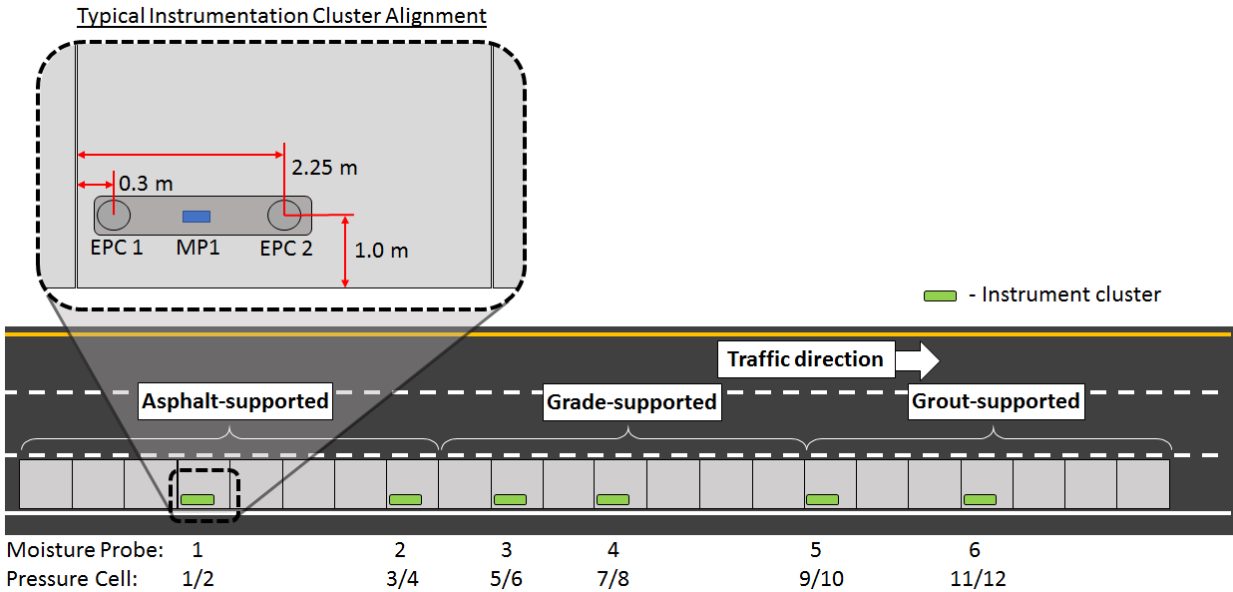


**Figure 6.14: Project instrumentation schematic**

In the location of each instrument cluster, a 25 mm deep trench was cut and chipped into the milled HMA surface. This provided a cavity in which to install the sensors, and also included a trench through the adjacent shoulder to run the instrumentation cabling. The sensors were seated and covered in packed sand with the surface of the pressure cells at the elevation of the milled surface. The moisture sensor was located between the pressure cells, adjacent to the channel where cabling was run to the side of the road. The cabling was run through a buried conduit to data-logger housed in a cabinet located approximately 10 m from the edge of the shoulder. Figure 6.15 shows a typical instrumentation cluster being installed on-site.

The instrumentation was planned to provide information relating to the distribution of load through the PCIP into the asphalt support layer and the presence of moisture at the PCIP-asphalt interface. Locating the EPCs adjacent to a joint and at the centre point of the panels was intended to provide any insight into the differential pressures associated with these locations.



**Figure 6.15: Instrumentation cluster installation**

The moisture sensor was located in a depression beneath the panels, and therefore the moisture levels measured by the sensor will provide an overestimate of the actual moisture conditions beneath the panels. They provide insight into the presence of moisture beneath the panels, including when it is first found, and whether it dissipates after it permeates beneath the panel.

## **6.2.2 Methodology**

### **6.2.2.1 Moisture Sensors**

The moisture sensors beneath the panels were monitored in conjunction with local precipitation information. The precipitation data was gathered from a weather station located 17.5 km northwest of the project site (44°14'02"N, 79°46'45"W) that provided daily cumulative precipitation amounts (mm/day). This weather station was the closest location that provided information relating to precipitation, and provides the best available data relating to site precipitation events. Comparing precipitation data with sub-panel moisture provides information into the permeability of the design.

The design includes concrete sitting in an asphalt “bath tub” so the ability of water to get and stay beneath the panel is an important consideration in the performance of the PCIP design, particularly in a climate susceptible to freeze/thaw cycling.

The presence of water beneath the panels can also influence panel warping. During initial curing following casting, moisture conditions can result in moisture gradients that cause shrinkage in areas of low moisture, and less or no shrinkage in areas of high moisture. This difference in shrinkage can result in warping. This warping is more prevalent in cast in place concrete in which the bottom maintains most of its moisture while the surface dries out under exposure to the environment. For precast concrete elements, the curing and subsequent drying is more consistent across all faces of the element as they are generally exposed to air on all sides. However, part of this initial shrinkage is considered to be reversible (Neville, 1997), that is saturation of the concrete will result in volume increase less than the initial volume loss due to shrinkage. Therefore, even in the case of precast concrete pavements, exposure to moisture beneath the panels can result in some warping. It should be noted that the relatively short joint spacing of precast concrete pavement panels can serve to mitigate the warping stresses associated with moisture gradients (Delatte, 2014).

#### **6.2.2.2 Earth Pressure Cells**

Since shortly after construction, data from the EPCs has been collected at 30 minute intervals. This process collects daily pressure variations that can be tracked over the course of the year.

Following the completion of construction, the MTO specified that falling-weight deflectometer (FWD) testing be undertaken on the PCIPs to gauge the load transfer efficiency across all of the inter-panel joints, which is discussed in Section 6.3. During the lane closure for this testing on October 6<sup>th</sup>, 2016, a fully-loaded gravel truck was brought to site in order to conduct static load testing on the panels. On each instrumented panel, the truck was parked in two positions to gauge the load imparted from the panel to the asphalt support layer. Each position was maintained for approximately five minutes and the sampling frequency on the EPCs was increased to 33 mHz. The two positions and a photo of the truck in Position #2 are shown in Figure 6.16.

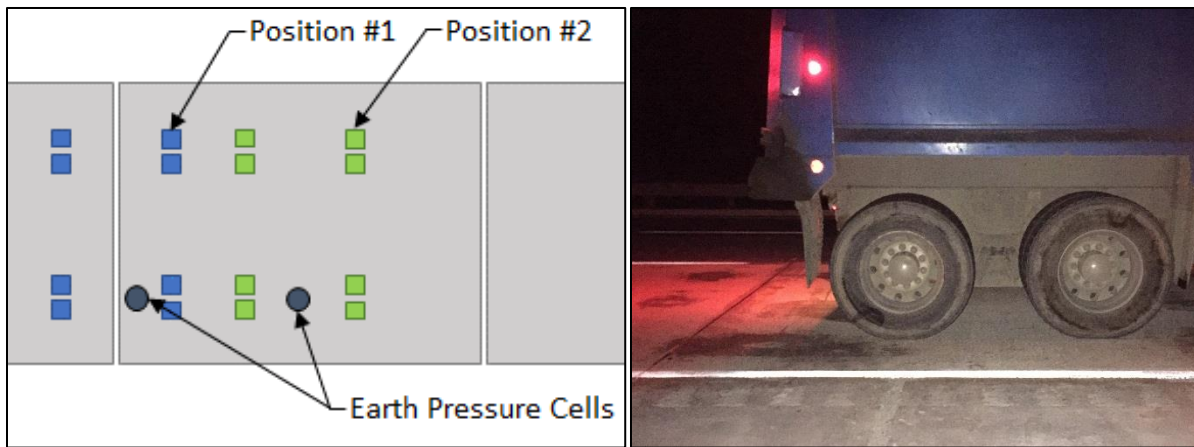


**Figure 6.16: Loaded truck axle configurations for static testing**

The truck had a total mass of 32,200 kg, or 316 kN. The tire-pavement interface for each of the 10 truck tires was found to have an area of 0.06 m<sup>2</sup>, therefore corresponding to an average pressure of 544 kPa beneath the truck tires. This average value likely underestimates the pressure under the rear two axles that support the majority of the loaded truck's mass, however individual axle weight data was not available.

The temperature readings from the EPC thermistors were used to determine the temperature at the bottom of the PCIPs. These data can be used with air temperature readings from local weather stations to determine a reasonable estimate of the temperature differential across the concrete panels. It is understood that pavement surface temperatures will generally be higher than air temperatures during sunny periods; however, no thermistors were installed in the concrete surface to get a more precise surface temperature value. Therefore air temperature was chosen to serve as a reasonable proxy.

Temperature differences can be considered as both positive and negative temperature differentials. Positive temperature differentials indicate that the top surface of the PCIP is warmer than the bottom surface and usually occur during the daytime. This situation corresponds with downward panel curling. Negative temperature differentials indicate that the bottom of the PCIP is warmer than the top, which corresponds to upward panel curling, and typically occurs during nighttime.

The edge stresses associated with the temperature differential can be calculated using Westergaard equations of relative stiffness and stress (Ioannides, Thompson, & Barenberg, 1985), combined

with curling stress correction factors developed by Bradbury (Bradbury, 1938). Bradbury developed a curling stress correction factor as a function of the ratio of panel length to the radius of relative stiffness. The radius of relative stiffness is a measure of the stiffness of the concrete pavement in relation to the stiffness of the supporting material. Its equation is shown in Equation 13.

$$l = \sqrt[4]{\frac{ED^3}{12(1-\nu^2)k}} \quad (13)$$

where:

$l$	= Radius of relative stiffness (cm)
$E$	= Modulus of elasticity of concrete (kg/cm <sup>2</sup> )
$D$	= Thickness of concrete (cm)
$\nu$	= Poisson's ratio of concrete (assumed to be 0.15)
$k$	= Modulus of subgrade reaction (kg/cm <sup>3</sup> )

Using the average values based on the 28-day measured concrete properties and an assumed support stiffness, as outlined in Section 4.3.2, the average radius of relative stiffness for the PCIP panels is 6.44 cm. For a 4.66 m panel length, this results in a Bradbury correction factor  $C$ , of 1.05. The edge stress associated with a temperature gradient can then be calculated using Equation 14.

$$\sigma_{\Delta t} = \frac{CE\alpha_t\Delta t}{2(1-\nu^2)} \quad (14)$$

where:

$\sigma_{\Delta t}$	= Calculated panel edge stress due to temperature gradient (MPa)
$C$	= Bradbury correction factor (1.05)
$\alpha_t$	= Concrete thermal coefficient of expansion (assumed $9 \times 10^{-6}/^{\circ}\text{C}$ )
$\Delta t$	= Temperature difference between top and bottom of panel ( $^{\circ}\text{C}$ )
$\nu$	= Poisson's ratio of concrete (assumed to be 0.15)

Weather data was collected from the Atmospheric Environment Service located northwest of King City, Ontario. This weather station is located adjacent to Highway 400, 17 km south of the project site (43°57'50"N 79°34'26"W). This data source represents the closest available approximation of the weather conditions on site.

## 6.2.3 Results

### 6.2.3.1 Moisture Sensors

Figure 6.17 shows moisture content readings and daily precipitation amounts from October 3, 2016 until November 7, 2016. While there were 6 instrument clusters, it can be seen that initially only 5 were reading properly, while the sixth was indicating a sensor error. It was found that environmental conditions affected the readings, and very cold temperatures occasionally resulted in these sensor errors. The volumetric water content (VWC, %) for each instrument cluster is shown on Figure 6.17. As there were two clusters per different support condition, VWC 1 and 2, 3 and 4, and 5 and 6, were located under asphalt-supported, grade-supported, and grout-supported panels, respectively.

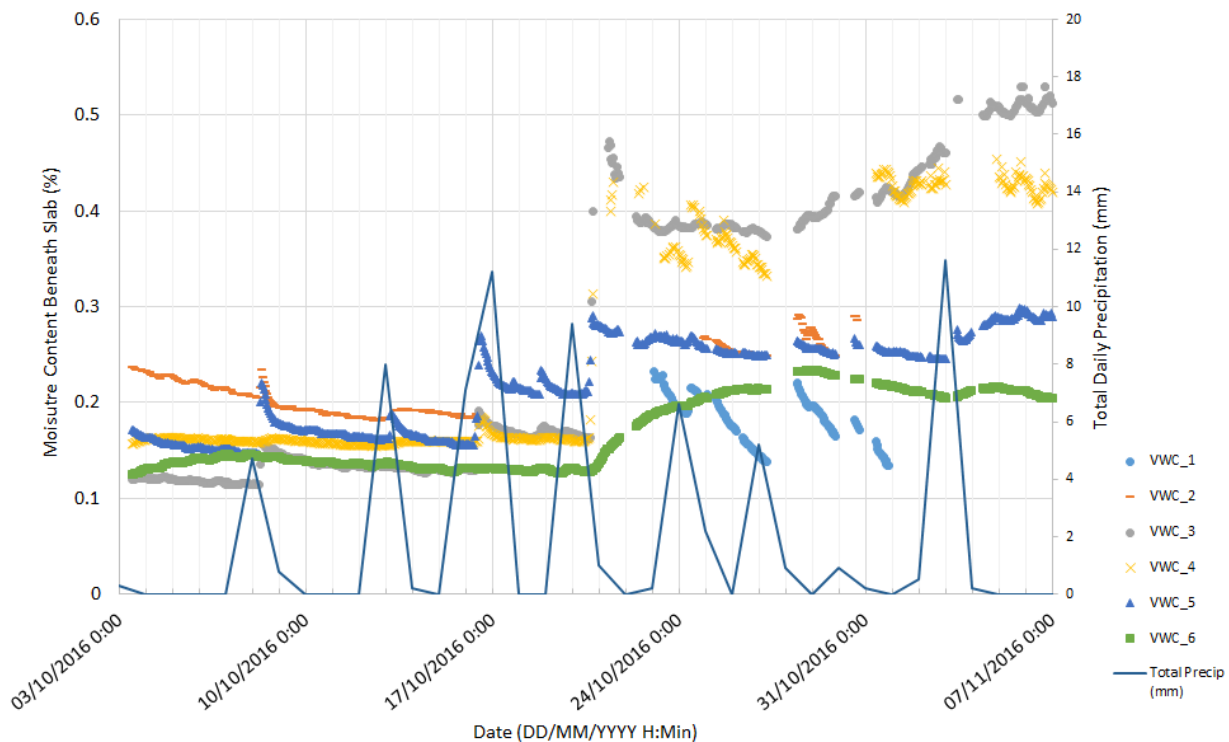


**Figure 6.17: Volumetric water content October 3 – November 7, 2016**

The moisture sensors were located in a trench beneath the milled asphalt surface, and therefore it is likely that these trenches collect water that infiltrates beneath the panel and the probes provide falsely high readings. For this reason, the magnitudes of volumetric water content readings do not reflect expected moisture content conditions in PCIP applications. However, the positive and

negative changes in moisture content measured beneath the panels do indicate the overall trends in moisture content beneath the panels, providing insight into infiltration and drainage characteristics.

The early dates shown on the plot correspond to days following construction. October 3, 2016 was the date when the data logging equipment was first brought on-line following the trial section construction. Very few, and minor precipitation events had taken place between the completion of construction on September 23, 2016 and this date. The moisture contents during this period represent the approximate moisture content of the bedding material as placed during construction.

During precipitation events observed on October 8<sup>th</sup>, 13<sup>th</sup>, and 17<sup>th</sup>, 2016 small increases in moisture content of Sensors 2, 3, and 5 indicated that some water was infiltrating the material beneath the panel. On the rain event occurring between October 20<sup>th</sup> and 21<sup>st</sup>, 2016, significant increases in moisture content indicate changes in the water infiltration rates throughout the site.

This change in infiltration rate could be attributed to environmental changes, such as moisture and temperature, which affect the material volume changes of concrete and asphalt. Immediately following the construction of the trial, it could be assumed that some bond was formed between joint and edge grouting materials and the adjacent existing asphalt. If the volumetric changes of these two materials were different enough, this may have instigated a loss of bond between the PCIP and the adjacent asphalt, resulting in a seam through that water could pass freely. Gaps between edge grout and HMA that could provide a path by which water could infiltrate beneath the panels were observed in the visual inspections described in Section 6.1.

Beyond October 21<sup>st</sup>, 2016, frequent precipitation events combined with an increased infiltration rate resulted in an average measured moisture content between 30% and 50%. This condition was observed throughout the months of December 2016 to March, 2017, though it should be noted that the sensors provided no data throughout significant portions of this period due to the cold temperatures.

The volumetric water contents measured at VWC 4 and 5 were seen to be consistently higher than in other locations within the project. While these two sensors were located beneath different support conditions, they were in consecutive instrument clusters. This may indicate site-specific

factors resulting in higher moisture levels in this area, such as relatively low elevation in comparison to the rest of the site.

Following the winter period, it was found that the moisture contents beneath the panels were generally found to drop during periods between precipitation events. Figure 6.18 illustrates this point in the period between April 25<sup>th</sup>, 2017 and June 13<sup>th</sup>, 2017.

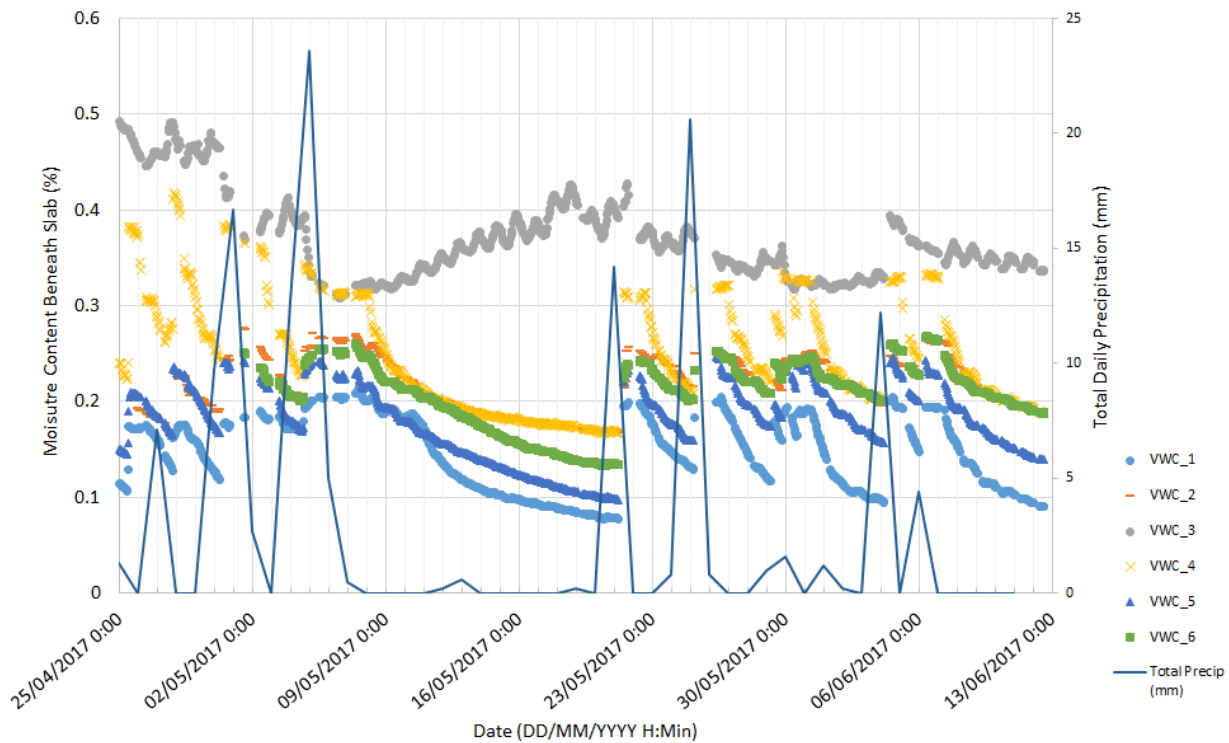


**Figure 6.18: Volumetric water content April 25 to June 13, 2017**

The moisture content of sensor #3 can be observed to have increased steadily from May 8<sup>th</sup>, 2017 until May 19<sup>th</sup>, 2017, with some daily fluctuations. This is despite almost no observed precipitation in the area. While this may indicate a secondary moisture source beneath the panel, it probably indicates that the readings from this sensor are not reliable.

The moisture content beneath the panels was found to generally follow the same trend for the remainder of 2017. Spikes in moisture content following precipitation events were followed by gradual decreases in moisture content. This period of time is shown in Figure 6.19. Following this period, the readings were found to drop severely, followed by a loss of readings in most of the sensors, indicating general sensor failure potentially brought on by winter conditions.

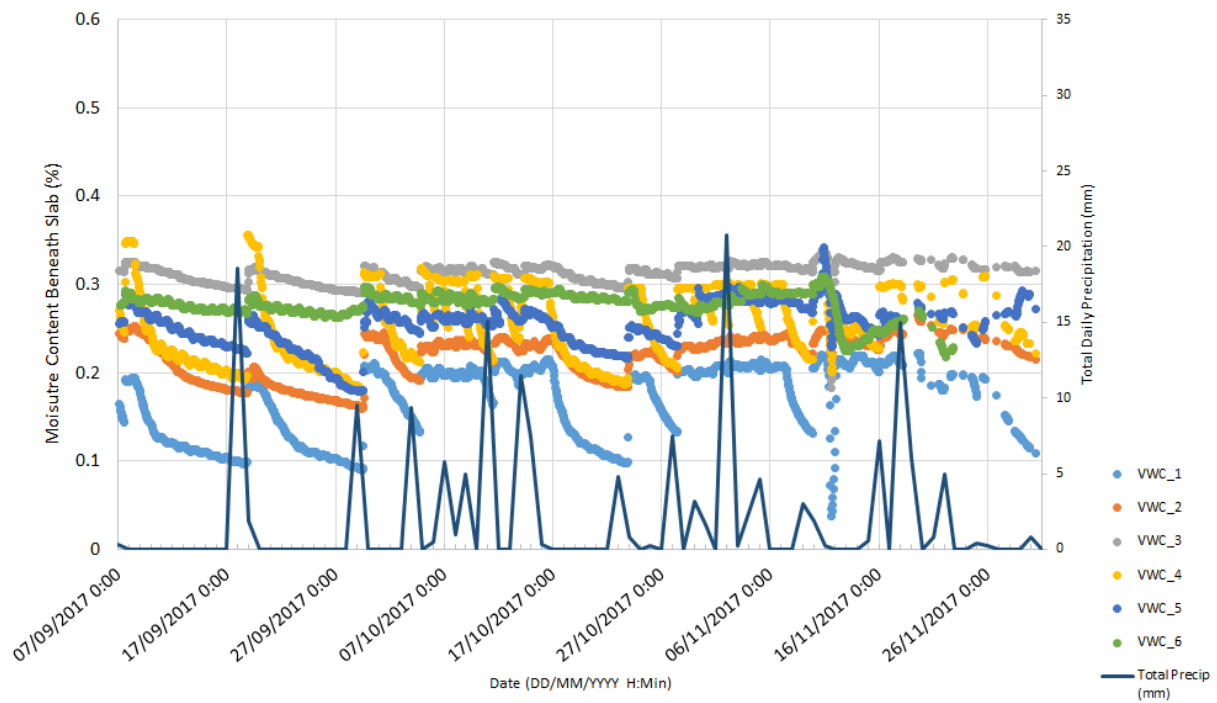
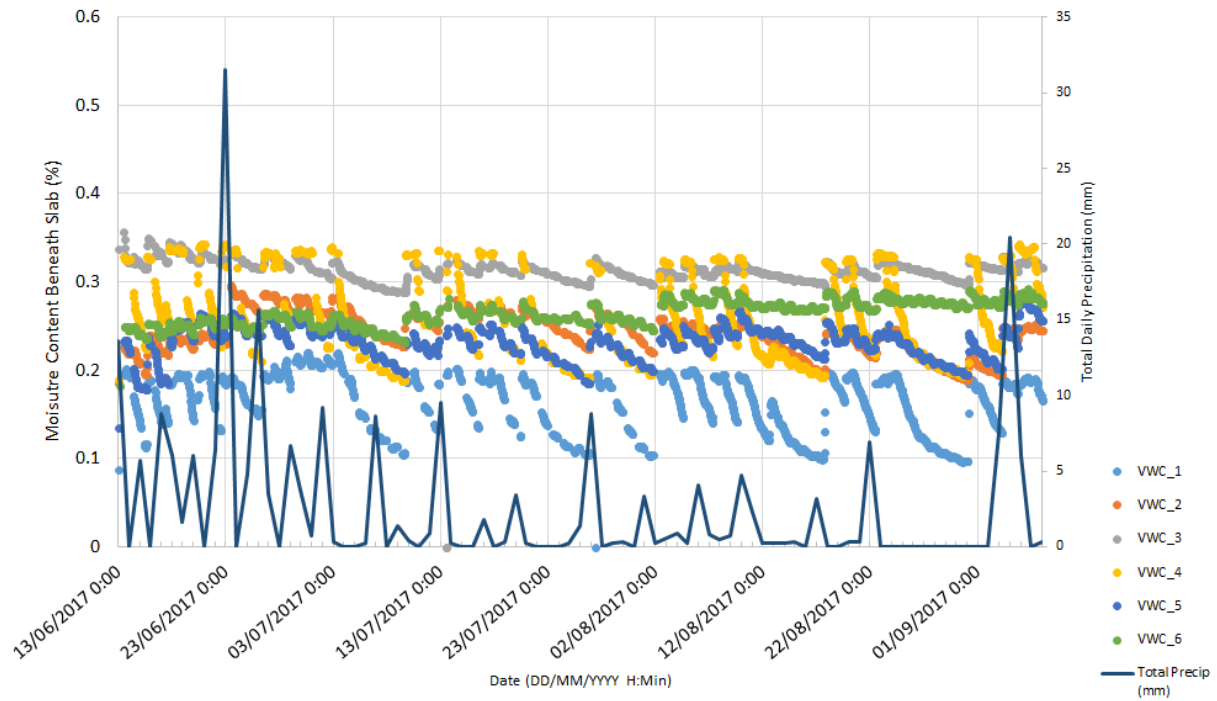


**Figure 6.19: Volumetric water content June 13, 2017 to November 30, 2017**

None of the three support conditions studied performed substantially differently with respect to sub-panel moisture penetration. This condition may change over time, but at this time no moisture conclusions can be drawn regarding the relative performance of the different support conditions.

Generally, all support condition types exhibited sharp increases in volumetric water content following precipitation events followed by slow decreases. This seems to indicate that water is draining from sub-panel area or evaporating from the original infiltration points, instead of remaining pooled beneath the panels; the exit point for this water is not clear and therefore, water located beneath the panels is a design consideration. This is especially relevant considering the PCIP is placed within a largely impermeable asphalt structure. It is expected that at least some of the drop in moisture content can be attributed to water draining via the channels used to run cabling for the instrumentation. These channels were generally at a lower elevation than the sensors, and would therefore serve as drainage paths. Considering this, it is recommended that a drainage detail be considered for any future applications of this rehabilitation technique. A discussion of this detail is included in Section 9.1.5

Figure 6.20, Figure 6.21, and Figure 6.22 show the average measured volumetric water contents and the daily cumulative precipitation values for 2016, 2017, and 2018, respectively. Much of the observed variation during winter months is due to the effects of several sensors providing error messages during cold weather.

The relatively steady state of average moisture content during 2017 corresponded to a continuous period where all moisture sensors functioned properly. During this time, it can be noted that the moisture content beneath the panels fluctuates slightly with precipitation events, but maintains a relatively consistent level of moisture.

The early portion of 2018, which is shown in Figure 6.22, corresponds to a period of low temperatures. During this time, there are substantial periods where as few as zero, one, or two sensors are registering readings that are contributing to the average moisture content. As shown in previous figures, the different sensors often provided significantly different results, therefore significant changes were seen as a function of which sensors were functioning at a given time.

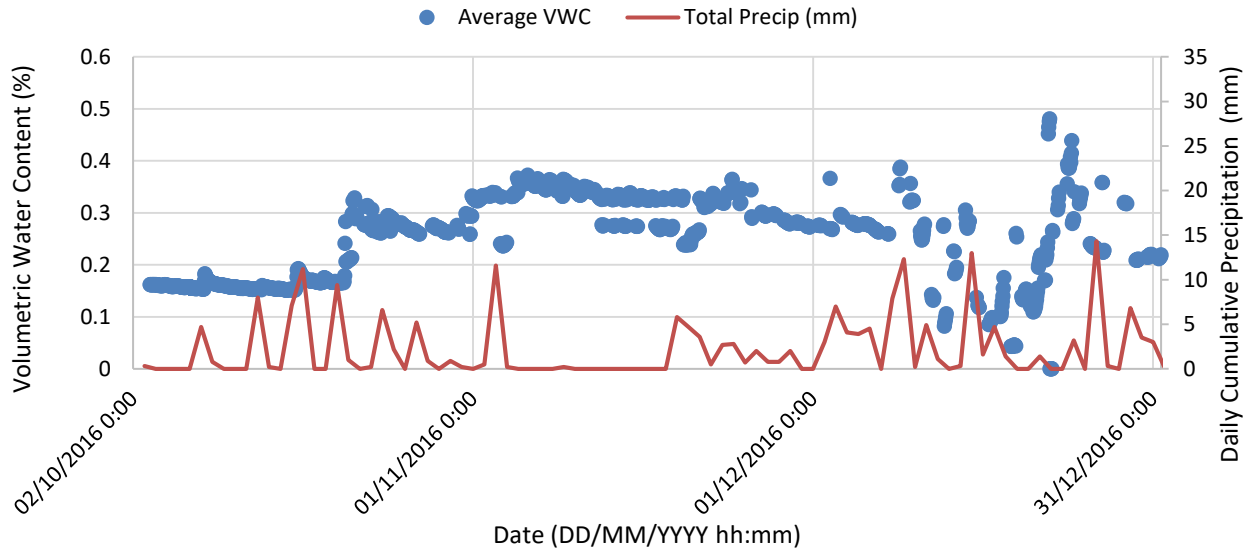


**Figure 6.20: Average volumetric moisture content and daily precipitation for 2016**

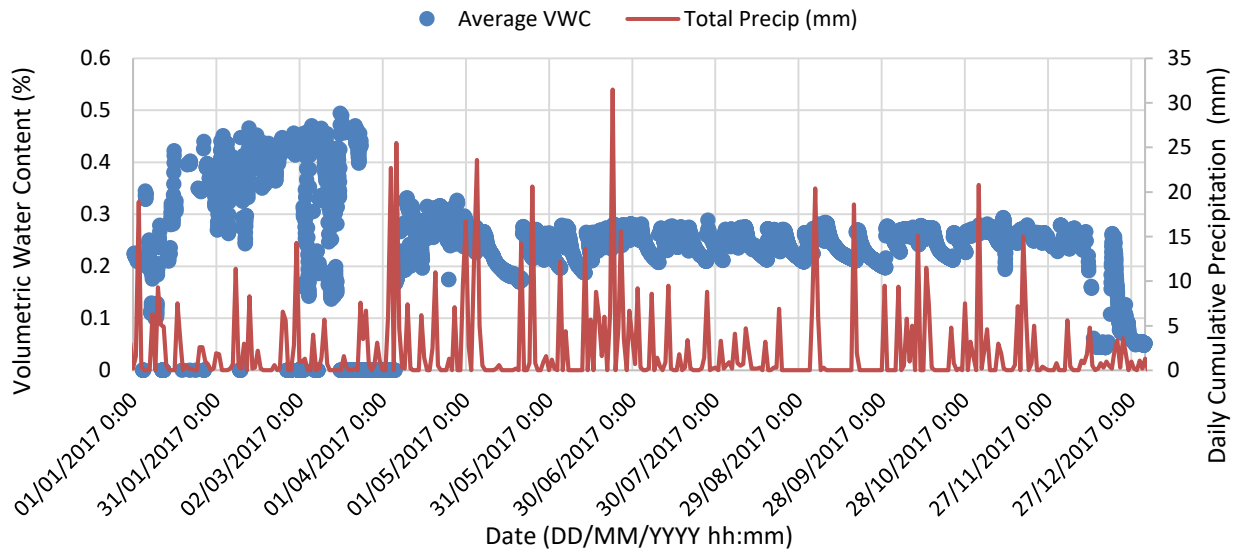


**Figure 6.21: Average volumetric moisture content and daily precipitation for 2017**

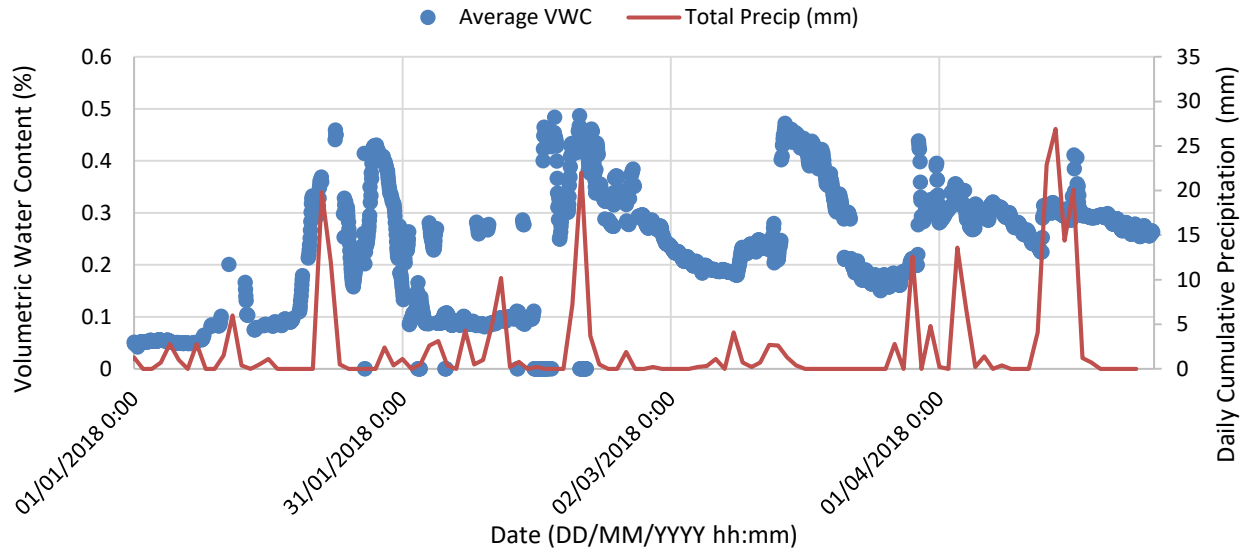


**Figure 6.22: Average volumetric moisture content and daily precipitation for 2018**

### 6.2.3.2 Earth Pressure Cells

The static load testing on October 6<sup>th</sup> and 7<sup>th</sup>, 2016 provided insight into the relative pressures imparted by the PCIP onto the supporting asphalt. The twelve total EPC sensors were paired within their instrument cluster: pairs 1/2 and 3/4, 5/6 and 7/8, 9/10 and 11/12, were located beneath asphalt-supported, grade-supported, and grout-supported panels, respectively. Following the static testing, it was found that sensor pairings 1/2, 3/4, 7/8, and 9/10 were producing readings based on significant panel loading. From these findings it was determined that sensor pairings 5/6 and 11/12 were not producing reliable results; one sensor in each of these pairings, was displaying pressure data while the second was not. For this reason, these sensor pairs were disregarded for other comparisons.

Figure 6.23 illustrates the typical shape of the response under the testing conditions described previously. The pressure readings were set to zero before the loads were applied to better show the effects of loading.

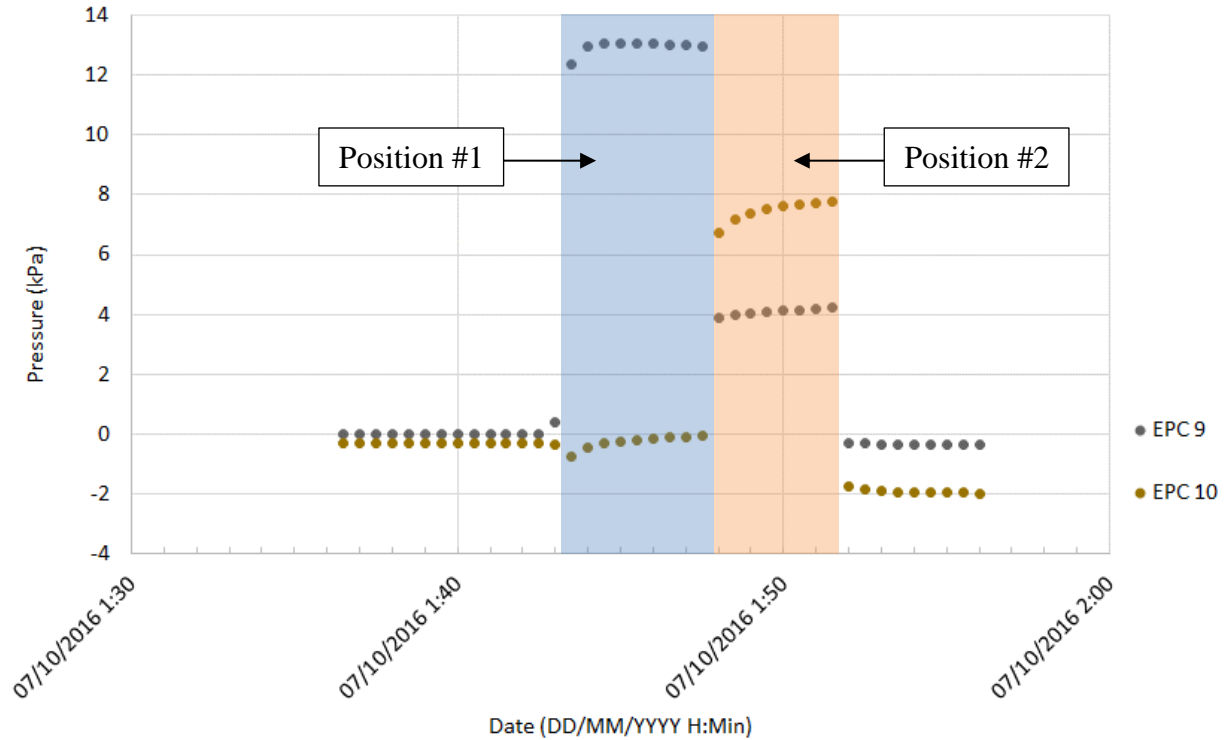


**Figure 6.23: Static load test results for panel instrumented with EPC 9/10**

Under load Position #1 (rear axle group spanning joint) approximately 13 kPa pressure was observed in the EPC 9 located adjacent to the joint, with very little pressure observed in the EPC 10 at the centre. When the rear axle group was positioned centrally on the instrumented panel (Position #2), the centre EPC 10 read approximately two times the joint EPC 9, but well less than the joint EPC 9 had read under Position #1. Similar trends were observed in the other functioning pairs, but the magnitudes of the pressure readings were found to range between 2 kPa and 13 kPa for the Position #1 readings.

Comparing the measured pressures under the two loading configurations may provide insight into the panel behaviour. In each case, one EPC is between the axles and one is outside of the axles. When the joint is loaded (Position #1), high pressures are measured between the axles but almost none are seen at the mid-panel, indicating that loads are largely supported by the materials directly beneath the joints. In fact, a slight pressure decrease was observed in three of the EPC pairings, which may indicate that the panel is lifting slightly in the centre when loaded at the joint. However,

when the centre of the panel is loaded (Position #2), increased pressures are measured at both sensors, indicating a distribution of the load across the full panel.

The pressure readings in each case are a function of the panel's downward deflection under load. As the panel deflects downward, the pressure cell is engaged. Therefore, the relative pressure readings under load Position #1 and Position #2 indicate that larger panel deflections are occurring at joints than at mid-panel under the same load. This larger deflection is also localized around the joint as the mid-panel pressure cell is not engaged under the Position #1 load, or is reduced. The differences between the deflection results are illustrated in Figure 6.24. The deflected and original shape is shown for each load position. The deflections shown in the figure are exaggerated for illustration and are not to scale.

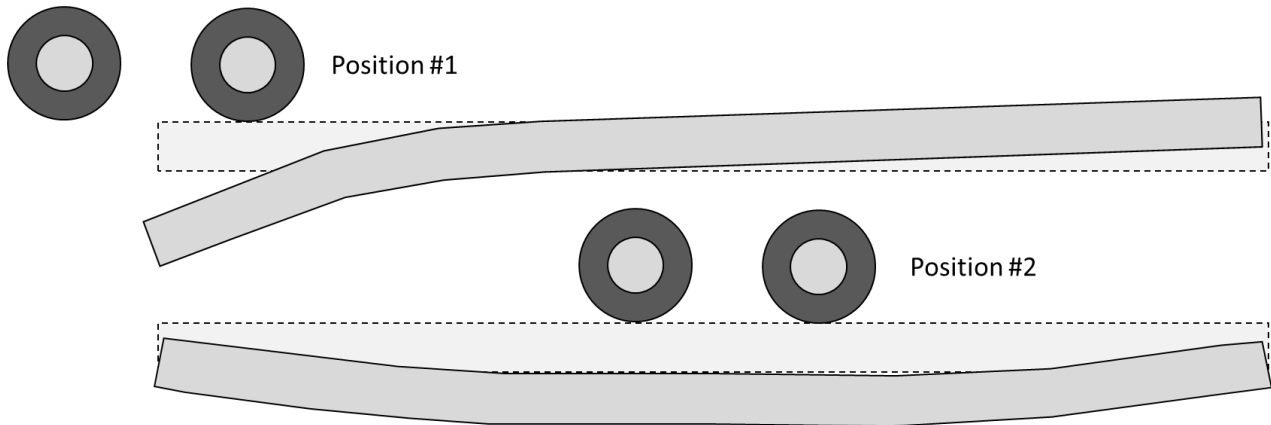


**Figure 6.24: Displacement shape under static load positions (not to scale)**

In typical concrete pavements, high deflections beneath joints could eventually result in pumping of base material in that area; however, the asphalt support layer should not generally be susceptible to this.

Falling weight deflectometer testing was undertaken following construction to gauge the performance of the joints, which is discussed in Section 6.3. The deflections under the FWD testing are presumed to correspond to the deflected shape of Position #1.

Relatively large deflections of adjacent panels under load Position #1 can result in high flexural stresses in the dowels and grout in the joint. Each panel will have opposite slopes at the joint under

that condition, placing the dowel between the panel under a significant moment couple. This can result in high bearing stresses between the dowel and the surrounding grout.

The pressure difference between the two EPCs in each working instrument cluster was tracked throughout the course of the study period. The difference in temperature between the air and the average EPC was also tracked during this time. Both sets of data are displayed in Figure 6.25, which shows these data types between the dates of October 15, 2016 and October 21, 2016. Each pairing shows the relative change in sub-panel pressure between a given panel's front joint and mid-panel locations.

This plot shows that during the period between October 18, 2016 and October 20, 2016, the system underwent rapid temperature changes. Throughout the course of those two days, the air temperature above the surface of the PCIP system went from approximately 6°C warmer to 8°C cooler twice, indicating two reversals from positive temperature gradient to negative temperature gradient and back again. During this period, the differences between the joint EPC readings minus the centre EPC readings were seen to fluctuate. Since changes in these readings are largely due to small panel deflections, changes in the difference between joint pressure and mid-panel pressure indicate the occurrence of minor panel curling. The joint and edge stresses related to curling could result in cracking of the joint and edge grouts. This may be the factor that resulted in higher sub-panel moisture contents after October 20, 2016 noted previously.

If this is the case, it indicates that a better sealant may be required at all edges and joints. Flexible sealant was only applied at transverse joints to account for temperature-induced changes in joint width. This material should be able to maintain its bond to both concrete and asphalt to reduce the amount of water that can penetrate beneath the PCIP. A drainage detail into the adjacent shoulder may also be a beneficial consideration where the situation allows for it. Both of these design changes are discussed in Section 9.1.

Panel curling can be exacerbated by the presence of water beneath the concrete panel, particularly in the case of a negative temperature differential between the top and bottom of the panel (Delatte, 2014). When this is considered in relation to the moisture sensor data presented previously, it indicates that the conditions of the PCIP may be conducive to panel curling, further indicating the

need for sub-panel moisture control. It is expected that the presence of PCIP reinforcement may make the panels resistant to curling.

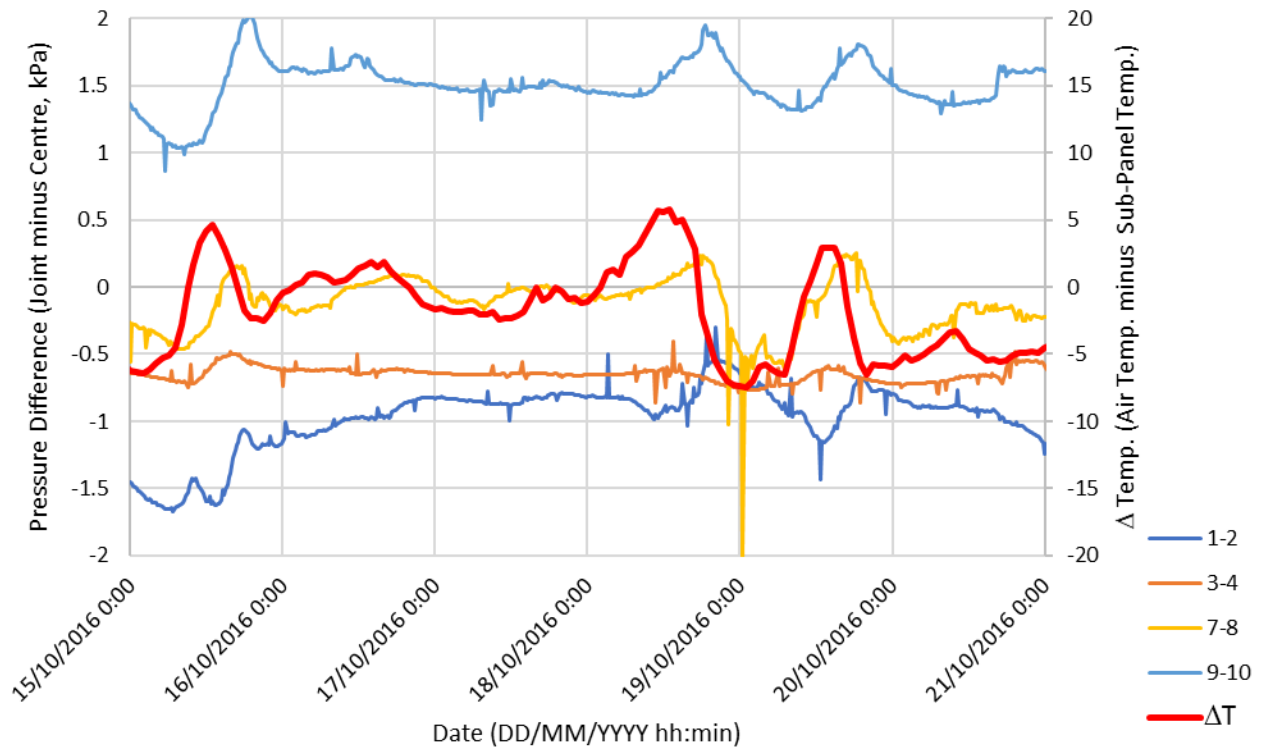


**Figure 6.25: Instrument cluster pressure differences and temperature differential (Oct 2016)**

Figure 6.26 and Figure 6.27 show the pressure and temperature differences for a period of warm weather (daily highs approximately 25°C) and a period of cold weather (daily highs approximately -6°C), respectively.

During the warm period, the temperature differential fluctuates from positive to negative on a daily basis. Each functioning pair of sensors can be observed to fluctuate similarly as a result of this temperature change. With average daily temperature difference fluctuations of 12.7°C, the average magnitude of these daily pressure fluctuations were 1.8, 0.9, 3.5, and 0.8 kPa, respectively.

During the cold period, a similar daily pattern in the temperature differential is observed; however, it remains generally negative, meaning that the surface temperature is generally colder than the temperature beneath the panels. The average daily temperature difference fluctuation of 8.1°C,

resulting in daily pressure fluctuations of 1.3, 1.0, 3.8, and 0.5 kPa, for each of the EPC pairs, respectively.

The pressure difference ranges seen in both cases are very similar, indicating that the curling pressures in both situations are similar. Asphaltic concrete materials have viscoelastic behaviour, and therefore the supporting layer beneath the PCIP will be stiffer in cold temperatures. When a concrete pavement is supported by a stiffer material, curling and warping stresses within the concrete are magnified. Therefore, despite similar curling pressures between seasons, the curling stresses may be magnified in colder months.

These findings should be qualified by noting that the accuracy of the sensors ( $\pm 3$  kPa) is on the same order as the readings.

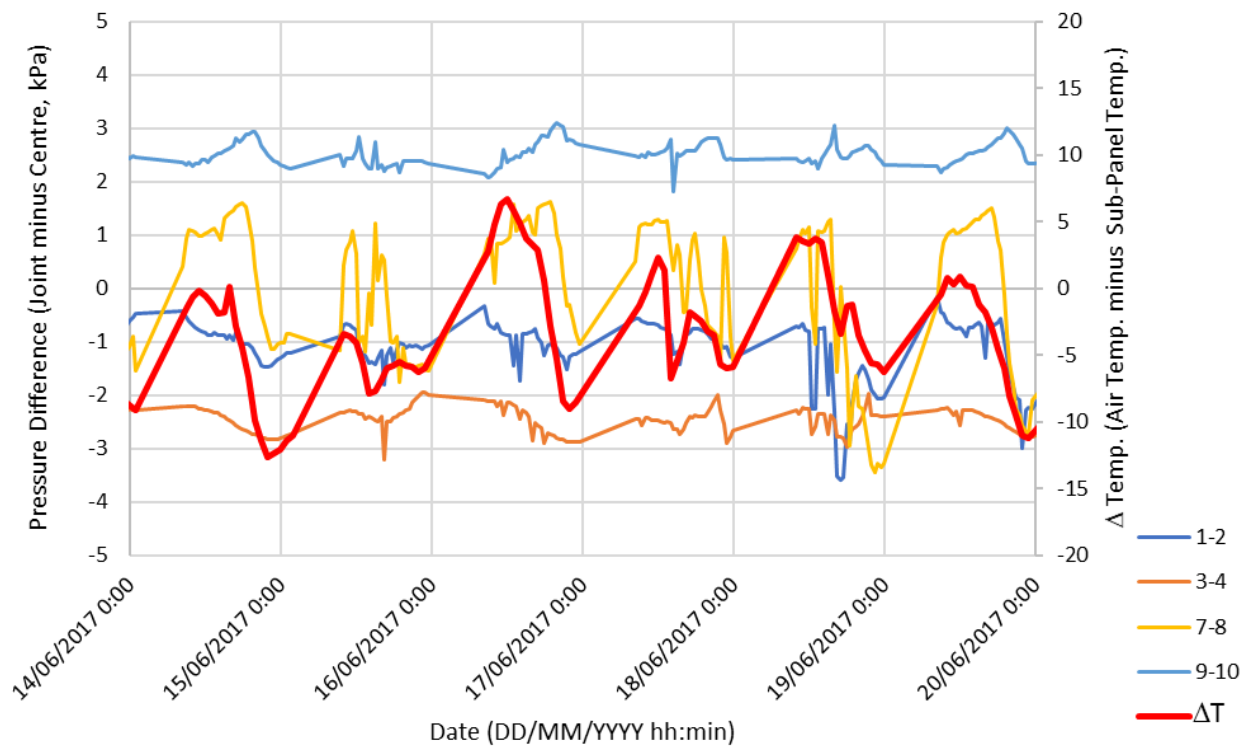


**Figure 6.26: Instrument cluster pressure differences and temperature differential (June 2017)**

Using the temperature difference, the resulting edge stress can be calculated as discussed previously. This edge stress was calculated for each temperature differential associated with pressure readings every half hour. The distribution of these calculated stresses over the one year

period from October 7<sup>th</sup>, 2016 to October 7<sup>th</sup>, 2017 are shown in Figure 6.28, while the distribution between April 24<sup>th</sup>, 2017 and April 24<sup>th</sup>, 2018 are shown in Figure 6.29. The time periods represented in the two plots overlap. This was done to show a full year distribution in each case, though less than 2 full years of data were collected.

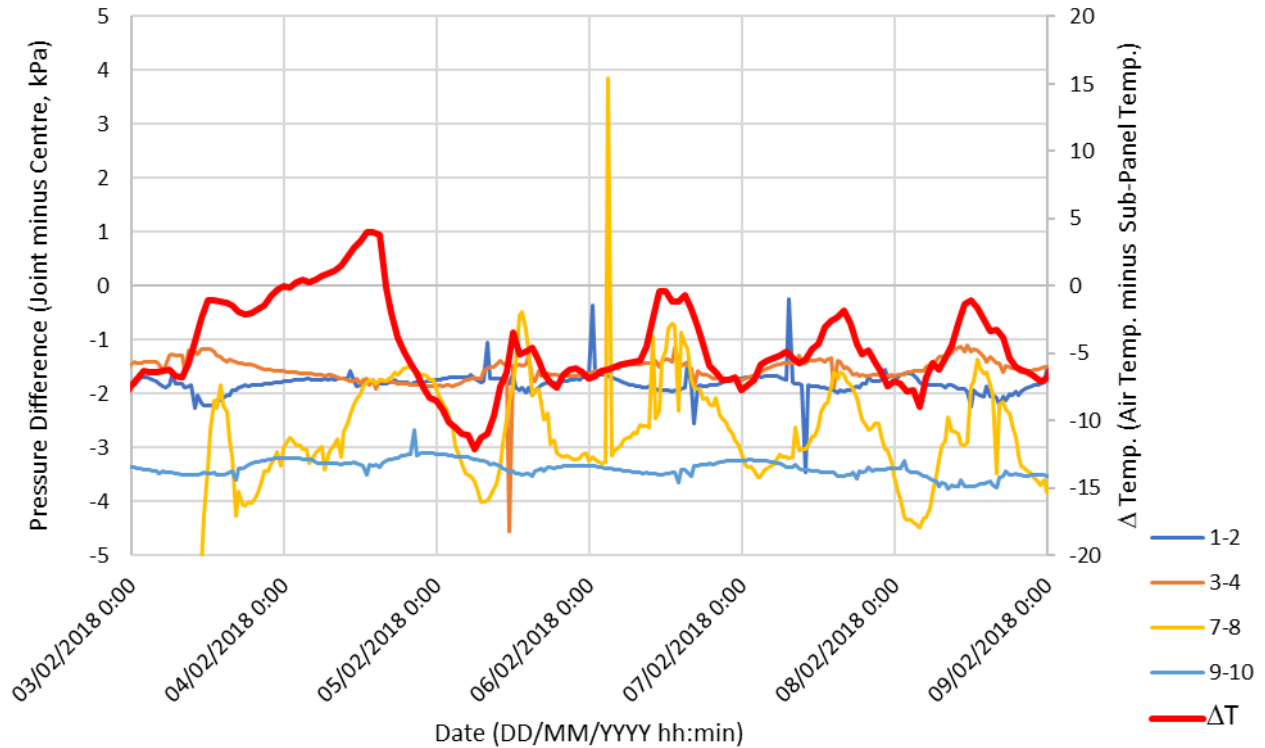


**Figure 6.27: Instrument cluster pressure differences and temperature differential (February 2018)**

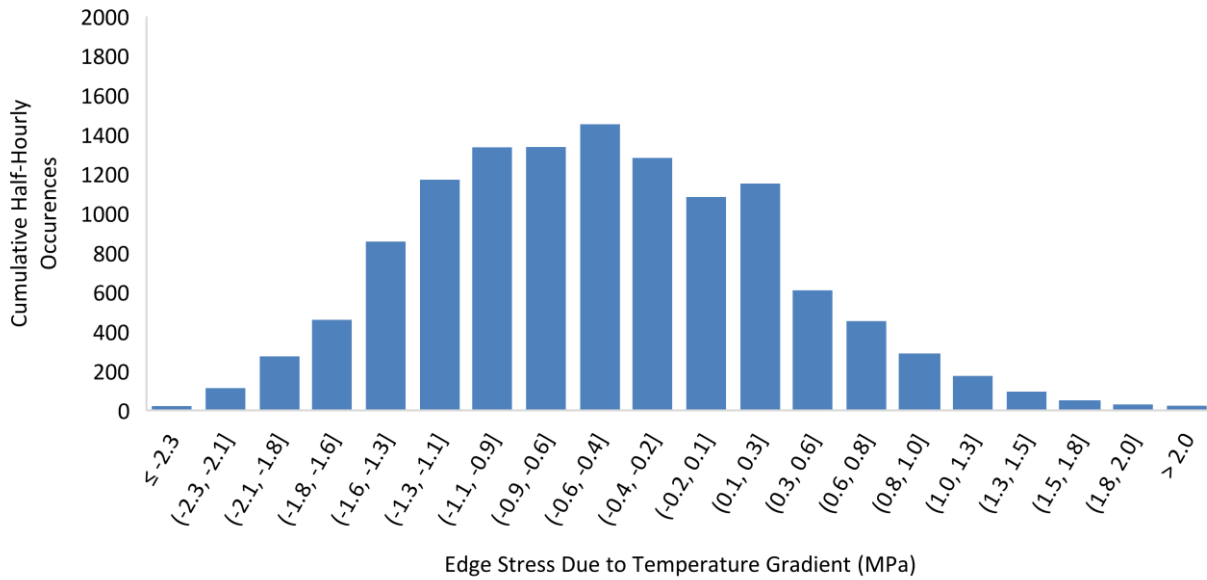


**Figure 6.28: Edge stress distribution 07/10/2016 to 07/10/2017 (half hour intervals)**

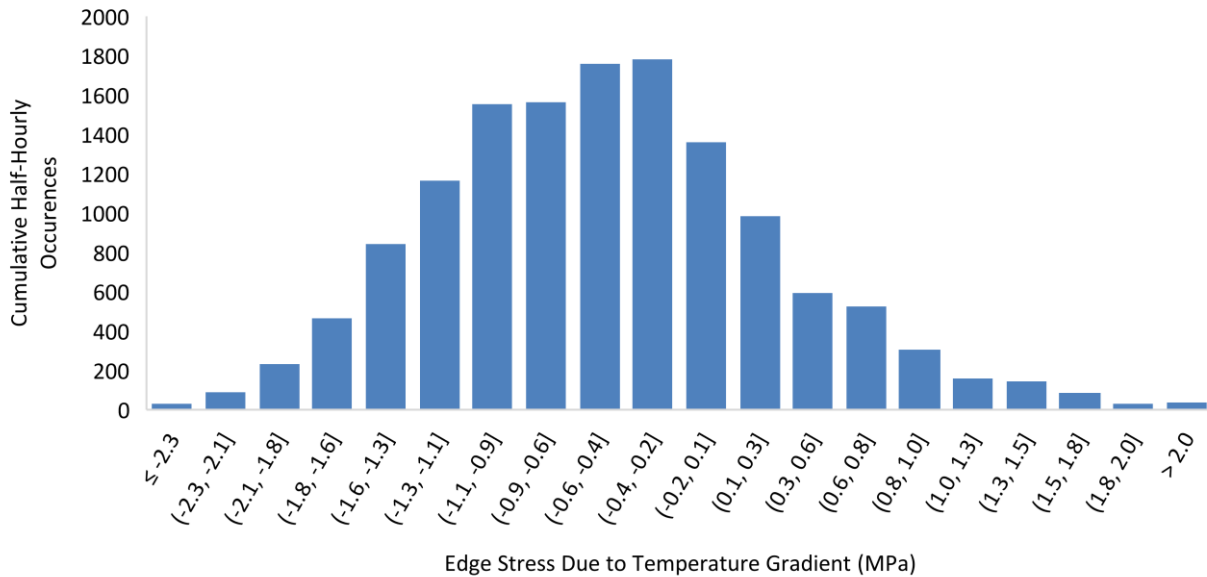


**Figure 6.29: Edge stress distribution 24/04/2017 to 24/04/2018 (half hour intervals)**

Over the course of each year, the average edge stress was found to be -0.5 MPa, which indicates that the surface was slightly cooler than bottom of the panels, resulting in a tensile stress. The magnitudes of these stresses were found to be generally normal in distribution, with 95% of the

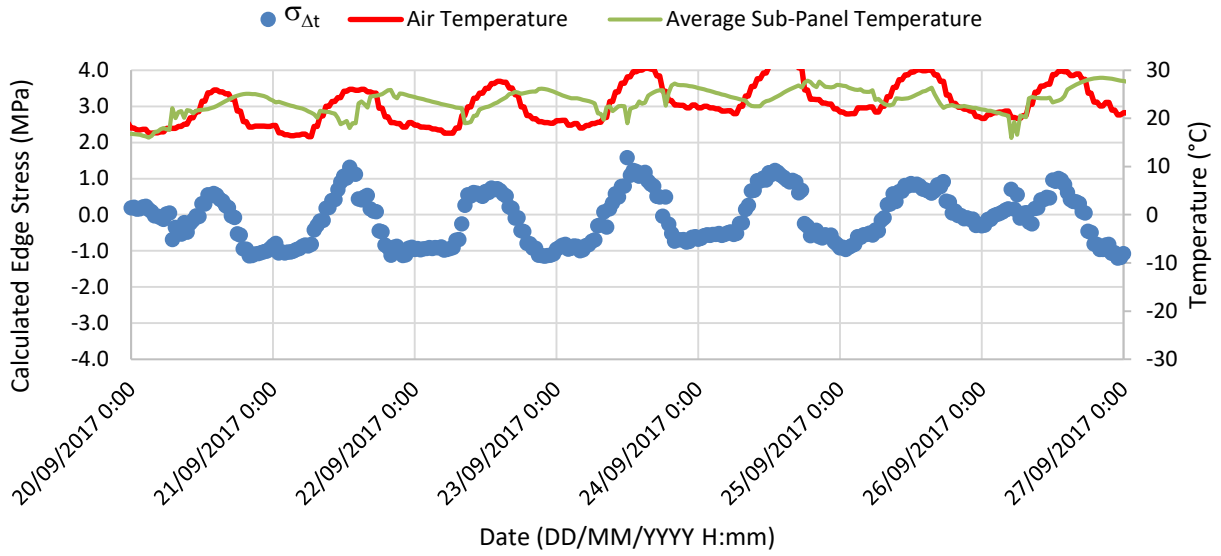
results in both cases being between approximately -2 MPa and +1.1 MPa. The maximum temperature related compressive and tensile stresses calculated throughout the study were 3.4 MPa and -2.8 MPa, respectively

These results indicate that temperatures should be considered in any fatigue analysis as the negative tensile stresses would magnify the stresses due to traffic loading. These stresses would therefore use a larger proportion of the total fatigue life according to Miner's fatigue principle. These effects would be offset in part by the edge stresses resulting in compressive stress at the bottom of the member, which would reduce the fatigue contribution of traffic loads. Since the mean stress in each case was negative, this indicates that the overall effect of the temperature loading would be a decrease in fatigue life.

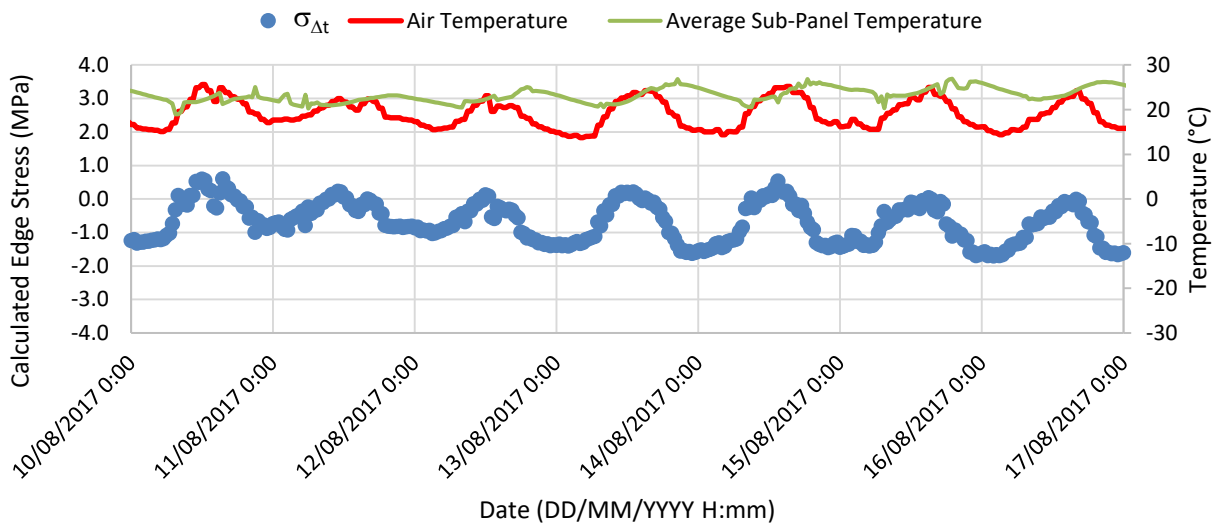
Again it should be noted that the reinforcement in the panels, which is not present in most Canadian concrete pavements, should arrest the propagation of cracks following fatigue failure.

Figure 6.30, Figure 6.31, and Figure 6.32 show the calculated edge stresses due to temperature gradients for hot, warm, and cold weather periods, respectively. In all cases, the insulating effect of the PCIP can be seen, as the temperature changes beneath the panel are smaller and slightly delayed as compared to the air temperatures. The sub-panel temperatures are generally warmer than the air temperature, resulting in a tensile stress. The high mid-day temperature peaks during the hot weather period result in a positive temperature gradient and compressive edge stresses. In the other two conditions, the warm mid-day air temperatures generally do not exceed the sub-panel temperature, resulting in consistent tensile stresses.

In each case, the panel surface temperature is likely higher than the measured air temperature during daylight periods. In general this would shift the temperature differential in the positive direction, resulting in increased compressive stresses at the panel bottom. This indicates that the tensile stresses displayed are likely over-estimates and would have a lesser impact on panel fatigue life.



**Figure 6.30: Calculated edge stress during hot weather period (20/09/2017 – 27/09/2017)**



**Figure 6.31: Calculated edge stress during warm weather period (10/08/2017 – 17/08/2017)**

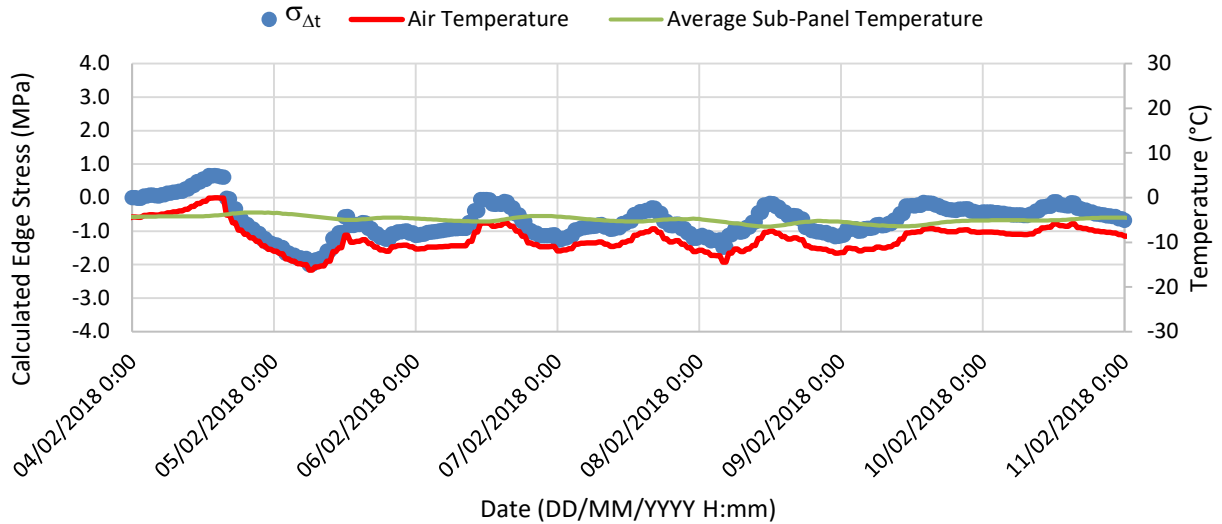


**Figure 6.32: Calculated edge stress during cold weather period (04/02/2018 – 11/02/2018)**

Figure 6.33 shows the distributions of the daily maximum daytime and nighttime temperature differentials between the top and bottom of panels, as considered based on EPC thermistor readings and local air temperature readings. This distribution considers the one year period between October 3, 2016 and October 3, 2017. It should be noted that in some instances, the maximum daytime differential is a negative value. This indicates that during that 24 hour period, the surface of the PCIP was never warmer than the base. Similarly, the maximum nighttime temperature differential was often positive.

The distribution is considered in terms of 1°C increment. The distributions of both daily maximum daytime and nighttime differentials are approximately normally distributed. During the time period the average daily maximum daytime and nighttime temperature differentials were 1.2°C and -6.6°C. Assuming a normal distribution, only approximately 7% of the days will have a maximum nighttime differential below -12.3°C or a maximum daytime temperature differential greater than 8.1°C.

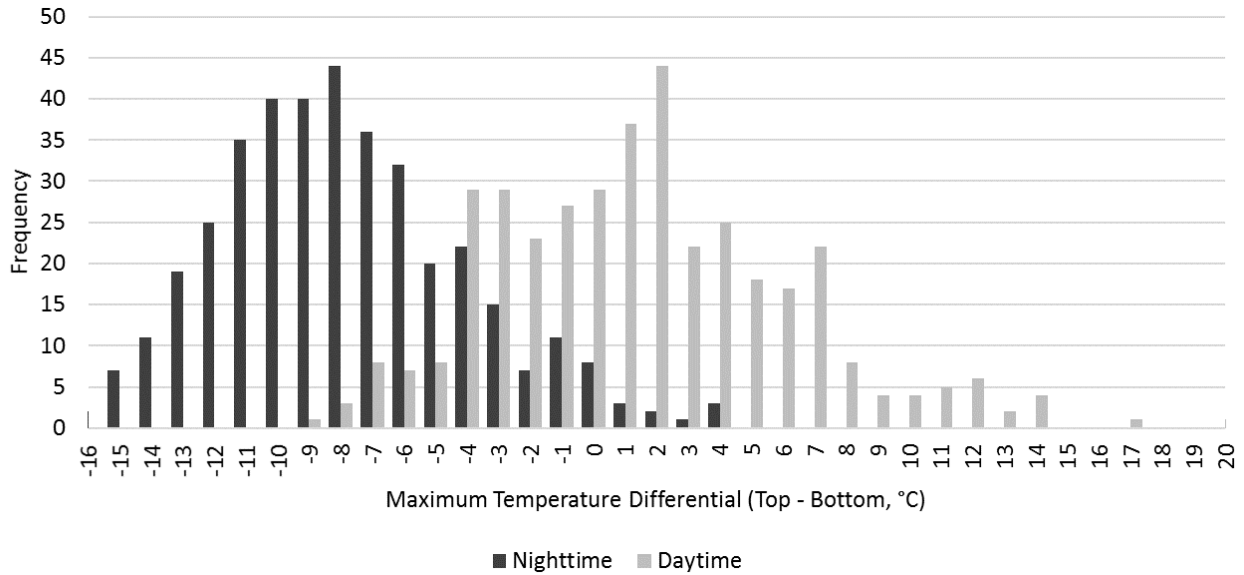


**Figure 6.33: Daily maximum and minimum temperature differentials, October 3, 2016 – October 3, 2017**

Reviewing the environmental and sub-surface data, it was found that during the first year, the air temperature underwent 51 cycles between above and below the freezing point (0°C), or freeze-thaw cycles. Due to the insulating effects of the PCIP, only 15 freeze-thaw cycles were observed below the PCIP. In the following year, October 7, 2017 to present, the air and sub-panel areas underwent 67 and 44 freeze-thaw cycles, respectively.

The presence of moisture beneath the panels combined with freeze-thaw conditions indicates that any support or grout material beneath the PCIP should be designed for these aggressive conditions.

#### 6.2.4 Conclusions and Recommendations

The instrumentation included six clusters, each of which consisted of two earth pressure cells (EPCs) and one moisture sensor. The sensors have been monitored since October 3, 2016, and this process is on-going.

Results indicate that as environmental temperatures began to drop at the end of the initial October of PCIP service, a change may have occurred that resulted in increased moisture infiltration rates beneath the panels. Beyond this point, significant amounts of moisture were observed beneath the panels for most of the winter season. During non-winter periods, sub-panel moisture contents have consistently dropped to relatively low levels following the increases associated with precipitation

events. This indicates that moisture is exiting the area beneath the PCIPs effectively, despite the impermeable nature of the asphalt support layer. The presence of moisture beneath the panels indicates that the bond between edge grouts and existing asphalt is allowing for the passage of water. A flexible sealant material should be considered at all joints and edges of the PCIP design.

Under static load testing using a fully loaded gravel truck, the functionality of the sensors was tested. All but two EPCs were found to be functioning, resulting in four functioning EPC pairs. Two load positions were observed for each instrumented panel: one with the tandem axle spanning the joint and one with the axle tandem axle centred on the panel. Under these conditions, it was found that the supporting material beneath the joint experiences loads from traffic as much as twice those experienced under the centre of the panel. This confirms the joint load transfer efficiency measured through FWD testing. Higher deflections at joints can place the dowels and their surrounding grout under stress due to the moment caused by opposite slopes of adjacent panels.

The temperature differentials across the PCIPs were approximated using air temperature as a surface temperature. The maximum daily daytime and nighttime temperature differentials were found to be approximately normally distributed, with average values of 1.2°C and -6.6°C, respectively. The largest negative temperature differential was found to be -16.7°C while the largest positive temperature differential was found to be 17.2°C. The edge stresses associated with the temperature differentials were found for the study period, and were found to be normally distributed across 1 year intervals, with average stresses of -0.5 MPa, indicating that generally the temperature related stresses increase the tension in the bottom of the panels, which can reduce the fatigue performance of a concrete pavement. This is based on the use of air temperature as a proxy for panel surface temperature, which can overestimate the tensile stresses during daytime periods.

51 freeze-thaw cycles were observed in the air temperature on site, while only 15 cycles were measured beneath the PCIP during the first year of service. In the second year (October 7<sup>th</sup>, 2017 to present), 67 air and 44 sub-panel freeze-thaw cycles were measured. Considering that moisture was found to be present beneath the panels, freeze-thaw resistant grouts and bedding materials are a necessary design feature of PCIP rehabilitation design.

The results do not differentiate any of the support conditions considered in terms of early-age performance. Each support condition provides similar moisture-penetration susceptibility, and

relative joint vs mid-panel pressures. These values will be tracked throughout the trial section's service life to determine the relative performance of the support conditions that could inform agencies when selecting the best PCIP strategy.

### **6.3 Joint Performance<sup>4</sup>**

As part of the Precast Concrete Inlay Panel (PCIP) trial, three different sub-panel support conditions were designed (Pickel et al. 2016). Support conditions are a large factor in the performance of precast concrete since the panels cannot flow to fit the shape of where it is placed, unlike concrete placed in the unhardened condition (Smith & Snyder, 2017; Tayabji, Ye, & Buch, 2012). A plane support surface is required to avoid high or low spots that can result in stress concentrations or bridging, respectively. A surface tolerance of  $\pm 3$ mm from plane was identified by the panel manufacturer as appropriate for support surfaces.

Each of the three support conditions on the trial had relative advantages and disadvantages relating to ease of construction, and the trial construction offered an opportunity to analyse each support condition according to both their constructability and performance. The three support conditions were asphalt-supported (AS), grout-supported (GroS), and grade-supported (GraS). Their designs and relative benefits and costs were discussed in Section 4.2. Table 6.2 summarizes the design components associated with each support condition.

In each case, load transfer between adjacent panels was achieved using smooth dowels that were cast integrally into one side of each PCIP. These dowels were then positioned within inverted dowel slots on the adjacent panel during placement. These dowel slots were then filled with structural grout to provide a bearing surface between the dowels and the adjacent panel. Each dowel was 38 mm in diameter and 355 mm long.

---

<sup>4</sup> The contents of this section of the chapter have been incorporated within a paper that has been submitted for publication. D. Pickel and S. Tighe, "*Joint performance evaluation for a Canadian precast concrete inlay panel trial*" Submitted to International Journal of Pavement Engineering. Submission date April 2, 2018

**Table 6.2: Summary of Support Conditions Studied**

		<b>Asphalt-Supported</b>	<b>Grade-Supported</b>	<b>Grout-Supported</b>
Precast Concrete Panel	Thickness (mm)	205	205	205
	Cast-in Levelling Feet	No	No	Yes
Milled HMA	Nominal Milling Depth (mm)	206	218	218
	Allowable Surface Texture (mm)	± 3	± 6	± 6
Support Material	Non-Structural Bedding Grout (mm)	0 to 4	0 to 4	-
	Rapid Setting Bedding Grout (mm)	-	-	7 to 19
	Cement-treated Bedding Material (mm)	-	3 to 19	-

A key performance measure of a jointed concrete pavement is the effectiveness of the joints at transferring loads from one panel to the adjacent panel. If a joint is unable to transfer load from a loaded panel to an adjacent, unloaded panel, then the loaded panel must support the full load, which results in very high stresses within the concrete panel and in the underlying material that supports the panel. These results can lead to early fatigue failure and support loss, respectively, which decrease the service life of a pavement or increase the frequency of required maintenance.

Various load transfer devices can be used in order to allow loads to be transferred across a joint, including smooth dowel bars, deformed tie-bars, plate dowels, and the concrete's constitutive aggregate. These mechanisms bridge the gap between adjacent sides of the joint and bear on both sides.

Field measurements of the effectiveness of joint load transfer are typically made using a falling weight deflectometer (FWD) or similar testing device. This test involves applying a load to one side of a joint and measuring the deflection of both the loaded ( $\delta_L$ ) and unloaded side ( $\delta_{UL}$ ) of the joint. The ratio of the unloaded deflection to the loaded deflection gives you the load transfer

efficiency ( $LTE_{\delta}$ ). Equation 15 shows the calculation of load transfer efficiency accepted by the American Association of State Highway and Transportation Officials (AASHTO, 1993).

$$LTE_{\delta} = \frac{\delta_{UL}}{\delta_L} \times 100\% \quad (15)$$

The  $LTE_{\delta}$  value provides an indication of the percent of deflection that is transmitted across a joint via a load transfer device. As the value approaches zero, it indicates that no load is being transferred across the joint and therefore the unloaded side is not deflecting at all (Figure 6.34, part a). As the value approaches 100%, it indicates that both sides of the joint deflect equally and therefore load is being very effectively transferred across the joint (Figure 6.34, part b). Part b of Figure 6.34 shows a steel dowel bar spanning the joint that is a common method of improving load transfer across a concrete pavement joint.

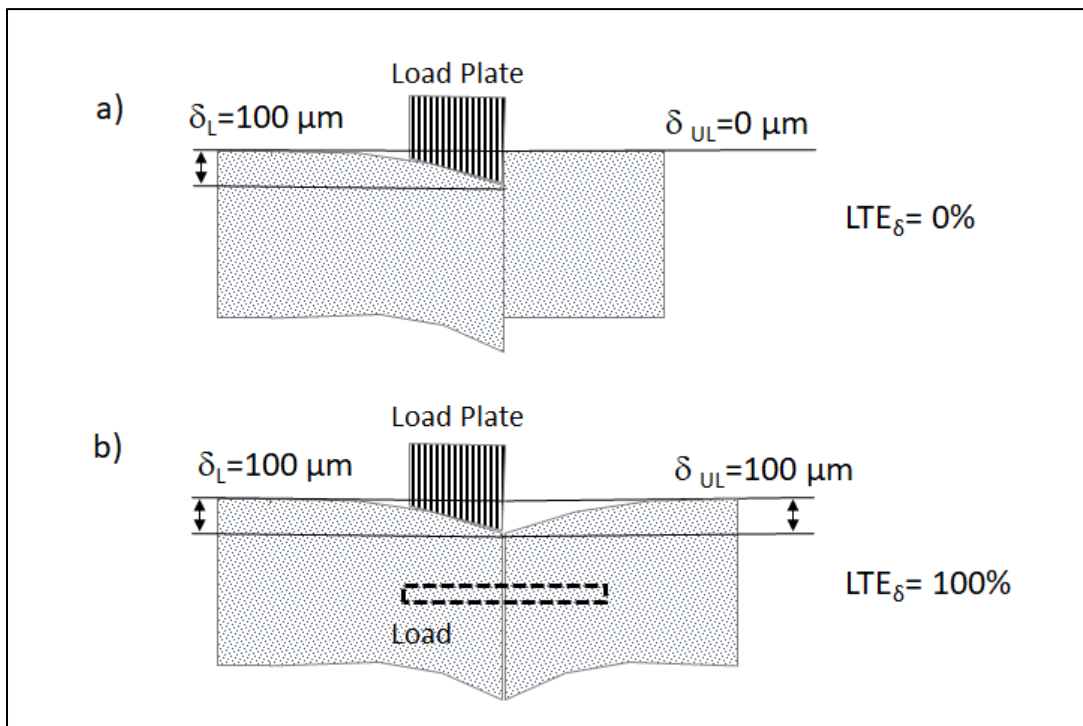


**Figure 6.34: Illustration of joint with no load transfer (a), and a joint with excellent load transfer (b)**

$LTE_{\delta}$  is a common method of measuring the performance of joints in concrete pavement. The test is easily performed, and the results are easily calculated and understood. The FWD testing

equipment is also useful for evaluating flexible pavement structures (such as HMA) and is therefore relatively common in the field of pavement testing.

The load transfer across a joint or a crack is provided in three main ways: aggregate interlock, load transfer devices, and stabilized support materials (Owusu-Antwi *et al.* 1990). When load transfer is evaluated using deflection-based testing, the support conditions beneath the joint play a secondary role in addition to the load transfer device being employed. Particularly in cases where the support material has shear capacity, a continuous layer beneath a concrete joint can affect the behaviour of a joint by increasing the overall shear capacity. The stiffness and durability of the material beneath a joint in a PCC pavement can affect the performance of that joint (Delatte, 2014; AASHTO, 1993).

In the case of the PCIP trial section, load transfer information can provide insight into the performance of the support conditions, as they represent the main variable in the overall load transfer system of the panels. The same dowel and grout system is used for each joint, however the support layer directly under the joints changes with each support condition. Therefore, to evaluate the different performance characteristics of the support conditions in the PCIP trials, their load transfer behaviour is analyzed.

### **6.3.1 Joint Evaluation Methodology**

Two separate instances of load transfer testing were undertaken on the PCIP trial section, both performed by members of the testing company EXP. The first was two weeks after the completion of the section's construction, on October 6, 2016. The second was following one year of service, on September 19, 2017. The air temperature for each of these nights ranged between 14-15°C and 17-19°C, respectively, while the measured concrete temperatures were 10°C and 19°C, respectively (Government of Canada, 2018). In both cases, the two right lanes of the highway were closed to traffic and the testing was done between the hours of 10 p.m. and 6 a.m. the following morning.

The testing included two passes along the trial: one along the inside wheel path (IWP) and one along the outside wheel path (OWP). In each pass, each joint was loaded on the approach side and on the leave side. For each test, drops were recorded for target loads of 40 kN, 55 kN, and 75 kN.

Displacements were measured at the location of the loading plate and at sensors 30 cm away from the loading plate. The sensors were centred around the joint such that each was spaced 15 cm on either side of the joint.

The trial section included eight AS panels, and seven of each GraS and GroS panels. Including the joints between the asphalt lane and the first and last PCIP, a total of 23 joints were tested for load transfer. This resulted in a total of 46 test IDs, one on each side of each joint, with two locations per ID (OWP and IWP).

For the purposes of this study, the transition joints between each type of support condition are ignored since these areas represent a transition between support conditions and the goal of the analysis is to differentiate between the different support types. The Asphalt/PCIP terminal joint results are presented, but are not included in the statistical comparisons between support condition types. Therefore, AS joints account for 13 test locations (ID # 3-16), GraS for 11 locations (ID # 19-30), and GroS for 11 locations (ID # 33-44). Asphalt/PCIP joints, at the very beginning and end of the trial, account for four locations (ID # 1, 2, 45, and 46) while transition joints account for four locations (ID # 17, 18, 31, and 32).

A visual inspection found that the load transfer dowels at each joint appeared to be functioning properly with the joints in good condition at both testing ages. The relative changes in the measured values discussed are assumed to be due to the differences in support condition that were the only substantial difference between the different parts of the trial section.

### ***6.3.1.1 Load Transfer Efficiency***

LTE<sub>s</sub> is the performance measure by which the MTO evaluates joint performance in PCC pavements. An LTE<sub>s</sub> value of  $\geq 70\%$  is used as an acceptance threshold for a well-performing joint. Severity of joint deterioration is also considered in order to make recommendations relating to joint repair (Chan & Lane, 2005).

The results of the two instances of FWD testing are summarized in Table 6.3. For each testing date, the table shows the minimum, maximum, and average LTE<sub>s</sub> values, as well as the standard deviation of all measurements for each of the three support conditions and the terminal interfaces between the PCIP and the HMA. Each LTE<sub>s</sub> value represents the average of the three LTE<sub>s</sub> values

determined at the three load levels. The cumulative number of  $LTE_{\delta}$  readings less than the 70% acceptance threshold are also shown.

**Table 6.3: Summary of  $LTE_{\delta}$  Results for Oct. 6, 2016 (Initial Construction) and Sept. 19, 2017 (One Year of Service)**

	Initial Construction					One Year of Service				
	$LTE_{min}$	$LTE_{max}$	$LTE_{avg}$	$\sigma$	Tests below 70%	$LTE_{min}$	$LTE_{max}$	$LTE_{avg}$	$\sigma$	Tests below 70%
AS	73.3%	86.0%	80.5%	3.2%	0	61.1%	92.9%	82.7%	9.4%	4
GraS	76.3%	84.8%	80.6%	2.5%	0	66.8%	94.7%	82.2%	7.0%	2
GroS	77.5%	89.3%	83.0%	3.4%	0	62.8%	97.2%	83.1%	7.9%	2
PCIP/HMA	50.9%	90.9%	70.4%	13.5%	5	7.8%	64%	37.7%	17.8%	8

After initial construction, all of the intermediate joints were found to adhere to the minimum 70% threshold. A least significant difference (LSD) statistical analysis was undertaken on the results that indicated that with 95% confidence, the load transfer efficiency of the GroS support condition was significantly higher than the other two support conditions. However, in all three cases the average  $LTE_{\delta}$  was acceptable based on the MTO's acceptance criteria.

One year after construction, the average  $LTE_{\delta}$  values were found to increase, however the standard deviation associated with each support condition type shows that this increase in average value corresponded to greater variance within the results. In each support condition, two separate joints were found to have at least one  $LTE_{\delta}$  test below the 70% threshold. In the case of the AS support condition, both the IWP and OWP tests at two separate joints were below 70%, resulting in four total results below 70%. The average  $LTE_{\delta}$  of the GroS condition was still the highest of the three, but due to the increased variance within the results, the difference was no longer statistically significant at 95% confidence.

During the first testing period, five of the eight tests on the PCIP/HMA joints were below the 70% threshold, indicating that there is significant differential deflection between the two materials

under loading conditions. In each case, the  $LTE_{\delta}$  was higher when the PCIP was loaded than when the HMA surface was loaded.

Following one year of service, the  $LTE_{\delta}$  values were found to drop even further. The average dropped well below the minimum acceptable threshold of 70% as the results of all eight tests were below this value. These joints only consisted of grout poured between two vertical faces, and this bond was generally found to have broken early in the pavement service life. Therefore, the only load transfer between the two materials is through the lower layers of the pavement structure, including the unmilled portion of the HMA and the base layers. It is likely that load transfer in these joints will be difficult to increase without the addition of a load transfer device, however a material that provides more adhesion to both the HMA and PCIP would at least improve the material bond in these joints.

Figure 6.35 displays the results of both testing dates. The 70% threshold is displayed as a horizontal line, while the vertical lines separate the support conditions, transition joints, and terminal joints.

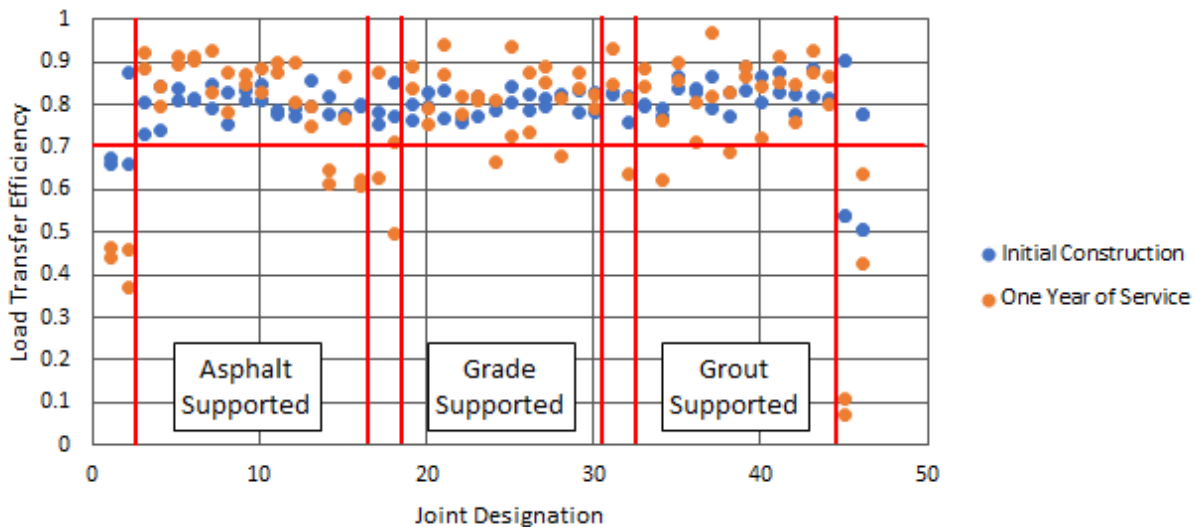


**Figure 6.35:  $LTE_{\delta}$  results for Oct. 6, 2016 (Initial Construction) and Sept. 19, 2017 (One Year of Service)**

The wider variation in results can be noted in the figure, including the drops below the acceptance threshold in some cases.

### 6.3.1.2 Void Detection

In addition to measuring the  $LTE_{\delta}$  across joints, the data collected from the FWD testing can also be used to provide insight into the presence of voids beneath joints and edges of panels. This test uses the three loading conditions (40 kN, 55 kN, and 75 kN) and their associated deflections ( $\delta_L$ ) in a linear regression to determine a line of best fit when the applied load is plotted against deflection. The y-intercept of the line of best fit then corresponds to the predicted deflection under a load of 0 kN. In an ideal and fully supported condition, this value would be anticipated to be zero, however as this value increases, it indicates the increased potential for the presence of a void beneath the joint. Traditionally, if this value is larger than 75  $\mu\text{m}$ , it is assumed to indicate a substantial void beneath the joint. This is often the threshold beyond which joint undersealing or another joint repair is recommended. Equation 16 represents the regression formula used to find the intercept,  $D_0$ .

$$D_0 = \overline{\delta_L} - \frac{\overline{L} \times \overline{\delta_L} - \overline{L} \times \overline{\delta_L}}{(\overline{L})^2 - \overline{L}^2} \times \overline{L} \quad (16)$$

Where  $L$  represents the applied load in kN,  $\delta_L$  represents the deflection corresponding to the applied load, in  $\mu\text{m}$ , and  $D_0$  represents the predicted deflection under no applied load, in  $\mu\text{m}$ .

Table 6.4 summarizes the results of the void detection analysis for each support condition type. The average  $D_0$  values for each support condition are shown for each year, as well as the standard deviation of the data.

As shown in the table, there was a significant increase in the  $D_0$  values for each support condition. While this does not necessarily indicate that significant and on-going deterioration of the joints is underway, it does show that conditions of the joint have changed since the as-constructed measurements were taken. This change was not clear in the  $LTE_{\delta}$  results, presented previously.

**Table 6.4: Summary of  $D_0$  Results for Oct. 6, 2016 (Initial Construction) and Sept. 19, 2017 (One Year of Service)**

	Initial Construction		One Year of Service	
	$D_{0avg}$ ( $\mu\text{m}$ )	$\sigma$ ( $\mu\text{m}$ )	$D_{0avg}$ ( $\mu\text{m}$ )	$\sigma$ ( $\mu\text{m}$ )
AS	-1.64	4.82	37.35	20.35
GraS	-1.51	6.30	28.20	11.64
GroS	-4.55	3.51	34.46	11.60

An LSD analysis indicated that the GroS support condition was statistically different than the other two conditions at 95% confidence in year 0. However, the increased variability at year 1 resulted in the differences between support conditions becoming not significant at 95% confidence. Considerably less variability was observed for the GraS and GroS support conditions than for the AS condition. This may indicate that these two conditions have performed better over the first year, however this difference is not significant at this point in time. Figure 6.36 illustrates the  $D_0$  results for both years of testing.

Unlike the  $LTE_8$  results, the void detection results indicate a clear difference in the joint behaviour over the course of the initial year of service. These changes should not be extrapolated to assume that year 2 will display a similar increase in  $D_0$ , as these changes may represent an “initial settling”. These results will be monitored throughout the pavement’s service life to track this.

As shown in the figure, at year 1 three AS joints exhibited  $D_0$  values above the 75  $\mu\text{m}$  threshold, indicating the potential for voids beneath the joints.

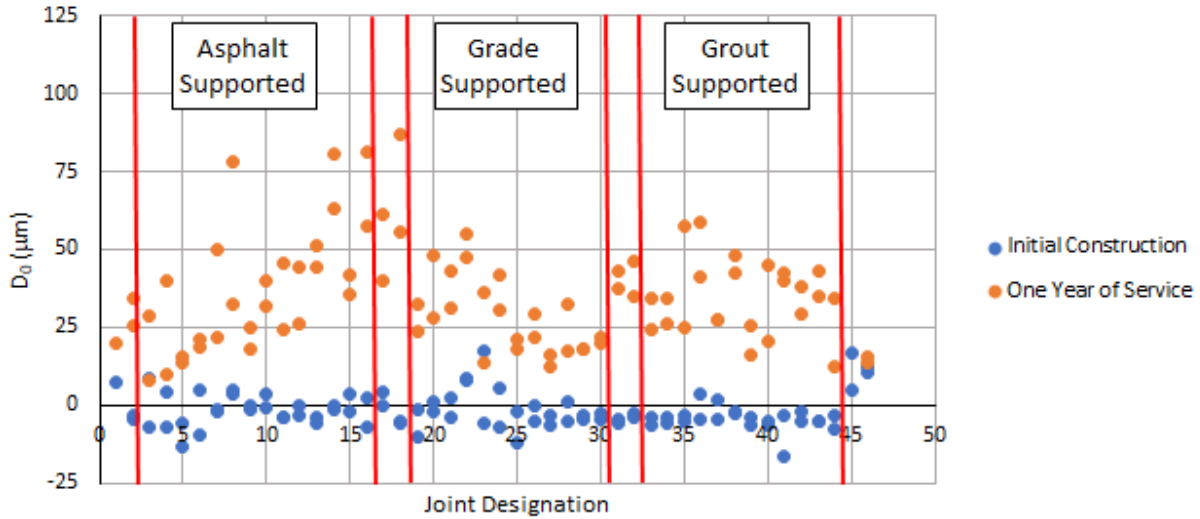


Figure 6.36: Sub-joint void analysis results

### 6.3.1.3 Relative Displacement

The use of  $LTE_{\delta}$  as a joint analysis method is a broadly useful technique that is easily performed and understood. However, the results do not provide a comprehensive representation of joint performance in all cases. In cases where very little deflection is observed on either side of a joint, the ratio of the two deflections can indicate a poor joint, when it is behaving well. Alternatively, if both sides of a joint deflect substantially, a significant difference between the two deflections can seem less significant in the ratio of deflections. Table 6.5 illustrates these particular cases for two joints, A and B, which behave differently according to  $LTE_{\delta}$ .

Table 6.5: Illustration of Potential Issues with  $LTE_{\delta}$

Joint	$\delta_L$ (μm)	$\delta_{UL}$ (μm)	$\Delta\delta$ (μm)	$LTE_{\delta}$	70% Acceptance
A	4	2	2	50%	Fail
B	120	85	35	71%	Pass

As shown, joint A would be considered as an unsatisfactory joint while joint B would be considered satisfactory and accepted, despite showing considerably higher overall deflections and differential deflections. This indicates that further information relating to a joint should be considered.

While the  $LTE_{\delta}$  formula is generally sufficient to identify poor joints, it cannot properly identify performance in situations such as those outlined above. Furthermore, the difference in deflection between the loaded and unloaded side is more indicative of joint performance than a ratio that can obscure the magnitude of the difference. Popehn, Schultz, and Snyder suggests the use of differential deflections, using the equation shown in Equation 17 (Snyder 2011, Popehn *et al.* 2003).

$$DD = \delta_L - \delta_{UL} \quad (17)$$

Where  $DD$  represents the differential deflection, and  $\delta_L$  and  $\delta_{UL}$  represent the peak deflections of the loaded and unloaded panels, respectively. This formula provides more context of the behaviour of a joint under load and was based on the assumption of a 40 kN load. Based on this formula, a performance requirement of 50  $\mu\text{m}$  (2 mils) has been recommended, and adopted by several state departments of transportation (Larson & Smith, 2011).

Equation 17 does not make any accommodation for varying load levels, which are unavoidable when field testing. Even with a target of 40 kN, the actual applied load will be largely dependent on machine calibration and operator inputs. Changes in the applied load results in changes to the differential deflection. Therefore, a different formula was developed and used for the evaluation of joints in this project. The formula, shown in Equation 18, considers the difference in actual deflection between the loaded and unloaded sides of the joint. Since this difference is linearly dependant on the magnitude of the load, the difference is then normalized by the measured load for the given measurement. For the purposes of this study, the 75 kN load level was used for the analysis, however any load level could be used similarly.

$$RD_{75} = \frac{\delta_L - \delta_{UL}}{\text{Measured Load}_{75kN}} \quad (18)$$

Using this formula, the testing data from both testing dates were analysed to consider the performance of the joints. Table 6.6 shows the average results for each support condition on both testing dates.

**Table 6.6: Summary of RD75 Results for Oct. 6, 2016 (Initial Construction) and Sept. 19, 2017 (One Year of Service)**

	Initial Construction		One Year of Service	
	RD <sub>75,avg</sub> ( $\mu\text{m}/\text{kN}$ )	$\sigma$ ( $\mu\text{m}/\text{kN}$ )	RD <sub>75,avg</sub> ( $\mu\text{m}/\text{kN}$ )	$\sigma$ ( $\mu\text{m}/\text{kN}$ )
AS	0.48	0.11	0.86	0.56
GraS	0.43	0.12	0.85	0.37
GroS	0.36	0.10	0.90	0.45
PCIP/HMA	0.76	0.49	3.87	3.68

The findings once again indicate that the GroS condition resulted in statistically better performance, at 95% confidence immediately following the completion of construction. Each support condition showed little relative deflection, with very consistent results.

After one year of service, the relative deflections observed for each support condition increased substantially. The average RD<sub>75</sub> for the GroS condition was observed to be the highest, though the variance shown in the AS condition shows that some of these joints experienced significant increase in joint relative deflection.

The PCIP/HMA terminal joints were found to show substantially higher relative displacement than all other joints at both testing ages. As discussed for the LTE<sub>δ</sub> results, this finding is expected based on the design of the joint. Following one year of service there were large differences in the displacements under loading, regardless of whether the PCIP or the HMA side of the joint was being loaded.

Figure 6.37 shows the results for RD<sub>75</sub> for both years of testing.

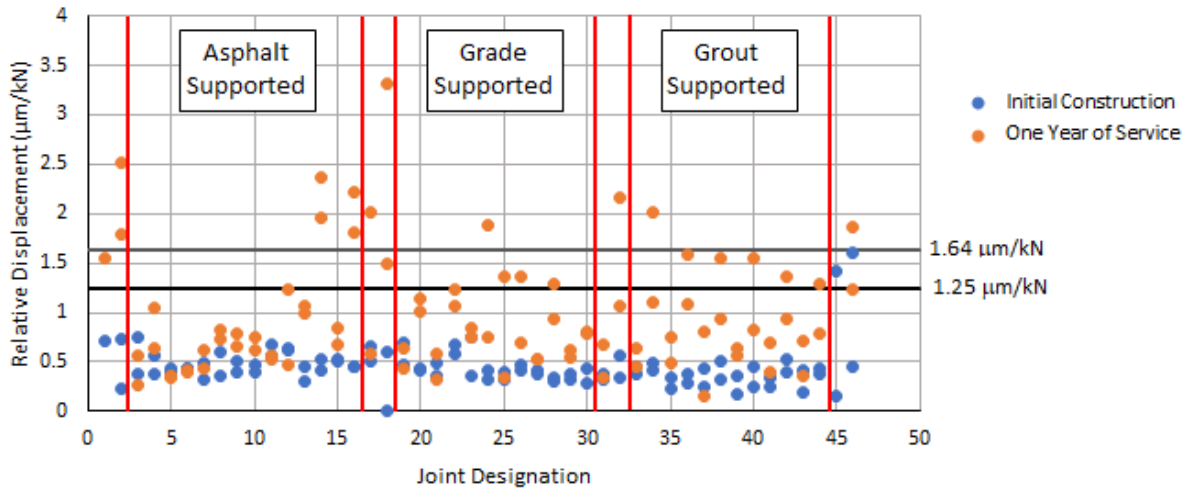


**Figure 6.37: RD<sub>75</sub> Results for Oct. 6, 2016 (Initial Construction) and Sept. 19, 2017 (One Year of Service)**

As shown, the RD<sub>75</sub> values generally increased for each support condition. Both GraS and GroS conditions increased relatively consistently throughout the trial. AS increased on average, but only with very small increases in some joints and substantial increases in others.

The observed pattern in AS may be a result of inconsistent surface milling. While the milled surface tolerance was specified as  $\pm 3\text{mm}$ , the milled surface was not thoroughly checked prior to the placement of PCIP panels. In some areas, the PCIP joints are fully supported by the asphalt pavement layer, which is stiff and durable, but some areas may be supported by the thin, weak bedding grout, which could deteriorate over time and repeated loading. This could explain the areas of excellent performance and relatively worse performance within the same section.

The consistent change in the GraS and GroS conditions, may indicate that the original stiffness of the supporting layers between the PCIP and the HMA layer (CTBM/bedding grout and rapid-setting bedding grout, respectively) lose some of their load transferring abilities through the course of the first year of service.

In all cases, the joints were found to be performing well at the time of testing. While joint responses were found to vary between support types, none were found to be unacceptable at this stage of the trial's life.

The other load levels that were used for the analysis of this project were compared using a LSD statistical analysis and it was found that the RD<sub>40</sub>, RD<sub>55</sub>, and RD<sub>75</sub> populations were not statistically distinct. This indicates that relative displacements at any load level could probably be compared when normalized by the magnitude of the applied load.

### **6.3.2 Incorporating RD<sub>75</sub> into Joint Evaluation**

While the LTE<sub>δ</sub> method of joint evaluation provides meaningful information relating to joint performance of PCC pavements, some information is omitted through the use of a ratio. Furthermore, as seen in this trial the LTE<sub>δ</sub> can provide somewhat misleading results. Even though some joint deterioration can be assumed to have happened, the LTE<sub>δ</sub> testing indicated a net improvement of joint performance over the course of one year of service. The intuitive idea of some deterioration was confirmed via void detection and relative displacement testing. For this reason, it is suggested that the use of relative displacement (RD<sub>75</sub>) be incorporated into a joint evaluation practice.

The RD<sub>75</sub> value provides a meaningful measure of joint behaviour with units that can clearly represent the behaviour of joints under loading.

Using all of the joints within the project scope, including terminal and transition joints, a reasonable correlation between LTE<sub>δ</sub> and RD<sub>75</sub> was found for the data collected as part of this project using a least squares analysis. An exponential function, with the y-intercept set to LTE<sub>δ</sub> = 1, fits the measured data well, with a coefficient of determination of approximately 0.5. The intercept is set at 1 because in a case when the RD<sub>75</sub> is 0 μm/kN, the load transfer efficiency of the joint should be 100%. The equation and corresponding shape of this correlation are outlined in Figure 6.38.

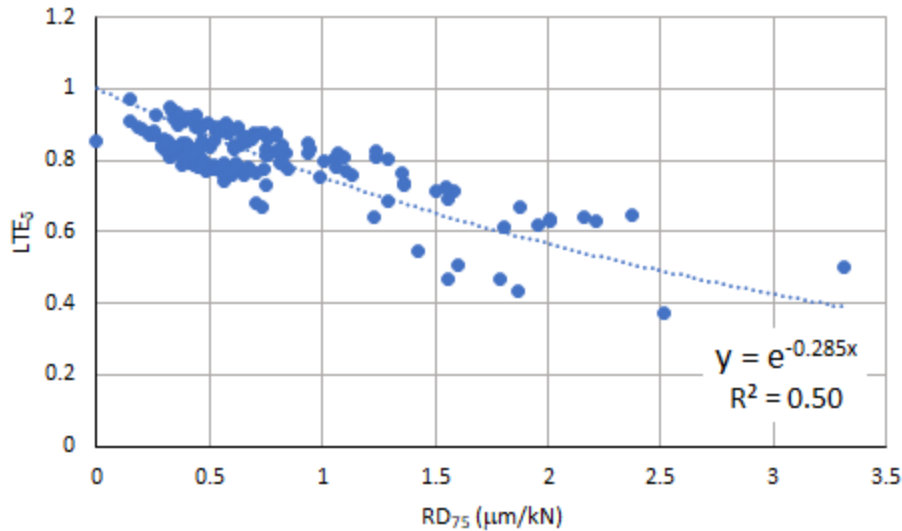


**Figure 6.38: Correlation between  $LTE_{\delta}$  and  $RD_{75}$**

Using this correlation, the relationship between  $LTE_{\delta}$  and  $RD_{75}$  can be approximated by Equation 19. This correlation and equation is based on a limited data set from a specific PCC application and requires further analysis prior to acceptance. The following discussion represents only a starting point for the use of the  $RD_{75}$  measure.

$$LTE_{\delta} = e^{-0.285RD_{75}} \quad (19)$$

The empirical studies that have been used to determine the threshold  $LTE_{\delta}$  value should not be discounted, and therefore the threshold  $RD_{75}$  value based on an  $LTE_{\delta}$  value of 0.7 is approximately equal to 1.25  $\mu\text{m}/\text{kN}$ . Using this value, the same joints that were near or below the 70% threshold value would exceed the  $RD_{75}$  threshold.

Additionally, the  $RD_{75}$  values linearly correlate reasonably with  $D_0$  analysis indicating voids, with a coefficient of determination of  $R^2=0.45$ . The linear correlation between  $LTE_{\delta}$  and  $D_0$  is not strong, with a coefficient of determination of  $R^2=0.03$ . These correlations are shown in Figure 6.39 and Figure 6.40, respectively.

While the relationship is not as clear as that shown Figure 6.38, the presence of voids could be reasonably correlated with  $RD_{75}$  values. On the other hand, there is no clear relationship between

LTE<sub>δ</sub> and D<sub>0</sub>. If a threshold RD<sub>75</sub> value was to be determined to indicate the presence of voids, the studies that were used to develop the D<sub>0</sub> = 75 μm threshold should not be discounted. Considering this, the correlation equation in Figure 6 can be evaluated for D<sub>0</sub> = 75 μm to produce an RD<sub>75</sub> value of 1.64 μm/kN.

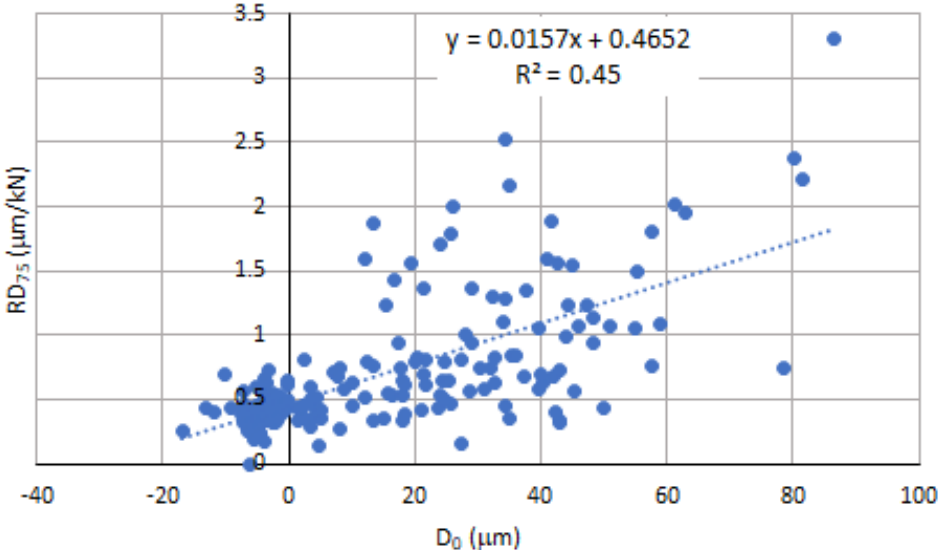


**Figure 6.39: Correlation between D<sub>0</sub> and RD<sub>75</sub>**

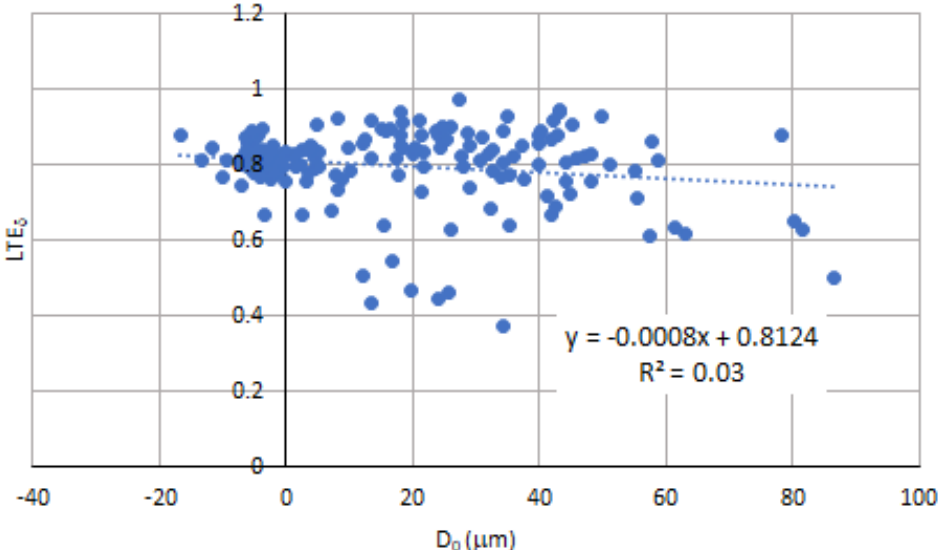


**Figure 6.40: Correlation between D<sub>0</sub> and LTE<sub>δ</sub>**

Based on this study, a load transfer evaluation of a PCIP application could evaluate RD<sub>75</sub> values as follows:

- $RD_{75} < 1.25 \mu\text{m/kN}$ , indicates a good joint performing well,
- $1.25\mu\text{m/kN} < RD_{75} < 1.64\mu\text{m/kN}$ , indicates sub-optimal joint performance,
- $RD_{75} > 1.64\mu\text{m/kN}$ , indicates poor joint performance with potential for void beneath the joint

In all cases, the condition of the joint as determined by a visual inspection should also be considered for comprehensive analysis of the joint condition and performance. These evaluation lines are shown on Figure 4 for illustration purposes.

While the  $RD_{75}$  thresholds suggested are based on the thresholds used in the more established tests, further use and refinement of the  $RD_{75}$  measurement could produce sufficient data to produce empirically-developed thresholds that could be used in conjunction with  $LTE_{\delta}$  values to produce a more comprehensive joint evaluation tool.

### 6.3.3 Conclusions

The PCIP trial section had three sections that each incorporated a different method of providing sub-panel support to the PCIPs: Asphalt-supported (AS), Grade-supported (GraS), and Grout-supported (GroS). Part of the evaluation of the trial section involved the testing of the joints between adjacent panels through the use of falling weight deflectometer (FWD) testing. FWD testing is typically used as method to obtain load transfer efficiency ( $LTE_{\delta}$ ) values for each joint, where  $\geq 70\%$  load transfer is considered acceptable joint performance. FWD testing was performed two weeks after the completion of the trial construction and again after one year of service.

Since the load transfer devices of each PCIP support method were the same, differences between each section of the trial were attributed to the support conditions beneath the joints. Joints between the PCIP and the adjacent asphalt pavement as well as transition joints between the different support conditions were generally ignored for the evaluation.

The  $LTE_{\delta}$  and  $RD_{75}$  for the terminal joints between the PCIP and the HMA were found to be considerably lower than the inter-panel joints at both testing ages. A better means of providing connection between the vertical faces of each element is required.

Following construction, all of the joints achieved the minimum acceptable threshold of 70%  $LTE_{\delta}$ , with little variation of results. The GroS condition was found to have a statistically higher  $LTE_{\delta}$  than the other support conditions. Following one year of service, some joints in each section were found to be below the acceptable threshold, with much higher variation in results. Overall, the average  $LTE_{\delta}$  was found to increase, counterintuitively.

Three load levels were used for FWD testing, and therefore void detection analysis could also be performed. This involves calculating the line of best fit between applied load and panel displacement and then determining the y-intercept of that line. This intercept ( $D_0$ ) indicates the predicted displacement in  $\mu\text{m}$  under zero load. When this value exceeds a threshold of 75  $\mu\text{m}$ , it indicates the presence of a void beneath the joint.

The intercept values were found to be low in all cases after construction, indicating that each joint was firmly supported. Following one year of service, the  $D_0$  values increased in all cases, indicating some deterioration of the support beneath the joint. This deterioration is not surprising under traffic loads and may represent “settling” more than significant, on-going deterioration. This result clashes with the  $LTE_{\delta}$  values that were seen to increase.

$LTE_{\delta}$  results do not give the full picture of joint performance, so a secondary value of relative displacement  $RD_{75}$  was developed to provide context to the magnitude of the displacement differences across a joint. This value can be calculated from data typically collected from  $LTE_{\delta}$  testing.

$RD_{75}$  indicated that the GroS condition provided the best load transfer following construction. The  $RD_{75}$  increased for all support conditions after one year of service, but the highest increase was observed for the GroS. Both GraS and GroS showed consistent increases in  $RD_{75}$ , that could indicate some deterioration of their support layers. The AS condition was seen to have either low or high  $RD_{75}$  with few intermediate values. This may indicate inconsistent milling practice, that could have left voids beneath joints that were initially filled with lean grout. This material may deteriorate quickly compared to other joints that are fully supported by the asphalt support layer.

Based on this analysis, it is suggested that a measure of relative displacement, such as  $RD_{75}$ , be considered when measuring joint performance. The value provides more context for the performance of a joint than  $LTE_{\delta}$  on its own.

Preliminary threshold values for acceptance were developed based on the information gathered as part of this study, including for joint acceptance and void analysis,  $RD_{75} = 1.25\mu\text{m/kN}$  and  $1.64\mu\text{m/kN}$ , respectively. These thresholds were developed based on correlations to existing thresholds, but with more comprehensive study, empirically calibrated  $RD_{75}$  values should be developed that can then be used in conjunction with  $LTE_{\delta}$  and visual joint inspection to develop a more comprehensive means for evaluating joint performance.

The joints of the trial section were generally found to be performing well after a year in service. While the GroS support seems to provide better joint performance initially, this does not appear to translate into better performance long-term. A more consistent method of milling the asphalt surface in the AS condition could result in this support condition providing the best long-term joint performance of the three conditions, based on the results of the  $RD_{75}$  test.

#### **6.4 Panel Surface Analysis**

The surface of a given pavement is very important when considering the overall performance of the pavement. Since the pavement surface is what interacts with the tires of the vehicles using the pavement, it can have a significant effect on the safety and comfort of the road users. The surface changes tire-pavement interactions, which govern noise, friction, and ride quality.

The description of a pavement's surface is generally made with respect to its texture, which is generally broken down into three distinct categories: microtexture, macrotexture, and megatexture. These texture categories are defined by ranges in wavelength ( $\lambda$ ) and amplitude (A), and each have effects on different parts of the tire-pavement interaction.

Microtexture ( $\lambda < 0.5\text{ mm}$ ,  $1\mu\text{m} < A < 500\mu\text{m}$ ) refers to the texture at a smaller-than-visible scale. It is generally associated with the properties of the aggregate used in the pavement construction.

Macrotexture ( $0.5\text{ mm} < \lambda < 50\text{ mm}$ ,  $0.1\text{ mm} < A < 20\text{ mm}$ ) refers to the texture that can be easily seen on the pavement surface. The size and distribution of aggregate particles will affect the

macrotexture, and in concrete pavements the macrotexture is often applied to the pavement by tining, burlap dragging, broom finishing, or diamond grinding.

Megatexture ( $50 \text{ mm} < \lambda < 500 \text{ mm}$ ,  $0.1 \text{ mm} < A < 50 \text{ mm}$ ) is on the same order of magnitude as the tire itself and is often manifested as deteriorations in the pavement (potholes, cracking, rutting, etc.). (Hall, Smith, & Littleton, 2008)

Pavement surfaces can be reasonably represented by a series of sine curves with different wavelengths and amplitudes. Each of these sine curves fall into one of the three categories for a scale that is meaningful for a pavement surface analysis. Figure 6.41 illustrates a simplified pavement surface as made up by sine curves of varying wavelengths and amplitudes. While the amplitudes and wavelengths are not to scale, the combination of different amplitudes and wavelengths to make up a pavement surface are illustrated.

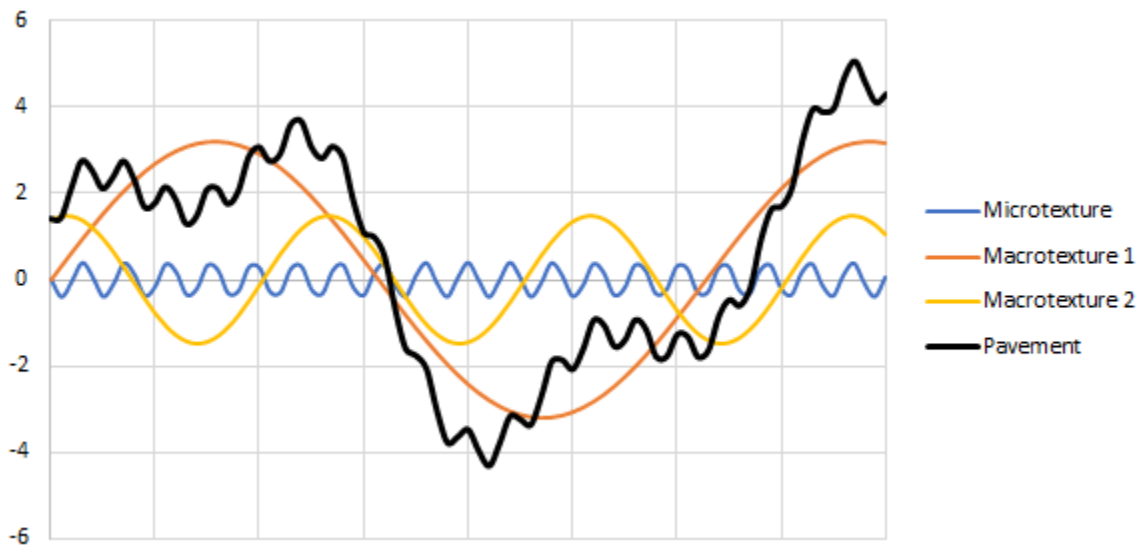


**Figure 6.41: Simplified pavement surface as combination of different sine waves**

When an actual pavement surface is measured, a Fourier transform on this data can provide wavelength distribution information for the pavement surface that effectively decomposes the actual pavement surface into its component sine waves. (Sayers & Karamihas, 1998)

In the case of the PCIP trial section, the surface textures can be generally associated with the following considerations:

- Microtexture: aggregate proportions and types, broom finish applied to the concrete surface following initial finishing
- Macrottexture: longitudinal tining, with a depth of 3 mm to 5 mm at 19 mm spacing was applied to the surface following the broom finish
- Megattexture: the joints provide some initial megattexture following installation, at a spacing of 4.66 m (panel length) and an amplitude defined by the vertical differential between adjacent panels, which was specified to be no greater than 3 mm.

Each of the three texture categories effect the tire-pavement interaction in different ways. When roads are dry, the microtexture has a significant effect on the frictional properties, while macrottexture plays a larger role when roads are wet, especially when vehicles are travelling at high speeds. Macrottexture and megattexture tend to influence the ride quality and noise characteristics of the pavement (Hall, Smith, & Littleton, 2008). In concrete pavements, one function of the macrottexture, specifically tining, is to remove water from the tire-pavement interface by providing a reservoir-like space below the riding surface and sometimes channelling water off of the pavement surface. Proper cross slope drainage ultimately plays the most significant role in removing water from the riding surface.

Therefore, when evaluating a new pavement type such as the PCIP, the pavement surface properties should be considered and evaluated. This section describes the surface evaluations that were undertaken on the PCIP trial section, including frictional properties testing, texture scanning, and surface roughness testing.

Due to the nature and location of the PCIP trial, the access to the pavement surface was limited. The testing of the various aspects of the pavement surface were generally done during over night highway closures, in conjunction with other scheduled tests, such as the Falling Weight Deflectometer. For this reason, the timing of the testing was limited and selected areas of the trial were focused on. Specifically the right wheel path and centre of the panels were the focus of this chapter, where relatively high and relatively low traffic loading, respectively, is expected. The differences found between the two areas provide insight into the effects of the traffic-related abrasion on the panels.

### 6.4.1 Surface Texture Measurement

Pavement surface texture can be measured using several direct and indirect methods, including the sand patch method, the outflow meter, and the circular track meter (Liu, 2015). One common method is the mean profile depth (MPD), which calculates the average depth of the surface's macrotexture based on a 2-dimensional profile of a 100 mm section (ASTM International, 2015). The 2-dimensional profile can be measured using spot laser technology that measures the surface height along the longitudinal direction of the pavement. The MPD has been found to correlate well with wet pavement frictional properties, however it is only an approximation of the 3-dimensional surface texture, and cannot represent tire-pavement interaction well (Liu, 2015).

For this reason, Liu (2015) developed a set of 3-dimensional texture indicators that could be obtained using laser line scanning technology. Similar to the laser spot technology, the line laser moves parallel to the pavement's longitudinal direction measuring surface height, however because the scanner spreads laser light across a defined width, the transverse direction is also measured during the laser sweep.

The method involves the development of a 3-dimensional texture height map using the output of a line laser scanner. The laser measures a patch of pavement of Length: 102 mm by Width: 100 mm, though the length of this section can be increased to 254 mm if required. The pavement surface measured is normalized based on the mean height and liner slopes of the various profiles measured within the scanned section. The texture map is then decomposed using discrete wavelets to provide indices based on the amplitudes and volumes of the macrotexture components. The indices developed by Liu are outlined in Table 6.7.

The volumetric indices related to the pavement texture are defined according to the bearing area curve of the texture, as shown in Figure 6.42. Using the measured texture, the curve is determined based on the normalized heights throughout the sample as a cumulative distribution. The peak material volume, or the highest 10%, is generally the first contact of the tire and wears away first. The core volumes, or the middle 70%, represent the bulk of the texture and provide insight into the texture's longevity. The valley void is the lowest region, and represents space available for water accumulate beneath the tire-pavement interface.

**Table 6.7: 3-Dimensional Pavement Texture Indices (Liu, 2015)**

<b>Symbol</b>	<b>Description</b>	<b>Type</b>	<b>Characterize</b>
<b>SMTD</b>	Simulated Mean Texture Depth (mm), simulates sand patch method based on highest measured elevation	Texture amplitude	Macrotexture
<b>S<sub>q</sub></b>	Root Mean Square Deviation (mm), summed Std. Dev. of the differences between texture height and mean texture height	Texture amplitude	Macrotexture
<b>S<sub>sk</sub></b>	Skewness, measurement of probability distribution's asymmetry	Texture amplitude	Macrotexture
<b>S<sub>ku</sub></b>	Kurtosis, statistical measure describing the width of distribution of texture components around the mean	Texture amplitude	Macrotexture
<b>V<sub>mp</sub></b>	Peak Material Volume (mL/m <sup>2</sup> ), volume of material in top 10% of bearing area curve (see Figure 6.42)	Material Volume	Macrotexture
<b>V<sub>mc</sub></b>	Core Material Volume (mL/m <sup>2</sup> ), volume of material between 10% and 80% of bearing area curve (see Figure 6.42)	Material Volume	Macrotexture
<b>V<sub>vc</sub></b>	Core Void Volume (mL/m <sup>2</sup> ), volume of voids between 10% and 80% of bearing area curve (see Figure 6.42)	Material Volume	Macrotexture
<b>V<sub>vv</sub></b>	Valley Void volume (mL/m <sup>2</sup> ), volume of voids in lowest 20% of bearing area curve (see Figure 6.42)	Material Volume	Macrotexture
<b>NPSE</b>	Normalized Power Spectra Energy (mm <sup>2</sup> /mm <sup>2</sup> ), summation of energy spectral density of microtexture details after Discrete wavelet transformation	Spectrum Index	Microtexture

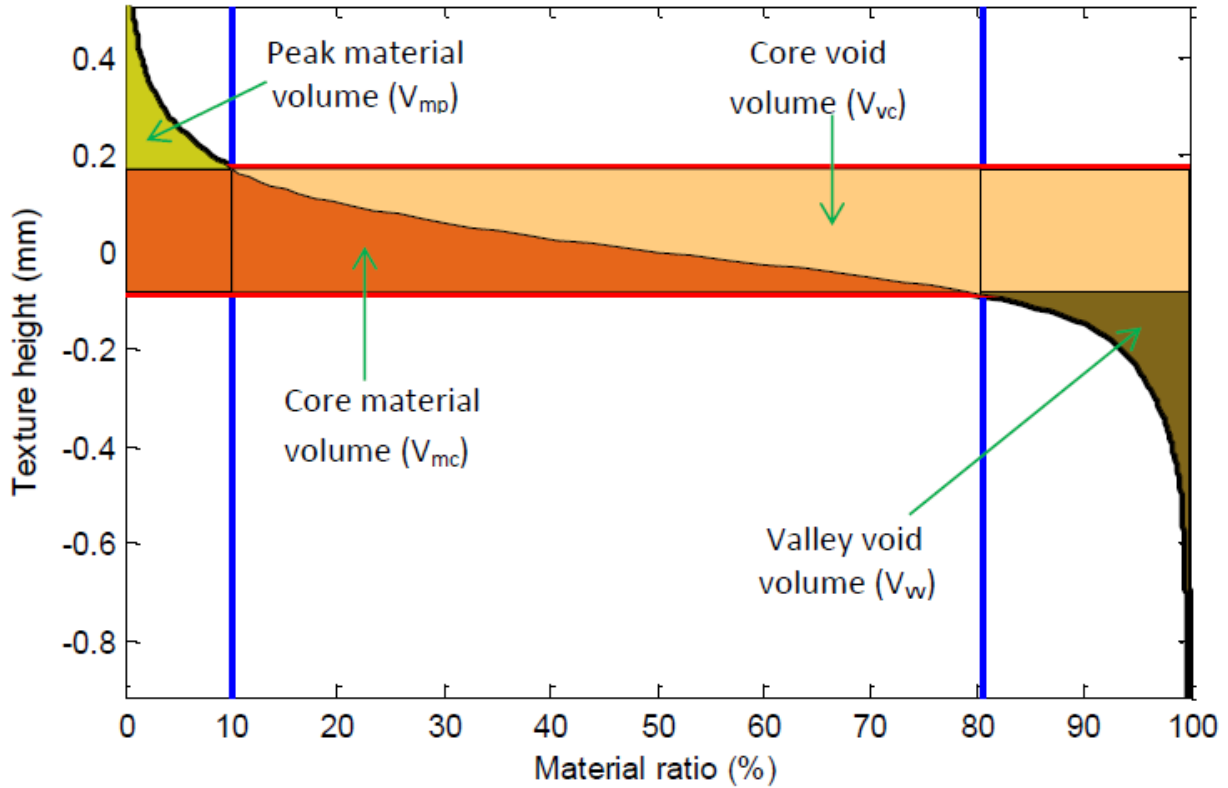


**Figure 6.42: Material bearing area curve for pavement texture (Liu, 2015)**

Liu (2015) found that the SMTD index correlated strongly ( $R^2 = 0.83$ ) with the more traditional mean profile depth (MPD) value. The MPD, in turn has been found to be capable of predicting the gradient,  $S_p$ , of pavement friction values, according to Equation 20 (Hall, Smith, & Titus-Glover, 2006).

$$S_p = 14.2 + 89.7 \times MPD \quad (20)$$

where:  $S_p$  = International Friction Index Speed Number  
 MPD = Mean profile depth, (ASTM E 1845)

$S_p$  provides insight into the rate of change of the coefficient of friction as a function of changes in velocity.

Figure 6.43, from Flitsch et al. (2002) illustrates the effects of the microtexture and macrotexture on the pavement coefficient of friction over a range of sliding speeds. Comparing the high

microtexture pavements, A' and B', the effects of high (B') and low (A') macrotexture can be seen. Pavements with high macrotexture maintain higher coefficients of sliding friction with increases in velocity.

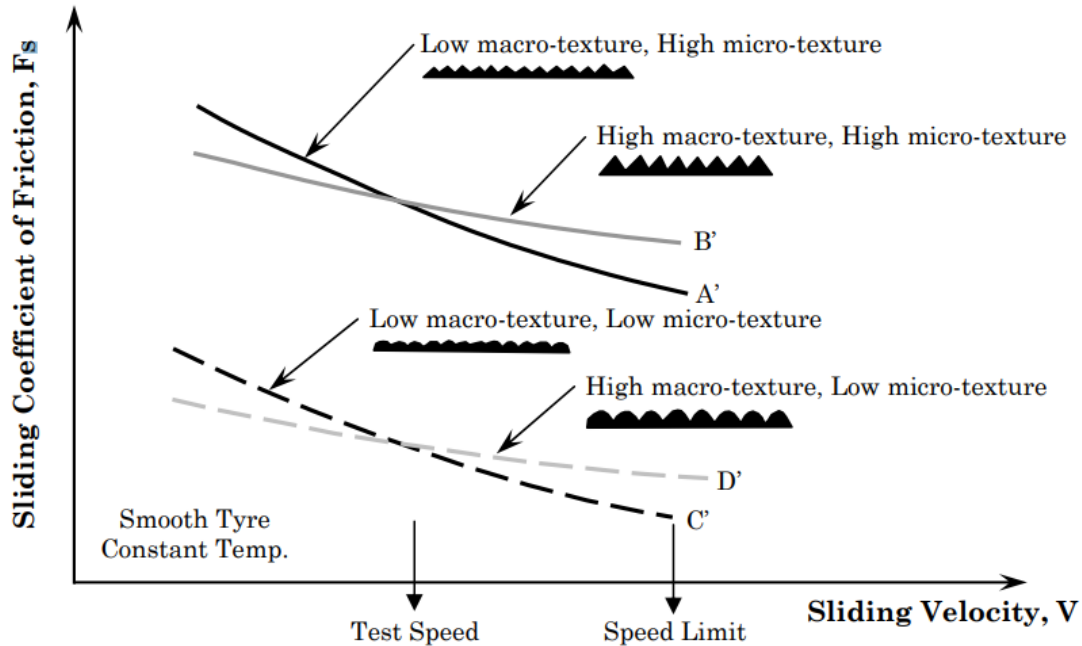


**Figure 6.43: Effect of micro-texture and macro-texture on pavement-tire friction at different sliding speeds (Flintsch, Al-Qadi, Davis, & McGhee, 2002)**

Therefore, increases in the 3-D index SMTD should correspond with increased  $S_P$  values. Similarly, the NPSE index that corresponds to microtexture should provide insight into the magnitude of the sliding coefficient of friction.

None of the indices studies by Liu (2015) were found to be sufficient to predict pavement friction, on their own, however a relationship was developed between the friction number, SMTD, and  $S_{ku}$  of a given pavement. The pavements considered in the development of the relationship were airport pavements including HMA and transversely tined PCC pavements. The friction number that the relationship considers was collected using a Transport Canada approved SARSYS Surface Friction Tester, which uses a smooth-tread tire travelling at 65 km/hr over a surface wetted to a 0.5 mm water depth. The relationship is shown in Equation 21 (Liu, 2015):

$$FN = 73.77 + 14.08 \times SMTD - 1.81 \times S_{ku} \quad (21)$$

where: FN = Friction number  
 SMTD = Simulated mean texture depth  
 S<sub>ku</sub> = Kurtosis of surface macrotecture  
 R<sup>2</sup> = 0.73

The SMTD and S<sub>sk</sub> were found to be correlated to tire-pavement noise, as predicted by On-board Sound Intensity measurements. In general, it was found that lower SMTD and negatively skewed texture result in quieter pavements, but lower friction. The V<sub>vc</sub> was also found to be a significant indicator of the friction number of a pavement.

Based on these findings, the SMTD, S<sub>ku</sub>, S<sub>sk</sub>, V<sub>vc</sub>, and NPSE indices were investigated for the PCIP trial.

#### **6.4.1.1 Surface Texture Measurement Methodology**

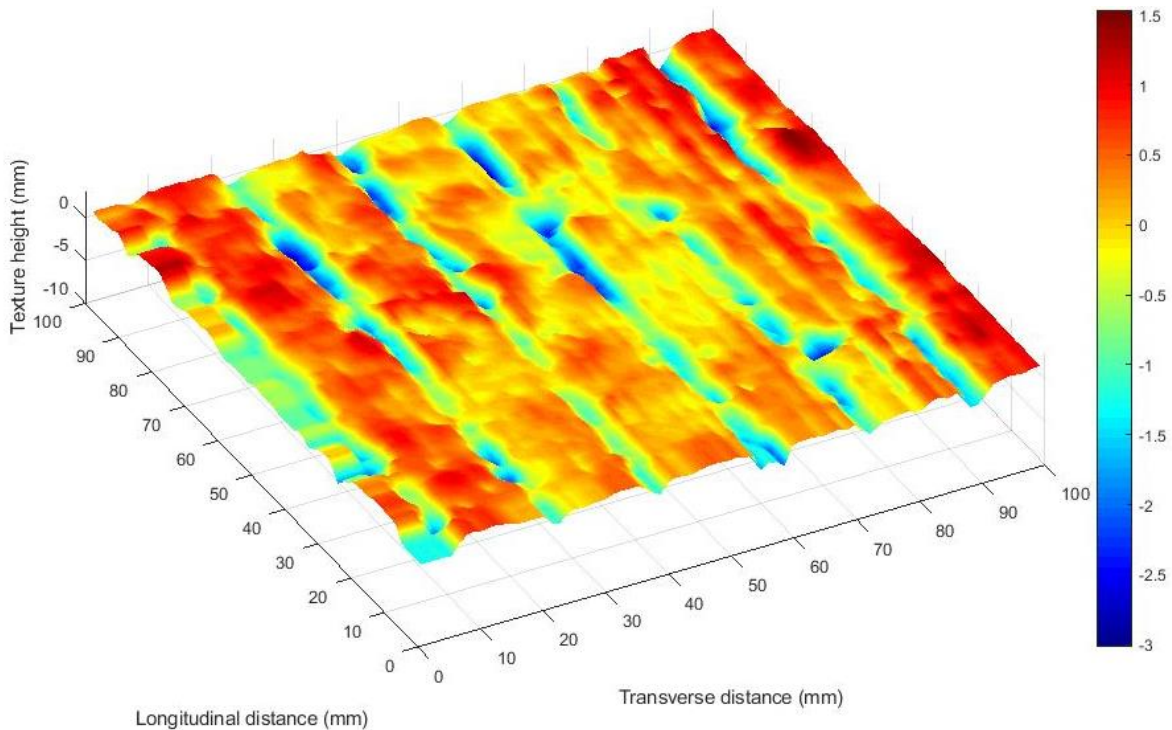
Testing of the surface texture of the precast panels was conducted on two occasions. The first was on September 7<sup>th</sup>, 2016 when 4 panels were tested while they were being stored prior to installation. The second occasion was on September 6<sup>th</sup>, 2017, after the panels had been subjected to service conditions for one year. In each case, the testing was performed in conjunction with British Pendulum testing, which is discussed later.

For each panel tested, two locations were analyzed. The first location was in the right wheel path of the panel, approximately 70 cm from the right edge of the panel, and the second location was at the centre of the panel, 183 cm from the right edge of the panel. Both locations were 135 cm from the front edge of the panel.

The laser scanning was performed using an LS-40 line-laser scanner, developed by HyMIT (2013). The data collected by the scanner was analyzed using MATLAB code provided by Dr. Qingfan Liu (2017). In each location, a texture scan was completed that yielded each of the indices outlined in Table 6.7.

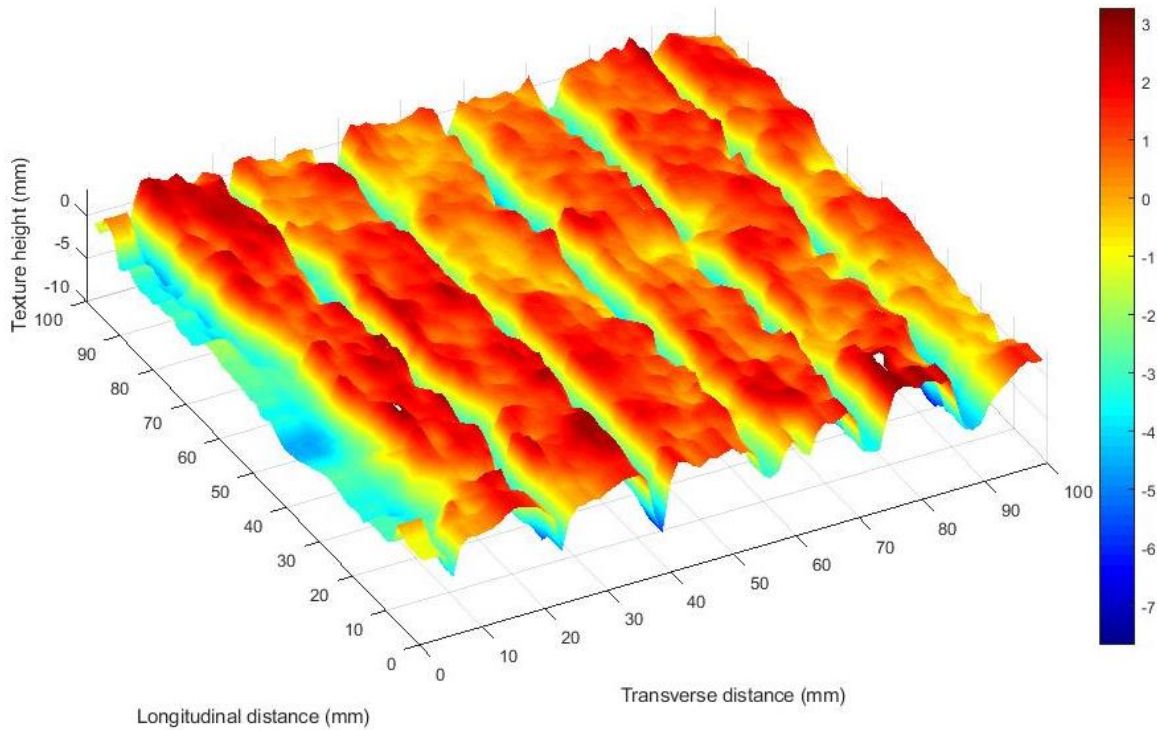
### 6.4.1.2 Surface Texture Measurement Results

Figure 6.44 and Figure 6.45 illustrate the texture maps recovered from the line-laser scanner data for the right wheel path and centre of Panel #1, respectively. The texture maps were produced using MATLAB software. While the axes scales remain the same for the two figures, the colour scheme associated with the texture height is a function of the maximum and minimum values mapped.



**Figure 6.44: Recovered 3-D surface texture height map of right wheel path on Panel #1**

As shown in the colour scales for Figure 6.44 and Figure 6.45, the wheel path appears to have been smoothed over the course of 1 year of service, while the centre of the panel still appears to have maintained a large degree of the asperities originally cast into the surface. In both cases, the longitudinal tines at 19 mm spacing can be observed. The plotting procedure determines a new reference point for each texture map, so the difference in tine depth is difficult to ascertain from the plots.



**Figure 6.45: Recovered 3-D surface texture height map of centre of Panel #1**

Four panels were tested during the pre-installation measurements taken at Armttec’s facility. The average results of these scans are summarized in Table 6.8. Two of the measurements taken at the panel centre were found to be corrupted, and therefore the averages shown in that column on include two measurements.

The kurtosis index averaged to be 4.81. A typical normal distribution has a kurtosis index of 3, so in the context of pavement texture, a value greater than 3 indicates that the texture is “peaked” as compared to a value that is less than 3, which is “flat”. A texture with a kurtosis value of 3 will have an even distribution of peaked and flat surfaces.

The skewness index was found to be negative. This indicates that the mean texture height is below the mode texture height, indicating that the texture surface is largely located beneath the median of the texture profile. Tined concrete pavements tend to be negatively skewed due to the regular, lower surfaces. A negative skew can indicate a macrotexture that can remove surface water from the tire-pavement interaction.

**Table 6.8: Average Results for Pre-Installation Measurements**

	Centre	Right Wheel Path	Average of All Measurements
SMTD (mm)	1.75	1.17	1.36
$S_{ku}$	4.42	5.01	4.81
$S_{sk}$	-1.17	-1.06	-1.10
$V_{vc}$ (mL/m <sup>2</sup> )	940.79	617.56	725.30
NPSE (mm <sup>2</sup> /mm <sup>2</sup> )	0.043	0.027	0.032

The remaining indices constitute a baseline for comparison for the measurements taken after the panels had been exposed to traffic conditions for one year. The initial readings only represent four of the 22 total panels, and therefore the baseline may not be fully representative and should be considered only as a reference.

Figure 6.46 shows the simulated mean texture depth values for each of the scans taken on September 6<sup>th</sup>, 2017, after the panels had been in service for one year. The line-laser scan results for each index are shown for the centre of the panel and the right wheel path. The right wheel path is expected to have experienced significantly higher abrasion due to traffic than the centre of the panels.

The SMTD for the centre was found to be consistently higher than the right wheel path. On average, the SMTD of the panel centre was found to be 0.41 mm higher than that of the right wheel path. Since the centre is exposed to less abrasion than the wheel path, this likely indicates a relative drop in SMTD over the one year of service. As discussed previously, this indicates a loss in macrotexture that probably corresponds to a drop in the pavement's  $S_P$  value. This indicates that the pavement's friction decreases more quickly with speed increases than when initially installed.

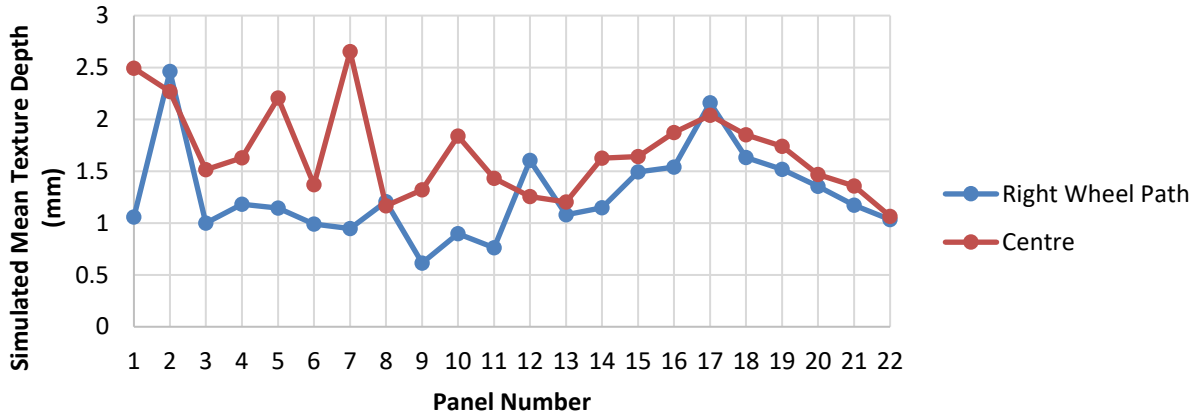


**Figure 6.46: Simulated mean texture depth results for all panels (right wheel path and centre)**

The decreased SMTD may indicate that the noise produced by the tire-pavement interaction is decreasing, as these two properties have a positive correlation.

Figure 6.47 shows the kurtosis indices for each of the panels.

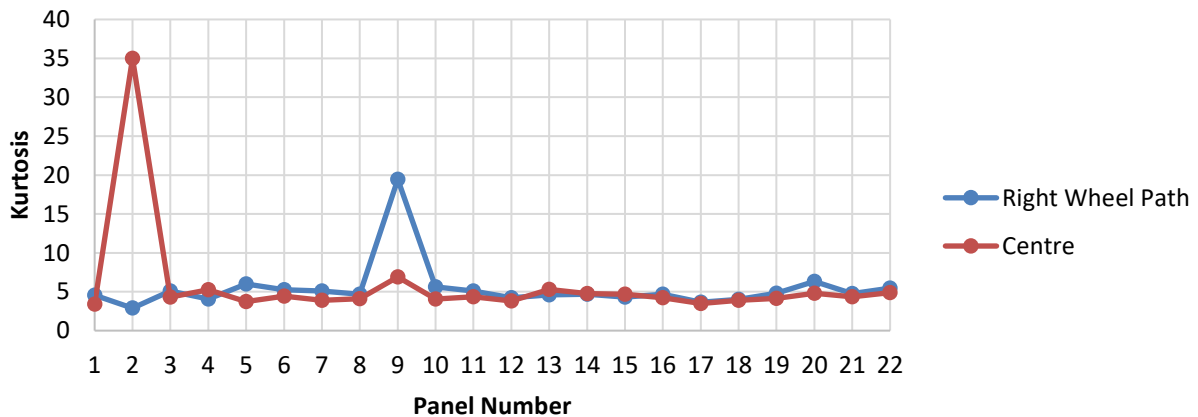


**Figure 6.47: Kurtosis of measured surface texture for all panels (right wheel path and centre)**

With the exception of the wheel path reading of panel #2 (2.89), all indices were greater than 3. This indicates that the shape of the texture continues to be peaked in shape, even after the effects of abrasion. Like the SMTD, the kurtosis index was found by Liu to be an indicator of frictional properties, with higher kurtosis values detracting from frictional properties. In general, the centre and wheel path kurtosis indices were indistinct from one another, indicating that the contribution to frictional properties from kurtosis was similar in either location.

Upon inspection, the centre scan from panel #2 was found to contain an error, which skewed the result. The scanner interpreted a ~30 mm deep point within the surface, which was not actually present. This “peak” dominated the kurtosis calculation, resulting in the outlier seen in Figure 6.47. A similar situation was observed for the wheel path measurement of panel #9, but the depth of the deep points were only approximately 4 mm, which is more likely to occur.

The effects of these points can also be seen in Figure 6.48, which shows the skewness of all readings.

The high kurtosis measurements for panels #2 and #9 were found to result in highly negative skewness for these areas. However, all of the measurements resulted in negative skewness values, which is a function of the tined surfaces. Generally, the centre and wheel path measurements were not largely different, except in the aforementioned cases. This indicates that the traffic-related abrasion does not largely affect the skewness distribution index.

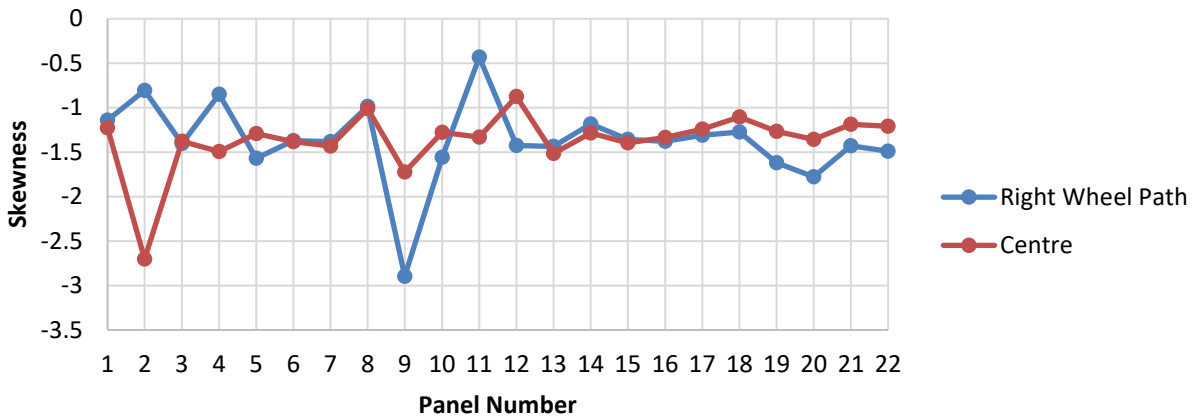


**Figure 6.48: Skewness of measured surface texture for all panels (right wheel path and centre)**

A negative skewness index was found to correlate with lower pavement noise. Since the two locations are not distinct in this index, it indicates that the contribution of skewness to pavement noise is not changing under the effects of traffic-related abrasion.

Figure 6.49 summarizes the results for the core void volumes as measured at the different test locations.

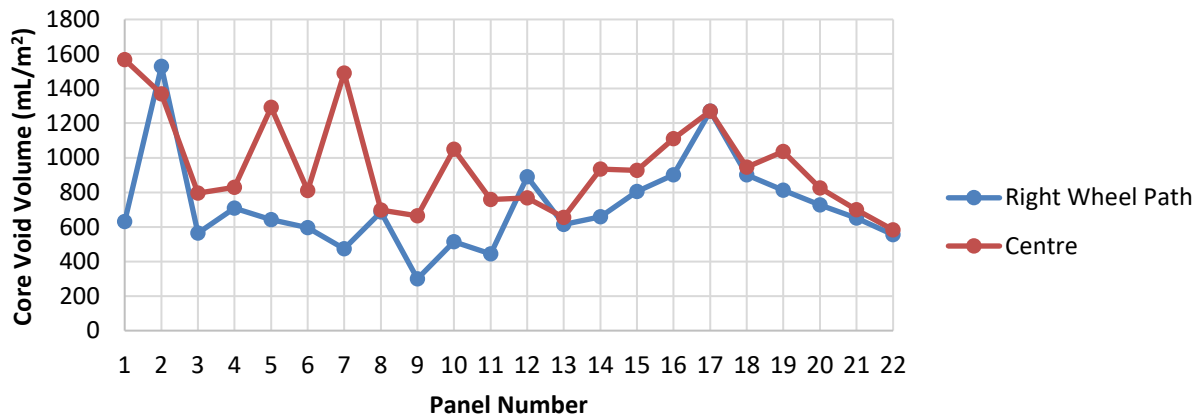


**Figure 6.49: Core void volume of measured surface texture for all panels (right wheel path and centre)**

Liu (2015) found the core void volume to correlate with friction number and like the SMTD, this index was found to decrease slightly between the centre and right wheel path. On average, the wheel path core void volume was 237 mL/m<sup>2</sup> less than the corresponding centre value.

Figure 6.50 shows the NPSE values associated with the tests.

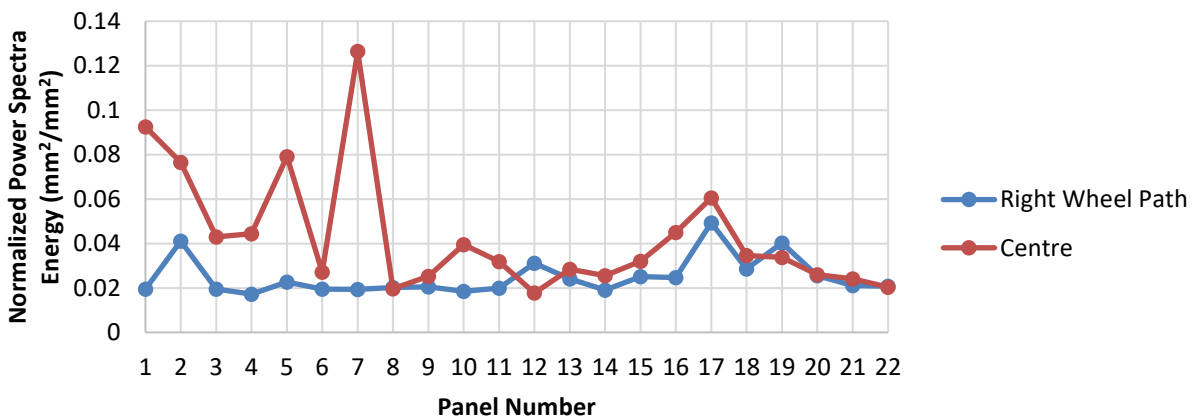


**Figure 6.50: Normalized power spectra energy for all panels (right wheel path and centre)**

The NPSE gives an indication of the microtexture of the measured texture area. Increased NPSE indicates a higher number of surface asperities on the microstructure scale ( $\lambda < 0.5\text{mm}$ ). The centre textures were found to consistently have higher microtexture than the wheel path textures. This may represent the biggest difference between the frictional properties of the two areas, for low

speed and dry friction, when microtexture of the pavement governs friction. Traffic-related abrasion appears to have some impact on the microtexture of the PCIP panels.

#### **6.4.1.3 Surface Texture Measurement Conclusions**

Based on the line-laser scan and analysis of the PCIP trial section after one year of service, the following conclusions can be made:

- The SMTD, which is correlated with mean profile depth and the  $S_p$  gradient of friction, was found to decrease in the wheel path relative to the centre of the panel, indicating a deterioration in friction
- The tined pavement surface resulted in consistently negative skewness indices, which are associated with lower pavement noise in comparison to positive skewness indices
- The NPSE, an indicator of pavement microtexture, was found to be lower in the wheel path than in the panel centre, indicating that the friction at low speeds and in dry conditions, when microtexture governs friction, may have decreased under one year of traffic-related abrasion

#### **6.4.2 PCIP Surface Roughness Properties**

Roughness (or alternatively smoothness) is a fundamental characteristic of any pavement. The roughness of a given pavement has been found to have effects on the fuel consumption (El Khoury, Akle, Katicha, Ghaddar, & Daou, 2014), vehicle maintenance costs (Zaabar & Chatti, 2014), and health (Li, Qiao, & Yu, 2016; Li, Qiao, & Yu, 2016) of the pavement's users and their vehicles. While these effects are not always fully understood or linear, a pavement's roughness is still an important characteristic that should be identified and monitored.

Pavement roughness is a function of several pavement attributes, including inherent characteristics like surface material type and placement techniques, and pavement joint spacing and design, and characteristics that develop and change over time like pavement deterioration types, frequency, and magnitude. Each affects the interaction between the pavement surface and the tires of the vehicles travelling across the pavement at speed, causing vibrations that effect both the vehicle and its passengers.

The magnitude of the vibrations caused by a given pavement's roughness and their effects generally increase with vehicle speed. Therefore, roughness becomes a greater concern for roadways that have higher posted speed limits and average speeds. The Precast Concrete Inlay Panel (PCIP) rehabilitation strategy is specifically for use on high-volume roadways that typically have posted speed limits in the range of 100 to 110 km/hr. For this reason, the roughness of the PCIP strategy is an important consideration.

It should be noted that the PCIP strategy would generally be employed on localized issues, resulting in relatively short lengths where the strategy is applied. This somewhat mitigates the effects of PCIP roughness.

The International Roughness Index (IRI) is a measure for assessing the roughness of a road surface that was developed by the World Bank from 1982-1986 (Sayers, Gillespie, & Paterson, 1986). The index is a filtered ratio between the cumulative movement in a vehicle's suspension and the distance that the vehicle has travelled. The index is commonly represented as a slope, with units of millimeters/meter, meters/kilometer, or inches/mile. The IRI is a measured and computed characteristic for a single longitudinal wheel track and is defined for a vehicle speed of 80 km/hr (Sayers, 1995). This is because even though the measurement procedure can be undertaken at a number of speeds through several methods, the movement of a vehicle's suspension due to road roughness will be a function of the vehicle's speed.

The IRI is based on the surface of the road, and therefore it is often calculated based on a measured profile. IRI is a standard measure that can be obtained by many different means, including surveys, response-type road roughness meters, and profiling devices, which was one of the determining factors in its wide acceptance by the World Bank (Sayers, Gillespie, & Paterson, 1986). Since it corresponds to vehicle interactions with the road surface, it provides a meaningful measure of road performance in terms of smoothness, which can be easily related to road users.

IRI typically increases as a road deteriorates, through cracks and distortions in the pavement surface. For this reason, and because IRI can be measured through several means, IRI is often used as a pavement network management index, where roughness values above a given threshold trigger maintenance activities.

Figure 6.51 summarizes the IRI roughness scale, as laid out by Sayers *et al.* (1986). As the IRI increases, the speed at which vehicles can safely use the pavement decreases. The various classifications of road and their approximate ranges of IRI are shown, along with typical distortions and surface defects seen at given IRI levels.

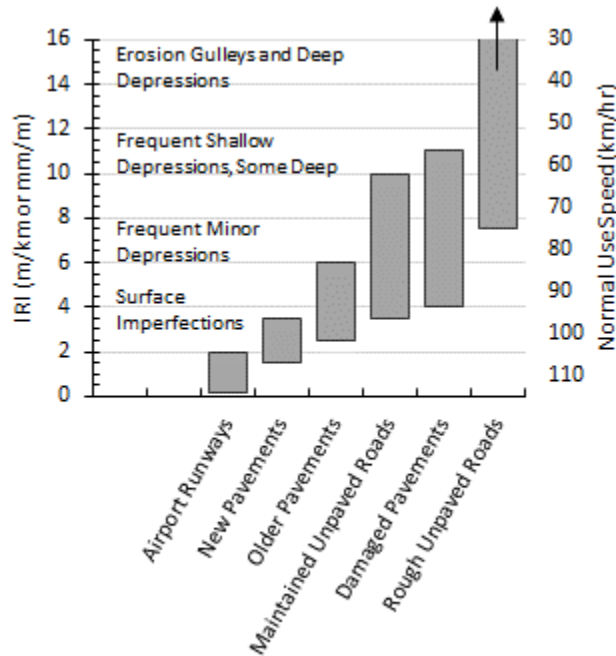


**Figure 6.51: The IRI Roughness Scale (from Sayers *et al.* 1986)**

An IRI value of 0 m/km indicates a perfectly flat pavement surface, and as the value increases it corresponds to higher distortions of the pavement surface. As shown, an IRI value of 14-16 m/km corresponds to a surface that is eroded and has deep depressions in the surface. For newly constructed HMA or PCC highway pavements, the MTO typically specifies an acceptance criteria of 1.25 m/km, above which repairs or replacements are required. Portland cement concrete (PCC) pavements are typically textured using tining and/or grinding, and these intentional surface textures, as well as pavement joints, are often captured by IRI measurements.

Furthermore, precast concrete pavements, such as the PCIP trial, present even more potential for relatively high IRI than conventional PCC pavements due to their method of placement. The adjacent panels are placed after hardening, and therefore the relative vertical alignment between adjacent panels depends on the support conditions beneath the panels. This can result in roughness as vehicles travel across displaced joints.

When precast concrete pavement panels are not placed well, post-construction diamond grinding can be used to smooth the pavement surface across the joints.

Two methods of measuring the IRI of the PCIP installation were used. These included the use of a walking profiler during a roadway closure and an Automatic Road Analyzer (ARAN) conducted at speed during normal traffic hours.

#### **6.4.2.1 Surpro Method**

The walking profiler that was used for data collection is a Surpro 4000, which is a Class 1 walking profiler that is manufactured by International Cybernetics Corporation. The profiler is walked along a longitudinal line corresponding to a wheel path at a near-constant speed. Inclinometers in the profiler measure the relative changes in elevation between the two wheels of the profiler that is digitally analysed to produce a profile of the surface that was measured. Figure 6.52 shows the profiler being used for the project.

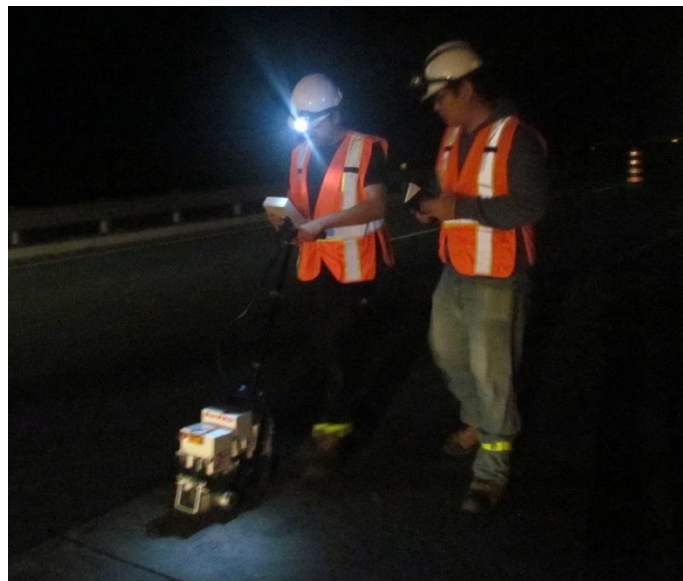


**Figure 6.52: Surpro 4000 measuring surface profiles on PCIP trial site**

The profile data is then analysed using proprietary software from International Cybernetics Corporation, called WinReport. The software interprets the profile data in 1 m increments that are then converted into an IRI value for that meter. These IRI values can be averaged over the total length being analyzed to determine a total IRI value.

Figure 6.53 illustrates the profile data as collected by the Surpro 4000. The data represented in this plot is shown prior to filtering and being converted to IRI data based on the accumulated measures of surface imperfections. The vertical lines labelled DO represent events on the course of the data collection. For this project, the events were used to denote the locations of joints between PCIP panels.

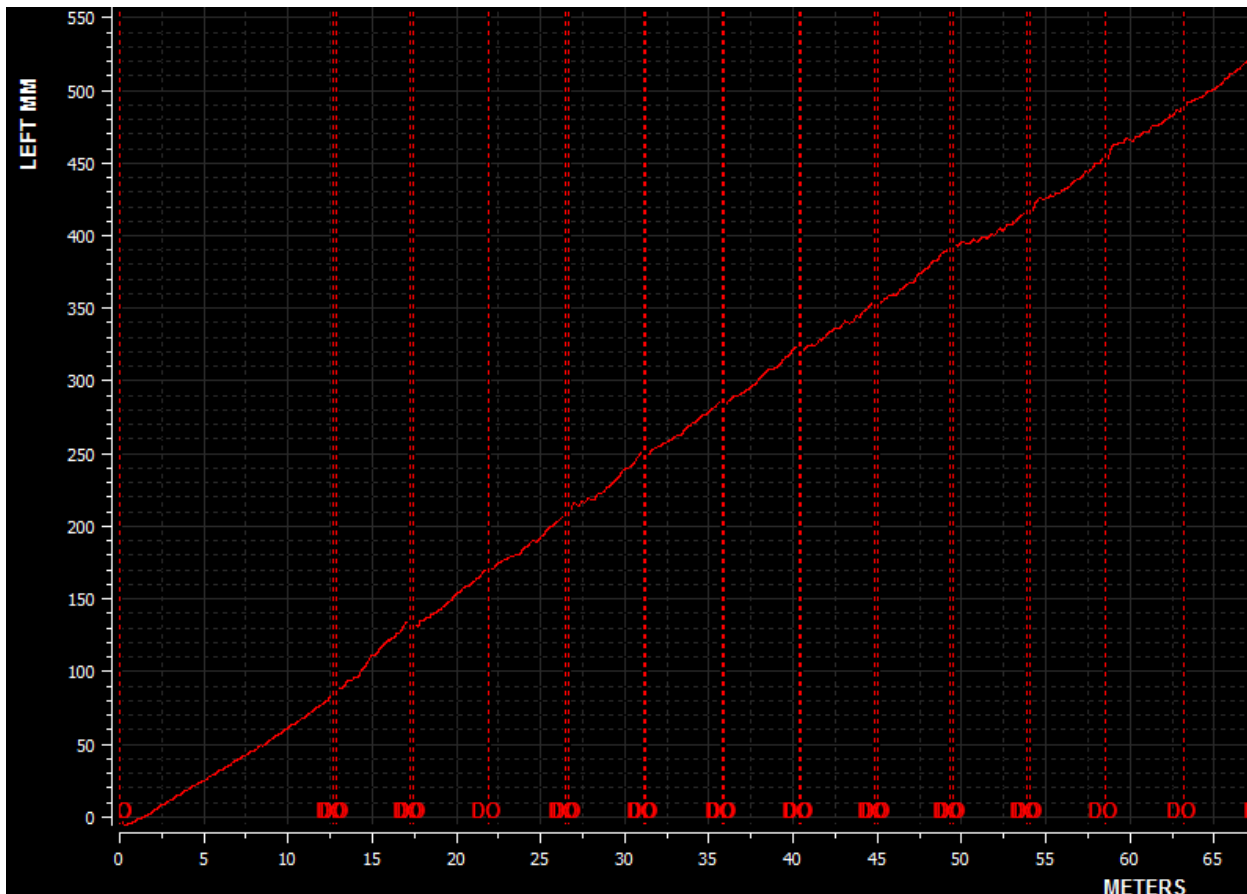


**Figure 6.53: A partial display of profile data as collected by Surpro 4000**

The collection of surface roughness data from the PCIP trial application took place on the evenings of September 6<sup>th</sup> and September 13<sup>th</sup>, 2017, roughly one year after the construction of the project. Two-lane closures of Highway 400 were scheduled to accommodate Falling Weight Deflectometer testing of the PCIP joints, the results of which are discussed in another chapter of this thesis. Data was collected for the left and right wheel paths of the PCIP surface separately, with four total data collection trips for each. Approximately 10 to 15 m of the existing asphalt pavement beyond either

end of the PCIP trial were also measured during this period. Figure 6.53 shows the portion of asphalt measured on this data collection between 0 m and approximately 12.5 m.

During data collection, the joints between panels were digitally marked on the profiler using events so that during data analysis the roughness results associated with each different support condition could be identified and analysed separately.

The IRI readings throughout the course of one data collection pass are shown in Figure 6.54. The HMA portions at either extent of the plot show the roughness values associated with the existing asphalt beyond either end of the PCIP trial. The vertical lines delineate the areas defined by the different support conditions as labelled on the plot.

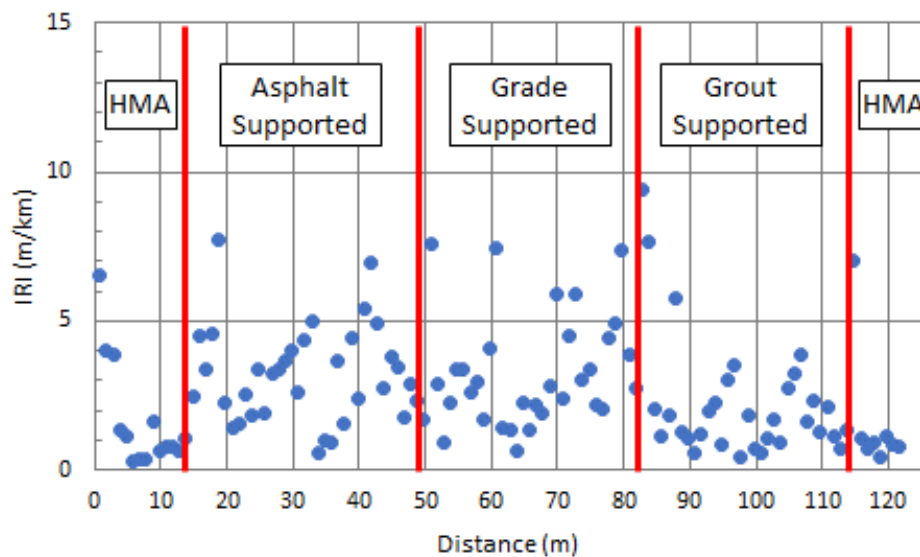


**Figure 6.54: IRI values on 1 m intervals for one data collection pass (Surpro)**

All the 1m interval readings from all passes were combined for each section of the test: HMA, Asphalt-supported, Grade-supported, and Grout-supported. The averages for the left and right wheel paths of these sections are shown in Figure 6.55. The overall average for each section, which is a combination of the left and right wheel paths, is also shown. The error bars in each case represent one standard deviation from the average in both the positive and negative directions.

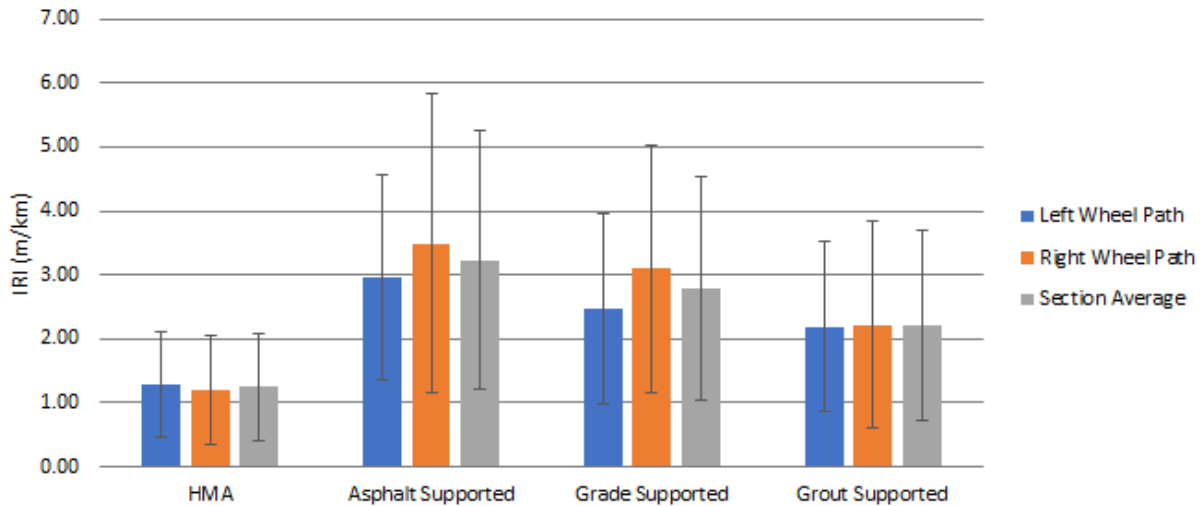


**Figure 6.55: Average IRI values for each section of the trial section**

As shown, the existing HMA pavement surface had considerably lower average IRI values than the PCIP sections. This result is intuitive as the HMA surface is relatively new and showed very little deterioration, in addition to having no joints or tined surface texture.

Within the PCIP sections, the least to most rough sections were Grout-supported, Grade-supported, then Asphalt-supported. A considerable amount of variation was observed in each, as evidenced by the error bars shown. According to a Least Significant Difference analysis, the difference between each support condition type was found to be significant at 95% confidence. The values associated with this analysis are shown in Table 6.9. The differences between the mean IRI values of AS and GraS, GraS and GroS, and AS and GroS were 0.44 m/km, 0.58 m/km, and 1.02 m/km, respectively. Each of these differences was above the LSD of 0.368 m/km, indicating each type of panel performed significantly distinctly.

It is theorized that the differences in roughness between sections can largely be attributed to differences in vertical differentials between adjacent panels. The surface finishes and conditions of the PCIPs throughout the trial at the time of testing were generally uniform. This leaves the connections between the panels as the primary source of differences in roughness. The construction specifications set the maximum value for the vertical differential between adjacent panels at 3 mm, and this maximum value was largely abided by. However, differentials of varying magnitudes were observed on site during testing.

**Table 6.9: Least Significant Difference Analysis for IRI Values**

<i>Groups</i>	<i>Count</i>	<i>Average</i>
Asphalt Supported	291	3.23
Grade Supported	258	2.79
Grout Supported	254	2.21

<i>ANOVA</i>						
<i>Source of Variation</i>	<i>SS</i>	<i>df</i>	<i>MS</i>	<i>F</i>	<i>P-value</i>	<i>F crit</i>
Between Groups	140.96	2	70.48101	22.21946	4.06E-10	3.006978
Within Groups	2537.63	800	3.17204			
Total	2678.59	802				

<i>LSD Analysis</i>	
<i>LSD Criteria</i>	
$\alpha_{overall}$	0.05
k	3
N	803
$n^*$	267.7
$\alpha_{modified}$	0.017
$t_{critical}$	2.393
SE	0.154
95% LSD	<b>0.368</b>

These vertical differentials are likely due to the amount of control that the contractor had over adjusting the relative elevations of the panels while placing them. These considerations are outlined in Table 6.10.

The inter-panel adjustment is related to the resiliency of the panels, as described in Section 5.5. Resiliency is a subjective measure of a design’s ability for adjustment on site.

Based on this analysis, the Grout-supported design for the PCIP is the optimum method for obtaining low IRI values in the design. The importance of the PCIP roughness should be considered by the MTO when determining the best practices for future applications. Concrete pavements generally have higher IRI values than HMA pavements, so taking steps to mitigate this difference in applications where concrete is deemed necessary should be considered. This is

particularly true on high volume roadways where the effects of high pavement IRI on fast moving vehicles can be magnified.

**Table 6.10: Panel Adjustment Practices and IRI Values**

<b>Support Condition</b>	<b>Method of Inter-Panel Adjustment</b>	<b>Control/Ease of Adjustment During Placement</b>	<b>Average IRI of Section (m/km)</b>
<b>Asphalt-supported</b>	<ul style="list-style-type: none"> <li>• Panels placed directly on milled surface</li> <li>• If misaligned, PCIP must be removed and the asphalt surface milled to suit</li> </ul>	Low	3.23
<b>Grade-supported</b>	<ul style="list-style-type: none"> <li>• CTBM placed and compacted to support panels</li> <li>• If misaligned, PCIP is removed and CTBM added or removed to improve alignment</li> <li>• If depth of milling is insufficient, localized re-milling may be required</li> </ul>	Medium	2.79
<b>Grout-supported</b>	<ul style="list-style-type: none"> <li>• Panels placed on milled surface then adjusted using integrally-cast levelling feet</li> <li>• Misalignment addressed directly while adjusting PCIP height</li> </ul>	High	2.21

It should be noted that improvements to the milling methods as discussed in previous chapters would improve the consistency of the milled asphalt surface that could in turn improve the vertical differential between panels and their overall IRI.

#### **6.4.2.2 Automated Road Analyzer (ARAN)**

The second method that was used to analyze the roughness of the PCIP section was the Automated Road Analyzer (ARAN). The ARAN measures the pavement surface while travelling at the speed of regular traffic. This data is then analyzed and converted into an IRI value based on 10 m intervals. Due to these intervals, the IRI data from the ARAN can not be partitioned into the different support conditions.

ARAN data was collected on October 7<sup>th</sup>, 2016, by members of the MTO. The data was then provided to CPATT as part of the research study.

Figure 6.56 shows the IRI data collected by the MTO's ARAN. The extents of the PCIP trial are marked on the plot as noted by the ARAN operator during collection.

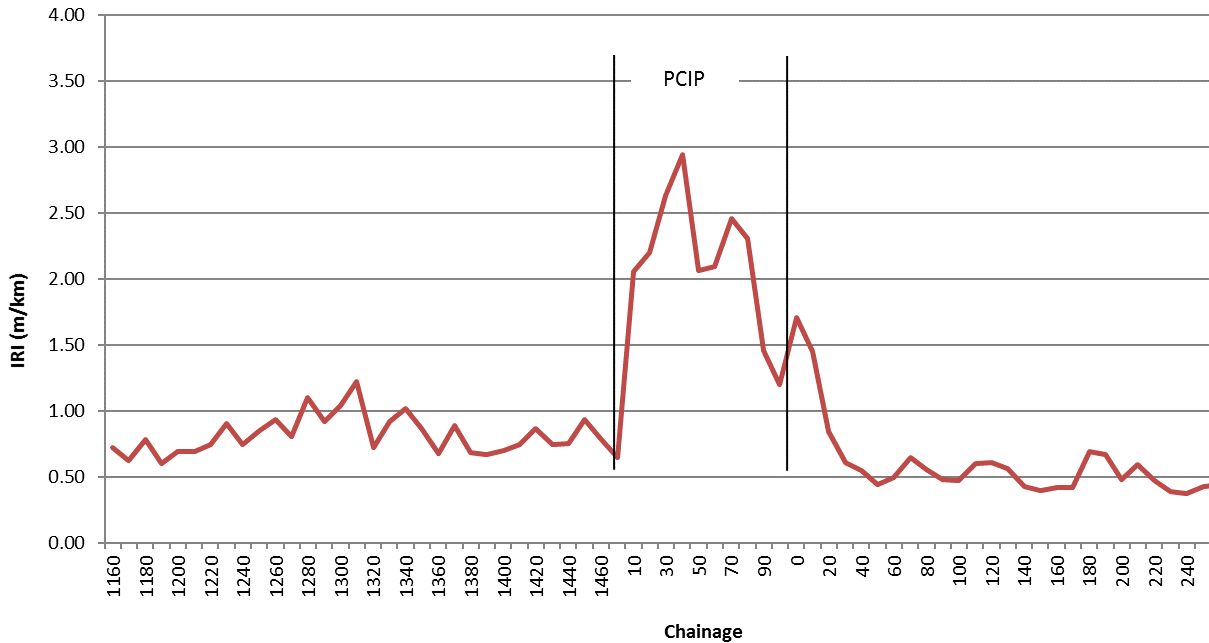


**Figure 6.56: IRI values on 10 m intervals for one data collection pass (ARAN)**

The ARAN IRI data roughly shows a similar trend to the Surpro roughness data regarding the roughness of the three support conditions, with roughness decreasing as the you move from AS to GraS to GroS. However, because of the sampling interval, the delineation between the three support conditions is unclear.

As shown, the roughness of the PCIP section is considerably higher than that of the HMA pavement prior to and after it, even considering the GroS condition that was found to have the lowest roughness.

### 6.4.2.3 Roughness Conclusions

The roughness of the PCIP trial section was measured using two methods, the Surpro walking profiler and the Automated Road Analyzer (ARAN).

The Surpro provided high enough resolution that the roughness associated with the different support conditions within the trial section could be differentiated. The roughness was found to be

lowest in the Grout-supported condition, followed by the Grade-supported then the Asphalt-supported conditions. This order corresponds to the decreasing level of control that the panel installer has over the final panel elevation. This results in a smoother transition between panels, and lower roughness.

Though the ARAN did not have sufficient resolution to differentiate between the different support conditions, the trend of the roughness throughout the section roughly corresponded to the findings of the Surpro.

In both cases, the roughness of the PCIP trial was found to be higher than the maximum acceptable threshold for new pavement used by the MTO of 1.25 m/km, while the adjacent HMA surface was found to generally be below this threshold.

Following construction, it may be necessary to undertake diamond grinding of the PCIP surface to address differential elevations between adjacent panels. This process will reduce the roughness of the section by producing a continuous profile along the section, and may have the additional benefit of allowing for the implementation of a next-generation concrete surface, which is a diamond grinding configuration that has been found to have good surface characteristics relating to noise. The diamond grinding may require that the riding surface of the panels be constructed with extra concrete cover to allow for repeated grinding efforts without encroaching on the panel's reinforcement.

### **6.4.3 PCIP Frictional Properties**

The frictional properties of a pavement surface are a key consideration in its performance. Low friction between the pavement and the tires of vehicles using the pavement can result in unsafe conditions wherein vehicles cannot safely stop or slow down. This can be exacerbated by weather conditions that can result in water, snow, and ice accumulations on the pavement surface, further reducing the pavement's frictional properties. Empirical evidence has been found to indicate that vehicle crashes are significantly correlated to the amount of available friction between tires and the pavement surface (Hall, Smith, & Titus-Glover, 2006). In the past, it was estimated that up to 13,000 deaths in the United States could annually be attributed to poor pavement condition, including insufficient texturing and friction (Larson, Scofield, & Sorenson, 2005).

The friction between a tire and pavement is largely made up of two components, hysteresis and adhesion, as shown in Figure 6.57 (Glennon & Hill, 2004). Hysteresis is the result of the energy loss caused by the deformation of the tire as it interacts with the macrotexture of the pavement (Hall, Smith, & Littleton, 2008), resulting in a horizontal force on the tire. The adhesion component of friction is the result of the Van Der Waals forces in the interaction of the tire particles with the pavement particles as they are brought into close proximity. This aspect of the friction is largely a function of the microtexture of the pavement as the microstructure of these small textures and that of the tire interact (Persson, 2000).

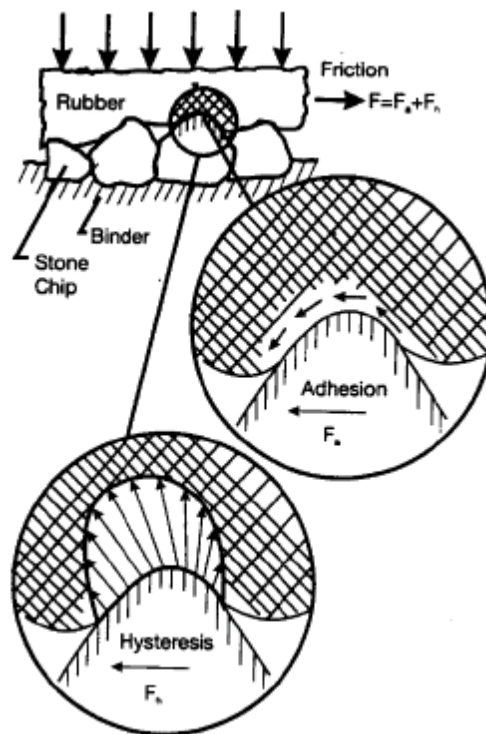


**Figure 6.57: Adhesion and hysteresis, the two principle components of pavement-tire friction (Glennon & Hill, 2004)**

The friction is also a function of the braking force being applied to the vehicle. When a vehicle undergoes a braking operation, the forces on the vehicle due to friction develop according to the changes in the coefficient of friction, as shown in Figure 6.58 (Hall, Smith, & Titus-Glover, 2006). As braking forces increase, the force due to braking increases to a peak. This increase occurs as the tire-pavement interface maintains a static condition (tire rolls over pavement instead of sliding) and therefore the coefficient of static friction is applicable. Beyond this point, the force imparted

by braking exceeds the maximum static friction force that the tire-pavement interface can impart to the tire and the interface begins to slip. This transitions from the coefficient of static friction to a kinetic coefficient of friction, which is lower than the static counterpart, and can ultimately result in tire lock up and skidding.

The skidding condition is dangerous as the driver loses much of the control of the vehicle. Anti-lock brakes in modern vehicles address this issue in the longitudinal direction, however transverse skidding resulting from low-radius, high-speed turns can have a similar effect.

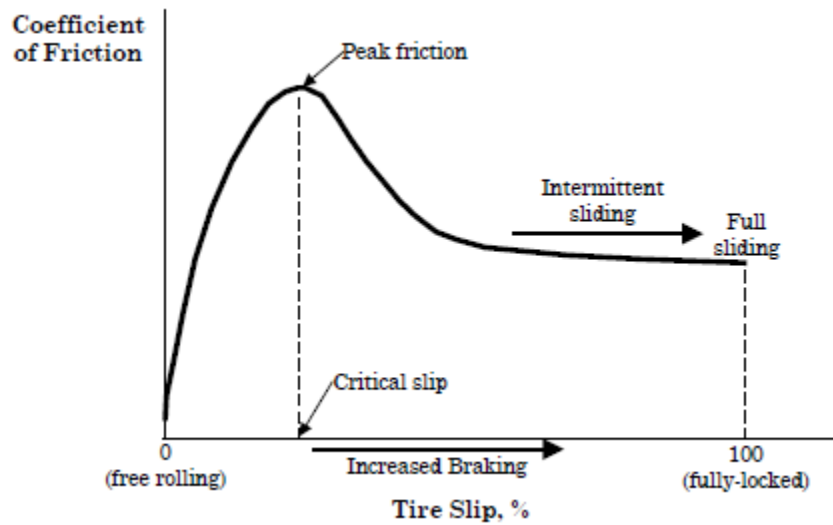


**Figure 6.58: Pavement friction versus tire slip (Hall, Smith, & Titus-Glover, 2006)**

The frictional characteristics of concrete pavements are initially dependant on the tining (macrotexture) and broom or burlap finishing (microtexture) (Delatte, 2014), which affect the hysteresis and adhesion properties of the pavement, respectively. As the pavement is subjected to service conditions, the durability of the initial friction characteristics becomes more important. The friction is due to asperities and surface shape, and therefore the polishing that occurs over time and smooths out these features reduces the friction. Therefore, the friction durability is due to abrasion resistance, which has been found to be a function of the concrete's strength and hardness of the concrete's aggregate (Taylor, Kosmatka, Voigt, & et al., 2007).

As discussed in a previous chapter, the surface texture used for the PCIPs included two parts to provide microtexture and macrotexture, a broom finish and longitudinal tining, respectively. Regarding the durability, the concrete used to construct the panels had an average 28-day compressive strength of 51.2 MPa. The coarse and fine aggregate used in the production of the PCIP concrete were found to adhere to OPSS 1002, which stipulates abrasion resistance in terms of Micro-Deval testing. For fine and coarse aggregate, the maximum allowable percent loss under these testing conditions is 20% and 14%, respectively.

Three methods were used to evaluate the frictional characteristics of the precast panels: British Pendulum, T2Go continuous friction analyzer, and the ASTM skid tester.

#### **6.4.3.1 British Pendulum**

The British Pendulum Skid Resistance Tester, commonly known as the British Pendulum (BP), is an impact tester that provides insight into the frictional properties of a flat surface (ASTM International, 2013). The BP consists of a dynamic pendulum with a rubber slider at its end. The pendulum is positioned such that the slider travels across a set gage length of contact with the surface being tested during the swing of the pendulum. The gage length is between 124 mm and 127 mm while the width of the slider is 76 mm, corresponding to a contact area of 94.2 cm<sup>2</sup> to 96.5 cm<sup>2</sup> for the test. The energy lost during this swing corresponds to the British Pendulum Number (BPN) that is measured at the highest point of the pendulum's swing path following contact with the surface. A higher BPN corresponds to a greater loss of energy, and therefore higher friction. The test is repeated four times to obtain an average BPN value for a given section. During the BP test, the pavement surface is thoroughly wetted and more water is applied between each subsequent reading. Therefore, the pavement is tested in the wet condition, which is generally the condition in which frictional properties are most relevant to safety considerations.

British Pendulums are generally associated with pavement microtexture, and their results are therefore often used to gauge aggregate polishing at the surface of the pavement (Hall, Smith, & Littleton, 2008).

Figure 6.59 shows the BP apparatus set up for use in the laboratory. The apparatus can also be used in the field, as was the case for the research outlined in this thesis.



**Figure 6.59: British Pendulum Skid Resistance Tester (Gonzalez, 2014)**

BP testing of the PCIPs was undertaken on two occasions. The first was undertaken on September 7, 2016 at the Armtex plant where the panels were being fabricated. During this visit, only four panels were available to be tested due to delays in the production schedule and panels stacked for curing purposes. During a previous site visit, members of the MTO were asked to choose a surface texture for the panels based on a test panel as discussed in Section 4.3.3.1. The four different panel textures (Burlap Drag + Light Tine (TFS 1), Broom Finish + Light Tine (TFS 2), Burlap Drag + Heavy Tine (TFS 3), and Broom Finish + Heavy Tine (TFS 4)) were retained following this initial visit and the test panel was tested for BPN during this visit.

The second BP testing took place on September 6<sup>th</sup>, 2017 after the PCIP had been in service for approximately one year. During this testing period, other tests were being conducted in parallel, including Falling Weight Deflectometer (FWD), which is discussed in a separate chapter. The FWD malfunctioned while on site and could not be moved from panels 15-17 where it broke down, which interrupted the BP testing. BP testing was only performed on panels 1-14, and 18-22 due to this interruption.

In each instance of testing, each panel was assessed in two locations. The locations were in the right wheel path, and in the centre of the panel, both 135 cm from the front edge of the panel. These two locations were chosen in order to track the effects of traffic-related abrasion. While the

centre of the panel will see some abrasion, the wheel paths will be subjected to the majority. Therefore the difference

Figure 6.60 shows the BP results for the first testing that took place at the Armtec facility in Mitchell, Ontario. The error bars in the figure represent one standard deviation in both the positive and negative direction based on the multiple BP readings taken for each test. The right wheel path (RWP) and centre readings are shown for each of the four panels tested. The four surface textures on the test panel are also shown on the right of the figure.

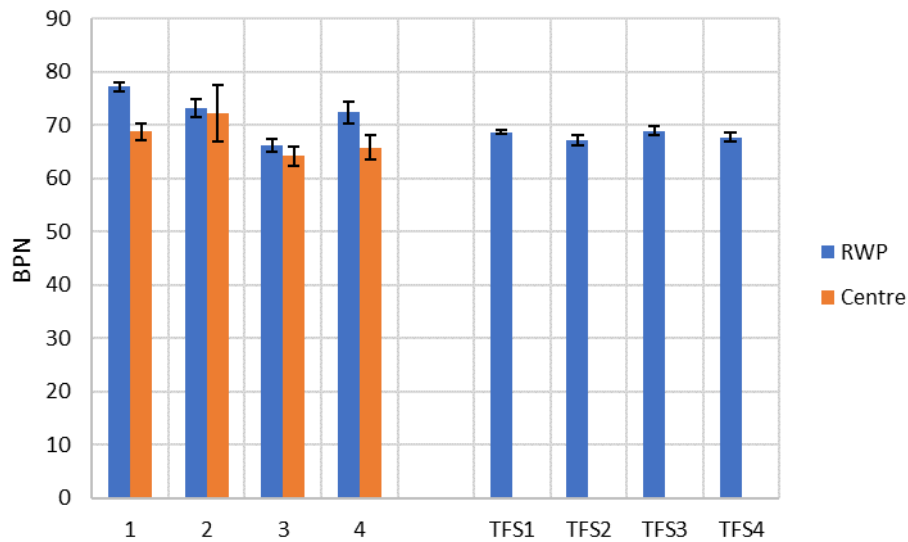


**Figure 6.60: British Pendulum Results for Testing at Armtec Facility (Sept. 7, 2016)**

The PCIP results were found to range between BPNs of 65 and 78. For each of the panels tested, the average BPN of the wheel path was found to be higher than that of the centre of the panel. This may indicate a systemic difference between the surface texture applications of the centre and wheel path areas, though with so few samples, the significance of this difference is small. When the averages of the centre and wheel path readings were analyzed using an Analysis of Variance, the two populations were found to be not significantly different at 95% confidence. The numbering of the four panels tested in this initial test does not correspond to the final numbering determined in the field. Due to a labelling issue, the BPNs of these panels can not be correlated to panels as measured in the field.

While there was a visual difference between the four different texture types on the test panel, there was no significant difference measured in terms of BPN value. The measured BPNs for the TFS 1-4 were 68.7, 67.2, 69, and 67.8, respectively.

Figure 6.61 shows the BP results for the in-situ testing of panels that occurred on September 6<sup>th</sup>, 2017. In this plot, the panel numbers correspond to the sequential numbering established in the field. Therefore panels 1-8 are asphalt-supported, 9-15 are grade-supported, and 16-22 are grout-supported. As discussed previously, no measurements were performed on panels 15-17 due to an equipment malfunction on site. The difference between the centre and right wheel path BPN values for each panel is also shown on the figure

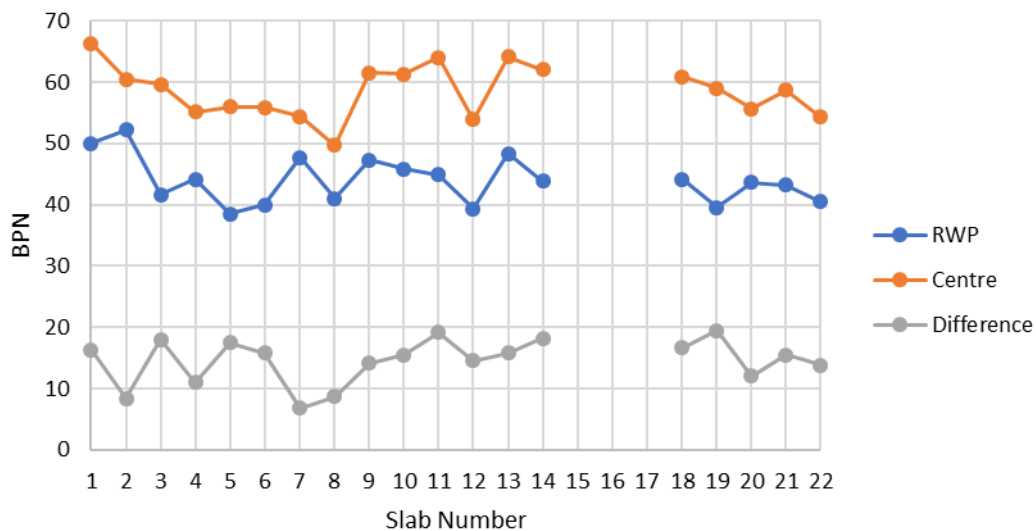


**Figure 6.61: British Pendulum Results for In-Situ Testing (Sept. 6, 2017)**

In this figure, it can be seen that the BPN for the areas within the wheel path, which have been subjected to traffic-related abrasion, are consistently lower than those areas in the centre of the panels, which have not. Over the full section, this difference was an average of 14.6 BPN. The BPNs of the centre locations were found to range from 49.7 to 66.3, while those of the wheel path locations ranged from 38.5 to 52.2. When compared using ANOVA, the two locations were found to be significantly different at 95% confidence.

This indicates that the frictional characteristics of the panel’s surface have changed significantly over the course of one year of traffic-related abrasion. Prior to placement, the two testing locations

were found to be statistically indistinct, based on a small sample of panels. However, in the more recent evaluation, the two locations were found to be distinct, despite drops in the average BPN for both. Some polishing of the surface aggregate can therefore be presumed to have occurred due to traffic-related abrasion.

Since the BP test is performed on an isolated section of the panel surface and does not incorporate any of the differentiating effects of inter-panel joints, unlike IRI, the three support conditions are not compared on the basis of BP.

#### **6.4.3.2 T2Go Friction Analyzer**

The T2Go Continuous Friction Analyzer, known as the T2Go, is a portable device used for analysis of surface friction. Figure 6.62 shows the T2Go device being used to analyze a concrete pavement.



**Figure 6.62: T2Go Testing on an Urban Concrete Street (Wafa, 2018)**

The two wheel device is developed by Airport Surface Friction Tester (ASFT) of Sweden. The device has two rubber tires that are used in the analysis. Based on a known mass and braking force, the coefficient of static surface friction is measured at approximately 0.5 m intervals.

The T2Go testing took place during the same closure as the in service British Pendulum testing, on September 6<sup>th</sup>, 2017. Figure 6.63 shows the results of the T2Go testing throughout the PCIP trial section. Due to the other tests that were taking place during the limited closure window for testing, the pavement surface could not be saturated prior to testing, therefore the results represent

static coefficients of friction (COF) in the dry condition. This condition is generally of less interest than the COF in the wet condition, as that is when friction is reduced overall and therefore a higher safety concern. However, dry friction is still an important safety consideration, particularly on a high speed, high volume roadway. Also, the analysis provides insight into the relative change in friction between the different longitudinal profiles of the PCIP trial.

The friction was measured along the longitudinal profiles of the right wheel path, left wheel path, and panel centre line. The vertical lines represent the inter-panel joints. Approximately 15 m of HMA surface beyond the last PCIP was also measured at the time of testing as a comparison.

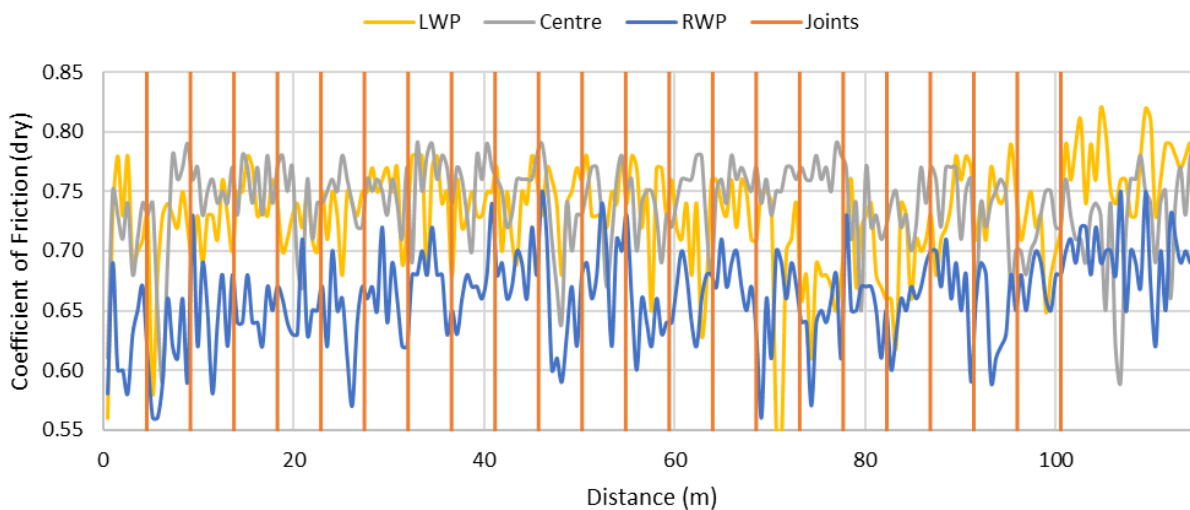


**Figure 6.63: Coefficient of Friction (dry) for PCIP Trial (Sept. 6, 2017)**

As shown, there is significant variation in COF throughout the longitudinal profiles of each of the right and left wheel path and centre line. The statistical analysis of the data sets is outlined in Table 6.11.

**Table 6.11: Least Significant Difference Analysis for Coefficient of Friction Values (T2Go)**

## SUMMARY

<i>Groups</i>	<i>Count</i>	<i>Sum</i>	<i>Average</i>	<i>Variance</i>
RWP	192	126.07	0.657	0.001
Centre	192	142.38	0.742	0.001
LWP	192	139.19	0.725	0.002

## ANOVA

<i>Source of Variation</i>	<i>SS</i>	<i>df</i>	<i>MS</i>	<i>F</i>	<i>P-value</i>	<i>F crit</i>
Between Groups	0.7783	2	0.3892	270.2225	0.0000	3.0114
Within Groups	0.8252	573	0.0014			
Total	1.6036	575				

## LSD Analysis

<i>LSD Criteria</i>	
$\alpha_{\text{overall}}$	0.05
k	3
N	576
n*	192
$\alpha_{\text{modified}}$	0.017
$t_{\text{critical}}$	2.395
SE	0.002
95% LSD	0.005

As shown in the table, the average COF for the right wheel path, left wheel path, and centre line are 0.657, 0.725, and 0.742, respectively. The results of the LSD analysis indicate that the LSD is 0.005 at 95% confidence. Since the difference between each pair of average COF values is larger than 0.005, therefore each of these longitudinal profiles is statistically distinct from the others. Similar to the findings of the BP testing, this indicates that traffic-related abrasion has resulted in the a change to the frictional characteristics of the wheel paths of the PCIP panels over the course of the first year of service. Interestingly, the change was more substantial in the right wheel path than the left. This is probably due in part to the cross slope of the panels that would shift the vehicle centres of gravity towards the right side of the lane, thereby increasing the abrasive effort in that wheel path.

The average COF value for the HMA section beyond the PCIP was found to be 0.73.

The average panel friction was determined based on the known locations of joints. These average friction values are shown in Figure 6.64. This figure shows the trends of Figure 6.63, but with some of the intra-panel variation replaced with an average value.

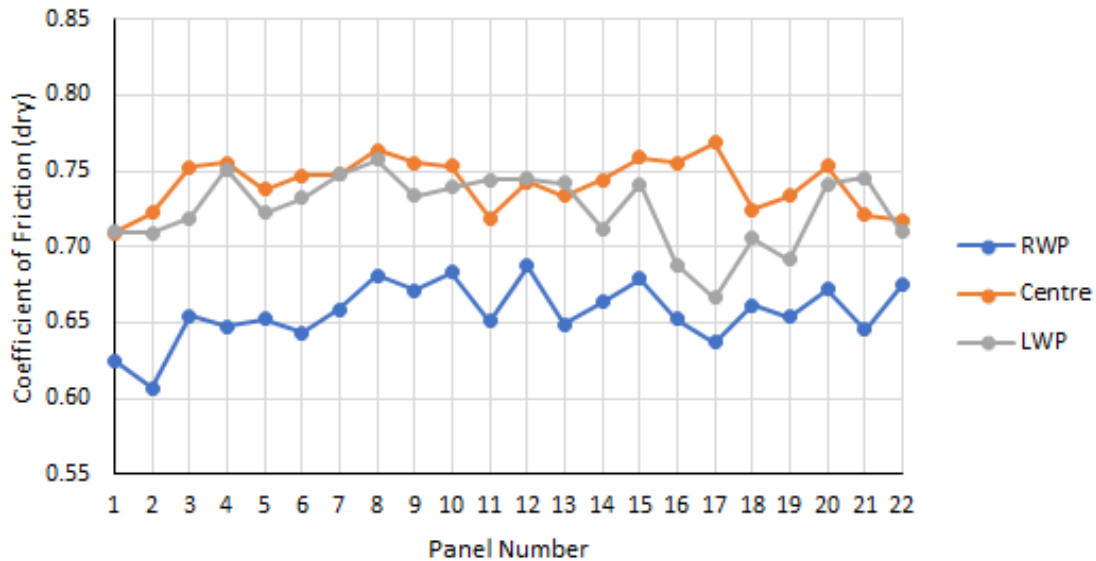


**Figure 6.64: Average coefficient of friction (dry) per panel for PCIP Trial (Sept. 6, 2017)**

The durability of the frictional properties of the PCIP should be monitored over the course of the trial’s service life. The drops in friction measured by the BP and T2Go methods may represent an initial drop in friction under the beginning of service conditions. This initial drop in friction may not represent a reasonable estimate of the expected annual drop in friction going forward.

### 6.4.3.3 MTO Skid Tester

The third method that was used to evaluate the friction of the PCIP test section was using the MTO skid tester in accordance with ASTM E274/E274M-15 (ASTM International, 2015). The test involves dragging a locked tire across the wet surface of a pavement at a constant speed of approximately 100 km/hr and calculating the coefficient of friction of the tire pavement interface based on the resulting force. The test was performed using an ASTM E 501 standard ribbed tire. The ribbed tire is not sensitive to the effects of macrotexture since it removes water from the tire-pavement interface, which is the main benefit of macrotexture in terms of friction.

The Friction Number (FN) is calculated using Equation 22.

$$FN = F/W \times 100 \quad (22)$$

where: FN = Friction number  
 F = Tractive force applied to the tire at the tire pavement interface, (N)  
 W = Dynamic vertical load on tire, (N)

The skid testing was undertaken on October 7<sup>th</sup>, 2016 following the completion of construction. The testing takes place at highway speed, and therefore only two tests were performed on the PCIP during this test, though several additional tests were undertaken on the HMA surface located prior to and after the PCIP section.

The FN values that were measured were found to be above the MTO acceptance threshold of 30. The specific data is not publicly available for inclusion in this document.

#### **6.4.3.4 Frictional Comparison to Liu Prediction Model**

The frictional model produced by Liu (2015), outlined in Equation 21, estimates the frictional number of a pavement based on two surface texture indices, Simulated Mean Texture Depth (SMTD) and the kurtosis index ( $S_{ku}$ ).

Using the surface textures measured in the field after one year of service, the relationship was used to estimate the friction numbers for the PCIP panels. The results of this analysis are shown in Figure 6.65.

It should be noted that the relationship was developed under the conditions outlined in Section 6.4.1, including a SFT system using smooth tires, continuous friction measurement at a slip ratio of 10% to 20%, and a testing speed of 65 km/hr. In general, it has been found that the device and methodology used to measure friction can have a large effect on the results of the test.

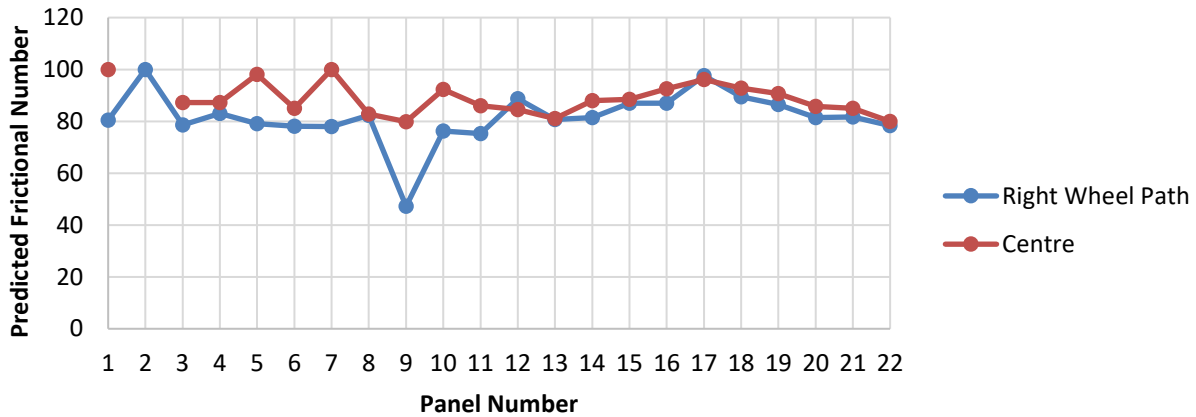


**Figure 6.65: Predicted friction numbers from surface texture measurement**

As shown, the predicted friction for the panels is quite high. In some instances, the prediction is above 100, which is not a practical result as 100 is the maximum theoretical level of friction under perfect conditions. As previously discussed, the kurtosis index for panel 2 was skewed by an erroneous reading, and has therefore been disregarded from the analysis.

Disregarding the erroneous reading and reducing all predictions greater than 100 to 100, the average friction for the right wheel path and the centre were 81.7 and 88.7, respectively.

While the values from the MTO skid tester are not known, it is expected that they would be lower than the values estimated by Liu’s relationship. The MTO skid tester used a ribbed tire that does not measure the benefit of water draining macrotexture. The test is also performed with a locked tire, which produces kinetic friction conditions that result in a lower friction number than partial slip. Further, the high testing speed results in a higher slip speed, which further reduces the frictional number being measured.

#### **6.4.3.5 Frictional Properties Conclusions**

Table 6.12 summarizes the friction results from the different methods used to analyze the PCIP trial. All analyses were undertaken in September 2017 after one year of service with the exception of the MTO Skid Tester, which took place immediately following the completion of construction.

**Table 6.12: Friction Test Results for Right Wheel Path and Panel Centre**

Test Method	Right Wheel Path	$\sigma$	Panel Centre	$\sigma$
British Pendulum	44.0	3.7	58.6	4.2
T2Go Continuous Friction (dry)	0.657	0.037	0.742	0.034
Liu Relationship	81.7	9.8	88.7	6.0
MTO Skid Tester	> FN 30			

As shown, there is considerable variation between the different methods of analyzing friction, which reinforces that friction analysis results are largely influenced by the method used to gather them. The friction related to the right wheel path was consistently less than that of the centre of the panel, with the relative difference between the two ranging from 8% to 25% difference. From these findings, it can be seen that there has been some friction loss associated with traffic over the year of service.

These findings indicate that friction test chosen by a given agency should be chosen with care to ensure that the test provides insight into meaningful pavement performance. The location of the testing within the pavement lane should also be considered carefully as the friction properties can vary across the width of a given pavement section.

#### 6.4.4 Conclusions

The pavement surface of the PCIP trial section was analyzed with respect to texture, roughness, and friction. Largely, the testing took place during over night lane closures, however some was performed during regular traffic conditions.

Based on the analysis, the following conclusions were made:

##### Surface Texture:

- The SMTD, which is correlated with mean profile depth and the  $S_p$  gradient of friction, was found to decrease in the wheel path relative to the centre of the panel, indicating a deterioration in friction
- The tined pavement surface resulted in consistently negative skewness indices, which are associated with lower pavement noise in comparison to positive skewness indices

- The NPSE, an indicator of pavement microtexture, was found to be lower in the wheel path than in the panel centre, indicating that the friction at low speeds and in dry conditions, when microtexture governs friction, may have decreased under one year of traffic-related abrasion

#### Roughness:

- The Surpro-measured roughness was found to be lowest in the Grout-supported condition, followed by the Grade-supported then the Asphalt-supported conditions
- This corresponds to the decreasing level of control that the panel installer has over the final panel elevation, which results in a smoother transition between panels, and lower roughness
- The trend of the ARAN-measured roughness throughout the section generally corresponded to the findings of the Surpro
- In both cases, the roughness of the PCIP trial was found to be higher than the maximum acceptable threshold for new pavement used by the MTO of 1.25 m/km, while the adjacent HMA surface was found to generally be below this threshold

#### Friction:

- There is considerable variation between the different methods of analyzing friction, which reinforces that friction analysis results are largely influenced by the method used to gather them
- The friction related to the right wheel path was consistently less than that of the centre of the panel, with the relative difference between the two ranging from 8% to 25% difference
- There has been some friction loss associated with traffic over the year of service
- The friction was initially found to be acceptable above the FN 30 threshold specified by the MTO

Following construction, it may be necessary to undertake diamond grinding of the PCIP surface to address differential elevations between adjacent panels. This process will reduce the roughness of the section by producing a continuous profile along the section, and may have the additional benefit of allowing for the implementation of a next-generation concrete surface,

which is a diamond grinding configuration that has been found to have good surface characteristics relating to noise and friction. The diamond grinding may require that the riding surface of the panels be constructed with extra concrete cover to allow for repeated grinding efforts without encroaching on the panel's reinforcement.

## **CHAPTER 7: LIFE CYCLE COST ANALYSIS**

Generally, the Ministry of Transportation of Ontario (MTO) considers the expected service life of a mill-and-overlay (M/O) rehabilitation on a freeway to be from 7-16 years (Ministry of Transportation of Ontario, 2013). This service life is dependent on several factors, including the number of lifts of hot mix asphalt (HMA) that is placed. More lifts (up to three) indicate more extensive rehabilitations that are expected to exhibit longer service lives. However, recent experience has shown a number of highways that are exhibiting rutting failure only 3-7 years after an M/O rehabilitation.

It is thought that frequent rutting failures are caused by deep-seated issues. These may be material or construction issues in the pavement subbase or subgrade layers, which cause the surface layers of the pavement structure to deform as ruts under loading. These issues cannot be rehabilitated by milling and replacing the upper HMA pavement layers, as these are not the layers causing the deformation.

Typically, the solution to these issues would be to excavate the pavement structure fully to locate and address the issue directly. This solution is both time and resource intensive but addresses the issues directly. However, under some circumstances the time requirements of a full excavation make it an unacceptable rehabilitation method for a given pavement. The long-term lane closures required to undertake a full excavation reduce the number of effective lanes of a highway, thereby reducing the road's capacity. When this capacity is below the typical traffic volumes, and there are no feasible alternate routes, significant user delays can result. User delays are associated with traffic delay costs, which include user time, and vehicle operating costs associated with stopping, accelerating, and idling (Kher & Phang, 1975). While this is not a cost borne directly by the agency, it is a significant cost that should be considered in any economic analysis. Similarly, there are environmental impacts associated with stopping, accelerating, and idling, though these are outside of the scope of this research.

In the context of the MTO's highway network, the 400-series highways represent circumstances where full excavation is difficult to justify. The traffic levels of the 400-series highways are very

high, particularly near and within the Greater Toronto Area. These highways have annual average daily traffic values above 100,000 vehicles per day, and some sections see approximately 420,000 vehicles per day (Ministry of Transportation of Ontario, 2016).

The MTO is interested in potential methods to address these areas prone to deep-seated rutting without causing the undue user-related costs associated with frequent M/O rehabilitations or extensive reconstructions to directly address the issue. For this reason, a design was developed that included the use of precast concrete inlay panels (PCIP) that are installed in overnight construction windows and reduce the effects of deep-seated pavement issues (Pickel D. , et al., 2016). The design was implemented as part of a trial on Highway 400, a high-volume highway in the province of Ontario (Pickel D. J., Tighe, Lee, & Fung, 2018).

For the PCIP strategy to be considered feasible, the life cycle cost (LCC) of the strategy should be studied, incorporating all associated costs throughout the strategy's service life.

Lane and Kazmierowski (2005) produced the document titled "Guidelines for the Use of Life Cycle Cost Analysis on MTO Freeway Projects". The guideline lays out the methods that the agency prescribes for life cycle cost analyses (LCCA), which are commonly used at the MTO for the analysis of alternate bids for a given freeway project. The MTO requires one asphalt and one concrete pavement design be analysed for a given freeway construction bid in an effort to promote equity within the pavement materials sector. The guidelines, as laid out consider the following costs and associated performance criteria encountered throughout the pavement life cycle as defined below:

- Initial construction costs.
- Initial pavement service life.
- Rehabilitation costs.
- Timing and service life of rehabilitation.
- Preventive treatment costs.
- Timing and service life of preventive treatment.
- Discount rate.
- Salvage value.

Each design is analyzed over a period of 50 years. Notably, the guidelines do not consider user costs as part of the LCCA. Some consideration has been given to the topic, but the current practice is to disregard its use. These guidelines form the basis of any LCCAs performed by the MTO.

In this chapter, the MTO LCCA guidelines are used to develop a comparison between the frequent M/O rehabilitation and the PCIP rehabilitation. This comparison includes the impacts of user costs associated with construction activities, despite their exclusion from the MTO guidelines.

Due to the novelty of the PCIP strategy, and therefore a lack of relevant historical performance data, the comparison is deterministic in nature. A probabilistic comparison can not be performed, and therefore a sensitivity analysis focusing on the most subjective inputs to the LCCA model is performed to validate the findings. Furthermore a factorial analysis focusing on the most impactful of these subjective inputs is used to gauge the likely scope of the results of LCCA model.

## **7.1 Rehabilitation Techniques**

In order for a LCCA to be undertaken, several broad constraints must be identified and considered in order to ensure that the findings of the analysis are meaningful.

### **7.1.1 Scope of Comparison**

The scope of the comparison is based on recommendations from the MTO LCCA guideline, but altered to suit the specific nature of the problem that is being considered. The comparison is considered for a one km stretch of Highway 400, in the area where the trial section was constructed. Highway 400 has three lanes in each direction in this location, and the LCCA guidelines typically consider the full width of a given road section in their comparisons, however the deep-seated rutting issue has generally been confined to the right lane that carries the majority of the highway's truck traffic. For this reason, the comparison only considers one lane being rehabilitated. All other lanes are considered to be independent of the comparison and are not included in the comparison.

### **7.1.2 Social Discount Rate**

The social discount rate (SDR) is a very important factor in LCCAs. It represents the rate at which future costs and savings of social projects, such as highway infrastructure, are discounted when calculating their present worth (PW). These values are difficult to determine as they are subject to the effects of numerous social and financial factors, which can change throughout the course of a

50-year analysis period. Nonetheless, SDRs are necessary to any LCCA in order to consider future costs at an acceptable discount. In Ontario, the SDR is a nominal social discount rate. This rate is used to account for alternate social benefits that are not realized as a result of the cost being considered (Moges, Ayed, Viaceli, & El Halim, 2017). In 2016, the Ontario Ministry of Finance set the nominal social discount rate (NSDR) for pavement design projects as a step function. From 0 to 30 years into the future, the NSDR is 4.5%, while from 31-75 years, the NSDR is 4.0% (Ministry of Transportation of Ontario, 2017).

### **7.1.3 Required Activities**

In order to develop reasonable cost estimates that can be used to compare the different rehabilitation strategies, the component activities of each strategy must be identified and quantified. Quantification includes estimates of time and cost required for each activity.

#### **7.1.3.1 Mill-and-Overlay (M/O)**

The M/O rehabilitation strategy is used frequently by the MTO and therefore information related to its component parts is easily found. Through discussions with MTO personnel, a “typical” method for performing a M/O rehabilitation of a section exhibiting premature deep-seated rutting was developed. Generally, the strategy involves the following:

1. Mill away the surface layer of pavement, which is then trucked off site for disposal or recycling.
2. Place a tack coat to promote bonding between the existing and new pavement layers.
3. Place and compact a 40 mm lift of new HMA pavement.
4. Place a second tack coat.
5. Place and compact the surface layer of HMA.

Following construction, the typical maintenance schedule includes routing and sealing cracks after three years of service, then subsequently performing mill and patch operations combined with routing and sealing and approximately six year intervals. Approximately 19 years after the initial construction, the pavement undergoes an 80 mm depth M/O rehabilitation that begins the cycle again. Figure 7.1 illustrates the typical schedule that is assumed for a deep strength asphalt concrete freeway pavement.

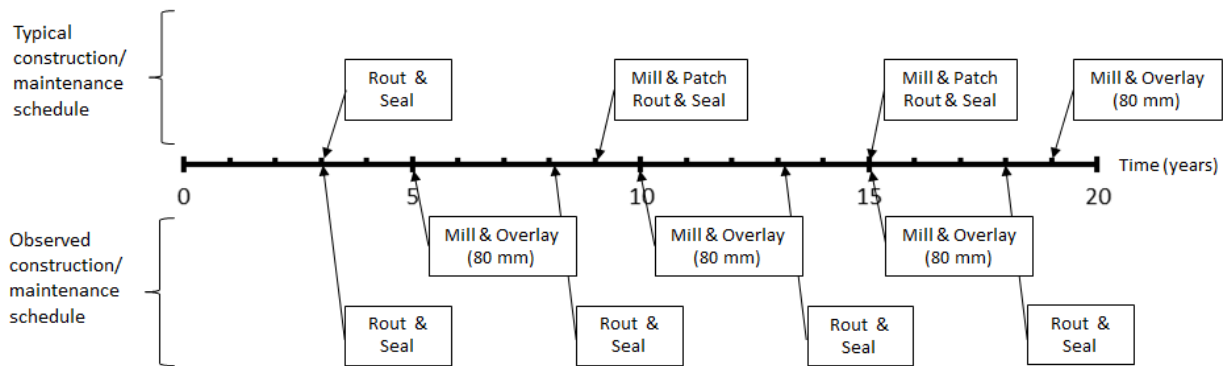


**Figure 7.1: Typical and observed construction and maintenance schedule for deep strength asphalt cement pavement**

As mentioned, when deep-seated rutting issues are present beneath the freeway pavements, the typical maintenance schedule does not apply. In these cases, the deep seated rutting typically manifests by 3-7 years after the initial construction, at which point it requires an 80 mm depth M/O rehabilitation. This effectively removes 12 to 16 years from the expected service life of the pavement. Figure 7.1 shows the potential maintenance and rehabilitation schedule in these cases, beneath the horizontal axis.

### 7.1.3.2 PCIP

The construction of the PCIP strategy, as performed on the Highway 400 trial section, is somewhat more complicated than the typical M/O strategy. In part, this is due to the nature of the trial, which included three designs, each with a unique panel support system. However, in simplified terms, the PCIP construction operation includes the following steps:

1. milling ~200 mm of existing HMA in the right lane,
2. cleaning the milling debris left on the surface,
3. preparing the support conditions, consisting of either
  - a. carefully cleaning the milled asphalt surface, or
  - b. placing, screeding, and compacting a cement-treated bedding material to provide a uniform support surface,
4. placing the panels on the support surface (using a crane), and
5. pumping grout around and beneath the panels.

Unlike the M/O rehabilitation strategy, the PCIP strategy does not have a comprehensive historical data set from which to formulate maintenance and repair strategies; the trial on Highway 400 represents the first PCIP trial under service conditions. Therefore, in order to produce a life cycle cost analysis, some assumptions must be made about the PCIP performance.

Significant data exists for conventional jointed plain concrete pavements (JPCP), so a typical maintenance schedule has been developed by the MTO. While there are many differences between PCIP and JPCP, it is a reasonable assumption that their maintenance schedules could be similar. This consideration assumes that the issues that were identified in the trial section would be addressed in future applications of the strategy. Specifically, an improved longitudinal joint detail, such as that outlined later in Section 9.1.4, and a surface grinding regime such as that outlined in Section 9.1.6 to address initial roughness, is assumed. Therefore, for the purposes of this analysis, the maintenance schedule for JPCP is applied to the PCIP.

Following construction, the first maintenance activity for the pavement involves resealing joints after 12 years of service. This is done on an as-needed basis, but an estimate of 50% of the transverse joints and 25% of the longitudinal joints has been found to be an acceptable assumption. At 18 years, a minor concrete pavement restoration (CPR) is performed, which includes diamond grinding the pavement's surface to provide surface texture, resealing joints (100% of transverse joints and 50% of longitudinal joints), and full and partial depth patching. The full and partial depth patching is done as required, but 0.5% and 0.3% of the total pavement surface area is an acceptable assumption.

The next repair is a major CPR operation at 28 years, which includes all of the same activities as the minor CPR, but with more patching. For this CPR, 1.7% and 1.0% of the total pavement surface area can be assumed to require full depth and partial depth patching, respectively.

At 38 years, the concrete pavement is sprayed with a tack coat and overlaid with 80 mm of HMA. The cracks that form in this asphalt layer are then routed and sealed at 41 years and again at 44 years.

Figure 7.2 illustrates the assumed construction and maintenance schedule for the PCIP rehabilitation strategy, which was developed based on the JPCP strategy outlined by the MTO in their LCCA guidelines.

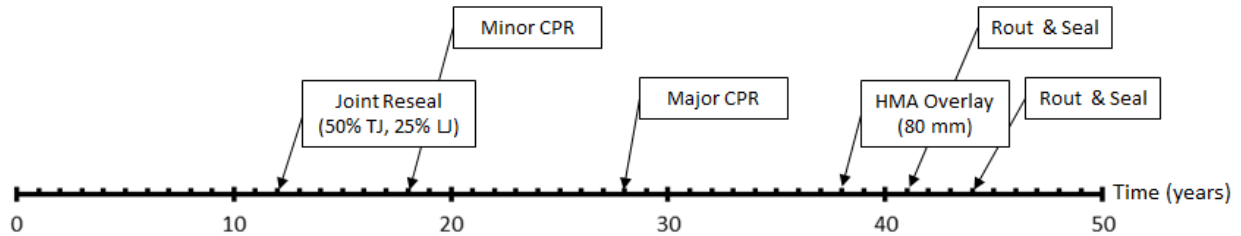


**Figure 7.2: Assumed construction and maintenance schedule for PCIP rehabilitation modelled on JPCP**

#### 7.1.4 Unit Costs

The unit costs associated with the relevant construction operations were obtained from two sources. Where applicable and available, cost estimates were taken from the MTO cost database. Since the PCIP strategy is novel, there is no cost information related to its construction in this cost database. In these cases, the costs associated with the trial section construction are used to estimate the costs associated with the PCIP construction.

The cost estimates in each case likely misestimate actual costs that would be encountered on a project repairing deep-seated rutting issues. In the case of the MTO database, the values are averages based on large paving projects. For smaller rehabilitations like localized deep-seated rutting, these estimates are probably low since the same economies of scale can not be achieved. In the case of the PCIP trial construction, the costs likely overestimate those that would be encountered. Since the trial was the first of its kind, there were high costs due to start-up activities (new forms for precast panels, new grout mixer/pump, specialized milling head, etc.) that could not be amortized across several or larger projects. Following construction, both the contractor and MTO indicated that the costs associated with the trial were larger than would be expected for a full-scale implementation of a PCIP rehabilitation. The previous MTO experience with intermittent precast repairs on highways 401 and 427 found the trial to have costs approximately 250% of the eventual full-scale implementation. However, because the trial was the lone source of PCIP costing, the costs used on the trial were often used for this analysis.

Following the completion of the trial, the unit cost of the panels was determined to be the largest contributor to the PCIP construction costs. For the trial, each panel cost approximately \$8000 including delivery to the site. In addition to delivery, the cost encompassed all of the costs associated with precasting, including mix designs, texturing, curing, etc. The trial represented the first project of its kind for Armtec, the precasting plant.

In discussions with the contractor, following the completion of construction, a per panel cost estimate was produced that is more representative of the panels for a full scale project using the PCIP rehabilitation. This cost estimate was produced assuming the same panel dimensions that were used on the trial, with no applicable taxes. The estimate was also for delivery between June and October, as April and May spring thaw load restrictions would increase delivery costs. The estimate included unit costs based on 400 to 1200 panels and 1200+ panels in the order. The cost estimates are outlined in Table 7.1.

**Table 7.1: Panel unit cost estimates for full-scale PCIP projects**

<b>Description</b>	<b>Unit</b>	<b>Est. Qty</b>	<b>Unit Price</b>	<b>Unit Price (incl. tax)</b>
Supply only including freight:	Each	400 (Min)	<b>\$4940</b>	<b>\$5582</b>
Alternate for Quantities > 1200 Panels	Each	1200+	<b>\$4100</b>	<b>\$4633</b>

The unit costs that were considered to calculate the cost of construction are shown in Table 7.2.

Maintenance costs were taken from the MTO cost database for both M/O and PCIP rehabilitations. The assumption used in the case of PCIP was that the maintenance activities and their associated costs would be similar to conventional concrete pavement. Since this type of pavement is more common, the MTO has cost estimates relating to its maintenance. In addition to unit costs, the MTO has estimates of the length of time that each maintenance or repair strategy should last. These values are summarized in Table 7.3.

**Table 7.2: Unit Costs used for Calculation of Construction Costs**

<b>Activity</b>	<b>Description</b>	<b>Cost</b>	<b>Unit</b>
<b>Asphalt Milling</b>	Milling the existing HMA to 40 mm or 80 mm depth (as required). Cost includes milling and material removal from site.	\$6	/m <sup>2</sup>
<b>Tack Coat</b>	Thin layer of bituminous material sprayed prior to placing HMA to promote and improve bonding between pavement layers. Cost includes material and placement.	\$0.50	/m <sup>2</sup>
<b>New Material</b>	New HMA (High-friction SP12.5 FC2) to replace milled surface material. Cost includes material, placement, and compaction.	\$127.70	/ton
<b>Traffic Control</b>	Includes development of traffic control plan, placement of required signs, pylons, and lights, and crash trucks.	\$1,800	/night
<b>Water Truck</b>	Water used for production of different grouts on site	\$95	/hour
<b>Cement Treated Base</b>	Cement treated base including cement and fine aggregate. Includes material and delivery to site.	\$150	/m <sup>3</sup>
<b>Grout</b>	Includes both flowable bedding grout and structural edge/joint grout. Cost includes material.	\$23	/bag
<b>Milling</b>	Milling the existing HMA to ~200 mm depth (as required). Cost includes milling and material removal from site. Higher price represents threshold nightly cost for smaller milled areas.	\$6,500	/night
<b>Crane</b>	Includes transportation and operation costs for crane to place panels from trucks to road. Based on 10 hour shift including 2 hours travel time.	\$3,500	/night
<b>Precast Panels</b>	Construction, curing, and transportation of panels to site.	\$5,582	/panel
<b>Concrete Pump</b>	Mixer/pump used to produce and distribute grout where required. Includes operator.	\$200	/hour

**Table 7.3: Unit Costs and Estimated Service Lives for Maintenance/Rehabilitation Activities**

Activity	Description	Cost	Unit	Estimated Service Life (years)
<b>Rout and Seal</b>	Routing cracks to remove loose material and provide a bonding surface, then pouring a rubberized asphalt sealant into the crack. Cost includes material and placement.	\$6	/m	
<b>Mill and Overlay Costs</b>	Same as described for mill and overlay construction operations	As shown previously		11 (typical)
<b>Concrete Joint Resealing</b>	Resealing longitudinal and transverse joints which have lost sealant	\$10.43	/m	
<b>Diamond Grinding</b>	Retexturizing concrete surface to improve friction properties, by grinding 1.5 - 19 mm from concrete surface.	\$10	/m <sup>2</sup>	10
<b>Full Depth Repair</b>	Degraded areas of concrete are cut out and replaced	\$250	/m <sup>2</sup>	10
<b>Partial Depth Repair</b>	Removing unsound concrete from pavement surface and replacing with new concrete.	\$450	/m <sup>2</sup>	10
<b>Overlay</b>	Following the end of the concrete pavement's service life, the pavement is overlaid by an asphalt pavement layer, with costs according to the previously listed overlay costs. Overlay is then subjected to rout and seal maintenance	As shown previously		12

### 7.1.5 User Costs

The MTO LCCA guidelines (2005) avoids the use of user costs in life cycle cost analyses, citing the significant effort to calibrate user cost models to Ontario conditions. However, part of the motivation to utilize the PCIP trial was to find a method to limit the number of construction operations and their associated effects on users. Therefore, it is reasonable to consider user costs when comparing the two rehabilitation strategies especially given that this treatment is most likely to be used on very high-volume highways in the Greater Toronto Area where user delays are a major issue.

To determine user costs, the Simplified Work Zone User Delay Analysis (SZUDA) tool, developed by a joint partnership between the University of Toronto and the University of Waterloo, was used (Mushtaq, 2011; Ahmadi, 2011). The tool uses a throughput model to estimate traffic levels of a highway throughout the day and the user delays associated with restricting the capacity of the highway through construction operations. The construction site and its capacity are defined by the total number of lanes, the number of lanes closed, the closure type (concrete barriers or temporary barrels), the length of the closure, and the percentage of the total traffic that is made up of trucks.

Once the restricted capacity is calculated, it is compared to the expected traffic for the given time, which is based on traffic counts performed by the developers of the software for various highways in Ontario. Where the expected traffic is higher than the restricted capacity, user costs are incurred. The assumed user costs are \$10/veh/hr for passenger cars and \$50/veh/hr for heavy vehicles.

The construction site considered for each rehabilitation strategy was developed based on the layouts described in the Ontario Traffic Manual for Temporary Conditions (Book 7) (Ministry of Transportation of Ontario, 2014). The closure for two lanes of a six lane road (TL-38) best describes the temporary closure used for each of the rehabilitation operations considered. The layout is shown in Figure 7.3.

As shown, the temporary closure is made up of various sections with lengths defined based on the normal posted regulatory speed limit. Considering that the strategies are being considered for 400-series highways, this speed limit is 100 km/hr. Therefore, using this speed and the values outlined in Tables C and D of the traffic manual, the length of the construction site is considered to be 1370 m plus the length of the construction zone. Since the M/O construction operation can be completed in one night, the full 1 km length of the assumed section is the nightly work zone, which results in a total length of 2370 m. For the PCIP strategy, the assumed nightly placement is 40 panels per night, which corresponds to a work zone length of approximately 200 m, and a total length of 1570 m.

The original design document for the section of highway where the PCIP was constructed indicated that the total traffic is made up of 12% heavy vehicles, and therefore this value was used for the calculations. The one-way average daily traffic for the software is approximately 63,000 vehicles/day based on the traffic counts that were performed. In 2016, the section of roadway chosen for the comparison had an average annual daily traffic value of 90,000 vehicles, or 45,000 vehicles/day in each direction. The section also showed an average annual growth rate over the previous 15 years of 1.2%. The summer average daily traffic (SADT) for the section was 109,800 vehicles/day in 2016, or 54,900 vehicles/day in each direction with an average annual growth rate of 1.1% over the previous 15 years (Ministry of Transportation of Ontario, 2016). The SADT can be considered since the majority of construction operations occur during this period of the year.

So while the software probably overestimates the actual traffic conditions, it provides a reasonable approximation since site-specific hourly traffic counts are not available.

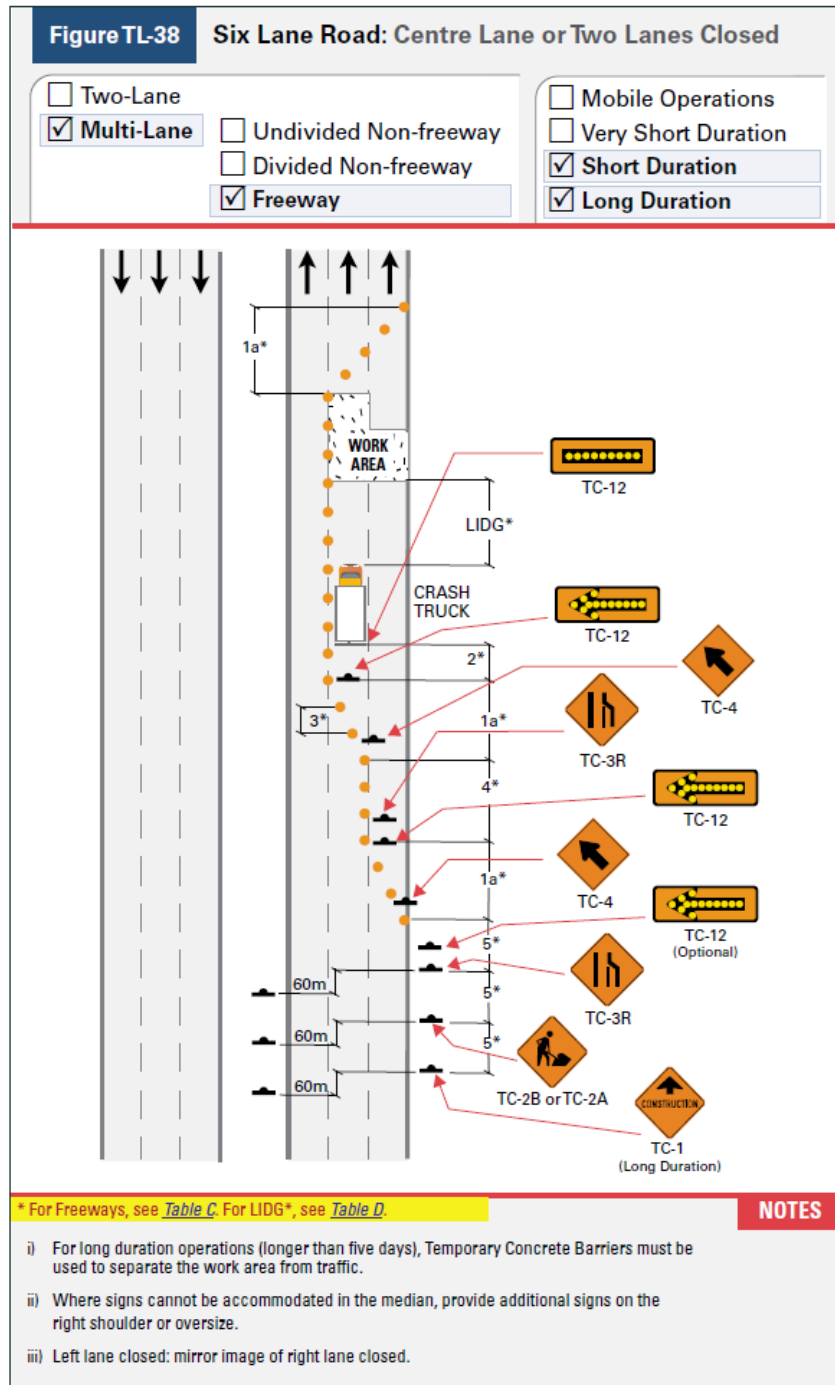


**Figure 7.3: Temporary closure layout for M/O and PCIP rehabilitations (Ministry of Transportation of Ontario, 2014)**

Considering these inputs, the average user cost for one night of construction is \$32,640.65 for the M/O rehabilitation. This value is the average over each weeknight, from Monday to Friday. Therefore, for one M/O operation, it costs \$32,640.65 for the users. Additionally, for each maintenance operation, such as routing and sealing cracks or repairing concrete joints, this user cost is considered under the assumption that the maintenance would take place over the course of one night.

The average cost of one night of PCIP rehabilitation, based on a full week is \$31,294.34. The slight difference is due to the shorter work zone length. Figure 7.4 shows the graphical representation of queue development for the PCIP construction operation over the course of one week. The MTO-specified construction window of 10 pm to 6 am results in slight queuing from 10 pm to 11 pm, and more substantial queuing from 5 am to 6 am. Based on the assumed rate of installation, the PCIP rehabilitation for 1 km would require six construction operations. Therefore, the total user cost associated with the PCIP installation over the six nights of construction is assumed to be \$187,766.04.

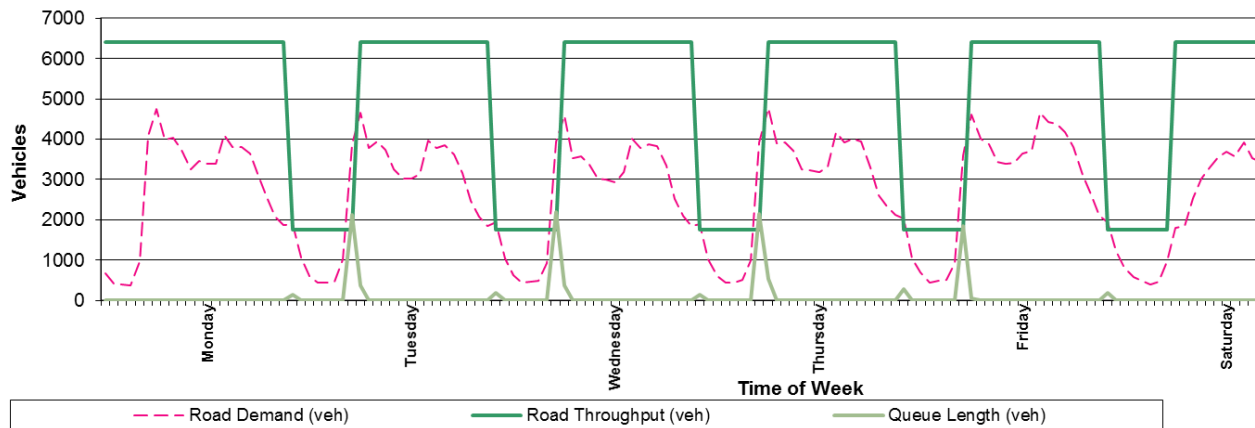


**Figure 7.4: Queue development for PCIP construction operations**

## 7.2 Life Cycle Cost

The life cycle cost analysis is conducted for a 50 year period. The costs for each of the required activities are calculated for the year they are expected to occur in. These values are then converted to a present worth using Equation 23 (Lane & Kazmierowski, 2005).

$$PW = C \times \left[ \frac{1}{1 + Dis} \right]^n \quad (23)$$

where: PW = Present worth cost (\$)  
 C = Future cost in present-day terms (\$)  
 Dis = Discount rate (decimal)  
 n = Time until cost is incurred (years)

At the end of the 50 year period, the economic value of the pavement remaining is accounted for using the salvage value. This value accounts for the remaining worth of the asset that would extend beyond the analysis period. The salvage value is calculated using Equation 24.

$$SV = \left[ \frac{L_{rem}}{L_{exp}} \right] \times C \quad (24)$$

where: SV = Salvage value of pavement (\$)  
 L<sub>rem</sub> = Remaining life of last rehabilitation treatment (years)  
 L<sub>exp</sub> = Expected total life of last rehabilitation treatment (years)  
 C = Cost of final rehabilitation treatment (\$)

Based on the assumed schedule of maintenance operations outlined in Figure 7.1 and Figure 7.2, the salvage value in both cases for the analysis is \$0 as the most recent rehabilitation has reached the end of its service after 50 years of total analysis. However, when the frequency of required M/O operations changes, the salvage value comes into play.

Using the unit costs, schedule, and nominal social discount rate described previously, the present worth cost of each rehabilitation strategy was found. The results of this analysis are shown in Figure 7.5. The PWC of each construction and maintenance operation is shown for each rehabilitation strategy, with a line showing the cumulative contribution to the total PWC of each operation.

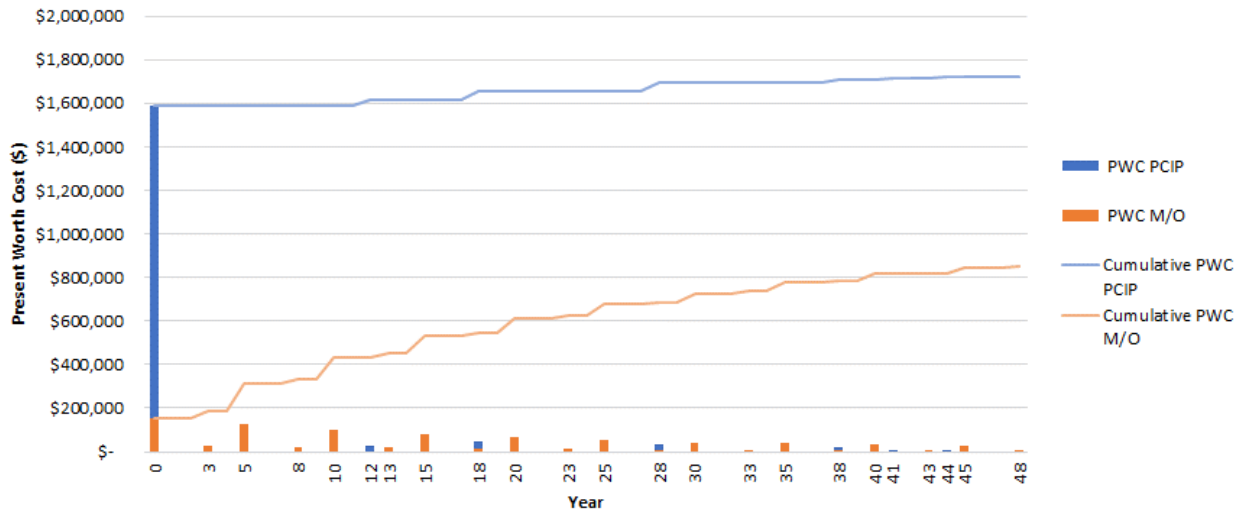


**Figure 7.5: Present worth costs for PCIP and M/O rehabilitation techniques**

As shown, the PCIP strategy has a substantially higher PWC, with a difference between the two strategies of \$872,480. The majority of the PCIP PWC is due to the initial cost of construction, with small contributions from the maintenance operations throughout the 50-year analysis period. The M/O strategy accrues relatively large costs at 5 year intervals associated with milling and overlaying, however the PWC of these operations is consistently reduced according to the nominal social discount rate. This can be seen in Figure 7.5, as the slope of the cumulative PWC for M/O flattens over time.

### 7.2.1 Sensitivity Analysis

For a deterministic life cycle cost analysis to be meaningful, it should consider the effect of changes to its inputs; sensitivity analyses are a method to analyze these changes. Sensitivity analyses are particularly useful when the actual value of a given input is subjective, unknown, or unreliable. When this is the case, seeing the magnitude of the effects of changes to the input can provide insight into whether the initial assumption is acceptable.

For this sensitivity analysis, the inputs that were considered to be the most subjective were the nominal social discount rate (NSDR), the user cost, the unit price of the panels, the frequency of the required M/O operations, and the rate at which the PCIPs can be placed on site.

For each sensitivity analysis, a sensitivity index was calculated according to the simple equation proposed by Hoffman and Gardner (1983), in Equation 25:

$$SI = \left[ \frac{D_{max} - D_{min}}{D_{max}} \right] \quad (25)$$

where:           SI = Sensitivity Index  
                    $D_{max}$  = Output result when parameter is at maximum value  
                    $D_{min}$  = Output result when parameter is at minimum value

The sensitivity index provides insight into the relative impact of a given parameter on the final output, which in this case is the difference between the PWC of the PCIP and M/O strategies. The index is dependant on the range limits of the parameter so having reasonable limits is an important consideration.

According to Moges et al. (2017), Canadian provincial agencies typically use a discount rate between 3% and 6%. Therefore, these limits were used as the limits for the sensitivity analysis for the NSDR analysis. The MTO uses a two part NSDR with a different rate for the first 30 years (4.5%) than for the next 45 years (4.0%) so the discount rates for the two time periods were considered to always have a difference of 0.5%. Therefore, the analysis considered NSDRs from 3.5 and 3.0% to 6% and 5.5%, for 0-30 years and 31-75 years respectively.

The average daily user costs were considered from approximately 75% to 125% of the original user cost value. The nightly user cost associated with the PCIP was approximately 96% of that for the M/O operation due to work zone length and therefore this ratio was maintained throughout the analysis. The limits of the range of the analysis were approximately \$24,000 per night and \$40,000 per night.

The unit price of the PCIPs is an input that has inherent variability due to its novelty. A unit cost of \$5582 represents the after-tax cost of the panels as estimated by the supplier for between 400 and 1200 panels, while a unit cost of \$4633 per panel corresponds to more than 1200 panels. Meanwhile, \$8000 per panel was the cost of the trial section. The sensitivity analysis considers unit prices from 100% of the trial construction cost, down to 50%. This encompasses both of the unit cost estimates for panels provided by Armtec, based on the size of the total order.

The frequency of the required M/O operations is unknown and largely dependant on site-specific considerations. The range of frequencies that has been discussed by members of the MTO for the areas that are potential PCIP candidates are from every 3 years to every 7 years. Therefore these frequencies define the limits of the analysis.

Finally, the rate at that the PCIPs can be installed represents the final major unknown to be considered in the sensitivity analysis. The scope of the PCIP trial was small and as a result the rate of installation under full production conditions was unknown. The members of the construction contractor who were involved in the trial section were polled following the construction, and the average estimate for nightly installation was 40 panels per night. This number is an estimate, and is therefore an unknown. Large continuous precast concrete projects have been found to have installation rates of 25 to 40 panels per night (Tayabji, Ye, & Buch, 2012). The PCIP design requires an extra step of asphalt milling, but reduces the amount of support material preparation that is required if the milling is done well. Since these considerations could conceivably result in an increase or decrease in the installation rate, the limits of the range of panel installation rates for the sensitivity analysis were selected as 20 panels per night and 45 panels per night.

The results of each sensitivity analysis are shown in Figure 7.6. In each case, the ranges of inputs discussed above are used to find the difference in 50-year present worth cost (PWC) between the PCIP and M/O strategies. A positive value represents a scenario where the PCIP strategy has a higher PWC than the M/O strategy.

Changes in the NSDR had a positive effect on the difference between the PWC for the two strategies. This is an intuitive result due to the relative cost structures of the two strategies; PCIP had a large initial cost with small future costs, while M/O had lower, but consistent costs throughout the 50 year analysis period. Therefore, discounting future costs at a greater rate reduces the PWC of the M/O strategy. The sensitivity index of the NSDR was found to be +0.22, indicating that changes between the minimum and maximum assumed NSDR values result in a change in the PWC difference of approximately 22%.

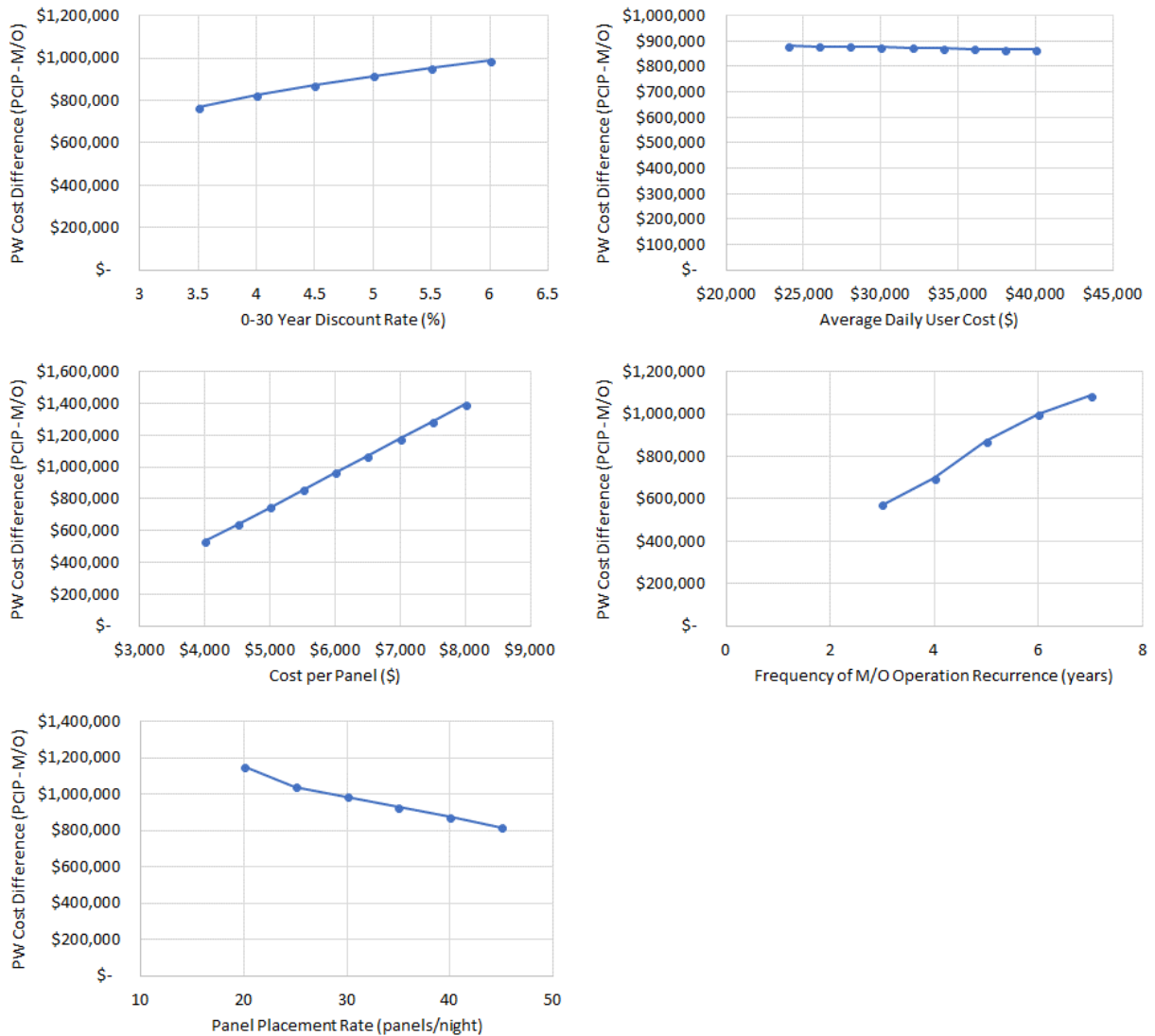


**Figure 7.6: Sensitivity Analyses for Discount Rate (upper left), Average Daily User Cost (upper right), Cost per Panel (centre left), Frequency of M/O Operation (centre right), and Panel Placement Rate (lower left)**

The average daily user cost was found to have a negligible effect on the PWC difference. As shown in Figure 7.6, the difference remains relatively consistent as the user cost changes. The sensitivity index of the model with respect to user cost was found to be -0.02, indicating that substantial changes to the user cost across the range considered resulted in a change of only 2% in the difference in PWC.

The unit price of the precast panels was found to be a very impactful input on the difference in PWC for the two strategies. With a sensitivity index of +0.62, the range considered for the PCIP

unit cost accounted for a 62% change in the PWC difference between the two alternatives. It should be noted that the index is dependant on the range being considered, so it is possible that the minimum consideration of \$4000 per panel is lower than is reasonable.

The required frequency of the M/O operation also had significant impact on the PWC difference between the two rehabilitation strategies. The sensitivity index for this input was found to be +0.47, or a 47% increase in the PWC difference due to increases in the frequency of operation from every three years to every seven years.

Finally, the panel placement rate also had a significant effect on the PWC difference. The sensitivity index was found to be -0.41, or a 41% decrease in the PWC difference due to the increase in placement rate considered, from 20 panels per night to 45 panels per night. Once again, this index is dependant on the range that is specified and 45 panels per night may not prove to be feasible.

A factorial analysis of the sensitivity results was undertaken to determine the combined effects of the changes to the different input values. The user cost had very little effect on the PWC difference, and so it was neglected for the analysis that only included NSDR, panel unit cost, M/O frequency, and panel installation rate.

For each of the four input types, the input values corresponding to the minimum and maximum outputs were considered for the factorial analysis. The PWC difference between the PCIP and M/O strategies were calculated for each combination of the maximum and minimum values in each case. The results of this factorial analysis are shown in Figure 7.7.

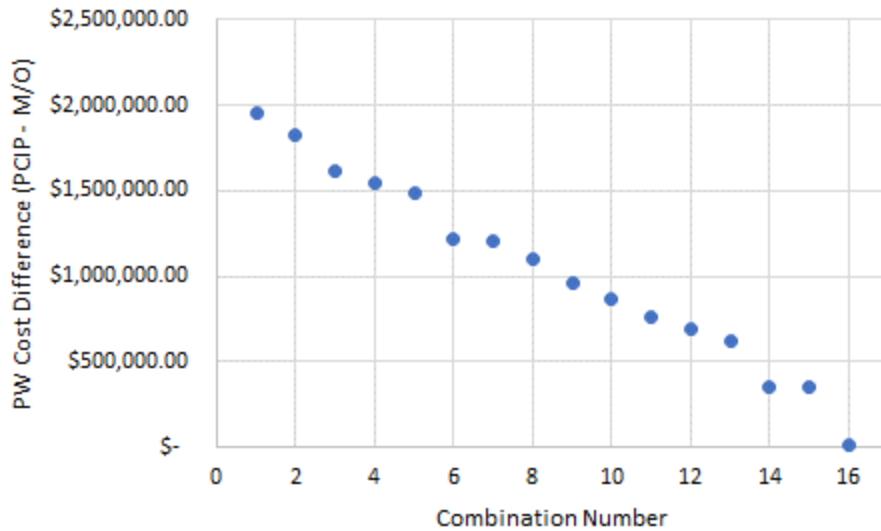


**Figure 7.7: Sensitivity Analysis Factorial Combination Results**

The results of the factorial combination in Figure 7.7 are arranged from highest PWC difference to lowest. The maximum difference observed within this analysis was \$1.95 M, which was a result of NSDR rates of 6% (0-30 years) and 5.5% (31-75 years), panel unit cost of \$8000, M/O frequency of once every 7 years, and a panel installation rate of 20 panels per night. The minimum PWC difference was approximately \$13,090, which was a result of NSDR rates of 3.5% (0-30 years) and 3% (31-75 years), panel unit cost of \$4000, M/O frequency of once every 3 years, and a panel installation rate of 45 panels per night.

The PCIP was found to have a higher PWC than the M/O strategy consistently throughout the analysis. Even considering PCIP-favourable inputs in each case, it was still found to have a higher cost, although this number is sufficiently small to be considered approximately equal.

Based on this analysis, it can be confidently stated that given these assumptions, the M/O strategy costs less than the PCIP strategy, based on the assumptions made within this analysis.

### 7.3 Tipping Point Analysis

The present worth cost of the PCIP rehabilitation strategy was found to be larger than that of the M/O strategy. In part, this may be due to the previously discussed overestimates and underestimates in construction costs due to the novelty of the PCIP strategy. The scale of the overestimates in PCIP cost are difficult to gauge without larger scale use of the strategy. While the

MTO has expressed a willingness to pay a higher cost in some circumstances in order to reduce some of the safety concerns associated with frequent M/O operations, it is clear that the cost of the PCIP must still be reduced in order to make this decision more feasible and defensible from the ministry's perspective.

The present worth cost of the PCIP rehabilitation strategy is largely due to the construction costs, with very little due to maintenance and repair operations in later years. Therefore, in order to define a "target cost" that would make the two strategies equivalent in terms of present worth cost, a significant reduction in PCIP construction costs must be realized. It was found that the unit costs of the panels had a significant effect on the PCIP construction costs and therefore the PWC difference, however this portion of the cost is being included within the overall construction costs for this analysis. While changes to the panel unit costs may make up a significant proportion of the required changes in PCIP construction cost, cost savings in other aspects of the construction process may also contribute.

A tipping point analysis was undertaken to determine the PCIP construction cost that would make the present worth costs of the two rehabilitation methods equivalent. The PCIP construction costs were varied until the 50-year PWC of both strategies were even. This analysis was performed with the initial assumptions and inputs. As shown in the sensitivity analysis, changes in these inputs can result in substantial changes to the difference in PWC between the two strategies. However, this analysis will show an approximation of what the initial construction cost of 1 km of PCIP should be in order to have comparable costs to M/O.

Based on this analysis, the initial cost of PCIP construction needs to be reduced to approximately \$528,000 in order to have the same 50-year PWC as the M/O operation. This represents a reduction of approximately 62% of the initial PCIP construction cost as used in this analysis, which is substantial. The life cycle costs of the two alternatives in this case are shown in Figure 7.8. It should be noted that the cost at year zero includes both the construction cost and the user cost, summing to approximately \$700,000.

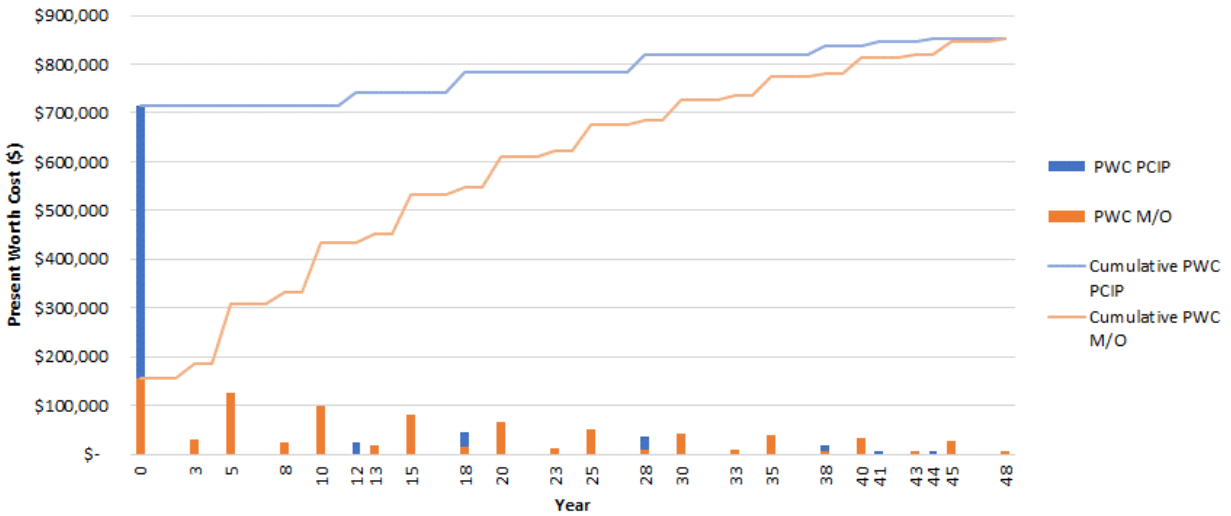


**Figure 7.8: Life cycle costs of PCIP and M/O strategies at “tipping point”**

The required construction cost reduction could be lessened if the MTO could provide an estimate of the benefits of PCIP in terms of present worth cost. For instance, if the MTO were to indicate that the safety benefits of PCIP are worth approximately \$500,000 in present worth, then the tipping point would occur when the PCIP initial construction cost was approximately \$1 M, which is a reduction of only 27% of the construction costs.

Some reduction in the construction cost is expected. As previously noted, the MTO has had experience with precast concrete highway trials where the cost of the trial was on the order of 250% of the actual cost realized for a full-scale implementation. The scale of this reduction must be on the order previously noted for the trial to be considered economically feasible, or some further justification of the PCIP value must be made.

#### **7.4 Initial Cost Reduction Estimate**

As discussed in Chapter 5.6.3, the MTO estimates that a reduction in initial cost on the order of 2.5 times is typical between trial sections and full-scale implementations for precast concrete pavements. This is only a rough estimate, but its potential effect was analyzed using the LCCA model developed for this research.

Table 7.4 summarizes the analysis of the effects of a reduction in the initial construction costs. The initial construction cost based on the trial project’s costs and pro-rated to a one km section was

found to be approximately \$1.92 M. This cost was developed based on the \$8000 unit cost for panels. When this cost is considered, the 50-year PWC difference between the two strategies being compared ranges between approximately \$1.1 M and \$1.6 M depending on the frequency of the M/O rehabilitation, with PCIP being consistently more expensive.

**Table 7.4: Initial Cost Reduction Effects**

			Difference in 50-year PWC (PCIP - M/O)		
	Initial Construction Costs	50-year Present Worth Cost	3-yr M/O Frequency	5-yr M/O Frequency	7-yr M/O Frequency
PCIP Trial Costs	\$ 1,920,418	\$ 2,244,589	\$ 1,092,294	\$ 1,392,350	\$ 1,606,096
PCIP Reduced Costs	\$ 768,167	\$ 1,092,339	-\$ 59,956	\$ 240,100	\$ 453,846

If the initial construction cost was reduced by a factor of 2.5, this would correspond to a cost of approximately \$770,000. When this cost is considered, the 50-year PWC cost difference ranges between approximately -\$60,000 and \$450,000. Therefore, if cost reductions on this scale can be realized, M/O operations required every three years could make the PCIP the more cost-effective option.

A part of this cost reduction has already been accounted for with the panel unit costs provided by the manufacturer. For large-scale orders of panels, the lower unit costs result in an initial construction cost that is approximately 1.6 times lower than the trial construction initial cost.

## 7.5 Life Cycle Cost Analysis Conclusions

Through the use of a life cycle cost analysis (LCCA), it was found that the PCIP strategy of 400-series highway rehabilitation has a higher present worth cost, based on this analysis. The difference in present worth cost based on the deterministic analysis indicated that the PCIP strategy cost approximately \$870,000 more than the M/O strategy.

A sensitivity analysis was undertaken to assess the reasonableness of the assumptions made regarding inputs in the LCCA. The analysis considered five of the inputs that were considered to be largely unknown or subjective. These included the nominal social discount rate, the average daily user costs associated with construction activities, the unit price of the precast panels, the required frequency of the M/O rehabilitation, and the placement rate of the panels on site. The

effect of changing these inputs was measured in the difference in present worth cost between the two rehabilitation strategies. In descending order of impact, with the sensitivity index in brackets:

1. Unit price of the panels (+0.62)
2. Frequency of the M/O operation (+0.47)
3. Panel placement rate (-0.41)
4. Nominal social discount rate (+0.22)
5. Average daily user cost (-0.02)

Based on these results, the average daily user cost was neglected for the factorial analysis, which indicated that, within the ranges set for the sensitivity analysis, the PCIP strategy was consistently more expensive. The difference in present worth cost was found to range from \$1.95 M to about \$13,000. This indicates that under some conditions the strategies were approximately similar, but more than 80% of the time the difference was larger than \$500,000.

It was found that for the two strategies to be approximately equal in terms of life cycle cost, the initial construction cost of the PCIP strategy would have to be reduced by approximately 62% from the value used in this analysis. The sensitivity analysis indicated that the life cycle cost of the PCIP strategy is very sensitive to change in the unit price of the panels, and this would be the primary area where these cost savings could be made.

The MTO has expressed that in some situations the PCIP might be considered despite its higher costs. If the external factors driving this decision could be given a monetary value, the required reduction in construction costs could also be readdressed to determine the tipping point considering this value.

## **CHAPTER 8:**

### **CONCLUSIONS AND RECOMMENDATIONS**

The conclusions and recommendations presented in this chapter are summarized by thickness design, construction, visual assessment, instrumentation, joint performance, surface evaluation, lifecycle cost, and overall feasibility.

#### **8.1 Thickness Design**

Using the panel thickness suggested by the Fort Miller Company and material characteristic assumptions outlined in Section 4.3.2, the expected fatigue life for the PCIPs range from  $1.55 \times 10^7$  to  $6.98 \times 10^{11}$  loads of 40 kN magnitude applied directly to the edge of the panels. A 40 kN axle load located on the pavement edge corresponds to an equivalent single axle. Over the course of 25 years in service, the panels are expected to be subjected to  $1 \times 10^8$  ESALs, indicating that there is some potential for premature panel fatigue failure. However, this should be considered with the following caveats:

- ESALs are a comparison tool that equate the loss of pavement serviceability to that of a given number of 80 kN axle loads. The tire loads associated with actual vehicles are generally lower than 40 kN, through the use of tandem and tridem axles and dual tires.
- The fatigue life of a pavement under lower applied loads increases exponentially.
- The majority of traffic runs in the wheel path of a pavement, as opposed to the edges, and the bottom of panel stress is significantly lower as the applied load moves away from edge.

Even with these considerations, the strengths of all but one batch of concrete had measured strength high enough to meet the design number of ESALs as single axle loads located on the edge of the pavement. Furthermore, the panels design included the presence of significant reinforcing steel in layers near the top and bottom of the panel, which would arrest the propagation of fatigue cracks once formed.

It is suggested that the design 28 day strength of the concrete be increased to 45 MPa. This is not an unreasonable target strength for precast members and would improve fatigue performance. This may become more critical if the joints are found to deteriorate, resulting in more frequent edge loading as vehicles cross deteriorated joints.

## 8.2 Construction Conclusions

During and immediately following construction, the process of constructing the PCIP rehabilitation strategy was analysed. The following conclusions were made regarding the construction of the PCIP strategy:

- Saw-cuts were not found to be necessary from the perspective of providing an adequate vertical face for the milled asphalt. The milling did produce a slightly rougher face than saw-cutting, though this may improve the adhesion between the HMA and the joint material. The saw-cuts also serve as a visual guide for the milling and facilitate the removal of HMA in areas where milling cannot reach, such as corners. If an improved means of milling control and asphalt removal are provided, then saw-cutting could be avoided, but otherwise provide some benefit to the HMA removal process.
- The grade control of the milling operation presents the biggest challenge remaining for the application of this technology. Challenges include inputting the existing and final surface characteristics into the milling machine as well as checking the milled surface for conformance.
- Future applications of PCIP should explicitly specify the use of milling equipment that can be laser guided off of a previously developed 3-D surface model or guided off of a reliable reference (such as a levelled rail) to produce a planar surface at a constant cross slope. The use of skis running on the surface of the shoulder or adjacent lane as a reference point cannot produce a consistent cross slope.
- The milling accuracy on site indicated that the HSS tubes were unnecessary and could likely be removed from the design in future iterations. A narrower gap could be milled to place grout along the longitudinal edges of the panels without reinforcement, and allowing the edges to be opened to traffic prior to grouting.
- The use of a specialized protection measure for the HMA edge beside the milled area should be used if the width of the longitudinal edge gaps are reduced substantially.
- The temporary panel used at the end of each night's work should be removed prior to the beginning of milling. This will ensure there is only one area that requires manual HMA removal and will result in a more consistent milled surface.

- Bedding grout was used at the following estimated rates: Asphalt-supported: 12 bags/panel, Grout-supported: 14 bags/panel, Grade-supported: 4 bags/panel.
- Future large-scale applications must consider that grout-supported panels require at least an hour of grout curing time before they can be opened to traffic loads. This is a significant staging consideration.
- In future applications, a “sacrificial layer” could be designed to account for diamond grinding both initially and throughout the pavement’s life. This would allow for adequate reinforcement cover to be maintained throughout the pavement’s service life. It is reasonable to expect 3±1 rounds of diamond grinding throughout a concrete pavement’s life cycle and this would be 4±1 if an initial diamond grind is required to smooth joint transitions.
- From the MTO’s perspective, the current ranking of the three support conditions is 1) Asphalt-Supported, 2) Grout-Supported, and 3) Grade-Supported.
- A hybrid of the AS and GroS conditions was the preference voiced by members of the contractor involved in construction.
- In general, the GroS panel was found to be most constructable, based on the criteria used in the AHP analysis, with AS ranking second. Under some conditions explored as part of the sensitivity analysis, it was found that the AS panels could be considered more ideal than the GroS panels, though this was generally not the case.

### **8.3 Visual Assessment**

Following one year in service, the PCIP trial was investigated during an overnight closure. This investigation included a visual assessment of the panels on site. The following conclusions were drawn from the visual assessment:

- The rehabilitation was found to generally be in excellent condition.
- The edge grout placed in the longitudinal joints and the terminal transverse joints was found to be ravelling throughout the site. This is likely due to the combined effects of the material production and placement and traffic. Some degree of ravelling of this material was observed in the longitudinal joints of 20 of the 22 panels in the trial.
- In addition to this ravelling, a gap between the edge grout and the adjacent was HMA was also observed throughout the trial.

- The sealant in all transverse joints was found to be in good condition, though incompressible materials (aggregate) were observed in several of the joints. The source of these materials is likely the raveling edge grout.
- Two panels were found to be cracked. This is thought to be due to improper milling on the first location of the trial, which required additional milling. The cracks were found to be held closed tightly by the reinforcement, with load transfer efficiencies of approximately 90%.

#### **8.4 Instrumentation**

During the construction of the trial section, six clusters of instrumentation were installed. Each cluster consisted of two earth pressure cells (EPCs) and one moisture sensor. The sensors have been monitored since October 3, 2016, and this process is on-going.

- As temperatures dropped at the end of the initial October of PCIP service, a change occurred that resulted in increased moisture infiltration rates beneath the panels. Beyond this point, significant amounts of moisture were observed beneath the panels for most of the winter season.
- During non-winter periods, sub-panel moisture contents have consistently dropped to relatively low levels following the increases associated with precipitation events. This indicates that moisture is exiting the area beneath the PCIPs effectively, despite the impermeable nature of the asphalt support layer.
- The presence of moisture beneath the panels indicates that the bond between edge grouts and existing asphalt is allowing for the passage of water. A flexible sealant material should be considered at all joints and edges of the PCIP design.
- 51 freeze-thaw cycles were observed in the air temperature on site, while only 15 cycles were measured beneath the PCIP during the first year of service. In the second year (October 7<sup>th</sup>, 2017 to present), 67 air and 44 sub-panel freeze-thaw cycles were measured. Considering that moisture was found to be present beneath the panels, freeze-thaw resistant grouts and bedding materials are a necessary design feature of PCIP rehabilitation design.
- The results do not differentiate any of the support conditions considered in terms of early-age performance. Each support condition provides similar moisture-penetration susceptibility, and relative joint vs mid-panel pressures.

## 8.5 Joint Performance

The PCIP trial section had three sections that each incorporated a different method of providing sub-panel support to the PCIPs: Asphalt-supported (AS), Grade-supported (GraS), and Grout-supported (GroS). Part of the evaluation of the trial section involved the testing of the joints between adjacent panels through the use of falling weight deflectometer (FWD) testing. FWD testing is typically used as method to obtain load transfer efficiency ( $LTE_{\delta}$ ) values for each joint, where  $\geq 70\%$  load transfer is considered acceptable joint performance. FWD testing was performed two weeks after the completion of the trial construction and again after one year of service.

Since the load transfer devices of each PCIP support method were the same, differences between each section of the trial were attributed to the support conditions beneath the joints. Joints between the PCIP and the adjacent asphalt pavement as well as transition joints between the different support conditions were left out of the statistical comparisons of support conditions.

- The  $LTE_{\delta}$  and  $RD_{75}$  for the terminal joints between the PCIP and the HMA were found to be considerably lower than the inter-panel joints at both testing ages. A better means of providing connection between the vertical faces of each element is required.
- Following construction, all of the inter-panel joints achieved the minimum acceptable threshold of 70%  $LTE_{\delta}$ , with little variation of results. The GroS condition was found to have a statistically higher  $LTE_{\delta}$  than the other support conditions.
- Following one year of service, some joints in each section were found to be below the acceptable threshold, with much higher variation in results. Overall, the average  $LTE_{\delta}$  was found to increase, counterintuitively.
- The intercept values were found to be low in all cases after construction, indicating that each joint was firmly supported. Following one year of service, the  $D_0$  values increased in all cases, indicating some deterioration of the support beneath the joint. This deterioration is not surprising under traffic loads and may represent “settling” more than significant, on-going deterioration. This result clashes with the  $LTE_{\delta}$  values that were seen to increase.
- $RD_{75}$  indicated that the GroS condition provided the best load transfer following construction. The  $RD_{75}$  increased for all support conditions after one year of service, but the highest increase was observed for the GroS.

- Both GraS and GroS showed consistent increases in  $RD_{75}$ , which could indicate some deterioration of their support layers. The AS condition was seen to have either low or high  $RD_{75}$  with few intermediate values. This may indicate inconsistent milling practice, which could have left voids beneath joints that were initially filled with lean grout. This material may deteriorate quickly compared to other joints that are fully supported by the asphalt support layer.
- Based on this analysis, it is suggested that a measure of relative displacement, such as  $RD_{75}$ , be considered when measuring joint performance. The value provides more context for the performance of a joint than  $LTE_8$  on its own.
- The joints of the trial section were generally found to be performing well after a year in service. While the GroS support seems to provide better joint performance initially, this does not appear to translate into better performance long-term.
- A more consistent method of milling the asphalt surface in the AS condition could result in this support condition providing the best long-term joint performance of the three conditions, based on the results of the  $RD_{75}$  test.

## 8.6 Panel Surface Evaluation

The pavement surface of the PCIP trial section was analyzed with respect to texture, roughness, and friction. Largely, the testing took place during over night lane closures, however some was performed during regular traffic conditions.

Based on the analysis, the following conclusions were made:

### Surface Texture:

- The SMTD, which is correlated with mean profile depth and the  $S_P$  gradient of friction, was found to decrease in the wheel path relative to the centre of the panel, indicating a deterioration in friction
- The tined pavement surface resulted in consistently negative skewness indices, which are associated with lower pavement noise in comparison to positive skewness indices
- The NPSE, an indicator of pavement microtexture, was found to be lower in the wheel path than in the panel centre, indicating that the friction at low speeds and in dry conditions,

when microtexture governs friction, may have decreased under one year of traffic-related abrasion

#### Roughness:

- The Surpro-measured roughness was found to be lowest in the Grout-supported condition, followed by the Grade-supported then the Asphalt-supported conditions. This corresponds to the decreasing level of control that the panel installer has over the final panel elevation, which results in a smoother transition between panels, and lower roughness.
- The trend of the ARAN-measured roughness throughout the section generally corresponded to the findings of the Surpro
- In both cases, the roughness of the PCIP trial was found to be higher than the maximum acceptable threshold for new pavement used by the MTO of 1.25 m/km, while the adjacent HMA surface was found to generally be below this threshold

#### Friction:

- There is considerable variation between the different methods of analyzing friction, which reinforces that friction analysis results are largely influenced by the method used to gather them
- The friction related to the right wheel path was consistently less than that of the centre of the panel, with the relative difference between the two ranging from 8% to 25% difference
- There has been some friction loss associated with traffic over the year of service
- The friction was initially found to be acceptable above the FN 30 threshold specified by the MTO

Following construction, it may be necessary to undertake diamond grinding of the PCIP surface to address differential elevations between adjacent panels. This process will reduce the roughness of the section by producing a continuous profile along the section, and may have the additional benefit of allowing for the implementation of a next-generation concrete surface, which is a diamond grinding configuration that has been found to have good surface characteristics relating to noise and friction. The diamond grinding may require that the riding surface of the panels be constructed

with extra concrete cover to allow for repeated grinding efforts without encroaching on the panel's reinforcement.

## **8.7 Life Cycle Cost Analysis**

Through the use of a life cycle cost analysis (LCCA), it was found that the PCIP strategy of 400-series highway rehabilitation has a higher present worth cost than frequent mill and overlay operations. The difference in present worth cost based on the deterministic analysis indicated that the PCIP strategy cost approximately \$870,000 more than the M/O strategy.

A sensitivity analysis was undertaken to assess the reasonableness of the assumptions made regarding inputs in the LCCA. In descending order of impact, with the sensitivity index in brackets:

1. Unit price of the panels (+0.62)
2. Frequency of the M/O operation (+0.47)
3. Panel placement rate (-0.41)
4. Nominal social discount rate (+0.22)
5. Average daily user cost (-0.02)

A factorial analysis of the different variables analyzed in the sensitivity found that the present worth cost difference between the two rehabilitation options ranged from \$1.95 M to about \$13,000. This indicates that under some conditions the strategies were approximately similar, but more than 80% of the time the difference was larger than \$500,000.

For the two strategies to be approximately equal in terms of life cycle cost, the initial construction cost of the PCIP strategy would have to be reduced by approximately 62% from the value used in this analysis.

The MTO has expressed that in some situations the PCIP might be considered despite its higher costs. The PCIP strategy is assumed to reduce the number of construction operations on a busy highway and provide the potential to use less virgin material over the course of the structure's life cycle. If the external factors driving this decision could be given a monetary value, the required reduction in construction costs could also be readdressed to determine the tipping point considering this value.

## 8.8 Overall Feasibility

The PCIP rehabilitation option was found to be a feasible method to rehabilitate high-volume highways that exhibit deep-seated rutting distress. The three support conditions that were investigated were all installed successfully in the trial section, and have performed well to date.

Based on both constructability, early joint performance, and surface roughness, the Grout-supported PCIP design was found to be the most ideal of the three designs constructed. Improvements to milling practices could improve the Asphalt-supported design to a point where a hybrid of the two designs, including levelling feet for areas of insufficient support, would be the most ideal design. This would remove the GroS necessity for same-night grouting, which may be found to be a larger factor affecting installation rate on full-scale PCIP installations.

In terms of Life Cycle Cost, the PCIP rehabilitation strategy was found to generally have a higher present worth cost than frequent mill and overlay procedures. The determining factor of this finding was the high initial cost of PCIP construction. Largely, the PCIP cost used in this analysis was based on the trial installation, which typically produces an inflated cost estimate. Future applications of this rehabilitation technique will provide further information regarding the cost of a full-scale implementation.

Even considering the higher cost, the safety aspects of limiting the number of construction operations on a 400-series highway could justify its use. Milling operations every 3 to 7 years expose the users of these highways to more dangerous conditions more frequently than is necessary.

While the PCIP rehabilitation as constructed is performing well, several improvements to the design are suggested based on the construction and performance of the trial. These improvements are outlined in the following section.

## **CHAPTER 9:**

### **IMPROVEMENTS AND SELECTION PROCEDURE FOR PCIP PROJECTS**

This chapter presents improvements that are suggested for future applications of PCIP technology and a selection procedure to be followed by an agency considering its use. These are based on the findings of the study, which were summarized in the previous chapter.

#### **9.1 Proposed Changes to the Initial PCIP Design**

Throughout the course of this research, a number of issues with the design of the PCIP trial were identified. These issues are not critical, but addressing them would improve the overall construction and performance of the PCIP rehabilitation strategy.

This section outlines the issues that were identified and proposes solutions where applicable.

##### **9.1.1 Concrete Strength Specification**

The original concrete strength specification for the material used to construct the precast panels was based on the specification for conventional cast-in-place concrete pavements. This included a compressive strength requirement of 30 MPa at 28 days. As outlined in Section 4.3.2 the actual measured compressive strengths were significantly higher than this requirement, due to the separate requirements of typical precasting procedures. These procedures include 24-hour stripping and lifting of precast members to allow for the construction of subsequent members.

As discussed in Section 4.3.2, the predicted fatigue performance of the PCIP members was very sensitive to changes in compressive strength, due to the stiff base and relatively thin member depths. Based on the assumptions listed in that section, a change in compressive strength from the specified 30 MPa to 45 MPa, results in an approximately 2000-fold increase in the number of 40 kN edge load applications before fatigue failure, from  $4.6 \times 10^4$  load applications to  $8.9 \times 10^7$  load applications. The increase in the minimum allowable compressive strength would have a substantial impact on the minimum expected fatigue performance.

For this reason, it is recommended that the minimum acceptable 28-day strength of the concrete used in the production of the PCIP members is increased to 45 MPa. This standard should not be difficult to achieve in practice but will provide some improvements to theoretical fatigue

performance. It should be noted that with a 30 MPa specified strength on the trial project, only one batch was found to have a 28-day strength below the 45 MPa threshold (41.7 MPa).

### **9.1.2 Advanced Milling Control**

The PCIP trial section included milling performed by a Wirtgen Model W120 CFI, with a 1.2 m-wide milling head. Each section was milled to a set depth and cross-slope based on the survey data collected prior to the beginning of construction. The milling depth was referenced off of the adjacent unmilled HMA surface. Following milling, the resulting surface was checked using manual techniques from the adjacent, unmilled HMA in the shoulder and adjacent lane. Therefore, both the milling and the following check are made from a fluctuating reference point. This can result in milled surfaces that exhibit similar distortions to the surface of the pavement.

Each of the three support condition types evaluated within this research had the potential to be affected by poor vertical milling control. The AS panels are placed directly on the milled surface and therefore require high precision in the milled surface. As discussed in Section 6.1.5, imprecise milling practices are thought to have resulted in two AS panels (#1 and #2) cracking under traffic loading. The GraS panels incorporate a layer of gradable bedding material to provide construction resiliency to poor milling, however on the trial it was noted that the milling was not done to a depth that allowed for the bedding material to be effective. Essentially, high areas on the milled surface were not covered with the bedding material. The GroS panels are adjusted above the milled surface, so provided the milling is deep enough, the PCIP surface should not be affected by inconsistencies with milling. The amount of structural bedding grout beneath the panels is highly dependent on the accuracy of the milling. Significant undulations in the milled surface or over-milled depth requires more grout material to fill the void beneath the panel following levelling. In this way, the milling accuracy even in the GroS condition can have a substantial effect on the material costs of the rehabilitation strategy.

The horizontal alignment of the milling was also controlled manually on site. Specifically, the milling machine operator visually referenced the saw-cuts that laid out the milling extents and adjusted the milling head accordingly. For most of the trial, this worked reasonably well, and the vertical cut HMA face was maintained. However, sections of the GraS portion of the trial saw horizontal over-milling by approximately 40 mm, as discussed in Section 5.3.

Both of these findings indicate a need for improved milling control. Several systems exist that use Global Navigation System Satellites (GNSS) technology in concert with surveys and engineered plans to provide precision locations for various aspects of civil engineering. The GNSS data, which is prone to variability caused by satellite geometry, atmospheric conditions, and more, can be corrected using a base station at a precisely known location to refine the GNSS data to provide accuracy of approximately 3 mm. This base station can often include a robotic total station. Given the information provided by these systems, the machines performing the milling can have automatic milling head control or alternately provide real-time feedback to the operator.

It is suggested that milling control be improved using this type of control system or similar on these projects. Particularly when AS support conditions are chosen for the given PCIP application.

### **9.1.3 Edge Protection**

One issue noted on the PCIP trial was the deterioration of edge grout that was exposed to traffic, as discussed in Section 6.1. Improvements to the edge grout material, mixing and placement practices could potentially improve this performance, however reducing the amount of exposed edge material is the best way to minimize its effects. The longitudinal gap between the PCIP and the existing HMA was 75 mm wide and was left primarily to avoid damaging the corner of the HMA left between the vertical milled face and the pavement surface. When lowering a panel using a crane on site, wind and cable twisting can result in unexpected panel movements. Providing this gap provided insurance against one of these unexpected movements causing the heavy suspended panel to be lowered onto the HMA, resulting in gouged pavement.

In order to minimize the longitudinal gap, a different means of providing edge protection is required. The detail shown in Figure 9.1 and Figure 9.2 illustrates the proposed method of providing this protection. The detail includes a 5 m long modified structural steel angle, L 76x51x6.4 made of CSA G40.21 350 W grade steel. The angle supports a guide plate of the same length that is inclined at a 45° angle and supported by triangular supports. The triangular supports also serve as stiffeners to the plate and are spaced at 500 mm on centre. All pieces are connected through welding. The sharp corner of the angle and the welding are grinded to a rounded shape, as shown. A 5 mm thick neoprene strip is connected the bottom of the angle on the face where the apparatus sits on the HMA surface to provide a uniform support beneath the angle.

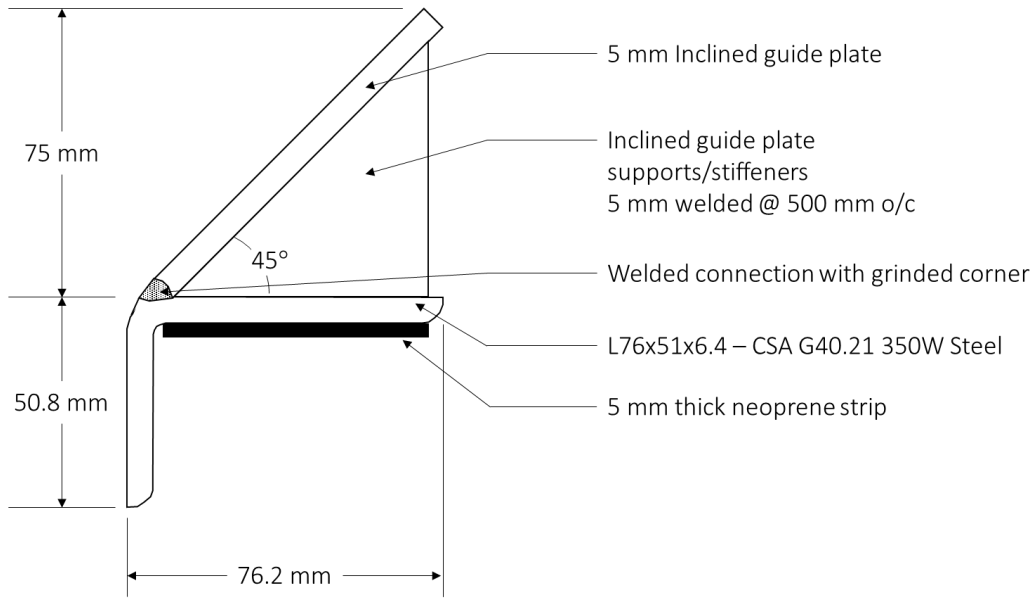


**Figure 9.1: Cross-section of HMA corner protection detail**

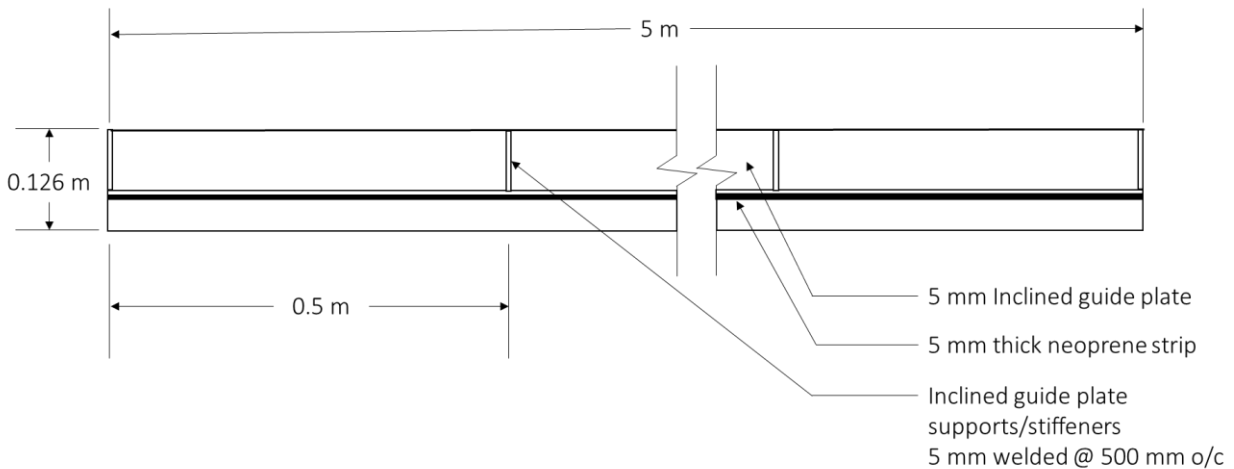


**Figure 9.2: Plan view of HMA corner protection detail**

The apparatus is designed to be placed on the HMA corners on either side of the milled recess prior to placing the panel. The inclined guide plate provides approximately the same 75 mm of protection as the longitudinal gap, but if the panel shifts, it serves to funnel it back into the right position. The stiffness of the apparatus ensures that any loads applied by the suspended panels will be transmitted across a substantial length of the HMA corner.

The stiff apparatus also allows for steel pry bars to be used by the placement crew to adjust the panel before it is resting on the milled HMA surface. Typically these bars could not be used because they would result in damage to the HMA, which would be used to brace the bars.

The longitudinal edge gap that is required when using this apparatus is only slightly larger than the width of the angle's flange, which is 6.4 mm wide, to allow the apparatus to be relocated to the next location; a 1 cm gap should provide sufficient space for panel placement. This gap width would also be small enough that filling the gap could be delayed until the following night without further protection measures, such as the HSS edge detail used for the trial.

Based on the unit weights of the constituent materials, each apparatus would weight approximately 56 kg. Therefore, it would require two labourers to move it between subsequent panel placements. The design could be modified to include handles at either end to better facilitate lifting.

The overall length of the apparatus could be changed to suit the panel lengths on a given project. The apparatus length should be longer than the panel length to avoid concentrated loads on the HMA. The corners of the panels being placed are the most likely areas of the panel to come into contact with the apparatus, and if a corner rests directly on the end of the apparatus, it will not distribute the load across very much of the HMA surface.

For the benefits of this detail to be realized, the accuracy of milling must be sufficient to maintain a consistent edge. This would be greatly helped by the improvements outlined in Section 9.1.1.

#### **9.1.4 Full Depth Mastic**

Generally, the use of cementitious grout at the vertical interfaces between HMA and the precast panels was found to be ineffective. These interfaces are found along both longitudinal edge joints and at the terminal transverse end joints. While bonding between the grout and HMA may have occurred upon initial placement, these bonds were found to have broken within one year of service, as discussed in Section 6.1. The bond and resulting load transfer characteristics were low at the initial load transfer testing, and got considerably worse after one year of service, as discussed in Section 6.3. This is probably due to the substantially different material properties between the precast concrete, HMA, and grout.

In the context of the PCIP trial, this results in two main issues. The first is that the gap at the terminal transverse edge is widening as the HMA has no tensile capacity at the vertical face. The second is that the gaps present a means by that water from the pavement surface can infiltrate beneath the panels.

When a tire travels from the PCIP to the adjacent HMA, it induces a field of stresses in the HMA structure. This stress field varies throughout the depth and width of the pavement, with different areas experiencing compressive or tensile stresses. A simplified illustration of the horizontal stresses and resulting deformation in the longitudinal direction (parallel to the direction of travel) is shown in Figure 9.3. The distortions in the pavement surface are exaggerated for illustration purposes. Part a) shows select stress conditions on a typical HMA surface, including compression beneath the applied load, and tension before and after the load and at the bottom of the section directly beneath the applied load. Parts b) through d) show similar distributions when a vertical discontinuity is introduced in the pavement, in the form of the HMA/PCIP transverse joint.

As shown, the interface between the HMA and the PCIP will be subjected to tensile stresses under the action of a vehicle passing across the joint. The rolling resistance between the tire and the pavement surface also results in a horizontal compression stress at the HMA surface. This is magnified if the vehicle is undergoing a braking action when travelling over this joint.

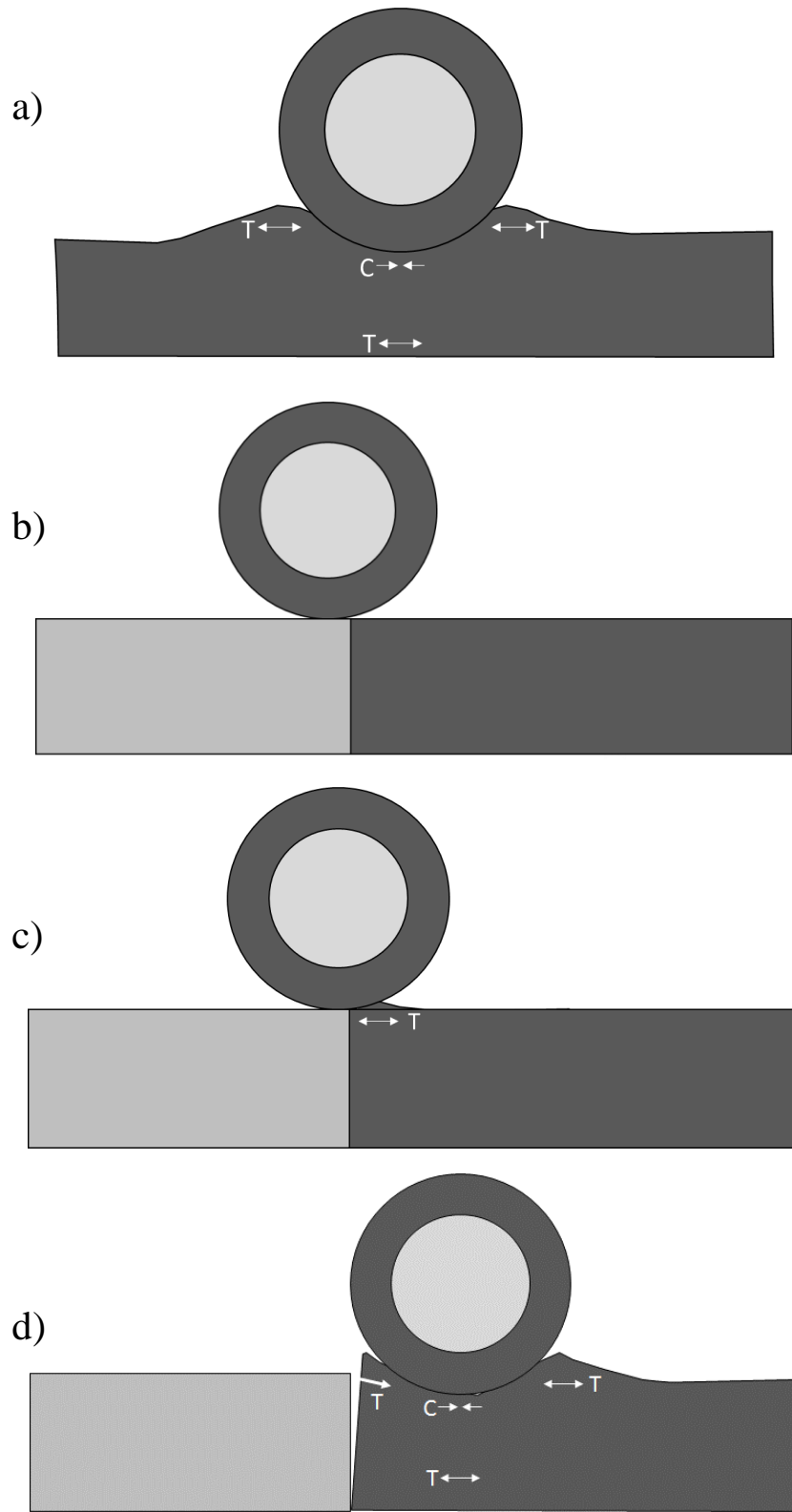


**Figure 9.3: Simplified longitudinal HMA stresses under tire load**

This behavior was reflected somewhat in the load transfer testing. When the HMA surface was loaded using the falling weight deflectometer, very little deflection was observed on the PCIP surface, indicating a lack of bond between the two materials.

Since this interface was found to have debonded after one year of service, the stress condition at this location consists of unbalanced primary stresses resisted by shear stresses. This condition results in increased strain due to the applied stresses. Strains in HMA are made up of viscous, elastic, and plastic components. The plastic component of strain, is non-recoverable and, like the elastic component, is proportional to the stress applied. As the overall strain increases, so does the non-recoverable component (Drescher, Kim, & Newcomb, 1993). Therefore, an interface that provides no tensile capacity results in quicker accumulation of plastic strains.

This is the case at the final transverse joint, which has been found to have accumulated plastic strains, particularly within the wheel paths. This has resulted in a substantial gap between the HMA surface and the edge of the PCIP. This gap provides a means for the ingress of surface water to the area beneath the panels, but could also lead to accelerated HMA deterioration. This could result in ride quality and potentially safety concerns.

The loss of the bond between the grout and the HMA surface along the longitudinal joints has also created a gap in these areas. The widths of these gaps are relatively small, generally measured to be less than 1 mm, but they are found along most of the length of the trial on both longitudinal edges. These gaps also present a path by which surface water can infiltrate beneath the panels to the level of the support conditions.

Water beneath the panels can result in an aggressive environment, particularly as it was found that regular freeze thaw cycles are observed beneath the panels. In addition to the deteriorating effects of frozen pore water in the materials at the PCIP support level, the volume changes associated with freezing water can result in stress concentrations in these areas. These considerations can result in deterioration of the support layer, which in turn could reduce the PCIP service life. This loss of support layer has not been observed in the PCIP trial, however reducing the amount of water that can penetrate beneath the panels is a reasonable preventative strategy.

In future applications, it is suggested that the design of these joints be modified. One potential method of providing bond between PCIP and HMA is through the use of a hot-applied mastic

material. The material is an elastic polymer modified binder that bonds well to both HMA and PCC. Hot-applied mastic is heated in specialized boilers then poured through a funnel to the intended location.

Generally, the material is tested using ASTM D5329-15 (ASTM, 2016), which tests the cohesion and adhesion properties of the material through a tension test. The sample is poured between two concrete blocks that are pulled until failure. Figure 9.4 shows the sample used to undertake this test.

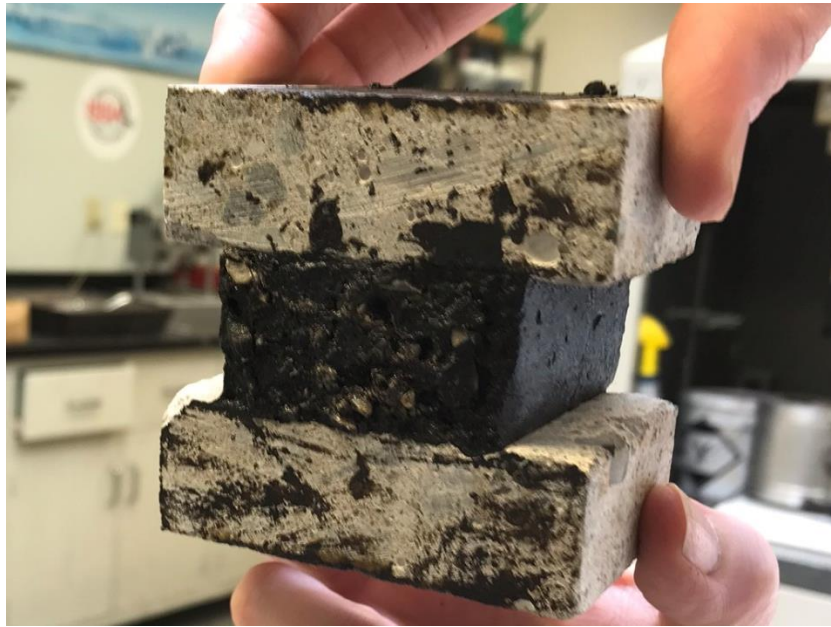


**Figure 9.4:** ASTM D5329 cohesion/adhesion sample (Varamini, 2018)

In the past, the mastic material has been used for bridge joints where an interface between PCC and HMA is necessary. Several proprietary hot-applied mastics are available, and they can generally be proportioned to suit the required application. A 160 to 180 kPa adhesion strength at 25°C is a common specification, though this range can be increased as needed.

The mastic will likely not match the tensile capacity of the adjacent HMA material, however providing any adhesion between the materials will provide benefit, and should maintain the waterproof seal.

The mastic has adhesive properties to both PCC and HMA and it should be applied to the full depth of the joint to maximize this bond. Figure 9.5 illustrates the design of the transverse edge

detail that was constructed as part of the trial section. It included a 12 mm gap between the PCIP and HMA that was filled with edge grout material to 25 mm below the pavement surface. The remaining gap was subsequently filled with a hot poured rubberized sealant. A 3 to 6 mm recess is provided beneath the pavement surface.

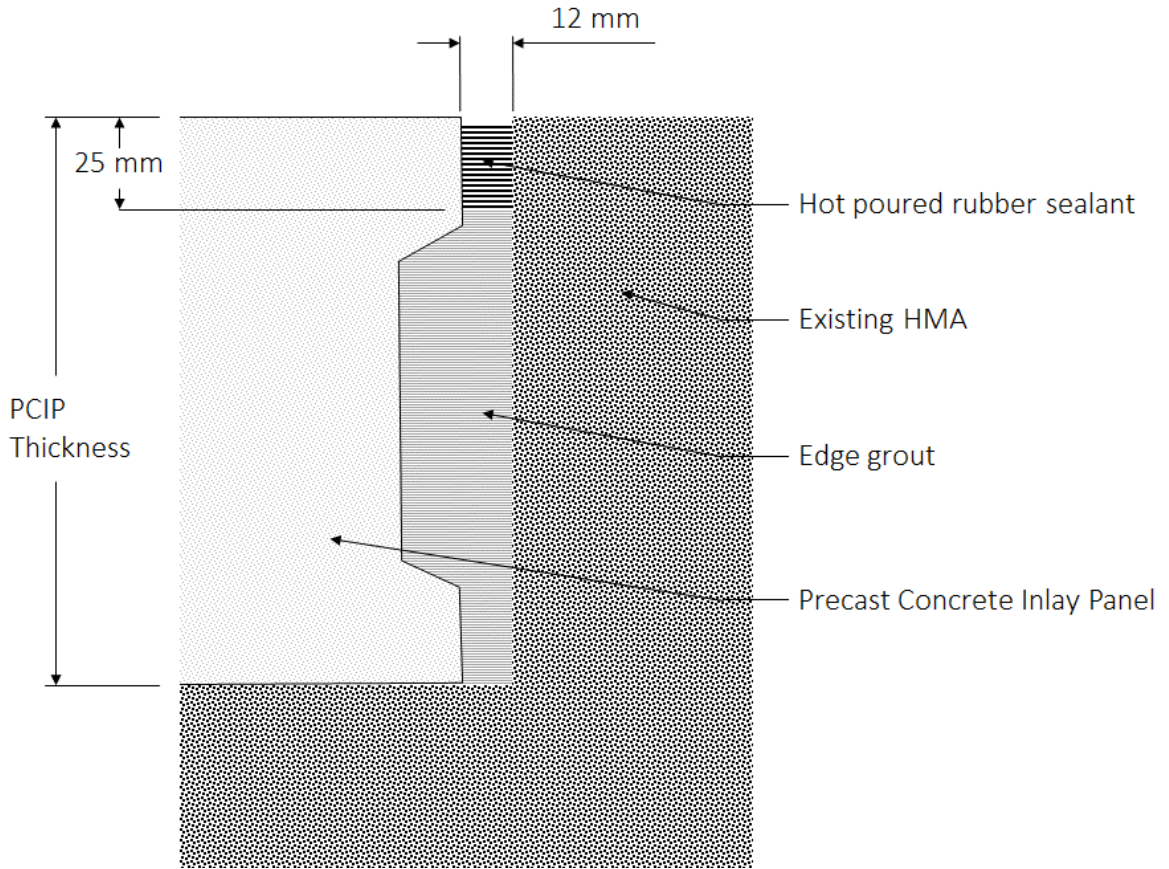


**Figure 9.5: PCIP trial transverse edge design detail**

The proposed transverse edge detail is shown in Figure 9.6. It is similar to the original detail in dimensions, however the full depth of the joint is to be filled with a hot-poured mastic material. A similar recess should be provided at the joint surface, instead of the typical overband application that is sometimes used for mastic crack repairs.

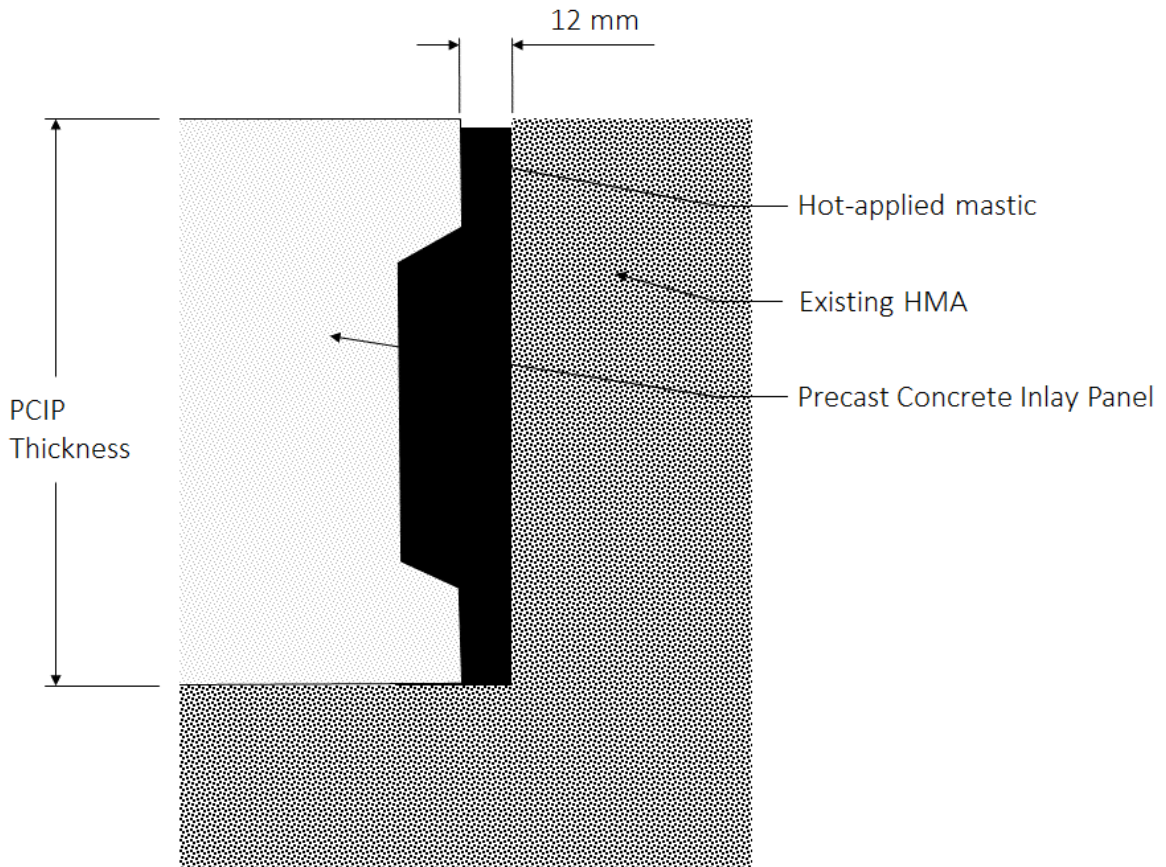


**Figure 9.6: Proposed PCIP transverse edge detail**

The shear key design, which improves the shear capacity of a grouted joint may not be necessary in this detail, though it would provide a greater surface area for the PCC-mastic bond and could be maintained unless it was found to interfere with the placement of the mastic material.

Similarly, the proposed longitudinal joint detail is shown in Figure 9.7. The original detail had a 75 mm wide gap that was filled with reinforced edge grout. The proposed apparatus, discussed in Section 9.1.3, would allow for a gap width of 8 to 10 mm, which could be filled with hot-applied mastic to provide a better seal and interface with the adjacent HMA section.

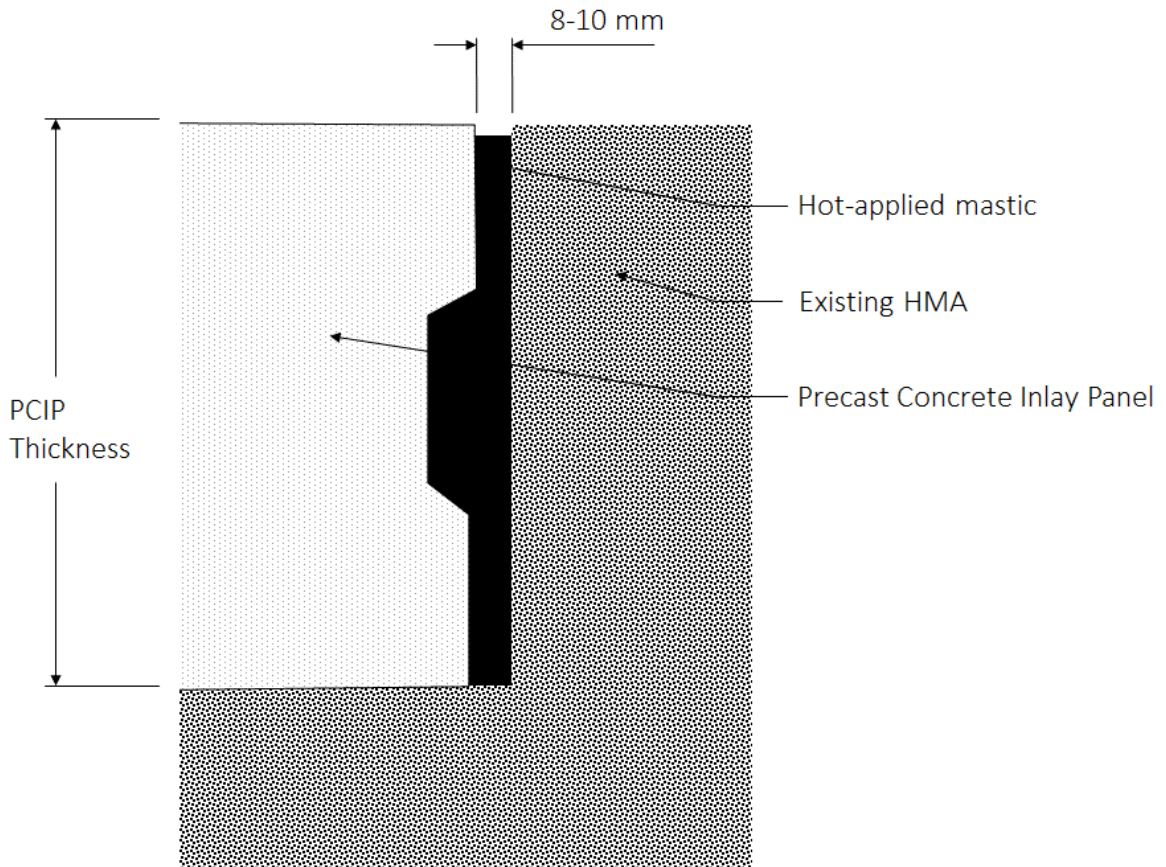


**Figure 9.7: Proposed PCIP longitudinal joint detail**

The production of edge grout, which was a mixture of dowel grout and pea gravel, was found to be somewhat problematic on site. The acceptance of the proposed details would negate the requirement for specialized edge grout as used on the PCIP trial.

The transverse joint design, which included dowel grout and a rubberized sealant was found to perform well in service. The original detail should be maintained in future PCIP applications, including the grout dams that were used to avoid dowel grout flowing into the longitudinal joint.

### 9.1.5 Drainage Details

Despite the expected improvements in the impermeability of the design, based on the proposed edge detailed in Section 9.1.4, the inclusion of a drainage detail beneath the PCIP support layer may be a prudent consideration. Incorporating a drainage detail into a PCIP project is an interesting consideration, since the construction operations only occur during limited-time, overnight closures. The addition of a separate construction operation that must take place in the same location

as the panel placement activities, could result in reducing the productivity of a given construction operation. However, since the presence of pooled water beneath the panels can result in freeze-thaw related deterioration, increased panel curling due to moisture gradients within the concrete (Mohamed & Hansen, 1997), and heaving forces, and because no joint sealing technique is perfect, some mechanism for drainage should be incorporated into the design.

On the PCIP trial section, moisture infiltration was found to occur within two months of construction (Section 6.2). It was also found that the moisture levels would generally drop between precipitation events, despite the lack of a designated drainage detail. It was theorized that drainage was occurring through the trenches that were dug into the pavement shoulders for running cables from the instrumentation to the data logger cabinet beyond the highway's shoulder.

Considering the unintended effectiveness of these details, a similar detail was developed for use on future PCIP applications. Figure 9.8 shows the proposed detail.

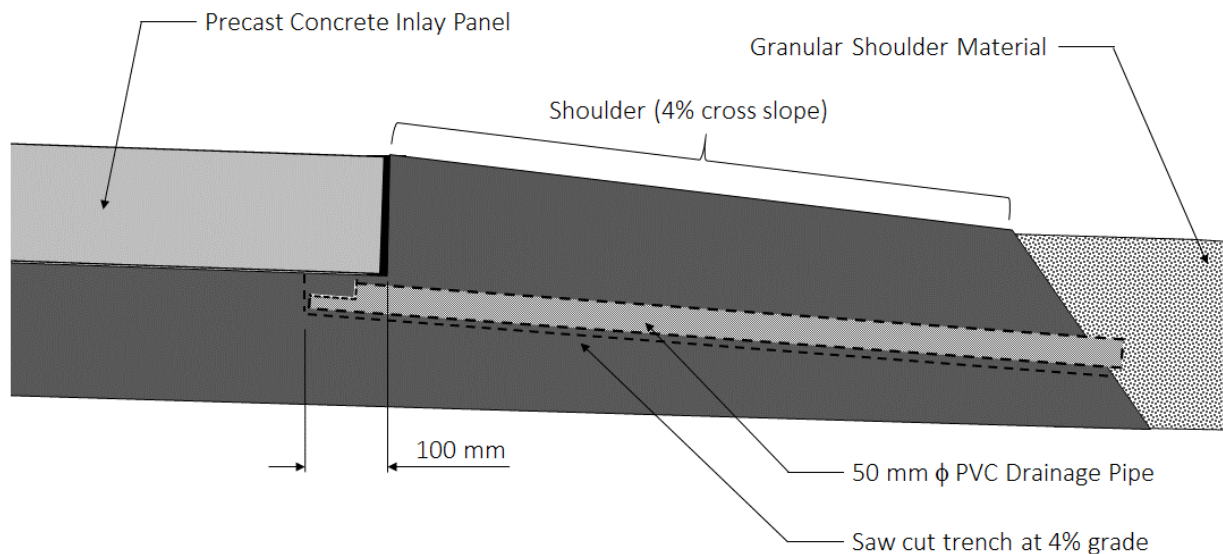


**Figure 9.8: Proposed drainage detail for PCIP rehabilitations**

The detail includes a trench cut into the shoulder with the same slope as the shoulder, using a micro trencher type machine or similar. Generally, the MTO specifies that shoulders have cross slopes of 4%. This is an acceptable slope for a drainage detail, so the trench should be made to the same slope. The trench should extend into the lane a distance of approximately 100 mm. The trenching can be performed prior to construction, but not the portion that extends into the lane.

A PVC pipe, with a diameter of 50 mm will be placed at the bottom of the trench as shown in the figure. The end of the pipe should extend into the granular material beyond the toe of the shoulder. The PVC should have the end detail shown in Figure 9.9. The PVC should be cut in half for a length of approximately 75 mm to facilitate the collection of water from the milled HMA surface. During the placement of panels, and subsequent grouting, the PVC should have a flexible block made of foam or similar located in the cut-out portion. This block will prevent the PVC from being filled with grout during the bedding grout installation. The block should be connected to a cable that extends through the length of the PVC that is capable of pulling the block through the PVC so that following grout hardening, the block can be removed from the shoulder. Following removal of the block, the shoulder end of the PVC should be protected with mesh to discourage animals from accessing and blocking the drain.

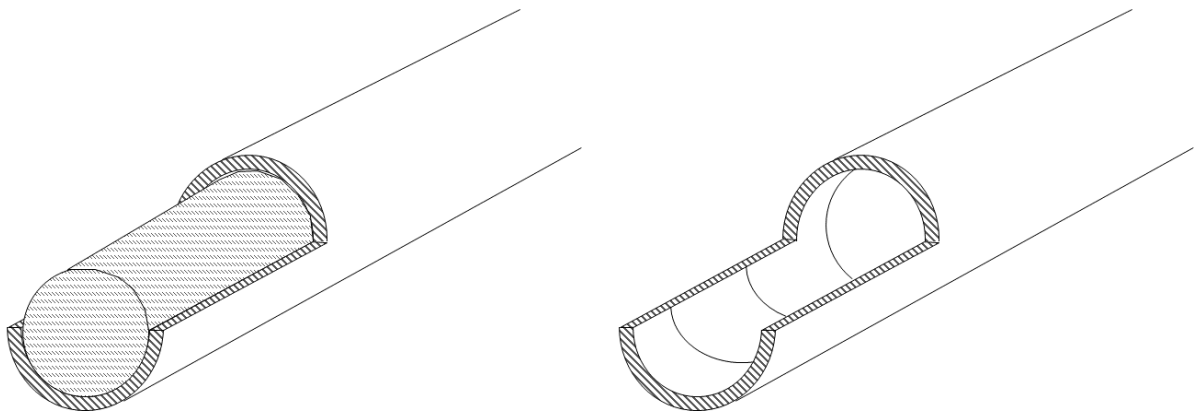


**Figure 9.9: PVC drainage detail end during panel placement (left), following block removal (right)**

The trench through the shoulder should be refilled with HMA patching material following the completion of PCIP placement.

The size and frequency of the drainage detail will be project specific and will depend on the precipitation in the area. The removal of trench material should begin as early in the nightly construction window as possible to avoid interrupting the placement of panels. Following the first pass of the milling machine on the right side of the lane, the portion of the trench beneath the panels should be removed.

### 9.1.6 PCIP Surface Diamond Grinding

Several aspects of the PCIP surface were found to have less than ideal characteristics, including relatively high roughness, grout port overflow, and noise generation. These characteristics could be mitigated by employing a post-installation surface finishing technique, specifically surface grinding.

Surface grinding is a technique used to smooth concrete surfaces by grinding the existing surface to a consistent elevation, using a series of diamond saw blades. The circular saw blades are aligned side by side to form a cylindrical grinding head, similar in shape to the milling heads used on this project. Figure 9.10 shows a typical arrangement of diamond saw blades for surface grinding.

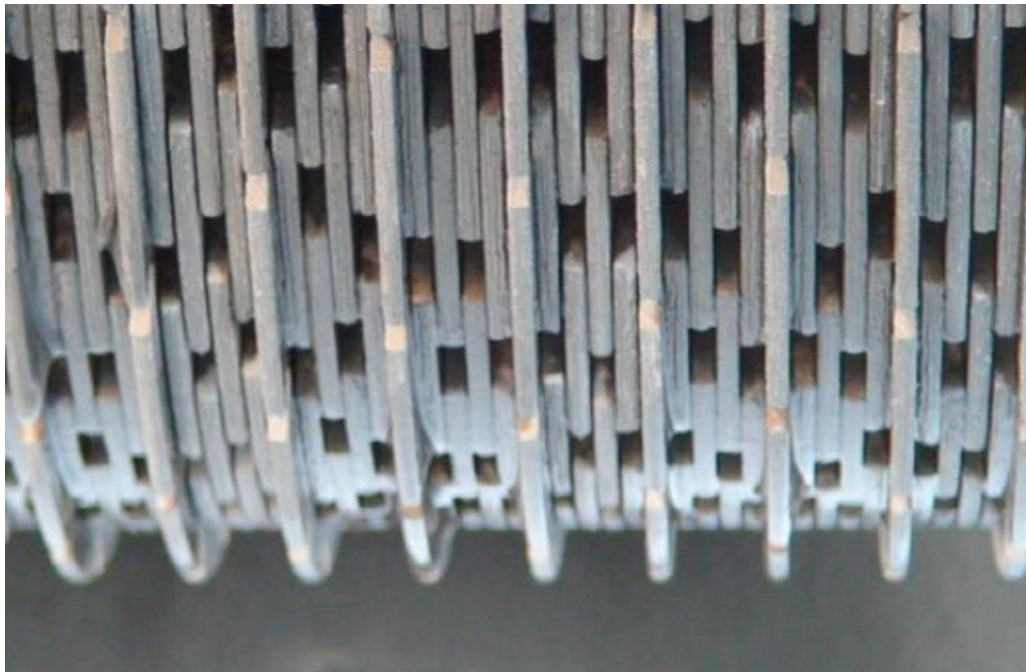


**Figure 9.10: Diamond grinding head for Next Generation Concrete Surface (adapted from (Scofield, 2017))**

Saw blades of different diameters result in a textured surface, with longitudinal grooves where required. One specific arrangement of diamond blades that has gained acceptance in the United States is the Next Generation Concrete Surface (NGCS). THE NGCS was developed at Purdue University to provide a concrete surface with better noise characteristics than typical PCC pavement surfaces. The NGCS, shown in Figure 9.11, is created using a 1.2 m wide milling head composed of 3.2 mm wide diamond blades, with 0.9 mm spaces between adjacent blades.

Grooving blades that produce a 3.2 to 4.8 mm deep groove are spaced at 12.7 to 15.9 mm intervals (Scofield, 2017).



**Figure 9.11: Next Generation Concrete Surface texture (adapted from (Scofield, 2017))**

Since its original conception in 2007, several concrete sections throughout the United States have had NGCS applied. The noise characteristics of the pavements have been found to be consistently better than all other conventional PCC pavement surface finishes, such as burlap dragged, longitudinally tined and grooved, and conventional diamond ground. The friction characteristics have also been found to be acceptable, with all sections constructed in the United States maintaining an SN40 friction number above 40 (Scofield, 2017). The MTO specification requires an SN value greater than 30.

The roughness characteristics outlined in Section 6.4.2, are attributed in part to the effects of vertical elevation differentials at the transverse joints of the PCIP. While construction placement tolerances attempt to minimize the magnitude of these differentials, it is reasonable to expect some difference from panel to panel. The use of diamond grinding after the installation of all panels in a given section would mitigate this issue by providing a consistent elevation. Any surface imperfections, such as the areas of grout overflow where tines were filled with material, would also be address through this method.

The MTO guidelines for life cycle cost analyses (Lane & Kazmierowski, 2005) indicate that a typical jointed plain concrete pavement will require retexturing after 18 years, with a standard deviation of 2.5 years. The life of diamond grinding has been found to last approximately 10 years, with a standard deviation of 1.5 years. This indicates that the expected service life of a diamond ground surface is approximately half as long as the original surface. However, a conventional diamond ground surface uses evenly spaced blades resulting in alternating longitudinal strips of negative texture, where the blades ran, and positive texture, made up of fins and lands, or high and low spots, as shown in Figure 9.12. The fins and lands are produced by concrete material breaking away during grinding, and produces a variable surface. The degradation of the milled surface corresponds to the loss of this positive texture under traffic-related abrasion, and is a function of the concrete mixture, aggregate type, equipment set up, and operator skill. The NGCS, as shown in Figure 9.12, has a more manufactured positive texture between the grooves, produced by closely spaced diamond blades, which is more durable under traffic loading (Scofield, 2017). Therefore, it is reasonable to expect that the 10 year service life of conventional diamond grinding may underestimate the expected service life of NGCS, though the new technology does not have long-term data supporting this conclusion at this time.

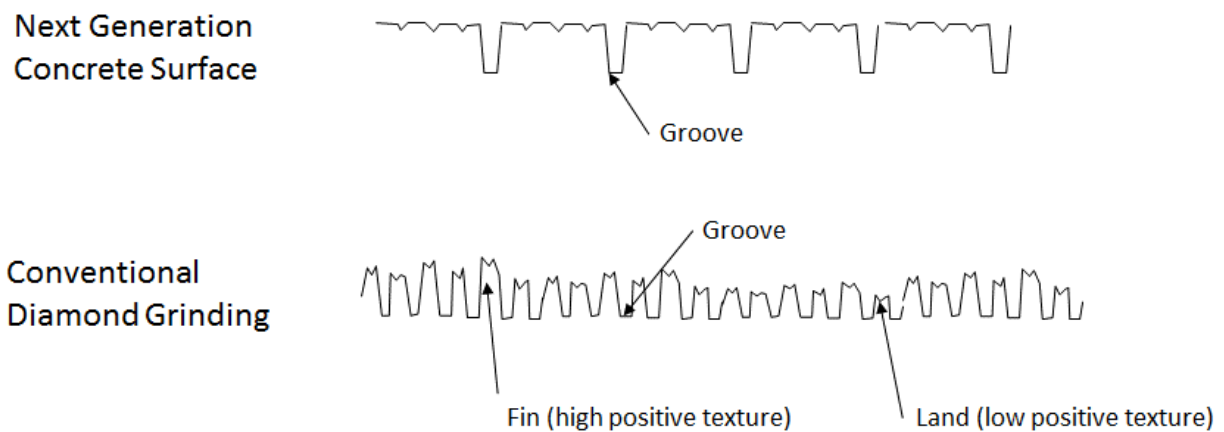


**Figure 9.12: NGCS and conventional diamond grinding surface profiles**

Regardless of the service time of the diamond ground surface, it is expected that several different diamond grindings will be required over the course of the pavement’s service life. Therefore, in

future applications of the PCIP rehabilitation strategy, it is proposed that the concrete cover over the top reinforcement be increased to allow for several consecutive diamond grinding operations.

The original PCIP panel design provided a concrete cover of 60 mm above reinforcement, as a class C1 panel structure, according to CSA A23.3-14 (CSA, 2014). A diamond grinding operation generally removes approximately 5 mm of concrete from the surface of the pavement (Delatte, 2014). Considering this and potentially conservative 10 year service life of a diamond grinding operation, the pavement could expect 5 diamond grinding operations in a 50-year service life, requiring an additional 25 mm of concrete cover to accommodate the milling and still maintain sufficient concrete cover.

It is recommended that the panel thickness be increased by 28 mm, beyond the thickness required for fatigue design in a given application. The 28 mm includes 25 mm for five rounds of grinding, each at a depth of 5 mm, and to account for the 3 mm maximum vertical differential placement tolerance. If the grinding is referenced off of the lower of the two adjacent panels, the 3 mm should provide sufficient depth. The overall increase in panel depth is dependant on the thickness of the existing pavement structure, and whether this extra depth can be accommodated.

The NGCS grinding operation should be specified based on the guide specification, “NGCS Construction on Existing or Newly Constructed Roadways”, provided by the International Grooving and Grinding Association (IGGA, 2014). This document is developed for American agencies, and includes imperial units and price adjustments in USD, which should be changed to units appropriate to a Canadian agency.

## **9.2 Selection Procedure for PCIP**

The selection of the PCIP rehabilitation strategy depends on a number of agency-specific factors, however the selection process in Figure 9.13 provides general considerations for use. The short construction windows, which are largely driven by high traffic volumes, combined with a deep-seated rutting pavement deterioration are the main factors for consideration of the appropriateness of the PCIP strategy.

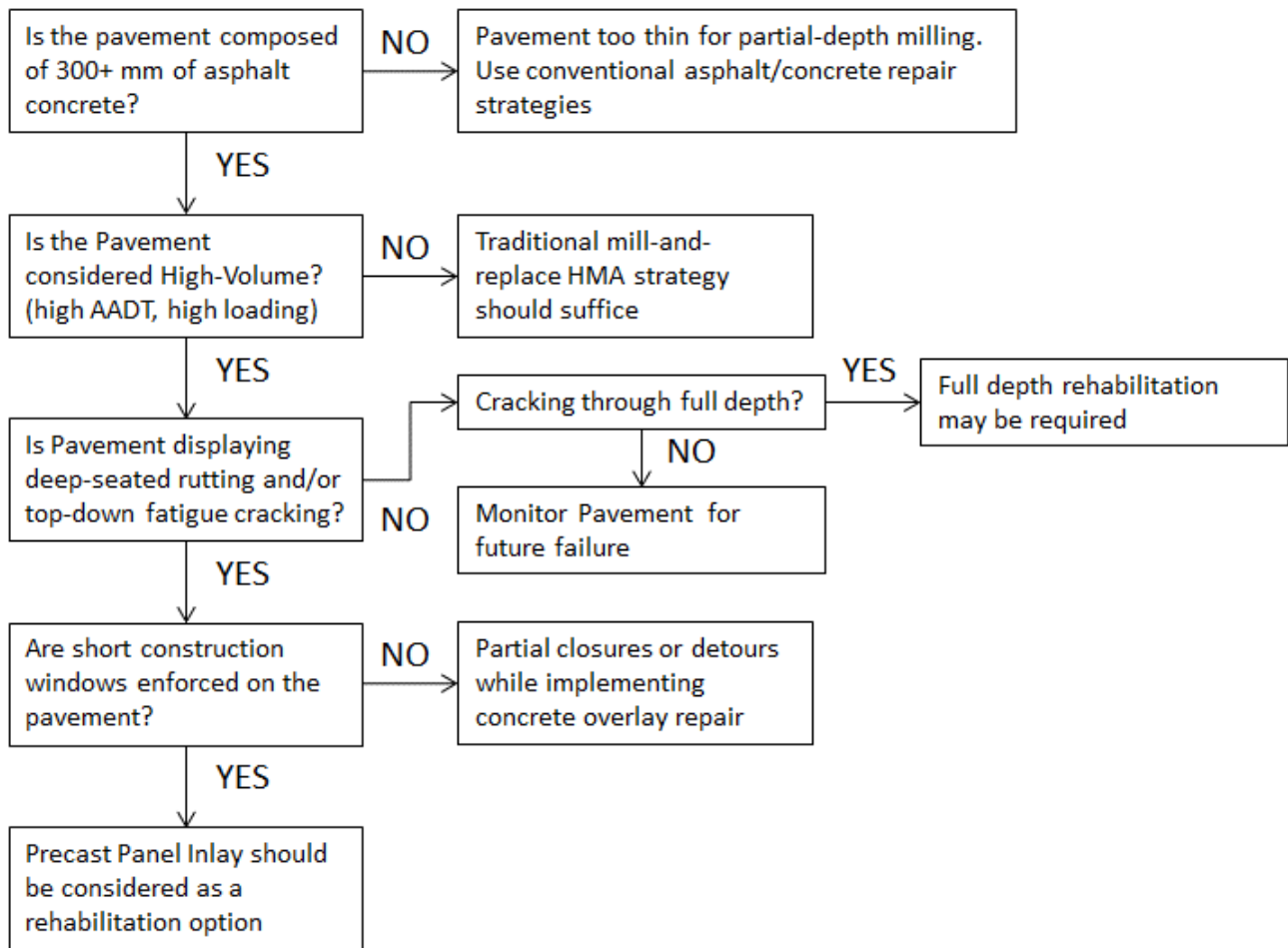


**Figure 9.13: Selection tree for Precast Concrete Inlay Panel use**

## **CHAPTER 10: SPECIFICATIONS FOR FUTURE APPLICATIONS**

The original specifications were developed for the PCIP trial based on existing MTO standards. The specifications included trial-specific considerations, including the placement of sub-panel instrumentation. These original specifications are shown in Appendix B. This chapter presents the guideline specifications for future PCIP projects. These specifications include aspects of the trial specifications, the MTO construction specifications for non-prestressed precast concrete bridge elements (Ministry of Transportation of Ontario, 2017), and the model specifications for precast concrete pavement systems developed as part of the SHRP2 Renewal Project R05 (Strategic Highway Research Program, 2013).

# **Guideline Specifications for Construction of Precast Concrete Inlay Panel Repairs of Asphalt Pavement**

## **TABLE OF CONTENTS**

- 1.0 SCOPE**
- 2.0 REFERENCES**
- 3.0 DEFINITIONS**
- 4.0 DESIGN AND SUBMISSION REQUIREMENTS**
- 5.0 MATERIALS**
- 6.0 EQUIPMENT**
- 7.0 CONSTRUCTION**
- 8.0 QUALITY ASSURANCE**
- 9.0 MEASUREMENT FOR PAYMENT**
- 10.0 BASIS OF PAYMENT**

### **1.0 SCOPE**

This specification covers the requirements for precast concrete inlay panel (PCIP) repairs of asphalt pavement.

The scope consists of the use of precast panels to be supported on a milled asphalt surface. The panels can be adjusted as required with levelling bolts and supported with rapid setting bedding grout.

Use of this document shall be according to the Contract Documents.

### **2.0 REFERENCES**

This specification refers to the following standards, specifications, or publications:

### **Ontario Provincial Standard Specifications, Construction**

OPSS 350	Concrete Pavement and Concrete Base
OPSS 369	Sealing or Resealing of Joints and Cracks in Concrete Pavement and Concrete Base
OPSS 510	Removal
OPSS 904	Concrete Structures
OPSS 905	Steel Reinforcement for Concrete
OPSS 929	Abrasive Blast Cleaning - Concrete Construction

### **Ontario Provincial Standard Specifications, Material**

OPSS 1001	Material Specification for Aggregates - General
OPSS 1002	Aggregates - Concrete
OPSS 1302	Water
OPSS 1153	Emulsified Asphalt Patching Material
OPSS 1350	Concrete - Materials and Production
OPSS 1440	Steel Reinforcement for Concrete
OPSS 1441	Load Transfer Assemblies

### **Ontario Ministry of Transportation Publications**

#### **MTO Laboratory Testing Manual:**

LS-433	Method of Test for Electrical Indication of Concrete's Ability to Resist Chloride Ion Penetration
LS-602	Sieve Analysis of Aggregates
LS-619	Resistance of Fine Aggregate to Degradation by Abrasion in the Micro-Deval Apparatus
LS-704	Plastic Limit and Plasticity Index of Soils

#### **MTO Materials Engineering and Research Report:**

MERO-019	Falling Weight Deflectometer (FWD) Testing Guideline (ISBN 0-7794-8720-6 Print)
----------	---

### **CSA Standards**

A23.1/23.2-14	Concrete Materials and Methods of Concrete Construction/Methods of Test and Standard Practices for Concrete
A3000-03	Cementitious Materials Compendium
A3004-C2	Test Method for Determination of Compressive Strengths [Part of CAN/CSA A3000-03, Cementitious Materials Compendium]
W47.1-09	Certification of Companies for Fusion Welding of Steel Structures
W59-03(R2008)	Welded Steel Construction (Metal Arc Welding)
W186-90 (R2007)	Welding of Reinforcing Bars in Reinforced Concrete Construction

### **ASTM International**

C 939-02	Flow of Grout for Preplaced-Aggregate Concrete (Flow Cone Method)
C 33	Concrete Aggregates

### 3.0 DEFINITIONS

For the purpose of this specification, the following definitions apply:

**Bedding Grout** means a thin non-structural grout pumped into the grout distribution system that is cast in the bottom of the precast panel to fill voids beneath the panels to provide uniform support to the panel.

**Continuous Precast Concrete Panel Repair** means the continuous replacement of multiple consecutive panels of concrete or sections of asphalt pavement with inter-connecting precast concrete panels.

**Diamond Grinding** means altering the profile and texture of a concrete pavement surface by using grinding equipment that employs diamond tip blades.

**Dowel Grout** means a non-shrink, non-expansive grout, otherwise defined as Proprietary Concrete Repair Material (PCRM) in this NSSP, that is pumped into cast-in slots to encase dowels.

**Low Permeability Concrete** means concrete typically containing silica fume and having rapid chloride permeability of 1000 coulombs or less when tested according to LS-433.

**Lot** consists of all of the same element types, of the same mix design produced over seven consecutive Days

**Micro Milling Equipment** means a cold milling machine whose cutting mandrel's carbide cutting teeth have a tooth spacing of 8 mm.

**Rapid Setting Bedding Grout** means a thin fast setting bedding grout, as described above, which is designed to reach a compressive strength of 5 Mpa in one hour.

### 4.0 DESIGN AND SUBMISSION REQUIREMENTS

#### 4.1 Submission Requirements

##### 4.1.1 Precast Concrete Pavement Panel Repair Plan

At least 2 weeks prior to the start of the work, details on the method of the following operations shall be submitted to the Contract Administrator:

- Fabrication, transportation, and installation of precast concrete panel repair method.
- Removal of existing asphalt pavement (i.e., sawcutting, partial depth removal, equipment, and disposal).
- Precast panel placement.
- Grouting (i.e., equipment to be used for mixing and installing).
- Edge sealing with hot-applied mastic (i.e., equipment to be used for mixing and installing).
- Drainage plan (i.e. number and location of drains, equipment to excavate trench, detail design).
- Method of protecting adjacent HMA surface during panel placement.

#### **4.1.2 Working Drawings**

Working Drawings shall include shop drawings and drawings for handling and installation of the elements.

The Contractor shall prepare and submit 3 sets of Working Drawings and all supporting documentation, to the Contract Administrator at least 5 Business Days prior to commencement of fabrication of the elements, for information purposes only. Prior to making a submission, the design Engineer and the design-checking Engineer shall affix their seals and signatures on the Working Drawings verifying that the drawings are consistent with the Contract Documents.

The Working Drawings shall include the following information:

- a) Element details.
- b) Steel reinforcement schedules.
- c) Lifting point locations.
- d) Details and location of all temporary supports.
- e) All other applicable details.

The supporting documents shall include the following information:

- a) Handling and installation procedures including calculations and lifting point locations.
- b) Details of bracing installed to provide adequate support and stability to the element during construction.

When other authorities are involved in the approval of the design or construction of a highway structure, submissions shall be made at least 5 weeks prior to commencement of work and one additional copy of the submission shall be provided for each authority. The requirements, as stated elsewhere in the Contract Documents of each authority and the Owner shall be satisfied prior to commencement of the Work.

#### **4.1.3 Precast Concrete Mix Design**

The Contractor shall submit the concrete mix design to the Contract Administrator according to the Mix Design requirements of OPSS 1350.

When self-consolidating concrete (SCC) is proposed to be used by the Contractor, the requirements for submission shall be according to the Specification for Self-Consolidating Concrete in Precast Products available from the Ministry's Materials Engineering and Research Office.

The precast concrete mix design shall be submitted to the Contract Administrator at least 2 weeks prior to the start of the work.

Documentation shall be included with the submission of the mix design that demonstrates the proposed mix design and materials meet the requirements of this specification, including the air void system in the hardened concrete and the minimum specified 28-Day compressive strength.

All supporting test data shall not be more than 12 months old at the time the concrete mix design is submitted to the Contract Administrator.

#### **4.1.4 Proprietary Concrete Repair Material (PCRM) - Product Details**

At least 7 Days prior to commencement of the work, the name of the PCRM selected for use and the manufacturer's specifications and recommendations for placement shall be submitted to the Contract Administrator. PCRM shall be Dayton Superior HD-50, ProSpec Slab Dowel Grout, or an approved equivalent. The submission shall also include documentation verifying the suitability of the product for the application and evidence of successful performance in a similar application. The PCRM and supporting information provided shall be acceptable to the Owner.

#### **4.1.5 Chipping Hammer**

At least one week prior to commencement of the work, a copy of the manufacturer's published specifications on the chipping hammers to be used shall be submitted to the Contract Administrator.

#### **4.1.6 Product Report**

A product report shall be submitted to the Contract Administrator for each shipment of elements, prior to shipping the elements.

The report shall contain the following information:

- a) List of elements including their ID number and description.
- b) Documentation of defects or deficiencies other than those listed in Table 1, and all related repair proposals.

The following documentation shall be made available upon request:

- a) The mill certificates for the steel reinforcement used in the elements.
- b) Temperature control records including location of thermocouple wires.
- c) Copies of all measurements and inspections carried out by the Contractor to verify compliance with this specification, including the concrete cover over steel reinforcement, crack measurement summary, tolerances, and surveys for geometric control.
- d) Documentation verifying that all repairable defects have been identified, evaluated and corrected as detailed elsewhere in the specification

## **5.0 MATERIALS**

### **5.1 Precast Concrete Panels**

### **5.1.1 General**

The minimum compressive strength of concrete at 28 Days shall be 45 MPa. Testing of the concrete compressive strength shall be carried out according to CSA A23.2.

The air void parameters of the hardened concrete shall be a minimum air content of 3% and a maximum spacing factor of 0.230 mm.

Rapid chloride permeability shall meet the requirements of low permeability concrete ( $RCP \leq 1000$  Coulombs) for each specified precast element listed.

Concrete shall meet the requirements of the materials section of OPSS 350 and OPSS 1350 with the following exceptions and additions:

- a) Concrete aggregates shall be according to OPSS 1002.
- b) The nominal maximum size of coarse aggregate shall be 19 mm.

### **5.1.2 Finishing**

Finishing of precast concrete panels shall be according to OPSS 350.

### **5.1.3 Texturing of Surface**

Texturing of the precast concrete panel surface shall consist of an initial texturing with a burlap drag that produces longitudinal striations parallel to the centerline. Final texturing shall be with a steel-tined device that produces longitudinal grooves with the steel tines to be 2 mm to 3mm wide at 19mm spacing, resulting in grooves 3 to 5 mm deep after the concrete has hardened.

### **5.1.4 Dimensions**

Precast concrete panels shall be one lane width wide and 4.0 to 5.0 m long. Panels shall be cast to a thickness as per the contract drawings.

### **5.1.5 Steel Reinforcement**

Steel reinforcement shall be according to OPSS 905.

## **5.2 Bedding Grout**

Bedding grout shall be a mixture of cement, water, and plasticizing admixture. The grout mixture shall have a flow rate of 17 to 22 seconds as measured by ASTM C 939 to ensure fluidity. The compressive strength of the bedding grout shall be a minimum of 2.0 MPa at 12 hours.

### **5.2.1 Rapid Setting Bedding Grout**

Rapid set bedding grout shall be bedding grout formulated to reach a compressive strength of 5 MPa in one hour.

### **5.3 Tie Bars and Dowel Bars**

Tie bars shall be according to OPSS 1440. Dowel bars shall be according to OPSS 1441.

### **5.4 Expansion Caps for Dowel Bars**

Caps shall be tight-fitting and made of compressible, non-absorptive, closed cell polyethylene that will allow approximately 6 mm movement at the end of the dowel bar.

### **5.5 Bond Breaker**

Dowel bars shall be coated with RC-250, Tectyl 506, or an approved equivalent.

### **5.6 Proprietary Concrete Repair Material (PCRM)**

The PCRM selected shall be suitable for the application.

The minimum compressive strength of the PCRM at 28 Days shall be 30 MPa.

The PCRM for use in the dowel grout shall be deemed suitable by the panel manufacturer and capable of being pumped into the dowel slots.

### **5.7 Joint Materials**

The joint sealant material used in inter-panel transverse joints shall be according to OPSS 369.

The hot applied, pourable mastic patching material for longitudinal joints and terminal transverse joints between PCIP and adjacent HMA shall be Macseal M.A.R.S. or an approved equivalent.

### **5.9 Water**

Water shall be according to OPSS 1302.

## **6.0 EQUIPMENT**

### **6.1 Chipping Hammer**

Chipping hammers shall be hand held and have a maximum weight of 9.0 kg prior to any handle modification, where applicable, and a maximum piston stroke of 102 mm. All hammers shall have the manufacturer's name and parts or model number engraved on them by the manufacturer. All information shall be clearly legible. The manufacturer's published specifications shall be the sole basis for determining weight and piston stroke.

## **6.2 Hand Finishing Equipment**

Hand finishing equipment shall be according to OPSS 904.

## **6.3 Straight Edges**

Straight edges shall be according to OPSS 904.

## **7.0 CONSTRUCTION**

### **7.1 General**

PCIP repairs for asphalt pavement shall be carried out at the locations identified in the Contract Documents.

### **7.2 Precast Elements**

#### **7.2.1 General**

Precast elements of the same type and for a given component shall be fabricated from the same mix design regardless of whether or not they are cast in the same facility.

#### **7.2.2 Element Identification**

Each precast element shall be identified with a tamper-resistant, permanently-affixed means of identification that includes a unique identification number, date of casting and location of the production facility.

#### **7.2.3 Dimensional Tolerances**

All elements shall meet the dimensional tolerance requirements of CSA 23.4 unless otherwise specified in the Contract Documents. For dimensional tolerances not specified, the maximum allowable dimensional variation shall be 1:800 or  $\pm 3$  mm, whichever is greater.

#### **7.2.4 Concrete Cover**

All elements shall meet the cover requirements of the Contract Documents.

#### **7.2.5 Surface Tolerance**

Formed and unformed surfaces shall be such that, when tested with a 3 m long straight edge placed anywhere in any direction on the surface, there shall be no gap greater than 3 mm between the bottom of the straight edge and the surface of the concrete.

#### **7.2.6 Production Facility**

The precast elements shall be fabricated in a facility that is certified to the requirements of:

- a) Canadian Standards Association (CSA A23.4) under the category Precast Concrete Products-Structural, Non-Prestressed and Prestressed, or
- b) Canadian Precast/Prestressed Concrete Institute (CPCI), Group B, Products and Group BA, Bridge Products with Architectural Finishes, Category, B1, or BA1, Precast Concrete Bridge Products

### **7.2.7 Welding**

Welding of steel hardware including shear studs shall be according to the Contract Documents and CSA W59. Welding shall be performed by a qualified welder working for a company certified by the Canadian Welding Bureau according to CSA W47.1. Welding of steel reinforcement shall be according to the Contract Documents and to CSA W186. Welding shall be performed by a qualified welder working for a company certified by the Canadian Welding Bureau according to CSA W186.

### **7.3 Operational Constraints**

Prior to starting precast panel inlay work, 3 (three) cores per 100 lane m, each 100 mm in diameter, shall be taken mid lane in in the lane to be repaired to measure the total thickness of asphalt pavement. Cores shall be labelled and core thicknesses recorded in the field and brought to the Contract Administrator. Core holes shall be backfilled and compacted with suitable cold mix material prior to opening the lane to traffic.

Perimeter sawcutting of the removal area shall not be carried out more than 1 week in advance of the expected date of repair.

Power broom all cold milled surfaces prior to precast inlay panel placement.

Bedding grout and dowel grout shall be carried out as soon as possible after the installation of the precast concrete inlay panel.

The PCRM shall not be placed when the air temperature is outside the manufacturer's recommended temperature range or is likely to fall or rise outside the range throughout the duration of the material placing operation. Prior to placing the PCRM, it shall be demonstrated to the Contract Administrator that the existing concrete temperature in the repair area meets the manufacturer's requirements by measuring and recording the substrate temperatures using a contact thermometer or infrared thermometer.

Construction vehicles, equipment, or traffic shall not be permitted to travel on the precast repair until the PCRM has attained a minimum compressive strength of 20 MPa.

Each repair location shall be completed within the time period specified in the Contract Documents. If the repair is not progressing at a rate that will permit the full restoration of traffic within the allowable time period, appropriate measures acceptable to the Contract Administrator shall be undertaken to allow opening of the road to traffic. PCIP repairs shall replace the above temporary work during the next scheduled closure.

### **7.4 Drainage**

Before commencing cold milling, trenches shall be cut in the shoulder asphalt to facilitate the placement of drainage details. The trench shall be cut from the outside edge of the shoulder to the

longitudinal sawcut denoting the outside edge of milling. This trench should be 50 mm deeper than the milling depth for the section.

The number and locations of these trenches shall be according to the approved drainage plan. The trenches will have PVC drainage details inserted following cold milling, but prior to panel placement to facilitate drainage. The PVC details will be temporarily blocked to prevent grout inflow during bedding grout placement. This blockage shall be removed following grout setting, and prior to completion of construction.

These trenches shall be backfilled and compacted with suitable HMA material as per OPSS.PROV 1153.

## **7.5 Removals**

### **7.5.1 General**

A detailed survey shall be carried out to precisely delineate the limits of the areas to be repaired within a tolerance of 5 mm as per the contract drawings. Inlay repairs shall be the full width of the lane and the depth of hot mix asphalt repair as specified in the contract drawings.

During pavement removal operations, care shall be taken to prevent contamination with granular and other foreign materials.

Removal shall be performed in such a manner as to leave adjacent pavement and structures remaining in place undisturbed.

When the roadway is to be opened to traffic, after the daily shut down, a temporary 1.0 meter long panel shall be installed as specified in the Contract Documents.

Asphalt pavement material from removal operations shall become the property of the contractor and immediately removed from the site.

### **7.5.2 Cutting Existing Pavement**

Pavement shall be sawcut for neat removal to the dimensions and depth specified in the Contract Documents.

Suitable mechanical sawing equipment and pavement cold milling equipment capable of producing a straight clean vertical face shall be used for cutting the pavement.

The outer limits of the removal area shall be sawcut to the depth specified in the contract drawings and shall not be overcut by more than 250 mm into the adjacent hot mix asphalt that is to remain in place. Overcuts shall be filled with a proprietary product acceptable to the Owner.

### **7.5.3 Removal of Asphalt Pavement, Partial-Depth**

The work shall include the partial-depth removal of asphalt pavement using cold milling equipment capable of milling to a width of 2 meters and depth of 300 mm in one pass.

The cold milling equipment used for partial depth removal shall be automatically controlled for grade and slope given location during removal, using GNSS technology combined with a base station for location correction, or similar. This control shall be based off of engineered drawings developed from the surveyed elevations on site. The surface remaining after removal shall have a constant and continuous crossfall matching the intended surface course crossfall. The surface remaining after removal shall have an even texture and be free of significantly different grooves and ridges in all directions.

The asphalt pavement shall be removed to the depth specified in the Contract Documents.

Removed asphalt pavement material shall not remain on the roadway after completion of the day's operation. Placing of the material on grade other than a bituminous surface prior to hauling to a stockpile shall not be permitted.

The final milled surface shall be attained using a micro milling machine where the gap between the top of micro milled surface and the bottom of a 3 m straightedge placed anywhere in any direction on the micro milled surface shall not exceed 3 mm.

Removals shall be carried out without damaging the adjacent asphalt pavement or asphalt shoulder.

Asphalt surfaces damaged during the removal process shall be repaired. A proposal for asphalt surface repairs shall be provided to the Contract Administrator for approval.

## **7.6 Panel Installation**

During installation, a method of protecting the adjacent HMA surface shall be provided. Design for this edge protection shall be submitted to the Owner for approval prior to beginning of construction.

Panels shall be guided into position during installation using guide bars inserted in bedding grout port holes to align panels during setting. The use of pry bars or wedges in joints between adjacent panels for alignment purposes shall not be permitted.

The vertical differential between adjacent precast inlay panels shall be a maximum of 3 mm. The levelling inserts (bolts) shall be adjusted until the differential does not exceed 3 mm prior moving on to the next panel.

## **7.7 Placing the Dowel Grout and Bedding Grout**

Foam grout dams shall be installed at the open ends of the transverse joint to be grouted to prevent dowel grout from escaping during the installation. Dowel grout shall be mixed in strict accordance with the instructions provided by the manufacturer. The volume of water shall be measured accurately for each batch by weighing the batch water or by using calibrated pails that are

perforated at a level to ensure the correct amount of water is mixed with each bag of grout. Dowel grout shall be pumped in the back port of each grouting location until it comes out the second port of the same. The same procedure shall be repeated for all grouting locations. The grout level in previously filled ports shall be continually monitored. Grout shall be added, as necessary, to keep the grout level in the ports even with the top of the panel.

Bedding grout shall be placed after the dowel grout has been installed. Bedding grout shall be mixed in strict accordance with the instructions provided by the manufacturer of the viscosity-reducing admixture. Bedding grout shall be pumped in the lowest port of the panel until it comes out the corresponding port at the other end of the panel. While filling the remaining ports in the panel, the grout level shall be continually monitored in previously filled ports and grout added, as required, to keep the grout level in the ports even with the top of the panel. This will maintain a safe and adequate head pressure on the bedding grout until all voids under the panel are filled.

When levelling bolts are used, a rapid setting bedding grout shall be used incorporating the same placement procedures as typical bedding grout.

Before the bedding grout fully sets, the top 50 mm of bedding grout in each port shall be removed and replaced with PCRM. The PCRM in all ports shall be finished flush and matching with the surface of the concrete and all excess material removed immediately.

## **7.8 Tolerances**

### **7.8.1 Surface Tolerances**

The surface of the precast concrete panel repair shall join 3 mm to 5 mm above the adjacent existing asphalt pavement, to be made flush with the initial diamond grinding. Final surface tolerance of continuous panels shall be so that the gap is not greater than 3 mm when the 3 meter straight edge is placed in any location and direction, including the edge of pavement, except across the crown or drainage gutters.

## **7.9 Next Generation Concrete Surface Diamond Grinding**

Following the completion of PCIP installation, including grouting, for the full project, the surface of the repaired area will be diamond ground to provide a Next Generation Concrete Surface (NGCS).

The grinding operation will provide a flush ground surface that contains longitudinal grooves and shall be constructed in one, single-pass operation. The diamond blade stack will consist of two types of diamond grinding blades arranged to provide a flush ground surface as well as those required to produce the longitudinal grooves. The diamond blade stack shall be mounted on a 1.2 m grinding head, stacked with 3.2 mm wide blades separated by 0.9 +/- 0.13 mm wide spacers. The blades used to produce the flush ground surface shall be flat across their contact surface and in the same plane with other flush grind blades (excluding grooving blades) when mounted. The complete head, when stacked with all blades, shall be straight across its length without bowing when mounted on the diamond grinding machine. No unground surface area between passes will

be permitted. The longitudinal grooving blades will be spaced among the flush grind blade stack on 12.7 mm to 15.9 mm centers and shall produce grooves 3.2 mm to 4.8 mm in depth. The grooves shall be constructed parallel to the centerline. The contractor shall use a guide to ensure proper alignment of the grooves to centerline.

The depth of the grinding shall be the minimum required to produce a continuous profile throughout the PCIP repair, based on the vertical joint differentials resulting from panel installation.

The NGCS grinding process shall produce a pavement surface that is true to grade and uniform in appearance with a longitudinal grooved texture. The flush ground surface shall appear smooth and shall contain no ridges that exceed 0.8 mm. The longitudinal grooves shall be constructed parallel to the centerline. At a minimum, 98% of the pavement surface shall be textured utilizing the NGCS.

### **7.9.1 Smoothness Requirement**

Each segment of the finished NGCS shall have a final profile with a Mean International Roughness Index (MRI) of 4 mm/m or less.

The smoothness profile shall be generated using lightweight profiler equipment with a laser that simulates the tire footprint that is approved by the Owner. All equipment shall have current certification and be approved by the Owner.

The contractor shall measure the profile in both wheel paths and average the IRI results to determine acceptance (MRI). The profiles shall be measured 0.9 m from each lane line. A guide shall be used to ensure proper alignment of the profile. The Owner shall have a representative with the lightweight profiler during all testing periods. This representative shall sign the resulting profile form.

The Owner shall run comparison profiles on no less than 10 percent of the segments using the same type of certified equipment as the contractor. It is of great importance that a proper guide is used to ensure that all testing is completed over the same track. The contractor and agency testing should be completed during the same time of day and under similar climatic conditions. The results of these verification profiles shall not vary more than 10 percent from the contractor profiles.

The Owner may choose to accept isolated sections if the variance between the two profiles is less than 15 percent. When the difference exceeds 15 percent on an isolated basis or 10 percent on a consistent basis, referee testing will be required to determine which device is providing an accurate evaluation of the pavement surface. The party found to have the inaccurate equipment will pay for the referee testing. The Owner may choose to withhold payment for segments that do not meet these criteria until the problem is resolved. The Owner may choose to run verification profiles on the entire project if the comparison profiles are constantly outside the allowable tolerance. The Owner will charge for the additional testing if the contractor's operation is found to be in error. Segments found not meeting the smoothness requirements will require regrinding at no additional cost to the Agency.

## **7.10 Joint Sealing**

All transverse joints between precast inlay panels shall be sealed according to OPSS 369. All longitudinal and transverse edge joints shall be filled with hot applied, pourable mastic patching material.

Joint sealing shall take place following the initial surface grinding of the pavement.

## **7.11 Sampling and Testing**

### **7.11.1 General**

All samples, including those handled by a commercial carrier shall be accompanied by a sample data sheet and any additional documents as specified elsewhere in the Contract Documents. When not specified or not included on the sample data sheet, samples shall be delivered with a transmittal form identifying the following information:

- a) Contract Number.
- b) Name of Contractor, name of contact person and telephone numbers.
- c) Name of Contract Administrator, and telephone numbers.
- d) Quantity and type of sample. When a sample consists of more than one item, each item shall be individually identified.
- e) Date sampled.
- f) Date shipped.
- g) Sample and lot number.
- h) Sample location.

### **7.11.2 Compressive Strength of Concrete in Precast Panel**

Concrete test cylinders shall be cast, cured, handled, and delivered for 28-Day compressive strength testing according to OPSS 1350 based on 1 set of 2 cylinders taken for each batch of concrete.

### **7.11.3 Acceptance of Rapid Chloride Permeability**

One core per lot shall be tested according to LS-433. Acceptance testing shall be carried out at 28 to 32 Days. Two samples 50 mm long shall be cut from the core representing a lot, and tested to determine the acceptance of the lot. Another core shall be retained for referee testing. Individual

test results shall be forwarded to the Contractor as they become available. Acceptance of rapid chloride permeability shall be based on the result obtained on the core representing the lot.

Where rapid chloride permeability of 1000 coulombs or less is specified, lots with a rapid chloride permeability result less than or equal to 1000 coulombs shall be considered acceptable. Lots containing silica fume with a rapid chloride permeability result greater than 1000 coulombs and less than or equal to 2000 coulombs shall be considered unacceptable and shall be repaired. Lots containing silica fume with a rapid chloride permeability results exceeding 2000 coulombs shall be rejected and replaced at the Contractor's expense.

#### **7.11.3.01 Referee Testing of Rapid Chloride Permeability**

Referee testing of rapid chloride permeability may only be invoked by the Contractor within 5 Business Days of receipt of the acceptance test result.

Referee testing shall be carried out on 2-50 mm samples obtained from the reserved core representing the lot for which referee testing was invoked, and the results shall be averaged to obtain the test result for the lot.

The referee laboratory shall be designated by Owner based on the applicable roster and cores shall be tested according to LS 433 by that laboratory.

Referee test results shall be forwarded to the Contractor as they become available.

When the referee result is greater than the acceptance test result or no more than 200 Coulombs below the acceptance test result, then the acceptance test result is confirmed and shall remain valid. When the referee test result for the lot is more than 200 Coulombs below the acceptance test result, the acceptance test result is not confirmed, and the referee test result shall replace the acceptance test result in the acceptance requirements of this specification.

#### **7.11.4 Compressive Strength of Proprietary Concrete Repair Materials**

Samples of PCRMs shall be taken from the mixer in the field for the determination of the early strength and 28-Day compressive strength. The PCRMs shall be moulded into cubes according to CAN/CSA A3004- C2.

Cubes shall be prepared on-site from the PCRMs to be used to fill the slots. For the 28-Day compressive strength, the PCRMs shall be sampled once for every 4 hours of production or a minimum of once per day, whichever is greatest. One set of six cubes shall be made from each sample of PCRMs.

Additional cubes for determination of early strength shall be prepared. One set of six cubes shall be made for the final repair area of each closure. These cubes shall be tested to verify that the PCRMs in the repair area has attained a compressive strength of 20 MPa. These test results shall be communicated immediately to the Contract Administrator prior to opening to traffic.

The timing of testing and frequency of testing of the early strength cubes shall be determined when the PCRM has attained a minimum compressive strength of 20 MPa.

The specimens shall be stored at a temperature between 15 °C and 25 °C and shall not be moved prior to demoulding. The specimens shall be demoulded and transported to the QA laboratory designated by the Owner within 24 hours ± 4 hours. The samples shall be transported in a sealed white opaque plastic bag containing at least 250 ml of water and maintained at a temperature between 15 °C and 25 °C.

### **7.12 Falling Weight Deflectometer Testing**

Within 2 weeks of panel placement and grouting, falling weight deflectometer (FWD) testing shall be carried out on the approach and leave joints of each precast panel and across the transverse end joints to determine the load transfer efficiency across the transverse joints. FWD testing, equipment calibration, and reporting shall be according to MERO-019 using the Load Transfer test with a Detailed Project Level data collection scenario and a JCP Test Plan configuration.

### **7.13 Repair or Removal of Unacceptable Concrete**

Precast concrete pavement panels that arrive on the job site cracked, honeycombed, or showing any other visually detectable deficiencies shall be rejected and not used in the work.

Precast concrete pavement panels that do not meet the surface tolerance requirements shall be removed and replaced, or corrected by diamond grinding.

Asphalt pavement adjacent to precast concrete panel inlay repair, damaged or displaced during installation of the precast panels shall be repaired to the satisfaction of the Contract Administrator.

### **7.14 Management of Excess Material**

Management of excess material shall be according to the Contract Documents.

## **8.0 QUALITY ASSURANCE**

### **8.1 Inspection**

Prior to installation and with notification, access shall be provided to the Contract Administrator to inspect the precast concrete pavement panels to ensure that they are properly textured and crack-free without any honeycombing or other visually detectable deficiencies.

### **8.2 Acceptance or Rejection**

Prior to opening to traffic, access shall be provided to the Contract Administrator to inspect the precast concrete inlay panel repairs to determine if the completed work contains:

- a) Cracking or spalling.

- b) UngROUTED saw over-cuts from the removal process.
- c) Rocking of precast concrete inlay panel.
- d) Precast concrete inlay panel that does not meet surface tolerance.

Precast concrete inlay panel repairs shall be rejected based on the presence of one or more of the defects identified above or one or more of the following conditions:

- a) FWD testing results indicate a load transfer efficiency of less than 70%.
- b) Air content of the hardened concrete in the precast panel is less than 3% or spacing factor is greater than 0.230 mm.

A detailed remedial plan shall be submitted to the Contract Administrator for approval to address identified deficiencies.

## **9.0 MEASUREMENT FOR PAYMENT**

### **9.1 Actual Measurement**

#### **9.1.1 Precast Concrete Panel Inlay Repair**

Measurement of the PCIP repair placed shall be by area in square metres. The total area shall be calculated to the nearest 0.1 m<sup>2</sup>.

### **9.2 Plan Quantity Measurement**

When measurement is by Plan Quantity, such measurement shall be based on the units shown in the clause under Actual Measurement.

## **10.0 BASIS OF PAYMENT**

### **10.1 Precast Concrete Inlay Panel Repair**

Lump sum payment at the Contract price for the above tender items shall be full compensation for all Labour, Equipment, and Material to do the work laid out.

Measures taken to permit full restoration of traffic within the allowable time period shall be at no additional cost to the Owner.

Precast concrete inlay panels that do not meet surface tolerance requirements shall be either removed and replaced or repaired by diamond grinding at no additional cost to the Owner.

Precast concrete inlay panels rejected by the Contract Administrator shall be removed and replaced with new precast concrete panels as specified elsewhere in the Contract Documents at no additional cost to the Owner.

Asphalt surfaces damaged during the removal process shall be repaired at no additional cost to the Owner.

### **10.2 Surface Diamond Grinding Payment**

NGCS construction will be paid for at the contract price per square metre, laid out in the table below. Payment shall be full compensation for all labor, equipment, material and incidentals to complete this work, including hauling and disposal of grinding residue.

<b>Speeds <math>\geq</math> 75 km/hr</b>	
<b>MRI (mm/m)</b>	<b>\$/m<sup>2</sup></b>
0-2	1.75
2-3	(3-MRI) * 1.75
3-4	0

## REFERENCES

- AASHTO. (1993). *AASHTO Guide for Design of Pavement Structures*. Washington DC: American Association of State Highway and Transportation Officials.
- Ahmadi, B. (2011). *Workzone Throughput Models for Southern Ontario (thesis)*. Toronto, ON, CAN: University of Toronto.
- American Concrete Institute. (2005). Building Code Requirements for Structural Concrete. In *ACI 318-05: ACI Manual of Concrete Practice Part 3: Use of Concrete in Buildings - Design, Specifications, and Related Topics*. Detroit, MI, USA: American Concrete Institute.
- Applied Research Associates. (2012). *Final Pavement Design Report: Highway 400 Median Barrier Replacement*. Toronto, ON, CAN: Applied Research Associates.
- Applied Research Associates: ERES Division. (2003). *Guide for Mechanistic-Empirical Design of New and Rehabilitated Pavement Structures: Appendix JJ Transverse Joint Faulting Model*. National Cooperative Highway Research Program of the Transportation Research Board.
- Ashtiani, R. S., Jackson, C. J., Saeed, A., & Hammons, M. I. (2010). *Precast Concrete Panels for Contingency Rigid Airfield Pavement Damage Repairs*. Tyndall Air Force Base, FL: Air Force Research Laboratory.
- ASTM. (2016). ASTM D5329: Standard Test Methods for Sealants and Fillers, Hot-Applied, for Joints and Cracks in Asphalt Pavements and Portland Cement Concrete Pavements. West Conshohocken, PA, USA: American Society for Testing and Materials.
- ASTM International. (2013). *Standard Test Method for Measuring Surface Frictional Properties Using the British Pendulum Tester*. West Conshohocken, P.A., U.S.A.: ASTM International.
- ASTM International. (2015). *Standard Practice for Calculating Pavement Macrotexture Mean Profile Depth*. West Conshohocken, P.A., U.S.A.: ASTM International.

- ASTM International. (2015). *Standard Test Method for Skid Resistance of Paved Surfaces Using a Full Scale Tire*. West Conshohocken, P.A., U.S.A.: ASTM International.
- Banuelas, R., & Antony, J. (2004). Modified analytic hierarchy process to incorporate uncertainty and managerial aspects. *International Journal of Production Research*, 3851-3872.
- Bradbury, R. (1938). *Reinforced Concrete Pavements*. Washington D.C., USA: Wire Reinforcement Institute.
- Campbell Scientific. (2017, April 24). *CS655: Soil Water Content Reflectometer 12 cm*. Retrieved from Campbell Scientific: <https://www.campbellsci.ca/cs655>
- Chan, S., & Lane, B. (2005). *Falling Weight Deflectometer (FWD) Testing Guideline (MERO-019)*. Downsview, Ontario: Ministry of Transportation Ontario.
- Chong, G. J., & Wrong, G. A. (1995). *Manual for Condition Rating of Rigid Pavements (SP-026)*. Donsview, ON: Ontario Ministry of Transportation.
- CSA. (2014). *A23.3-14: Design of Concrete Structures*. Mississauga, ON, CAN: Canadian Standards Association.
- Delatte, N. J. (2014). *Concrete Pavement Design, Construction, and Performance: Second Edition*. Boca Raton, FL: CRC Press.
- Drescher, A., Kim, J. R., & Newcomb, D. E. (1993, February). Permanent Deformation in Asphalt Concrete. *Journal of Materials in Civil Engineering*, 5(1), 112-128.
- El Khoury, J., Akle, B., Katicha, S., Ghaddar, A., & Daou, M. (2014). A microscale evaluation of pavement roughness effects for asset management. *International Journal of Pavement Engineering*, 15(4), 323-333.
- Flintsch, G. W., Al-Qadi, I. L., Davis, R., & McGhee, K. K. (2002). Effect of HMA Properties on Pavement Surface Characteristics. *Proceedings of the Pavement Evaluation 2002 Conference*. Roanoke, VA, USA.

- Gaspard, K. (2008). *Assessment of Tri-Dyne Precast Concrete Panels*. Baton Rouge, LA: Louisiana Transportation Research Center.
- Glennon, J. C., & Hill, P. F. (2004). *Roadway Defects and Tort Liability* (2nd ed.). Lawyers & Judges Publishing Company.
- Gonzalez, M. (2014). *Nanotechnology Applied in the Design of the Next Generation of Canadian Concrete Pavement Surfaces*. Waterloo, ON: University of Waterloo.
- Government of Canada. (2018). *Historical Weather Data*. Retrieved February 1, 2018, from [http://climate.weather.gc.ca/historical\\_data/search\\_historic\\_data\\_e.html](http://climate.weather.gc.ca/historical_data/search_historic_data_e.html)
- Hajek, J. J., Smith, K. L., Rao, S. P., & Darter, M. I. (2008). *Adaptation and Verification of AASHTO Pavement Design Guide for Ontario Conditions*. Champaign, IL: Ministry of Transportation of Ontario.
- Hall, J. W., Smith, K. L., & Titus-Glover, L. (2006). *Guide for Pavement Friction Final Report*. Washington, D.C., U.S.A.: National Cooperative Highway Research Program (NCHRP).
- Hall, J. W., Smith, K., & Littleton, P. (2008). *Texturing of Concrete Pavements*. Washington, D.C., U.S.A.: National Cooperative Highway Research Program.
- Harrington, D., & Fick, G. (2014). *Guide to Concrete Overlays: Sustainable Solutions for Resurfacing and Rehabilitating Existing Pavements*. Washington DC: American Concrete Pavement Association (ACPA).
- Heavy Haul Trucking. (2016, November 09). *Ontario Oversize Permits*. Retrieved from <http://www.heavyhaul.net/ontario-oversize-permits/>
- IGGA. (2014, September 30). *Guide Specification: NGCS Construction on Existing or Newly Constructed Roadways*. Retrieved from International Grooving and Grinding Association: [http://7e846f23de4e383b6c49-2fba395bb8418a9dd2da8ca9d66e382f.r19.cf1.rackcdn.com/uploads/resource/301/NGCS\\_Construction\\_Existing\\_Newly\\_Constructed\\_Roads\\_093014.pdf](http://7e846f23de4e383b6c49-2fba395bb8418a9dd2da8ca9d66e382f.r19.cf1.rackcdn.com/uploads/resource/301/NGCS_Construction_Existing_Newly_Constructed_Roads_093014.pdf)

- International Organization for Standardization. (2008). *Buildings and Constructed Assets, Service-life planning Part 5: Life-cycle Costing (ISO 15686-5)*. Geneva, Switzerland: International Organization for Standardization.
- Ioannides, A. M., Thompson, M. R., & Barenberg, E. J. (1985). Westergaard Solutions Reconsidered. *Transportation Research Record, No. 1043*, 13-22.
- Khanal, S., Tighe, S., & Bowers, R. (2013, April 8). Pavement performance mechanics of interlocking concrete paver crosswalk designs. *Canadian Journal of Civil Engineering*, pp. 583-594.
- Kher, R., & Phang, W. A. (1975). *Economic Analysis Elements: Ontario Pavement Analysis of Costs*. Downsview, ON: Ministry of Transportation and Communications, Ontario.
- Lane, B., & Kazmierowski, T. (2005). *Guidelines for the use of life cycle cost analysis on MTO freeway projects (MERO-018)*. Downsview, Ontario: Ministry of Transportation Ontario.
- Lane, B., & Kazmierowski, T. (2011). Performance of Precast Concrete Pavement Repairs on an Urban Freeway in Toronto. Edmonton: Transportation Association of Canada.
- Larson, R. M., & Smith, K. D. (2011). *Evaluation of Alternative Dowel Bar Materials and Coatings*. Washington D.C.: Federal Highway Administration.
- Larson, R. M., Scofield, L., & Sorenson, J. (2005). Providing durable, safe, and quiet highways. *Proceedings of the 8th International Conference on Concrete Pavements. II*, pp. 500-522. Colorado Springs, C.O., U.S.A.: International Society for Concrete Pavements.
- Li, Q., Qiao, F., & Yu, L. (2016). Clustering Pavement Roughness Based on the Impacts on Vehicle Emissions and Public Health. *Journal of Ergonomics*, 6(1), 1-4.  
doi:10.4172/2165-7556.1000146
- Li, Q., Qiao, F., & Yu, L. (2016). Impacts of pavement types on in-vehicle noise and human health. *Journal of the Air and Waste Management Association*, 66(1), 87-96.  
doi:<https://doi.org/10.1080/10962247.2015.1119217>

- Liu, Q. (2015). *Three-Dimensional Pavement Surface Texture Measurement and Statistical Analysis (Thesis)*. Winnipeg, MB, CAN: University of Manitoba.
- Ministry of Transportation of Ontario. (2013). *Pavement Design and Rehabilitation Manual: Second Edition*. Downsview, ON: Materials Engineering and Research Office, Ministry of Transportation of Ontario.
- Ministry of Transportation of Ontario. (2014). *Ontario Traffic Manual- Book 7: Temporary Conditions*. St. Catharines, ON: Ministry of Transportation of Ontario.
- Ministry of Transportation of Ontario. (2016, 11 08). *iCorridor*. Retrieved February 15, 2018, from Ministry of Transportation of Ontario:  
[http://www.mto.gov.on.ca/iCorridor/map.shtml?accepted=true#tab\\_5](http://www.mto.gov.on.ca/iCorridor/map.shtml?accepted=true#tab_5)
- Ministry of Transportation of Ontario. (2017). *RAQS Consultant: What's New in RAQS*. Retrieved March 1, 2017, from <https://goo.gl/R3pZQe>
- Ministry of Transportation of Ontario. (2017). *Special Provision No. 999F31: Construction Specification for Non-prestressed Precast Concrete Bridge Elements*. Ministry of Transportation of Ontario.
- Ministry of Transportation of Ontario: Highway Standards Branch. (2013). *Traffic Volumes*. Retrieved from Ministry of Transportation of Ontario:  
[http://www.raqsb.mto.gov.on.ca/techpubs/TrafficVolumes.nsf/fa027808647879788525708a004b5df8/88c66a2279555c798525788d0048cca4/\\$FILE/Provincial%20Highways%20Traffic%20Volumes%201988-2013.pdf](http://www.raqsb.mto.gov.on.ca/techpubs/TrafficVolumes.nsf/fa027808647879788525708a004b5df8/88c66a2279555c798525788d0048cca4/$FILE/Provincial%20Highways%20Traffic%20Volumes%201988-2013.pdf)
- Ministry of Transportation Ontario. (2016, 11 08). *iCorridor*. Retrieved from Ministry of Transportation of Ontario:  
[http://www.mto.gov.on.ca/iCorridor/map.shtml?accepted=true#tab\\_5](http://www.mto.gov.on.ca/iCorridor/map.shtml?accepted=true#tab_5)
- Moges, M., Ayed, A., Vecili, G., & El Halim, A. A. (2017). A Review and Recommendations for Canadian LCCA Guidelines. *2017 Conference of the Transportation Association of Canada*. St. John's, NL.

- Mohamed, A. R., & Hansen, W. (1997). Effect of Nonlinear Temperature Gradient on Curling Stress in Concrete Pavement. *Transportation Research Record*, 1568, 65-71.
- Mushtaq, M. A. (2011). *Measuring Work Zone Throughput and User Delays (thesis)*. Waterloo, ON, CAN: University of Waterloo.
- Neville, A. M. (1997). *Properties of Concrete*. New York: John Wiley & Sons, Inc.
- Ontario Provincial Standards (OPS). (1998). *Construction Specification for Concrete Pavement and Concrete Base*. Downsview, ON, CAN: Ministry of Transportation of Ontario.
- Ontario Provincial Standards (OPS). (2013). *Material Specification for Aggregates - Concrete*. Downsview, ON, CAN: Ministry of Transportation of Ontario.
- Ontario Provincial Standards (OPS). (2016). *Material Specification for Concrete- Materials and Production*. Ministry of Transportation of Ontario.
- Pavement Interactive. (2011, September 20). *Micro-Milling – The Finer Side of Milling*. Retrieved from Pavement Interactive:  
<http://www.pavementinteractive.org/2011/09/20/micro-milling-the-finer-side-of-milling/>
- Perera, O., Morton, B., & Perfrement, T. (2009). *Life Cycle Costing in Sustainable Public Procurement: A Question of Value*. Winnipeg, Manitoba: International Institute for Sustainable Development.
- Persson, B. (2000). *Sliding Friction: Physical Principles and Applications* (2 ed.). New York, N.Y., U.S.A.: Springer-Verlag Berlin Heidelberg.
- Pickel, D. J., Tighe, S. L., Lee, W., & Fung, R. (2018). Highway 400 Precast Concrete Inlay Panel Project: Instrumentation Plan, Installation, and Preliminary Results. Washington D.C., United States: Transportation Research Board 97th Annual Meeting.
- Pickel, D., Tighe, S., Fung, R., Lee, S., Smith, P., & Kazmierowski, T. (2016). *Using Precast Concrete Inlay Panels for Rut Repair on High Volume Flexible Pavements*. San Antonio, TX: International Conference on Concrete Pavements.

- Priddy, L. P., Bly, P. G., Jackson, C. J., & Flintsch, G. W. (2014). Full-scale field testing of precast Portland cement concrete panel airfield pavement repairs. *International Journal of Pavement Engineering*, 15(9), pp. 840-853.
- Saaty, T. L. (2005). Chapter 9: The Analytical Hierarchy and Analytical Network Processes for the Measurement of Intangible Criteria and for Decision-Making. In *Multiple Criteria Decision Analysis: State of the Art Surveys* (pp. 345-407). Boston, MA, USA: Springer Science and Business Media.
- Saaty, T. L. (2013). The Modern Science of Multicriteria Decision Making and Its Practical Applications: The AHP/ANP Approach. *Operations Research*, 61(5), 1101-1118.
- Sayers, M. W. (1995). On the Calculation of International Roughness Index from Longitudinal Road Profile. *Transportation Research Record*, 1501, 1-12.
- Sayers, M. W., & Karamihas, S. M. (1998). *The Little Book of Profiling*. Ann Arbor: The University of Michigan.
- Sayers, M. W., Gillespie, T. D., & Paterson, W. D. (1986). *Guidelines for Conducting and Calibrating Road Roughness Measurements*. Washington, D.C., U.S.A.: The World Bank.
- Scofield, L. (2017). *Development and Implementation of the Next Generation Concrete Surface*. International Grooving and Grinding Association & American Concrete Pavement Association.
- Scott, M. J. (2002). Quantifying Certainty in Design Decisions: Examining AHP. *ASME Design Engineering Technical Conference*. Montreal.
- Smith, P. (2014, October 29-31). Vice President, Market Development and Product Engineering at The Fort Miller Co., Inc. (D. Pickel, Interviewer)
- Smith, P., & Snyder, M. (2017). *Manual for Jointed Precast Concrete Pavement*. National Precast Concrete Association.

- Snyder, M. B. (2011). *Guide to Dowel Load Transfer Systems for Jointed Concrete Roadway Pavements*. Institute for Transportation at Iowa State University. Ames, IA: National Concrete Consortium.
- Strategic Highway Research Program. (2013). *Model Specifications for Precast Concrete Pavement Systems*. Retrieved from SHRP 2 Report R05:  
[http://onlinepubs.trb.org/onlinepubs/shrp2/SHRP2\\_R05\\_modelspecifications.docx](http://onlinepubs.trb.org/onlinepubs/shrp2/SHRP2_R05_modelspecifications.docx)
- Tayabji, S., Ye, D., & Buch, N. (2012). *Precast Concrete Pavement Technology Project R05 – Modular Pavement Technology*. The Strategic Highway Research Program 2 Transportation Research Board of The National Academies.
- Taylor, P. C., Kosmatka, S. H., Voigt, G. F., & et al. (2007). *Integrated Materials and Construction Practices for Concrete Pavement: A State-of-the-Practice Manual*. Washington, D.C., U.S.A.: Federal Highway Administration, United States Department of Transportation.
- The Fort Miller Company Inc. (2015). *Super Slab Detailed Drawings*. Schuylerville, NY: Fort Miller Co. Inc.
- Tighe, S. (2001). Guidelines for Probabilistic Pavement Life Cycle Cost Analysis. *Transportation Research Record*(1769), 28-38.
- Titus-Glover, L., Mallela, J., Darter, M. I., Voigt, G., & Waalkes, S. (2005). Enhanced Portland Cement Concrete Fatigue Model for StreetPave. *Transportation Research Record: Journal of the Transportation Research Board, No. 1919*, 29-37.
- Transportation Association of Canada (TAC). (2013). *Pavement Asset Design and Management Guide*. Ottawa: Transportation Association of Canada (TAC).
- US Department of Transportation Federal Highway Administration. (2015, April 6). *Work Zone Road User Costs - Concepts and Applications*. Retrieved August 24, 2015, from Work Zone Mobility and Safety Program:  
<http://ops.fhwa.dot.gov/wz/resources/publications/fhwahop12005/sec2.htm>

- Vaidya, O. S., & Sushil, K. (2006). Analytic Hierarchy Process: An Overview of Applications. *European Journal of Operational Research*, 169(1), 1-29.
- Wafa, R. (2018). *Evaluating Unbonded Concrete Overlay for Usage on Ontario Residential Streets*. Waterloo, ON, CAN: University of Waterloo.
- Walls III, J., & Smith, M. R. (1998). *Life-Cycle Cost Analysis in Pavement Design -Interim Technical Bulletin*. Washington, DC: Federal Highway Administration.
- Williams, L. J., & Abdi, H. (2010). Fisher's Least Significant Difference (LSD) Test. In N. Salkind (Ed.), *Encyclopedia of Research Design*. Thousand Oaks, CA, USA: Sage.
- Zaabar, I., & Chatti, K. (2014). Estimating Vehicle Operating Costs Caused by Pavement Surface Conditions. *Transportation Research Record: Journal of the Transportation Research Board*, 2455(10.3141/2455-08), 63-76.

## **APPENDIX A: LEAST SIGNIFICANT DIFFERENCE CALCULATION**

---

Sample Calculation:

Consider the following load transfer efficiency values for each of the support conditions tested.

LTE	AS	GraS	GroS
#1	0.810	0.802	0.799
#2	0.733	0.767	0.804
#3	0.743	0.831	0.777
#4	0.848	0.798	0.795
#5	0.813	0.838	0.840
⋮	⋮	⋮	⋮
Mean	0.805	0.806	0.830

To determine the 5% LSD value:

1. Set the significance level  $b = 0.05$  for 5% significance (95% confidence).
2. Set  $k = 3$  as the total number of support conditions (AS, GraS, GroS).
3. Set  $N = 76$  as the total number of results for the three support conditions.
4. Calculate  $n = 25.33$  as the average number of results for each support condition.
5. Calculate “ $\alpha$ ” for use in the t-test calculation:

$$\alpha = 1 - (1 - b)^{\left(\frac{1}{k}\right)} = 1 - (1 - 0.05)^{\left(\frac{1}{3}\right)} = 0.01695$$

6. Calculate the t-statistic as:

$$t_{\alpha, N-k} = t_{0.01695, 73} = 2.44$$

7. Calculate the mean square within groups as the sum of squares ( $SS = 0.072$ ) divided by the degrees of freedom with support types (i.e.,  $N - k = 73$ ).

Note: a one-way or single-factor ANOVA analysis was carried out using EXCEL to calculate these values:

Anova: Single Factor

SUMMARY

<i>Groups</i>	<i>Count</i>	<i>Sum</i>	<i>Average</i>	<i>Variance</i>
AS	28	22.54119	0.805042	0.001062
GraS	24	19.33314	0.805547	0.000641
GroS	24	19.91528	0.829803	0.001237

ANOVA

<i>Source of Variation</i>	<i>SS</i>	<i>df</i>	<i>MS</i>	<i>F</i>	<i>P-value</i>	<i>F crit</i>
Between Groups	0.009882	2	0.004941	5.019333	0.009069	4.332794
Within Groups	0.071864	73	0.000984			
Total	0.081746	75				

8. Calculate the standard error of the difference between two means:

$$SE = \sqrt{\frac{2(MS)}{N - k}} = \sqrt{\frac{2(0.000984)}{73}} \cong 0.005$$

9. Calculate the 5% LSD:

$$5\% LSD = t_{stat} \times SE = (2.44)(0.005) = 0.0127$$

This 5% LSD represents the smallest significant difference between two means in the given set of values. Therefore, the mean LTE of AS and GraS are not significantly different since the difference of their means is approximately 0.0005, which is smaller than the 5% LSD. However, the mean LTE of GroS is significantly higher than both AS and GraS, with differences in means of 0.025 and 0.024, respectively. Both differences are higher than the 5% LSD.

## **APPENDIX B: TRIAL SPECIFICATIONS AND DESIGN DRAWINGS**

---

## **NONSTANDARD SPECIAL PROVISION (NSSP) FOR CONSTRUCTION OF PRECAST CONCRETE INLAY REPAIRS OF ASPHALT PAVEMENT**

### TABLE OF CONTENTS

1.0	SCOPE
2.0	REFERENCES
3.0	DEFINITIONS
4.0	DESIGN AND SUBMISSION REQUIREMENTS
5.0	MATERIALS
6.0	EQUIPMENT
7.0	CONSTRUCTION
8.0	QUALITY ASSURANCE
9.0	MEASUREMENT FOR PAYMENT
10.0	BASIS OF PAYMENT

### 1.0 SCOPE

This specification covers the requirements for inlay repair of asphalt pavement 100 meters in length using precast concrete slabs based on the Fort Miller Super-Slab Method. The repair area is located in the Hwy 400 NBL, in lane 3 from Sta 17+550 to Sta 17+650, south of Hwy 89.

The work consists of 3 options:

- Option 1. Grade Supported Slabs: these precast slabs are placed on cement-treated base material (CTBM) with bedding grout
- Option 2. Asphalt Supported Slabs: these slabs are placed on the micro milled asphalt surface with bedding grout
- Option 3. Grout Supported Slabs: these slabs incorporating levelling bolts are placed on the milled asphalt surface with rapid setting bedding grout

Long term monitoring instrumentation will be installed as part of the work.

### 1.1 NSSP Use

Use of this NSSP shall be according to the Contract Documents.

### 2.0 REFERENCES

This specification refers to the following standards, specifications, or publications:

#### **Ontario Provincial Standard Specifications, Construction**

OPSS 350	Concrete Pavement and Concrete Base
OPSS 369	Sealing or Resealing of Joints and Cracks in Concrete Pavement and Concrete Base
OPSS 510	Removal

OPSS 904 Concrete Structures  
OPSS 905 Steel Reinforcement for Concrete  
OPSS 929 Abrasive Blast Cleaning - Concrete Construction

### **Ontario Provincial Standard Specifications, Material**

OPSS 1001 Material Specification for Aggregates - General  
OPSS 1002 Aggregates - Concrete  
OPSS 1302 Water  
OPSS 1350 Concrete - Materials and Production  
OPSS 1440 Steel Reinforcement for Concrete  
OPSS 1441 Load Transfer Assemblies

### **Ontario Ministry of Transportation Publications**

#### **MTO Laboratory Testing Manual:**

LS-602 Sieve Analysis of Aggregates  
LS-619 Resistance of Fine Aggregate to Degradation by Abrasion in the Micro-Deval Apparatus  
LS-704 Plastic Limit and Plasticity Index of Soils

#### **MTO Materials Engineering and Research Report:**

MERO-019 Falling Weight Deflectometer (FWD) Testing Guideline (ISBN 0-7794-8720-6 Print)

### **CSA Standards**

A23.1/23.2-04 Concrete Materials and Methods of Concrete Construction/Methods of Test and Standard Practices for Concrete  
A3000-03 Cementitious Materials Compendium  
A3004-C2 Test Method for Determination of Compressive Strengths [Part of CAN/CSA A3000-03, Cementitious Materials Compendium]

### **ASTM International**

C 939-02 Flow of Grout for Preplaced-Aggregate Concrete (Flow Cone Method)  
C 33 Concrete Aggregates

#### **3.0 DEFINITIONS**

For the purpose of this specification, the following definitions apply:

Bedding Grout means a thin non-structural grout pumped into the grout distribution system that is cast in the bottom of the Fort Miller Super-Slab □□ Method to fill voids beneath the slabs to provide uniform support to the slab.

Rapid Setting Bedding Grout means a thin fast setting bedding grout, as described above, which is designed to reach a compressive strength of 5 Mpa in one hour.

Dowel Grout means a non-shrink, non-expansive grout, otherwise defined as Proprietary Concrete Repair Material (PCRM) in this NSSP, that is pumped into cast-in slots to encase dowels.

Edge Grout is dowel grout extended 60% by weight with clean, saturated surface dry (SSD), Pea gravel with an approximate size of 9.5 mm and conforming to the requirements of ASTM C 33.

Continuous Precast Concrete Slab Repair means the continuous replacement of multiple consecutive slabs of concrete or sections of asphalt pavement with inter-connecting precast concrete slabs.

Diamond Grinding means altering the profile and texture of a concrete pavement surface by using grinding equipment that employs diamond tip blades.

Micro Milling Equipment means a cold milling machine whose cutting mandrel's carbide cutting teeth have a tooth spacing of 8 mm.

#### 4.0 DESIGN AND SUBMISSION REQUIREMENTS

##### 4.1 Submission Requirements

##### 4.1.1 Precast Concrete Pavement Slab Repair Plan

At least 2 weeks prior to the start of the work, details on the method of the following operations shall be submitted to the Contract Administrator:

- Fabrication, transportation, and installation of each precast concrete slab repair method.
- Removal of existing asphalt pavement (i.e., sawcutting, partial depth removal, equipment, and disposal).
- Base preparation.
- Precast slab placement.
- Grouting (i.e., equipment to be used for mixing and installing).

##### 4.1.2 Precast Concrete Mix Design

The precast concrete mix design shall be submitted to the Contract Administrator at least 2 weeks prior to the start of the work.

Documentation shall be included with the submission of the mix design that demonstrates the proposed mix design and materials meet the requirements of this specification, including the air void system in the hardened concrete and the minimum specified 28-Day compressive strength.

All supporting test data shall not be more than 12 months old at the time the concrete mix design is submitted to the Contract Administrator.

##### 4.1.3 Proprietary Concrete Repair Material (PCRM) - Product Details

At least 7 Days prior to commencement of the work, the name of the PCRM selected for use and the manufacturer's specifications and recommendations for placement shall be submitted to the Contract Administrator. The only PCRM grouts approved for the Fort Miller System are Dayton Superior HD-50 or ProSpec Slab Dowel Grout. The submission shall also include documentation verifying the suitability of the product for the application and evidence of successful performance in a similar application. The PCRM and supporting information provided shall be acceptable to the Owner.

##### 4.1.4 Chipping Hammer

At least one week prior to commencement of the work, a copy of the manufacturer's published specifications on the chipping hammers to be used shall be submitted to the Contract Administrator.

#### 5.0 MATERIALS

##### 5.1 Precast Concrete Slabs

##### 5.1.1 General

The minimum compressive strength of concrete at 28 Days shall be 30 MPa. Testing of the concrete compressive strength shall be carried out according to CSA A23.2.

The air void parameters of the hardened concrete shall be a minimum air content of 3% and a maximum spacing factor of 0.230 mm.

Concrete shall meet the requirements of the materials section of OPSS 350 and OPSS 1350 with the following exceptions and additions:

- a) Concrete aggregates shall be according to OPSS 1002.
- b) The nominal maximum size of coarse aggregate shall be 19 mm.

#### 5.1.2 Finishing

Finishing of precast concrete slabs shall be according to OPSS 350.

#### 5.1.3 Texturing of Surface

Texturing of the precast concrete slab surface shall consist of an initial texturing with a burlap drag that produces longitudinal striations parallel to the centerline. Final texturing shall be with a steel-tined device that produces longitudinal grooves with the steel tines to be 2 mm to 3mm wide at 19mm spacing, resulting in grooves 3 to 5 mm deep after the concrete has hardened.

#### 5.1.4 Dimensions

Precast concrete slabs shall be 3.66 m. wide and 4.57 m. long. Slabs shall be cast to a thickness as per the contract drawings.

#### 5.2 Cement Treated Base Material (CTBM)

Cement treated base material shall consist of a uniform mixture of fine concrete aggregate (concrete sand) and Portland cement mixed at a ratio of 6 (six) parts fine aggregate to 1 (one) part Portland cement.

Fine aggregate for CTBM shall meet the physical and gradation requirements for concrete fine aggregate specified in OPSS 1001 and 1002.

Portland cement shall be Type GU cement according to CSA A3000.

#### 5.3 Bedding Grout

Bedding grout shall be a mixture of cement, water, and plasticizing admixture. The grout mixture shall have a flow rate of 17 to 22 seconds as measured by ASTM C 939 to ensure fluidity. The compressive strength of the bedding grout shall be a minimum of 2.0 MPa at 12 hours.

##### 5.3.1 Rapid Setting Bedding Grout

Rapid set bedding grout shall be bedding grout formulated to reach a compressive strength of 5 MPa in one hour.

#### 5.4 Tie Bars and Dowel Bars

Tie bars shall be according to OPSS 1440. Dowel bars shall be according to OPSS 1441.

#### 5.5 Expansion Caps for Dowel Bars

Caps shall be tight-fitting and made of compressible, non-absorptive, closed cell polyethylene that will allow approximately 6 mm movement at the end of the dowel bar.

#### 5.6 Bond Breaker

Dowel bars shall be coated with RC-250, Tectyl 506, or an approved equivalent.

### 5.7 Proprietary Concrete Repair Material (PCRM)

The PCRM selected shall be suitable for the application.

The minimum compressive strength of the PCRM at 28 Days shall be 30 MPa.

The PCRM for use in the dowel grout of the Fort Miller Super-Slab® Method shall be capable of being pumped into the inverted dovetail slots.

### 5.8 Epoxy Adhesives

Epoxy adhesives shall be from the Owner's approved product list and shall be of the type intended for horizontal dowel application and mixed in the cartridge nozzle.

### 5.9 Joint Materials

The joint sealant material shall be according to OPSS 369.

### 5.10 Water

Water shall be according to OPSS 1302.

## 6.0 EQUIPMENT

### 6.1 Screeding Device for Base Preparation

The screeding device used for fine grading for base preparation shall be laser or otherwise mechanically controlled and shall be capable of fine grading fully compacted CTBM to a tolerance of 3 mm.

### 6.2 Chipping Hammer

Chipping hammers shall be hand held and have a maximum weight of 9.0 kg prior to any handle modification, where applicable, and a maximum piston stroke of 102 mm. All hammers shall have the manufacturer's name and parts or model number engraved on them by the manufacturer. All information shall be clearly legible. The manufacturer's published specifications shall be the sole basis for determining weight and piston stroke.

### 6.3 Hand Finishing Equipment

Hand finishing equipment shall be according to OPSS 904.

### 6.4 Straight Edges

Straight edges shall be according to OPSS 904.

## 7.0 CONSTRUCTION

### 7.1 General

Precast inlay slab repairs for asphalt pavement shall be carried out at the locations identified in the Contract Documents.

For the purposes of this trial, the only acceptable method of precast inlay slab repairs is the Fort Miller Super-Slab® Method as modified by the requirements of this NSSP.

#### 7.1.1 Fort Miller Super-Slab® Method

In the Fort Miller Super-Slab® Method, the work shall consist of fabricating precast concrete pavement slabs (i.e. Super-Slab®) for inlay repairs of asphalt pavement, sawcutting, partial depth removal (cold milling) of the existing asphalt pavement, placing and grading CTBM, placing precast slabs, installing PCRMs in inverted dovetail slots, installing bedding grout beneath the slabs, and sealing of joints.

## 7.2 Operational Constraints

Prior to starting precast slab inlay work, 3 (three) cores, each 150 mm in diameter, shall be taken mid lane in NBL lane 3, at Sta 17+570, 17+600, and 17+630 to measure the total thickness of asphalt pavement. Cores shall be labelled and core thicknesses recorded in the field and brought to the Contract Administrator for pickup by CPATT staff. Core holes shall be backfilled and compacted with suitable cold mix material prior to opening the lane to traffic.

Perimeter sawcutting of the removal area shall not be carried out more than 1 week in advance of the expected date of repair.

Power broom all cold milled surfaces prior to precast inlay slab placement.

Immediately prior to precast inlay slab installation, bolt temporary 4.50 m tubes to longitudinal face of precast slabs to maintain traffic over the temporary longitudinal joint. Remove tubes prior to installing grout as per contract drawings

Bedding grout and dowel grout shall be carried out as soon as possible after the installation of the precast concrete inlay slab.

The PCRMs shall not be placed when the air temperature is outside the manufacturer's recommended temperature range or is likely to fall or rise outside the range throughout the duration of the material placing operation. Prior to placing the PCRMs, it shall be demonstrated to the Contract Administrator that the existing concrete temperature in the repair area meets the manufacturer's requirements by measuring and recording the substrate temperatures using a contact thermometer or infrared thermometer.

Construction vehicles, equipment, or traffic shall not be permitted to travel on the precast repair until the PCRMs has attained a minimum compressive strength of 20 MPa.

Each repair location shall be completed within the time period specified in the Contract Documents. If the repair is not progressing at a rate that will permit the full restoration of traffic within the allowable time period, appropriate measures acceptable to the Contract Administrator shall be undertaken to allow opening of the road to traffic. Precast concrete inlay slab repairs shall replace the above temporary work during the next scheduled closure.

## 7.3 Instrumentation Plan

### 7.3.1 Trenching

Before commencing cold milling each night, a trench shall be cut in the shoulder asphalt. This trench will allow cabling from instrumentation to a data cabinet located inside the ROW fence. The trench shall be cut from the outside edge of the shoulder to the longitudinal sawcut denoting the outside edge of milling. This trench should be at least as deep as the milling depth for the section.

The location of this trench shall be specified by a member of the Centre for Pavement and Transportation Technology (CPATT) based on the extents of nightly milling.

A trench shall also be excavated from the outside edge of the asphalt shoulder, coinciding with the cable trench in the shoulder, to the data collection system housing unit at a continuous width and depth of 600 mm. This trench shall be backfilled and compacted with suitable earth material as per OPSS 510 under the direction of CPATT staff without damage to the installed cabling.

### 7.3.2 Recessed Milled Sections

Following the partial depth asphalt removal, but prior to the placement of CTBM or installation of the precast slabs, the contractor shall remove asphalt in specified locations for instrumentation placement. These recessed areas will be milled to a depth of approximately 25mm. The dimensions of these removals will be smaller in area than 0.5 m<sup>2</sup>. The locations of the milled areas will be specified by an onsite member of CPATT, and will consist of a maximum three (3) locations per night.

### 7.3.3 Sub-Slab Slot

A 50mm wide by 12mm deep slot for running of instrumentation cabling shall be removed from each recessed area to the shoulder trench specified previously. This slot can be connected to adjacent recessed sections to allow for cabling from multiple recessed areas to use the same slot.

All instrumentation installation beneath a precast slab shall occur prior to the placement of CTBM or precast slab.

### 7.3.4 Data Collection System Housing Unit Base

A concrete base for a data collection system housing unit (300mm x 1m x 1m) shall be poured smooth and level, located 1 meter offset from the ROW fenceline. This concrete base shall have a 250mm diameter opening in the center to allow for running instrumentation cabling from buried trenches.

## 7.4 Removals

### 7.4.1 General

A detailed survey shall be carried out to precisely delineate the limits of the areas to be repaired within a tolerance of 12 mm as per the contract drawings. Inlay repairs shall be the full width of the lane and the depth of hot mix asphalt repair as specified in the contract drawings.

During pavement removal operations, care shall be taken to prevent contamination with granular and other foreign materials.

Removal shall be performed in such a manner as to leave adjacent pavement and structures remaining in place undisturbed.

When the roadway is to be opened to traffic, after the daily shut down, a temporary 1.0 meter long slab shall be installed as specified in the Contract Documents.

Asphalt pavement material from removal operations shall become the property of the contractor and immediately removed from the site.

### 7.4.2 Cutting Existing Pavement

Pavement shall be sawcut for neat removal to the dimensions and depth specified in the Contract Documents.

Suitable mechanical sawing equipment and pavement cold milling equipment capable of producing a straight clean vertical face shall be used for cutting the pavement.

The outer limits of the removal area shall be sawcut to the depth specified in the contract drawings and shall not be overcut by more than 250 mm into the adjacent hot mix asphalt that is to remain in place. Overcuts shall be filled with a proprietary product acceptable to the Owner.

### 7.4.3 Removal of Asphalt Pavement, Partial-Depth

The work shall include the partial-depth removal of asphalt pavement using cold milling equipment capable of milling to a width of 2 meters and depth of 300 mm in one pass. The cold milling equipment used for partial depth

removal shall be automatically controlled for grade and slope during removal. The surface remaining after removal shall have a constant and continuous crossfall matching the intended surface course crossfall. The surface remaining after removal shall have an even texture and be free of significantly different grooves and ridges in all directions.

The asphalt pavement shall be removed to the depth for each precast inlay Option specified in the Contract Documents.

Removed asphalt pavement material shall not remain on the roadway after completion of the day's operation. Placing of the material on grade other than a bituminous surface prior to hauling to a stockpile shall not be permitted.

For Options 1 and 3, after partial depth removal, the gap between the top of milled surface and the bottom of a 3 m straightedge placed anywhere in any direction on the milled surface shall not exceed 6 mm.

For Option 2, the final milled surface shall be attained using a micro milling machine where the gap between the top of micro milled surface and the bottom of a 3 m straightedge placed anywhere in any direction on the micro milled surface shall not exceed 3 mm.

Removals shall be carried out without damaging the adjacent asphalt pavement or asphalt shoulder.

Asphalt surfaces damaged during the removal process shall be repaired. A proposal for asphalt surface repairs shall be provided to the Contract Administrator for approval.

## 7.5 Base Preparation

### 7.5.1 General

For the grade support option, Option 1, levelling material shall be cement treated base material (CTBM) meeting the requirements of this specification.

For the asphalt support option, Option 2, micro-milling of the cold milled asphalt surface shall be carried out to achieve a tolerance of 3 mm along 3 meter straightedge.

### 7.5.2 Cement Treated Base Material (CTBM)

CTBM shall be compacted then fine graded using a screeding device capable of grading the fully compacted bedding material to an accuracy of 3 mm +/- 1mm. Immediately prior to placement of the precast inlay slab, the compacted and fine graded CTBM shall be lightly sprayed with water to thoroughly dampen the CTBM throughout without puddling of water on the CTBM surface.

## 7.6 Steel Reinforcement

Steel reinforcement shall be according to OPSS 905.

## 7.7 Slab Installation

Slabs shall be guided into position during installation using guide bars inserted in bedding grout port holes to align slabs during setting. The use of pry bars or wedges in joints for alignment purposes shall not be permitted.

The vertical differential between adjacent precast inlay slabs shall be a maximum of 3 mm. For Option 1, if the vertical differential is greater than 3 mm, the slab shall be removed, the base re-graded, and the slab reset until the differential does not exceed 3 mm prior moving on to the next slab.

For Option 2, if the vertical differential is greater than 3 mm, the slab shall be removed, the milled surface micro milled and the slab reset until the differential does not exceed 3 mm prior moving on to the next slab.

For Option 3, the levelling inserts (bolts) shall be adjusted until the differential does not exceed 3 mm prior moving on to the next slab.

For Option 1, if un-grouted slabs under traffic are vertically displaced so that the vertical differential is greater than 3 mm as described above, the slab shall be removed, the base re-graded, and the slab reset prior to grouting, or the surface shall be brought to the required tolerance by grinding as required by this specification.

#### 7.8 Placing the Dowel Grout and Bedding Grout

Foam grout dams shall be installed at the open ends of the transverse joint to be grouted to prevent dowel grout from escaping during the installation. Dowel grout shall be mixed in strict accordance with the instructions provided by the manufacturer. The volume of water shall be measured accurately for each batch by weighing the batch water or by using calibrated pails that are perforated at a level to ensure the correct amount of water is mixed with each bag of grout. Dowel grout shall be pumped in the back port of each dowel slot until it comes out the second port in the same slot. A foot shall be placed over the second port and pumping shall be continued until the grout flows along the joint to the next slot. The same procedure shall be repeated for the back port of the next slot. The grout level in previously filled ports shall be continually monitored. Grout shall be added, as necessary, to keep the grout level in the ports even with the top of the slab and in the joints above the top of the slots.

For Options 1 and 2, bedding grout shall be placed after the dowel grout has been installed. Bedding grout shall be mixed in strict accordance with the instructions provided by the manufacturer of the viscosity-reducing admixture. Bedding grout shall be pumped in the lowest port of the slab until it comes out the corresponding port at the other end of the slab. While filling the remaining ports in the slab, the grout level shall be continually monitored in previously filled ports and grout added, as required, to keep the grout level in the ports even with the top of the slab. This will maintain a safe and adequate head pressure on the bedding grout until all voids under the slab are filled.

For Options 3, a rapid setting bedding grout shall be used incorporating the same placement procedures as bedding grout.

Before the bedding grout fully sets, the top 50 mm of bedding grout in each port shall be removed and replaced with PCRM. The PCRM in all ports shall be finished flush and matching with the surface of the concrete and all excess material removed immediately.

#### 7.9 Tolerances

##### 7.9.1 Surface Tolerances

The surface of the precast concrete slab repair shall join flush with the existing asphalt pavement. Surface tolerance of continuous slabs shall be so that the gap is not greater than 3 mm when the 3 meter straight edge is placed in any location and direction, including the edge of pavement, except across the crown or drainage gutters.

#### 7.10 Joint Sealing

All transverse joints between precast inlay slabs shall be sealed according to OPSS 369. All longitudinal and transverse edge joints shall be filled with dowel grout mixed with fine crushed stone at a ratio of 1 (one) part grout to 4 (four) parts stone.

#### 7.11 Sampling and Testing

##### 7.11.1 General

All samples, including those handled by a commercial carrier shall be accompanied by a sample data sheet and any additional documents as specified elsewhere in the Contract Documents. When not specified or not included on the sample data sheet, samples shall be delivered with a transmittal form identifying the following information:

- a) Contract Number.
- b) Name of Contractor, name of contact person and telephone numbers.
- c) Name of Contract Administrator, and telephone numbers.

- d) Quantity and type of sample. When a sample consists of more than one item, each item shall be individually identified.
- e) Date sampled.
- f) Date shipped.
- g) Sample and lot number.
- h) Sample location.

#### 7.11.2 Compressive Strength of Concrete in Precast Slab

Concrete test cylinders shall be cast, cured, handled, and delivered for 28-Day compressive strength testing according to OPSS 1350 based on 1 set of 2 cylinders taken for each batch of concrete.

#### 7.11.3 Compressive Strength of Proprietary Concrete Repair Materials

Samples of PCRMs shall be taken from the mixer in the field for the determination of the early strength and 28-Day compressive strength. The PCRMs shall be moulded into cubes according to CAN/CSA A3004- C2.

Cubes shall be prepared on-site from the PCRMs to be used to fill the slots. For the 28-Day compressive strength, the PCRMs shall be sampled once for every 4 hours of production or a minimum of once per day, whichever is greatest. One set of six cubes shall be made from each sample of PCRMs.

Additional cubes for determination of early strength shall be prepared. One set of six cubes shall be made for the final repair area of each closure. These cubes shall be tested to verify that the PCRMs in the repair area has attained a compressive strength of 20 MPa. These test results shall be communicated immediately to the Contract Administrator prior to opening to traffic.

The timing of testing and frequency of testing of the early strength cubes shall be determined when the PCRMs has attained a minimum compressive strength of 20 MPa.

The specimens shall be stored at a temperature between 15 °C and 25 °C and shall not be moved prior to demoulding. The specimens shall be demoulded and transported to the QA laboratory designated by the Owner within 24 hours ± 4 hours. The samples shall be transported in a sealed white opaque plastic bag containing at least 250 ml of water and maintained at a temperature between 15 °C and 25 °C.

#### 7.12 Falling Weight Deflectometer Testing

Within 2 weeks of slab placement and grouting, falling weight deflectometer (FWD) testing shall be carried out on the approach and leave joints of each precast slab and across the transverse end joints to determine the load transfer efficiency across the transverse joints. FWD testing, equipment calibration, and reporting shall be according to MERO-019 using the Load Transfer test with a Detailed Project Level data collection scenario and a JCP Test Plan configuration.

#### 7.13 Repair or Removal of Unacceptable Concrete

Precast concrete pavement slabs that arrive on the job site cracked, honeycombed, or showing any other visually detectable deficiencies shall be rejected and not used in the work.

Precast concrete pavement slabs that do not meet the surface tolerance requirements shall be removed and replaced, or corrected by diamond grinding.

Asphalt pavement adjacent to precast concrete slab inlay repair, damaged or displaced during installation of the precast slabs shall be repaired to the satisfaction of the Contract Administrator.

#### 7.14 Management of Excess Material

Management of excess material shall be according to the Contract Documents.

8.0 QUALITY ASSURANCE  
8.1 Inspection

Prior to installation and with notification, access shall be provided to the Contract Administrator to inspect the precast concrete pavement slabs to ensure that they are properly textured and crack-free without any honeycombing or other visually detectable deficiencies.

Access shall also be provided to CPATT personnel to coordinate instrumentation placement.

8.2 Acceptance or Rejection

Prior to opening to traffic, access shall be provided to the Contract Administrator to inspect the precast concrete inlay slab repairs to determine if the completed work contains:

- a) Cracking or spalling.
- b) UngROUTED saw over-cuts from the removal process.
- c) Rocking of precast concrete inlay slab.
- d) Precast concrete inlay slab that does not meet surface tolerance.

Precast concrete inlay slab repairs shall be rejected based on the presence of one or more of the defects identified above or one or more of the following conditions:

- a) FWD testing results indicate a load transfer efficiency of less than 70%.
- b) Compressive strength of the precast slab less than 30 MPa at 28 Days.
- c) Air content of the hardened concrete in the precast slab is less than 3% or spacing factor is greater than 0.230 mm.

A detailed remedial plan shall be submitted to the Contract Administrator for approval to address identified deficiencies.

9.0 MEASUREMENT FOR PAYMENT  
9.1 Actual Measurement  
9.1.1 Precast Concrete Slab Inlay Repair

Measurement of the precast concrete slab repair placed shall be by area in square metres. The total area shall be calculated to the nearest 0.1 m<sup>2</sup>.

9.2 Plan Quantity Measurement

When measurement is by Plan Quantity, such measurement shall be based on the units shown in the clause under Actual Measurement.

10.0 BASIS OF PAYMENT  
10.1 Precast Concrete Inlay Slab Repair, Option 1 – Item  
Precast Concrete Inlay Slab Repair, Option 2 – Item  
Precast Concrete Inlay Slab Repair, Option 3 – Item

Lump sum payment at the Contract price for the above tender items shall be full compensation for all Labour, Equipment, and Material to do the work for each option.

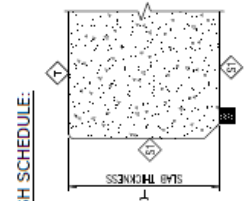
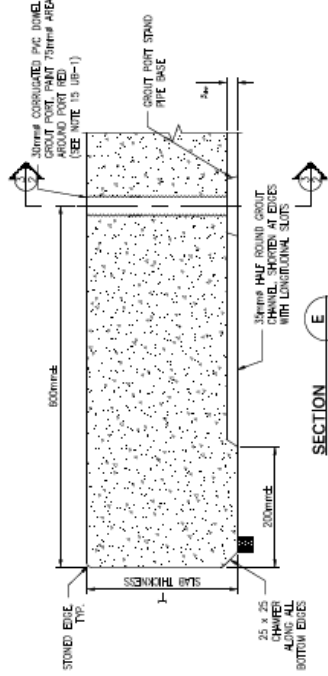
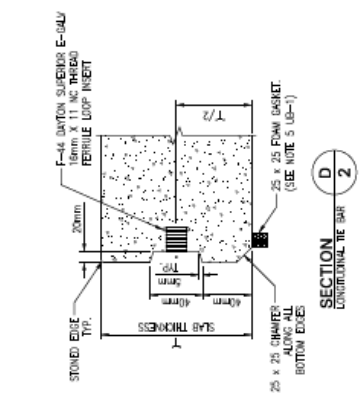
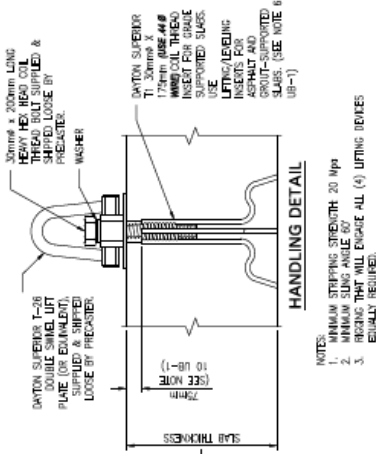
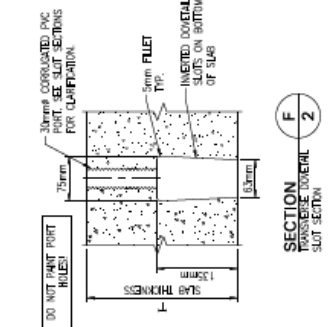
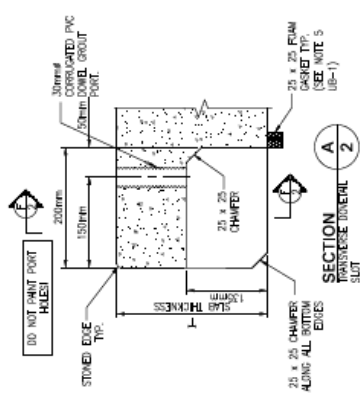
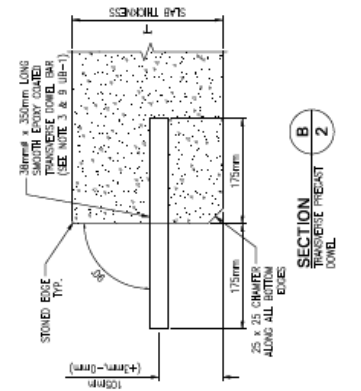
Measures taken to permit full restoration of traffic within the allowable time period shall be at no additional cost to the Owner.

Precast concrete inlay slabs that do not meet surface tolerance requirements shall be either removed and replaced or repaired by diamond grinding at no additional cost to the Owner.

Precast concrete inlay slabs rejected by the Contract Administrator shall be removed and replaced with new precast concrete slabs as specified elsewhere in the Contract Documents at no additional cost to the Owner.

Asphalt surfaces damaged during the removal process shall be repaired at no additional cost to the Owner.





FINISH SCHEDULE:  
 (1) BURLAP DRAG AND LONGITUDINAL TINED FINISH (SEE NOTE 13 ON UB-1)  
 (2) = STEEL FORM FINISH

"SUPER-SLAB IS PROTECTED UNDER AT LEAST ONE OF US PATENT NUMBERS: 6,607,329 B2, 7,068,874, 7,068,875, 7,068,876, 7,068,877, 7,068,878, 7,068,879, 7,068,880, 7,068,881, 7,068,882, 7,068,883, 7,068,884, 7,068,885, 7,068,886, 7,068,887, 7,068,888, 7,068,889, 7,068,890, 7,068,891, 7,068,892, 7,068,893, 7,068,894, 7,068,895, 7,068,896, 7,068,897, 7,068,898, 7,068,899, 7,068,900, 7,068,901, 7,068,902, 7,068,903, 7,068,904, 7,068,905, 7,068,906, 7,068,907, 7,068,908, 7,068,909, 7,068,910 OTHER U.S. AND FOREIGN PATENTS PENDING. SUPER-SLAB IS A REGISTERED US TRADEMARK OWNED BY THE PORT MILLER CO., INC.

PROVINCE OF ONTARIO MINISTRY OF TRANSPORTATION	
MAINTENANCE PROJECT	
CONTRACT ADDRESS	
SUPER SLAB® FABRICATION DETAILS	DWG # UB-2

THE PORT MILLER CO., INC. P.O. BOX 50 1500 W. 15th ST. NEW YORK 12877 PH: (518) 655-5500 FAX: (518) 655-4970 www.portmiller.com	REV #	DATE	BY	CHK'D BY	DATE
	2 of 2				





## **APPENDIX C: VISUAL ASSESSMENT RESULTS**

---

Panel #	Joint Gap				Vertical Differential Outside Allowable Range (mm)				Longitudinal Joint Grout Ravelling						
	LWP	C	RWP	AVG	Range (mm)				PCIP Cracking	Edge Grout	Slight	Medium	Severe		
1	19	14	16	16.33					X						
2	14	17	21	17.33					X						
3	19	15	15.5	16.50						X					
4	16	15	14	15.00							X				
5	14	15	16	15.00						X					
6	14	15	15	14.67								X			
7	15	19	-	17.00								X			
8	13	14	14	13.67									X		
9	15	15	14	14.67						X					
10	14	15	14	14.33									X		
11	17	16	17	16.67						X					
12	14	12	15	13.67									X		
13	17	17	21	18.33	10.00						X				
14	19	13	17.2	16.40											
15	12	15	15	14.00							X				
16	14	22	15	17.00									X		
17	15	14	15	14.67									X		
18	14	15	15	14.67								X			
19	14	14	14	14.00								X			
20	15	16	15	15.33							X				
21	15	13	15	14.33											
22	14	14	15	14.33								X			
<b>Count</b>										1	2	20	7	8	5

Panel #	Grout Overflow at Panel Edge				Grout Port Not Filled Completely	Spalling of PCIP Edge	Incomp. Material Lodged in Joint	Gap Between Edge Grout and Asphalt
	Grout Overflow Filling Grooves	Grout Port Overflow (>30 cm)	Transverse	Longitudinal				
1					X			
2								
3	X		X				X	X
4						X		
5							X	X
6							X	X
7	X		X		X		X	
8	X	X			X			
9	X		X				X	X
10	X		X				X	X
11	X		X	X			X	X
12	X		X				X	X
13					X			X
14	X		X	X				X
15	X		X	X			X	X
16					X		X	X
17	X		X				X	X
18								
19								X
20								X
21	X		X					X
22					X		X	
<b>Count</b>	11	1	10	3	6	1	11	14